MATHEMATICAL MODELING FOR HELMINTHS AND MYCOBACTERIUM TUBERCULOSIS CO-INFECTION

ARISTIDE G. LAMBURA

A Dissertation Submitted in Partial Fulfilment of the Requirements for the Degree of Doctor of Philosophy in Mathematical and Computer Sciences and Engineering of the Nelson Mandela African Institution of Science and Technology

Arusha, Tanzania

October, 2021

ABSTRACT

Tuberculosis continues to be a life-threatening disease in Sub-Saharan African countries despite the available vaccine whereas soil-transmitted helminth is among the neglected tropical disease that causes threats to pre-school, school-aged children and child-bearing mothers. The infection by helminths increases susceptibility to tuberculosis. Thus, there is a need to investigate the possibility of co-infection of the two diseases due to its geographical overlap at cellular and population levels. This dissertation presents deterministic mathematical models that are aimed at describing the transmission dynamics of soil-transmitted disease and the co-infection with tuberculosis. The first model that describes the transmission dynamics of soil-transmitted helminth with optimal control is presented. The model was qualitatively analyzed and the threshold that governs the spread of the disease derived. The best control model was developed, and numerical simulations were run using a variety of control measures to determine the most cost-effective method for effectively containing the disease. According to the findings, the most cost-effective method for combating the spread of soil-transmitted helminths is a combination of health education and sanitation. The soil-transmitted helminth model was modified to form the second model for the co-infection with tuberculosis. The qualitative analysis was made to determine the equilibrium points and the conditions for the disease eradication. The impact of helminth infection on tuberculosis and vice-versa were discussed and it was observed that helminth infection enhances tuberculosis in the community. Numerical simulation for the model revealed that the interventions that include a combination of measures for controlling helminth infection, vaccinating the babies with bacille Calmette-Guérin vaccine and the treatment of individuals with active tuberculosis were effective in controlling the spread of the diseases. The last model considered the interaction of the helminth parasites, mycobacterium tuberculosis pathogens, and the immune competence within an individual host. Numerical simulations showed that primary infection by either helminth parasite or Mtb bacteria is unsuccessful within the host when the basic reproduction number is less than the unit.

DECLARATION

I, ARISTIDE G. LAMBURA do hereby declare to the Senate of Nelson Mandela African Institution of Science and Technology that this dissertation is my own original work and that it has neither been submitted nor being concurrently submitted for degree award in any other institution.

Name and signature of candidate	**Date**

The above declaration is confirmed

Name and signature of supervisor 1	**Date**
Name and signature of supervisor 2	**Date**
Name and signature of supervisor 3	**Date**

COPYRIGHT

CERTIFICATION

The undersigned certify that they have read and found the dissertation acceptable by the Nelson Mandela African Institution of Science and Technology.

Name and signature of supervisor 1	**Date**
Name and signature of supervisor 2	**Date**
Name and signature of supervisor 3	**Date**

ACKNOWLEDGEMENTS

I sincerely express my gratitude to Almighty God for granting me the opportunity to pursue Ph.D. studies at NM-AIST.

I would like to express my heartfelt thanks and deepest appreciation to my academic supervisors Dr. Gasper Mwanga, Prof. Livingstone Luboobi, and Prof. Dmitry Kuznetsov for providing me with valuable and dedicated guidance, encouragement, devotion, and constant feedback throughout my study. Your insightful comments and feedback pushed me to sharpen my thinking abilities and brought this work to a higher level. May God bless you.

Without the support and funding given by the African Development Bank (AfDB) and the United Republic of Tanzania under project number $P-ZI-IAO-016$ and grant number 2100155032816, I would not have been able to complete this work. I'm also thankful to Mr. Julius Lenguyana, the project manager, for his warm welcome and willingness to help me meet the project's objectives.

I would like also to thank my tutors Prof. Dr-Ing. Verdiana Grace MASANJA and Prof. Dmitry Kuznetsov for their valuable guidance throughout my studies. I would like to convey my profound appreciation to my tutors for providing me with the right tools I needed and had the right direction for the completion of the dissertation.

Warm thanks go to my collegues at NM-AIST, Ms Edwiga Renald, Mr. Geradius Kikumi, Hegespol Mwanyika, Nkuba Nyerere, Mlyashimbi Helikumi, Maranya Mayengo, Paul Lucas Luchemba, Rene Costa, Edwin Ndibalema and Theresia Sabini for their cooperation, caring and social life at the campus. Thank you for being the wonderful companion and making my journey successful.

I would also like to thank my lovely and supportive wife, Rose, and my two sons Michael and Raphael for being patient with me and your immerse faith in me. I also thank my parents Genes Anaklet Lambura and Benedicta Shayo for their wise counsel and sympathy and all family members for their continued support and prayers.

DEDICATION

Mrs. Rose Shayo

&

Michael, and Raphael

This dissertation is dedicated to you, my beloved wife, and my children.

TABLE OF CONTENTS

LIST OF TABLES

LIST OF FIGURES

LIST OF APPENDICES

LIST OF ABBREVIATIONS

CDC	Center for Disease Control
WHO	Word Health Organization
TB	Tuberculosis
Mtb	Mycobacterium tuberculosis
Th1	T-helper-1
Th2	T-helper-2
STH	Soil-Transmitted Helminth
MDA	Mass Drug Administration
WORMSIM	Worm Simulation
WASH	Water, Sanitation and Hygiene
DFE	Disease Free-Equilibrium
TV	Television Video
ICER	Incremental Cost Effective Ratio
BCG	Bacille Calmetre-Guerin
FBSM	Backward Sweep Method
MATLAB	Matrix Laboratory
EEP	Endemic Equilibrium Point

CHAPTER ONE

INTRODUCTION

1.1 Background of the Problem

1.1.1 Basic Information about Soil-transmitted Helminths

The worldwide burden of helminths (worms) infection cannot be underestimated. It is estimated that over 1.5 billion people worldwide are infected with helminths (WHO, 2018). Helminths are parasitic worms that infect the intestine and are spread through contaminated soil in areas with poor sanitation. They are transmitted by eggs found on human faces. Ingestion of eggs or larvae in contaminated food or skin penetration by infective larvae in the soil are two other ways that helminths can be transmitted (CDC, 2018). The main species of worms that infect people are the roundworm (*Ascaris lumbricoides*), the whipworm (*Trichuris trichiura*) and the hookworms (*Necator americanus* and *Ancylostoma duodenale*). Intestinal manifestations (diarrhea, abdominal pain), general malaise, and weakness are all symptoms of these worms. Hookworms cause chronic intestinal hemorrhage and that lead to anemia. Helminth infection is widespread in tropical and subtropical areas, and it is attributed to a lack of sanitation as a result of extreme poverty. Individuals at risk in endemic areas include pre-school infants, school-aged children, and women of childbearing age (Uneke, 2010).

According to the WHO, there are several methods for controlling soil-transmitted helminths, including regular deworming to eliminate the infecting worms, health education to prevent re-infection, and improved sanitation to reduce the contamination of the soil with ineffective eggs.

1.1.2 Basic Information about Mycobactrium Tuberculosis

In 2019, a quarter of the world's population was estimated to be infected with Mycobacterium tuberculosis (Mtb), with 9.6 million people developing active tuberculosis and 1.5 million tuberculosis-related deaths recorded (Harding, 2020). Despite the huge infectious population about 90% to 95% are asymptomatic for a long period of time and they have 10% lifetime risk of developing active tuberculosis (Monin *et al.*, 2015). Mycobacterium tuberculosis is a bacteria that cause tuberculosis (TB) after inhalation of aerosolizing nuclei from an individual with active TB and infects predominantly human being but may also infect other diverse hosts. These bacteria have a slow growth rate, are aerobic, and can expand within human cells (an intracellular bacterium).

Tuberculosis is treated in two ways: for latent tuberculosis (chemoprophylaxis) and for active tuberculosis (treatment) (therapeutics). A successful treatment strategy to reduce the prevalence of TB infection is by considering both chemoprophylaxis and therapeutic. The control strategies have been developed for compliance with TB treatment due to its long-lasting treatment procedures (Ozcaglar *et al.*, 2012). However, treatment efficacy has lead to the development of Mtb resistant to the first line anti-TB drugs but still individuals can be infected with Mtb bacteria.

1.1.3 Helminth-Mycobacterium Tuberculosis Co-infection

It is well known that these two diseases have a geographical overlap which in turn increases the likelihood of co-infection with both pathogens and as a result competition become more intense within host. TB is most prevalent in societies where individuals are infected with helminth while helminth is reported as the most common parasite found in TB patients (Elliott & Weinstock, 2012). Figure 1 shows the world geographical distribution of the burden of helminths and tuberculosis co-infection. Immunologic studies show that asymptomatic helmith infection is associated with the increase in the regulatory T-cell and Th2-type responses which affect the host ability to mount an effective TH1-type immune-mediated protection against Mtb (Abate, 2013). Co-infection may significantly inhibit a host immune system, affects the antibacterial therapy which is detrimental to the prognosis of disease and impairs protective immune responses to vaccination against Mtb.

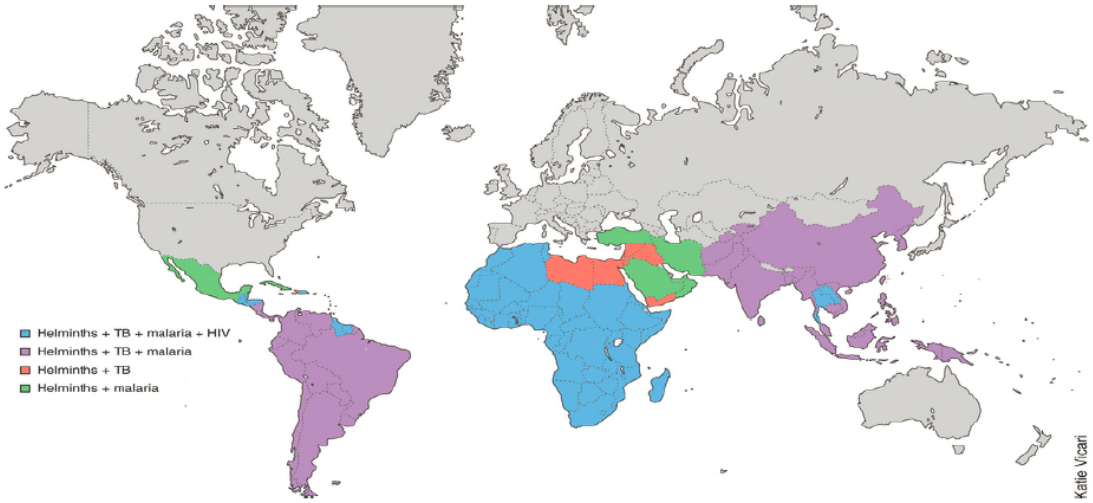

Figure 1: World map showing the geographical distribution of the burden of helminths and tuberculosis co-infection (Salgame *et al.*, 2013)

.

1.2 Statement of the Problem

The study of both helminths and Mtb is important because of co-occurrence of these two diseases in same geographical location. Literature shows that in resource-poor areas, co-infection with helminth and Mtb pathogens frequently occurs. The pathogen competition against hosts limited resources and virulence may differ from that of the single infection as in co-infection there is more than one pathogen or strain co-infecting a single host. Furthermore, infection by helminth parasites increases the susceptibility to tuberculosis and the consequences associated with such dual infections are tremendously serious in the cognitive development of the pre-school and school aged children (Mkhize-Kwitshana *et al.*, 2017). Previous mathematical models have concentrated on single infections in an attempt to control the diseases and the virulence caused by the two diseases which is not always the case. Thus this study considered inter-host and intra-host mathematical models for helminths and Mycobacterium tuberculosis co-infection and incorporated the aspects of immune responses and therapeutic measures. Furthermore, this study employed the power of optimal control in determining the best combination of control measures to combat the spread of the two diseases.

1.3 Rationale of the Study

This study is motivated by the fact that helminths and Mtb co-infections continue to pose a great threat in Sub-Saharan Africa due to limited resources. Co-infection is of particular importance and the interaction of co-infecting pathogens can either have positive or negative impact (Bhunu *et al.*, 2009; Mushayabasa & Bhunu, 2011). Helminths and Mycobacterium tuberculosis infections have large overlap at the population level and geographical level and both show different and complex immune responses (Babu & Nutman, 2016). Literature review shows that the helminth infection can impair the immunologic host control, which in turn leads to the increase in the risk of occurrence and progression of Mtb (Chatterjee & Nutman, 2015). Furthermore, studies show that infection by helminth is associated with an increased incidence of Mycobacterium disease. However, single infection mathematical models (Anderson & May, 1985; Medley *et al.*, 1993; Farrell *et al.*, 2018; Pullan *et al.*, 2014; Bhunu *et al.*, 2008a; Nkamba *et al.*, 2019; Du *et al.*, 2017) have proposed various interventions on an attempt to control the disease but had limited impact on eradication of both helminth infection and tuberculosis from the community. Thus mathematical modeling of soil-transmitted helminth and Mtb co-infection is of particular importance in understanding the transmission dynamics and control of these diseases in the community.

1.4 Objectives of the Study

The objectives of this study are classified in general objective and specific objectives.

1.4.1 General Objective of the Study

The general objective of this study is to develop and analyze mathematical models for helminths and Mycobacterium tuberculosis co-infection with the effect of treatment and immune responses.

1.4.2 Specific Objectives of the Study

The specific objectives of this study are:

(i) To formulate and analyze mathematical models for soil-transmitted helminth with the application of optimal strategies.

(ii) To formulate and analyze inter-host mathematical model for helminth and Mycobacterium tuberculosis co-infection with the application of optimal control strategies.

(iii) To formulate and analyze intra-host mathematical model for helminth and Mycobacterium tuberculosis co-infection with the effect of immune responses.

1.5 Research Hypothesis

(i) It is possible to formulate and analyze mathematical models for soil-transmitted helminth with the application optimal strategies.

(ii) It is possible to formulate and analyze inter-host mathematical model for helminth and Mycobacterium tuberculosis co-infection with the application of optimal control strategies.

(iii) It is possible to formulate and analyze intra-host mathematical model for helminth and Mycobacterium tuberculosis co-infection with the effect of immune responses.

1.6 Significance of the Study

(i) The developed mathematical models will help the decision makers and stakeholders to understand the transmission dynamics and control of helminth and Mycobacterium tuberculosis co-infection in order to make precise policies for interventions and also provides an understanding to the society on how helminth and tuberculosis can be controlled.

(ii) The findings of this study add up new knowledge to the existing literature and provide a platform for further research and studies to develop more suitable mathematical models for parasitic diseases of human and tuberculosis.

1.7 Delineation of the Study

Mathematical modeling of the co-infection of helminth infection and tuberculosis is of paramount importance. This study intended to cover various modeling techniques to come up with mathematical models for Helminth and Mtb co-infection at the population level and cellular level. The study was limited by the availability of secondary data to estimate model parameters. However, few data set obtained from the published articles were used to validate the soil-transmitted helminth model.

CHAPTER TWO

LITERATURE REVIEW

2.1 Introduction

This chapter presents a review of the mathematical models/framework and contribution of other scholars on helminth infection and the co-infection of helminth infection with Mtb.

2.2 Basic Mathematical Concepts

In this study, mathematical models for soil-transmitted helminths, inter-host mathematical model for soil-transmitted helminths and tuberculosis co-infection and intra-host model for Helminths and tuberculosis co-infection are analyzed using various techniques described here under.

2.2.1 Autonomous System

In this work, biological models are represented by autonomous system of the form:

$$\frac{d\mathbf{x}}{dt} = f(\mathbf{x}) \tag{2.1}$$

where, $\mathbf{x} = (x_1, x_2, ..., x_n)$ represents the state variables. The function $f(\mathbf{x})$ denote collection of real-valued functions of state variables x_i, $i = 1, 2, ..., n$ and time t.

2.2.2 Stability of Steady States

Local stability explains what happens near the equilibrium point. The equilibrium point is said to be stable if noise is added (perturbation) to the solution starting with the initial condition, over time the system will return to its equilibrium point. Global stability of the equilibrium point explains the inevitability of the system to return to its equilibrium point regardless of the starting point. For local stability of disease free equilibrium (DFE), the jacobian of system (2.1) is of the form:

$$J = \begin{pmatrix} \frac{\partial f_1}{\partial x_1} & \frac{\partial f_1}{\partial x_2} & . & . & . & \frac{\partial f_1}{\partial x_n} \\ \frac{\partial f_2}{\partial x_1} & \frac{\partial f_2}{\partial x_2} & . & . & . & \frac{\partial f_2}{\partial x_n} \\ . & . & . & . & . & . \\ . & . & . & . & . & . \\ . & . & . & . & . & . \\ \frac{\partial f_n}{\partial x_1} & \frac{\partial f_n}{\partial x_2} & . & . & . & \frac{\partial f_n}{\partial x_n} \end{pmatrix} \tag{2.2}$$

The conclusions can be drawn on the stability of the system (2.1) by studying the signs of the eigenvalues of J. However, Routh-Hurwitz conditions may applied to the system (2.2) to draw conclusion on the behavior of stability around the equilibrium point.

2.2.3 Bifurcation Analysis

Definition 2.1. *Bifurcation is defined as the sudden change in qualitative behavior of a dynamical system when a small change is made to the corresponding parameter value (bifurcation parameter).*

To investigate the local bifurcations at the endemic equilibrium points, Center Manifold Theorem by Castillo-Chavez and Song (2004) is employed. The theorem is stated here under for convenience.

Theorem 2.1. *(See Castillo-Chavez and Song (2004)) Consider the following general system of ordinary differential equations with a parameter ϕ:*

$$\frac{d\boldsymbol{x}}{dt} = f(\boldsymbol{x}, \phi), f : \mathbb{R}^n \times \mathbb{R} \to \mathbb{R}^n \text{ and } f \in \mathbb{C}^2(\mathbb{R}^n \times \mathbb{R}) \tag{2.3}$$

It is assumed that 0 is an equilibrium for system (2.3) for all values of the parameter ϕ: that is, $f(0, \phi) = 0$ for all ϕ. Assume

A1: $A = D_x f(0,0) = \left(\dfrac{\partial f_i(0,0)}{\partial x_j}\right)$ *is the linearisation of system (2.3) around the equilibrium 0 with ϕ evaluated at 0. Zero is a simple eigenvalue of A and other eigenvalues of A have negative real parts:*

A2: Matrix A has a right eigenvector w and a left eigenvector v corresponding to the zero eigenvalue.

Let f_k be the k^{th} component of f and

$$\begin{aligned} a &= \sum_{k,i,j=1}^{n} v_k w_i w_j \frac{\partial^2 f_k(0,0)}{\partial x_i \partial x_j}, \\ b &= \sum_{k,i=1}^{n} v_k w_i \frac{\partial^2 f_k(0,0)}{\partial x_i \partial \phi}. \end{aligned} \tag{2.4}$$

The local dynamics of (2.3) around 0 are governed by a and b in the following manner:

(i) $a > 0; b > 0$. *When $\phi < 0$ with $|\phi| \ll 1$, 0 is locally asymptotically stable, and there exists a positive unstable equilibrium; when $0 < \phi \leq 1$: 0 is unstable and there exists a negative and locally asymptotically stable equilibrium:*

(ii) $a < 0$*:* $b < 0$*. When* $\phi < 0$ *with* $|\phi| \ll 1$ *is unstable; when* $0 < \phi \leq 1$*; 0 is locally asymptotically stable, and there exists a positive unstable equilibrium:*

(iii) $a > 0$*:* $b < 0$*. When* $\phi < 0$ *with* $|\phi| \ll 1$*, 0 is unstable, and there exists a locally asymptotically stable negative equilibrium; when* $0 < \phi \leq 1$*; 0 is stable, and a positive unstable equilibrium appears:*

(iv) $a < 0$*:* $b > 0$*. When* ϕ *changes from negative to positive, 0 changes its stability from stable to unstable. Correspondingly, a negative equilibrium becomes positive and locally asymptotically stable.*

2.2.4 Optimal Control Theory

Optimal control theory is a branch of mathematics that involves finding a piece-wise continuous control $u(t)$ and the related state variables $x(t)$ to maximize the given objective functional of the form:

$$\begin{aligned} \max_{u} \int_{t_0}^{t_f} f(t, x(t), u(t))dt, \\ \text{subject to } x'(t) = g(t, x(t), u(t)), \\ x(t_0) = x_0 \text{ and } x(t_f) \text{ is free.} \end{aligned} \tag{2.5}$$

2.2.5 Pontryagin's Maximum Principle

Pontryagin's Maximum Principle Pontryagin (2018) is used to solve optimal control problem and must satisfy the following necessary and sufficient condition for the existence of an optimal control problem. If $u^*(t)$ and $x^*(t)$ are optimal for problem (2.5), then there exists a piece-wise differentiable adjoint variable $\lambda(t)$ such that $H(t, x(t), u(t), \lambda(t)) \leq H(t, x^*(t), u^*(t), \lambda(t))$ for all controls u at each time t where the Hamiltonian H given by:

$$\begin{aligned} H &= f(t, x(t), u(t), \lambda(t), g(t, x(t), u(t))), \text{ and} \\ \lambda'(t) &= \frac{\partial H(t, x^*(t), u^*(t), \lambda(t))}{\partial x}, \\ \lambda(t_f) &= 0. \end{aligned} \tag{2.6}$$

Algorithm 2.1 Foward-Backward Sweep Method (FBSM)

INPUT: Piecewise-constant control $u(t), t \in [t_j, t_{j+i}]$, where $j = 0, 1, ..., N-1, N$ is the number of time instants

OUTPUT: State and control optimal trajectory

while *Error in termination condition is larger than specified tolerance* **do**

-Solve $\dot{x}(t) = m(x(t), u(t), t), t \in [t_0, t_f]$, using foward RK4 with initial condition $x(t_0) = x_0$ and control vector $u(t)$.

-Solve $\dot{p}(t) = -g_x(x(t), u(t), t) - m_x(x(t), u(t), t)p(t), t \in [t_0, t_f]$, using backward RK4 with state $x(t)$, the transvesality condition $p(t_f) = 0$ and control vector $u(t)$.

-Compute the new control $u^{k+1}(t)$ by solving the characterization equation: $g_u(x(t), u(t), t) + m_u(x(t), u(t), t)p(t) = 0$.

-Compute error in terminal conditions.

Using the relative error: $\frac{||x^{k+1}-x^k||}{||x^{k+1}||} < \epsilon$ and/or $\frac{||u^{k+1}-u^k||}{||u^{k+1}||} < \epsilon$ or using absolute error. Here, k stands for the k^{th} iteration and ϵ is the tolerance level.

-Update control using a convex combination of the current and previous control.

end while

2.2.6 Numerical Solution of Optimal Control Problems

Most optimal control problems arising from engineering or biological sciences can not be solved analytically and hence numerical solutions are often sought. Solving the optimality system which comprises of the state, adjoint and optimal control, requires an iterative scheme. In this dissertation the Forward-Backward sweep method (FBSM) is presented and applied because it is the best method for solving problems arising from PMP. The method use Runge-Kutta method of order four in the integration. Any specific optimal control problem can be implemented and the algorim 2.1 summarizes the FBSM.

2.3 Mathematical models for Soil-transmitted helminths

It is critical to understand how the immune system regulates infection in individuals with exposed and chronic helminth infection, what immune traits allow some hosts to maintain low infection burdens, and how anthelminthic treatment and the resulting reduction in parasite burdens affect those protective immune traits (Babayan *et al.*, 2018).

Mathematical modeling and analysis of helminths has drawn the attention of many researchers since the first papers in understanding its transmission and the impact of control measures (Anderson &

May, 1985, 1992; Truscott *et al.*, 2016). The deterministic model used did not consider particular helminth species and results show that selective treatment can be effective in reducing worm burden per unit drug provided. Anderson and May (1985) developed a mathematical model to investigate the transmission dynamics of helminth infections including mathematical models for intestinal nematodes, models for schistosome flukes and policies for the control of helminth infection in human societies. A range of mathematical models have been developed as an extension of the model by Anderson and May framework to allow host worm burden to adopt dynamically to treatment and reinfection process (Medley *et al.*, 1993). However, none of these models have applied optimal control theory to determine the best combination of control measures and the cost effective strategy for the eradication of helminth infection.

Medley *et al.* (1993) developed a model that expressed the proportion of individuals harboring an intense infection and the distribution of helminths in the host population to achieve community treatment. The model adopted the deterministic framework by Anderson and May (1982, 1985) comprised the system describing the dynamics of parasites in the community and the distribution of parasites between hosts. Then the model was modified to the hybrid structure which may predict treatment programs in the community. However, community treatment alone can not sufficiently eradicate helminth infection in the community and the hybrid model proposed can not be extended to include other control measures. The current study propose a deterministic model that can be extended to include regular community treatment by MDA, health education, and sanitation and hygiene.

Farrell *et al.* (2018) developed two sets of soil-transmitted helminth (STH) mathematical models to test the efficacy of current and modified World Health Organization (WHO) guidelines for the control of soil-transmitted helminth infection. The findings show that current treatment guidelines should be expanded to include treatment for people of all ages. However, the proposed stochastic model does not permit the inclusion of control measures other than the repeated use of mass drug administration which is not sufficient for the eradication of helminth infection. Models for helminth show that elimination of infection from the community by the mass drug administration (MDA) alone is not achievable in some settings. Therefore, it is recommended to consider other control interventions such as water, sanitation, and hygiene (WASH) and improved health education (Pullan *et al.*, 2014). The current study proposes a deterministic model for soil-transmitted helminth which allow the application of the aforementioned control measures.

Coffeng *et al.* (2015) developed WORMSIM modeling framework for transmission and control of helminths and parameterize the model using published data. Their findings indicate that a minimum

of semi-annual preventive chemotherapy with albendazole at 90% coverage, combined with health education and/or WASH interventions, can control hookworm infection in highly endemic areas. The model did not consider the application of optimal control measures which is crucial in resources limited societies.

2.4 Mathematical models for the Inter-host co-infection of Mtb with other infectious diseases

Bhunu *et al.* (2009) developed a TB and HIV/AIDS co-infection model which considered the treatment of latent and active forms of TB and antiretroviral therapy. The analysis of the model was considered by separately analyzing the sub-models i.e TB-only model and HIV-only model and finally the full HIV-TB co-infection model.They concluded that treatment of AIDS cases resulted in a significant reduction in the number of individuals that progressed to active TB and treatment of all types of TB resulted in a delayed onset of the AIDS stage of HIV infection. Their findings suggest that only one control measure for the effective control of the HIV/AIDS and tuberculosis co-infection which is not sufficient for the eradication of the diseases. The current study considered co-infection of tuberculosis and soil-transmitted helminth to study the interaction of Mtb and helminth parasites so that pattern of control measures can be proposed with the application of optimal control.

Yakob *et al.* (2013) developed a mechanistic model of macro-parasite that demonstrated how optimal control strategy should be applied to macro-parasite co-infection. Previous studies by Anderson and May (1978) modeled the micro-parasite (e.g. virus, bacteria) using classic SIR (Susceptible Infectious Recovered) which provides an updated record on the prevalence of the infection. The studies of macro-parasite (e.g nematode, trematode) disease transmission and co-infection models have used the negative binomial function to explain the aggregation of parasites within the host population. The methodology applied does not allow the application of control measures and can not be applied in scenarios where infection rates vary temporally. In this study, deterministic models are used to allow the application of optimal control theory.

Tasman (2016) developed and analyzed an optimal control TB-HIV co-infection model that considered the treatment of anti-TB and antiretroviral for the control of TB and HIV infected individuals. They found that a combination of anti-TB and ARV treatments was the effective strategy for the control of TB-HIV infection. Moreover, the use of one control measure could reduce the infection and the use of anti-TB treatment was better than ARV treatment only for the elimination of TB-HIV co-infection in the populations which is not always the case. In this study, we propose the Mtb-helminth co-infection model that focuses on the treatment of infected individuals with the application of com-

bination of control measures and the effect of helminth infection on tuberculosis.

Okosun and Robert (2017) developed and analyzed the mathematical model for malaria and schistosomiasis in the presence of treatment. They considered three sub-populations namely the human population, the mosquito population, and the snail population which is the intermediate host for the miracidium population. The co-infection model was developed based on the assumption that susceptible individuals cannot be simultaneously infected by both pathogens at the same time. Their results revealed that prevention and effective treatment of schistosomiasis infection would assist in the effective control and eradication of malaria. The current study proposed the co-infection of Mtb and helminth infection to determine the effect of helminths on the transmission dynamics of Mtb with the application of optimal control strategies.

2.5 Mathematical models for the Intra-host co-interaction of Mtb with other infectious diseases

Mayer *et al.* (1995) developed a basic mathematical model for the interaction of the target population (viruses, parasites, bacteria, or tumor cells) with the immune response. The model was described by two ordinary differential equations that explained the single target population and the immune system. Their findings demonstrated that combining a few mechanisms and interaction rules in a simple and idealistic model can result in a wide range of immune reactions corresponding to a wide range of phenomena in different diseases or within a single disease. The current study extends the work by considering the co-interaction of two target populations (Mtb pathogen and helminth parasites) with the effectiveness of the immune system.

Kirschner (1999) developed a mathematical model for the dynamics of Mtb and HIV-1 co-infection. To investigate immune system dynamics in the presence of infection by both Mtb and HIV pathogens, the model represented the relationship between the immune system, Mtb, and HIV. Their results showed that in the presence of Mtb alone, HIV-infected individuals deteriorate the clinical picture and HIV-infected individuals activate latent TB. They further showed that the presence of infection with Mtb in the body worsens the clinical picture of HIV and infection by HIV activates Mtb. It is therefore important to consider the intra-host mathematical model of Mtb with other pathogens to examine the effects of the co-infecting pathogens. In this study, we explore the effect of the immune system in the absence of any infection and the presence of both Mtb and helminth parasites.

The study by Xiao and Bossert (2010) provides more insights on the interacting pathogens with the immune system. They proposed a mathematical model for the interaction between HIV and malaria

at the cellular level. The model comprised of three non-linear differential equations describing the interaction of the concentration of meteorites and HIV and the immune competence. Their results revealed that infection by the two pathogens among individuals depends on several factors which include immunity thresholds of the host, pathogenic factors, immunological factors, and the strengths of immunostimulation. The current study considered the an intra-host mathematical model for the interaction of the parasitic worms, Mtb and the immune system to study the dynamics of the pathogens and the resulted immune responses.

Anderson and May (1985) developed a stochastic model to investigate the transmission dynamics of human helminths and estimation of parameter values from epidemiological data.The current study propose deterministic models over stochastic model because we didn't consider any element of randomness. In addition deterministic models offers a functional way of getting adequate knowledge of the dynamics of a population when the population is sufficiently large as compared to stochastic model which is more appropriate for small population (Keeling & Rohani, 2011).

Although a lot has been done for a single epidemics infection (helminths or Mycobacterium tuberculosis) not much work has been done on helminth and mycobacterium tuberculosis co-infection. To the best of our knowledge this study will possibly be the first attempt to propose and analyze comprehensive mathematical models for helminths and Mycobacterium tuberculosis co-infection.

CHAPTER THREE

MATERIAS AND METHODS

3.1 Introduction

In this chapter we develop and analyze deterministic models of soil-transmitted helminth using non-liner differential equations.The model is later modified to include optimal control measures. The inter-host mathematical model for Helminth and Mtb co-infection was formulated by extending the basic helminth model. Epidemiological studies indicates that infection with helminths increases the susceptibility to Mtb infection. Therefore, the co-infection model was developed to capture this aspect and later optimal control was applied to determine the best strategy for the control of Helminth-Mtb infection. Finally, the intra-host mathematical model for the interaction between Mtb and helminth infection was formulated and analysed. The model was formulated by considering the two co-infecting pathogens, i.e helminth parasites , Mtb and the immune responses encountered. The goal is to figure out what happens when helminth parasites, Mtb bacteria and the host's immune system interact with the immune system.

3.2 Mathematical Model for Optimal Control of Soil-transmitted Helminth Infection

3.2.1 Model Formulation

For modeling, the total human population is divided into four sub-populations $S(t)$, $E(t)$, $I(t)$, $R(t)$. $S(t)$ represents the number of individuals who are not infected but can be infected by helminth parasites. The subclass $E(t)$ represents the number of individuals exposed to helminth infection but not infectious. The subclass $I(t)$ represents the number of individuals infected with parasitic worms. The subclass $R(t)$ represents the number of individuals recovered from helminth infection. The subclass $M(t)$ represents the parasite population in the environment. Individuals in the susceptible class contracts infection after a sufficient contact with the contaminated environment. All the newborns enter susceptible class at the rate b and are moved to the exposed class at the rate λ. Individuals in the exposed class are being re-infected as they interact with contaminated environment but remain latent for a period of $\frac{1}{\rho}$, where ρ is the progression rate from the exposed to infective class. Again we assume that an infected individual contaminate the environment at rate ϵ but do not acquire new infection, hence individuals in the infected class are moved to the recovered class as the result of

natural immunity at the rate q. Furthermore, we believe that these infected people develop a temporary immunity to the infection. As a result of the loss of immunity, individuals in the recovered class revert to the susceptible class at a rate γ.

The infected individuals contaminate the environment at the rate ϵ as they defecate outside the latrines to increase the concentration of parasitic worms in the soil. The parasitic worms in the soil infect human population at the rate,

$$\lambda = \frac{\beta M}{K + M} \tag{3.1}$$

where β is the intake rate of eggs in contaminated food or larvae that has penetrated the skin to lead the transmission of infection and K is the number(density) of the helminths at which the infection rate is half the maximum rate. The natural mortality in each human class is denoted by μ and the infectious individuals have added helminths induced death rate denoted by d. Further, we assume that the parasitic worms die naturaly at the rate μ_M. The aforementioned assumptions and explanation gives the dynamics of the helminth model as illustrated in Fig. 2. Model parameters are fully described in Table 1. The model has five non linear ordinary differential equations given by system (3.2).

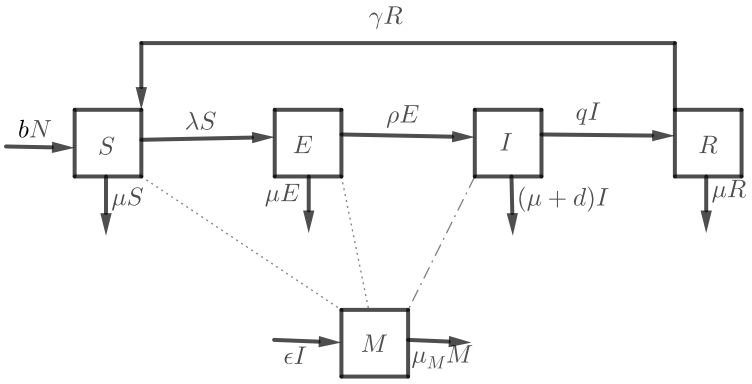

Figure 2: Compartmental diagram for the helminth model. The dashed lines indicate the interaction of human population with contaminated environment to ingest parasitic worms while the dashed line with dot indicate the rate at which individuals infected with helminths releases eggs to contaminate the environment

Table 1: Description of the model parameters

Parameters	Definition	Units
b	Per capita birth rate	Day^{-1}
μ	Per capita mortality rate	Day^{-1}
β	Ingestion rate of parasites	Day^{-1}
	or skin penetration by infective larvae	
K	Carrying Capacity of parasites in the soil	-
q	Natural recovery rate	Day^{-1}
γ	Immunity warning rate for	Day^{-1}
	recovered individuals	
d	Disease induced rate	Day^{-1}
μ_M	Clearance rate for parasitic worms	Day^{-1}
ϵ	Shading rate of parasite to the soil	Day $^{-1}$
ρ	Progression rate from exposed	Day^{-1}
	class to infective class	

$$\begin{aligned}
\frac{dS}{dt} &= bN + \gamma R - (\mu + \lambda)S, \\
\frac{dE}{dt} &= \lambda S - (\mu + \rho)E, \\
\frac{dI}{dt} &= \rho E - (d + \mu + q + \epsilon)I, \\
\frac{dR}{dt} &= qI - (\mu + \gamma)R, \\
\frac{dM}{dt} &= \epsilon I - \mu_M M,
\end{aligned} \tag{3.2}$$

with the condition $S + E + I + R = N$.

From equations (3.2) we have:

$$\frac{dN}{dt} = (b - \mu)N - (d + \epsilon)I. \tag{3.3}$$

To make our analytical analysis easier, it would be instructive to work with fractions instead of total number of populations. Hence the dynamics of the helminth model can be investigated by normalizing the model (3.2).

Let $s = \frac{S}{N}$, $e = \frac{E}{N}$, $i = \frac{I}{N}$, $r = \frac{R}{N}$ and $m = \frac{M}{K}$.

Then equation (3.3) can be written in terms of fractional variables as:

$$\frac{dN}{dt} = (b - \mu - (d + \epsilon)i)N. \tag{3.4}$$

Using equation (3.4) and differentiating the fractional variables with respect to t leads to the following normalized model:

$$\begin{aligned}
\frac{ds}{dt} &= b + \gamma r - (b + \frac{\beta m}{1+m} - (d+\epsilon)i)s, \\
\frac{de}{dt} &= \frac{\beta m}{1+m}s - (b + \rho - (d+\epsilon)i)e, \\
\frac{di}{dt} &= \rho e - (b + d + q + \epsilon - (d+\epsilon)i)i, \\
\frac{dr}{dt} &= qi - (b + \gamma - (d+\epsilon)i)r, \\
\frac{dm}{dt} &= \epsilon i - \mu_M m.
\end{aligned} \tag{3.5}$$

The solutions of the system (3.5) enter the region that is positively invariant given by:

$$\Omega = \{(s, e, i, r, m) \in \mathbb{R}^5_+ | s + e + i + r \leq 1, 0 \leq m \leq 1\}.$$

The following theorem guarantee the well posedness of the system (3.5) such that the solutions with non-negative initial conditions will remain non-negative for all future time.

Theorem 3.1

The region $\Omega \in \Re^5_+$ is positively invariant with respect to the system (3.5) and non-negative solutions exist for $t > 0$.

Proof. Given the non-negative initial conditions, it can be shown that the solutions to the system (3.5) , $s(t), e(t), i(t), r(t)$ and $m(t)$ are non-negative for $t > 0$ otherwise we assume a contradiction that there exists a first time t_0 such that $s(t_0) = 0$, $s'(t_0) \leq 0$ and $s(t) > 0$, $e(t) > 0$, $i(t) > 0$, $r(t) > 0$, $m(t) > 0$ for $0 < t < t_0$.

Consider the first equation of the system (3.5) with the aforementioned condtion, we have:

$$\frac{ds(t_0)}{dt} = b + \gamma r(t_0) - \left(b + \frac{\beta m(t_0)}{1 + m(t_0)} - (d+\epsilon)i(t_0)\right) s(t_0), \tag{3.6}$$

Then,

$$\frac{ds(t_0)}{dt} = b + \gamma r(t_0) > 0. \tag{3.7}$$

Equation (3.7) is a contradiction of the previous assumption i.e $s(t_0) = 0$ and $s(t_0) < 0$.

Therefore, it follows that for any $t > 0$: $0 < t < t_0$, we have $s(t_0) > 0$. Also, it can be shown that the remaining variables are all positive for $t > 0$.

□

Thus the helminth model is well posed epidemiologicaly and mathematically. Thus it is sufficient to consider the dynamics of (3.5) in Ω.

3.2.2 The Disease Free Equilibrium and Basic Reproduction Number

The disease free of the model (3.5) is obtained by equating all the derivatives equal to zero and then setting $e = 0$, $i = 0$, $r = 0$ and $m = 0$. Thus we obtain the DFE as:

$$\mathcal{E}_0 = (1, 0, 0, 0, 0).$$

The basic reproduction number denoted by $\mathcal{R}_0$ is the quantity that quantify the ability of the disease to invade the community and it is the quantity that governs the spread of the disease. Furthermore, it helps in deciding on control strategies to be adopted for disease eradication. Therefore, in our case $\mathcal{R}_0$ determines the role of parasitic worms/larvae present in the soil to produce secondary infections to the individual hosts.

The next generation approach is used to obtain $\mathcal{R}_0$ following (Diekmann & Heesterbeek, 2000). Using the principles of next generation matrix, let:

$$\mathcal{F} = \begin{pmatrix} \dfrac{\beta m}{1+m} s \\ 0 \\ 0 \\ 0 \end{pmatrix}$$

and

$$\mathcal{V} = \begin{pmatrix} (b + \rho - (d + \epsilon)i)e \\ (b + d + q + \tau + \epsilon - (d + \epsilon)i)i - \rho e \\ (b + \gamma - (d + \epsilon)i)r - (\tau + q)i \\ (\mu_M - \theta)m - \epsilon i \end{pmatrix}.$$

be the appearance of new infections and transfer on individuals between compartments, respectively. Applying linearization technique, the Jacobian matrices of $\mathcal{F}$ and $\mathcal{V}$ at DFE $\mathcal{E}_0$ are:

$$F = \begin{pmatrix} 0 & 0 & 0 & \beta \\ 0 & 0 & 0 & 0 \\ 0 & 0 & 0 & 0 \\ 0 & 0 & 0 & 0 \end{pmatrix} \text{ and } V = \begin{pmatrix} b + \rho & 0 & 0 & 0 \\ -\rho & b + d + q + \epsilon & 0 & 0 \\ 0 & -(\tau + q) & b + \gamma & 0 \\ 0 & -\epsilon & 0 & \mu_M \end{pmatrix}$$

Therefore:

$$FV^{-1} = \begin{pmatrix} \frac{\beta(b\rho\epsilon + \gamma\rho\epsilon)}{(b+\gamma)(b+\rho)\mu_M(b+d+q+\epsilon)} & \frac{\beta\epsilon}{\mu_M(b+d+q+\epsilon)} & 0 & \frac{\beta}{\mu_M} \\ 0 & 0 & 0 & 0 \\ 0 & 0 & 0 & 0 \\ 0 & 0 & 0 & 0 \end{pmatrix}.$$

The basic reproduction number $\mathcal{R}_0$ is the spectral radius of the next generation matrix FV^{-1}. Thus,

$$\mathcal{R}_0 = \frac{\rho\epsilon\beta}{\mu_M(b+\rho)(d+b+q+\epsilon)}. \tag{3.8}$$

It is important to unpack the basic reproduction number into components that can tell fitness and opportunities for selection i.e the duration of infectiousness, transmission per contact and number of contacts per unit time. To do this limit theory can be applied to equation (3.8) to have the fraction $\frac{\beta}{b+d+q+\epsilon}$ that represent the average number of susceptible individuals being infected during the infectious period, and the fraction $\frac{\rho}{b+\rho}$ represent the proportion of individuals that survives the latent period while $\frac{\epsilon}{\mu_M}$ represent the fraction of parasites diminish from the environment.

3.2.3 Stability of DFE

Theorem 3.2

The disease free equilibrium of the model (3.5) is LAS if $\mathcal{R}_0 < 1$ *and unstable if* $\mathcal{R}_0 > 1$.

Proof. To investigate the local stability of the DFE at $\mathcal{E}_0$ we obtain the Jacobian matrix of equation (3.5) i.e:

$$J_{\mathcal{E}_0} = \begin{pmatrix} -b & 0 & -(d+\epsilon) & \gamma & -\beta \\ 0 & -(b+\rho) & 0 & 0 & \beta \\ 0 & \rho & -(b+d+q+\epsilon) & 0 & 0 \\ 0 & 0 & q & -(b+\gamma) & 0 \\ 0 & 0 & \epsilon & 0 & -\mu_M \end{pmatrix}. \tag{3.9}$$

Clearly, $\lambda_1 = -b$ and $\lambda_2 = -(b+\gamma)$ are the first and second eigenvalues of the Jacobean matrix $J_{\mathcal{E}_0}$ which are strictly negative. The remaining three can be obtained by considering the sub matrix $J^1_{\mathcal{E}_0}$:

$$J^1_{\mathcal{E}_0} = \begin{pmatrix} -(b+\rho) & 0 & \beta \\ \rho & -(b+d+q+\epsilon) & 0 \\ 0 & \epsilon & -\mu_M \end{pmatrix}. \tag{3.10}$$

From equation (3.10), the characteristic equation is given by:

$$f(\lambda) = \lambda^3 + d_2\lambda^2 + d_1\lambda + d_0 = 0. \tag{3.11}$$

where,

$$\begin{aligned} d_2 &= 2b + d + q + \rho + \epsilon + \mu_M, \\ d_1 &= (b+\rho)(b+d+q+\epsilon) + \mu_M(2b+d+q+\rho+\epsilon), \\ d_0 &= \mu_M(b+\rho)(b+d+q+\epsilon)[1-\mathcal{R}_0]. \end{aligned} \tag{3.12}$$

Applying the Routh-Hurwitz criteria, the conditions in (3.12) $d_0 > 0$, $d_1 > 0$, $d_2 > 0$ and $d_2 d_1 > d_0$. Here $d_1 > 0$, $d_2 > 0$ and $d_0 > 0$ when $\mathcal{R}_0 < 1$, and then $d_2 d_1 > d_0$. Hence according to the Routh-Hurwitz criteria, the sub-matrix $J^1_{\mathcal{E}_0}$ has negative real parts whenever $\mathcal{R}_0 < 1$.

Thus, the DFE $\mathcal{E}_0$ is locally asymptotically stable if $\mathcal{R}_0 < 1$. □

3.2.4 Global Stability of the Disease-Free Equilibrium

For the proof of global stability we consider the Theorem developed by Chavez *et al.* (2002) and later applied by Mafuta *et al.* (2013).

To apply the theorem, system (3.5) is written in the form:

$$\begin{aligned} \frac{d\mathbf{X}}{dt} &= F(\mathbf{X}, \mathbf{Z}), \\ \frac{d\mathbf{Z}}{dt} &= G(\mathbf{X}, \mathbf{Z}), G(\mathbf{X}, 0) = 0 \end{aligned} \tag{3.13}$$

where, $\mathbf{X} = (s, r) \in \mathbb{R}^2_+$ denote the number of uninfected components (individuals) and $\mathbf{Z} = (e, i, m) \in \mathbb{R}^3_+$ denotes infected components (individuals) including the latent and infectious individuals.

The disease free equilibrium is now denoted by $\mathcal{E}_0 = (X^*, 0) = (1, 0)$.
The conditions (H1) and (H2) in the system (3.14) must be satisfied to guarantee local asymptotic stability:

$$\begin{aligned} H1: &\ \text{For } \frac{d\mathbf{X}}{dt} = F(X^*, 0), X^* \text{ is globally asymptotically stable, and} \\ H2: &\ G(\mathbf{X}, \mathbf{Z}) = A\mathbf{Z} - \widehat{G}(\mathbf{X}, \mathbf{Z}), \widehat{G}(\mathbf{X}, \mathbf{Z}) \geq 0 \text{ for} (\mathbf{X}, \mathbf{Z}) \in \Omega \end{aligned} \tag{3.14}$$

where, $A = D_{\mathbf{Z}} G(X^*, 0)$ is the Metzeler-matrix (the off-diagonal elements of A are non-negative) and Ω is the region where the model makes biological sense.
If the system (3.13) satisfy the two conditions in 3.14 then the following theorem holds.

Theorem 3.3

The disease fixed point $\mathcal{E}_0 = (X^*, 0)$ is globally asymptotically stable of the system (3.13) provided that $\mathcal{R}_0 < 1$ and that conditions H1 and H2 are satisfied.

Proof. From the system (3.5) we have:

$$F(\mathbf{X},\mathbf{Z}) = \begin{pmatrix} b+\gamma r-(b+\dfrac{\beta m}{1+m}-(d+\epsilon)i)s \\ qi-(b+\gamma-(d+\epsilon)i)r \end{pmatrix}, \tag{3.15}$$

and

$$G(\mathbf{X},\mathbf{Z}) = \begin{pmatrix} \dfrac{\beta m}{1+m}s-(b+\rho-(d+\epsilon)i)e \\ \rho e-(b+d+q+\epsilon-(d+\epsilon)i)i \\ \epsilon i-\mu_M m \end{pmatrix}, \tag{3.16}$$

Then system (3.15) can be reduced to:

$$\frac{d\mathbf{X}}{dt}\Big|_{Z=0} = \begin{pmatrix} b(1-s) \\ 0 \end{pmatrix} \tag{3.17}$$

Now, condition $H1$ is satisfied as it can be observed from the solution namely $s(t) = 1 + (s(0)-1)\,e^{-bt}$. As $t \longrightarrow \infty$, the solution $s(t) \longrightarrow 1$ implying global convergence of solution of (3.17) in Ω. Thus condition H1 is satisfied.

Let

$$A = \begin{pmatrix} -(b+\rho) & 0 & \beta \\ \rho & -(b+d+q+\epsilon) & 0 \\ 0 & \epsilon & -\mu_M \end{pmatrix},$$

Then

$$\widehat{G}(\mathbf{X},\mathbf{Z}) = \begin{pmatrix} \widehat{G_1}(\mathbf{X},\mathbf{Z}) \\ \widehat{G_2}(\mathbf{X},\mathbf{Z}) \\ \widehat{G_3}(\mathbf{X},\mathbf{Z}) \end{pmatrix} = \begin{pmatrix} \Big(1-\dfrac{s}{1+m}\Big)\beta m-(d+\epsilon)ie \\ -(d+\epsilon)i^2 \\ 0 \end{pmatrix}.$$

From above $\widehat{G}(\mathbf{X},\mathbf{Z}) \geq 0$ if and only if $d=\epsilon=0$. Thus $\mathcal{E}_0$ may not be globally asymptotically stable for some parameter values. This suggest the possibility of backward bifurcation of section 3.2.6. □

3.2.5 Existence of Endemic Equilibrium

The endemic equilibrium $\mathcal{E}^*$ of the model (3.5) is defined as the steady state solution which occurs when disease persists in the community and is obtained by equating the derivatives of the system (3.5) to zero. If we denote the force of infection as $\lambda^* = \dfrac{\beta m}{1+m}$ at steady states and let $z^* = b-(d+\epsilon)i^*$ for any choice of i^* at the endemic equilibrium, then the endemic equilibrium can be expressed in terms of the force of infection as:

$$
\begin{aligned}
s^* &= \frac{b\left(\gamma+z^*\right)\left(\rho+z^*\right)\left(d+q+z^*+\epsilon\right)}{\triangle_3+\left(z^*\right)^3\left(\lambda^*+\triangle_1\right)+\left(z^*\right)^2\left(\lambda^*\triangle_1+\rho(\gamma+\triangle_2)+\gamma\triangle_2\right)+z^*\triangle_4+\left(z^*\right)^4},\\
e^* &= \frac{b\lambda^*\left(\gamma+z^*\right)\left(\triangle_2+z^*\right)}{\left(\gamma+z^*\right)\left(\lambda^*+z^*\right)\left(\rho+z^*\right)\left(\triangle_2+z^*\right)-\gamma\lambda^*q\rho},\\
i^* &= \frac{b\lambda^*\rho\left(\gamma+z^*\right)}{\triangle_3+\left(z^*\right)^3\left(\lambda^*+\triangle_1\right)+\left(z^*\right)^2\left(\lambda^*\triangle_1+\rho(\gamma+\triangle_2)+\gamma\triangle_2\right)+z^*\triangle_4+\left(z^*\right)^4},\\
r^* &= \frac{b\lambda^*q\rho}{\triangle_3+\left(z^*\right)^3\left(\lambda^*+\triangle_1\right)+\left(z^*\right)^2\left(\lambda^*\triangle_1+\rho(\gamma+\triangle_2)+\gamma\triangle_2\right)+z^*\triangle_4+\left(z^*\right)^4},\\
m^* &= \frac{b\lambda^*\rho\epsilon\left(\gamma+z^*\right)}{\mu_M\left(\triangle_3+\left(z^*\right)^3\left(\lambda^*+\triangle_1\right)+\left(z^*\right)^2\left(\lambda^*\triangle_1+\rho(\gamma+\triangle_2)+\gamma\triangle_2\right)+z^*\triangle_4+\left(z^*\right)^4\right)}.
\end{aligned}
\tag{3.18}
$$

where,

$\triangle_1 = \gamma + d + q + \rho + \epsilon,$

$\triangle_2 = d + q + \epsilon,$

$\triangle_3 = \gamma\lambda^*\rho(d+\epsilon),$

$\triangle_4 = \left(\lambda^*(\rho(\gamma+\triangle_2)+\gamma\triangle_2)+\gamma\rho\triangle_2\right).$

Using equation five of (3.18) and the force of infection $\lambda^* = \dfrac{\beta m^*}{1+m^*}$ with the model parameters then (3.18) satisfies the following polynomial:

$$
\lambda^* P(\lambda^*) = \lambda^*(A\lambda^* + B) = 0 \tag{3.19}
$$

where,

$A = \mu_M\left(\gamma\rho(d+\epsilon)+z^*\left(\rho(\gamma+d+q+\epsilon)+\gamma(d+q+\epsilon)+z^*\left(\gamma+d+q+\rho+z^*+\epsilon\right)\right)\right),$

$B = \mu_M z^*(\gamma+z^*)(\rho+z^*)(d+q+\epsilon+z^*)(1-\mathcal{R}_0).$

In equation (3.19), $\lambda^* = 0$ corresponds to the disease free equilibrium and the polynomial $P(\lambda^*) = 0$ correspond to the existence of endemic equilibrium which co-exist with disease free equilibrium point when $\mathcal{R}_0 < 1$.

3.2.6 Bifurcation Analysis

To investigate the type of bifurcation the model (3.5) exhibits, we use the center manifold theory of Castillo-Chavez and Song (2004). To apply the center manifold theory we make the change of variables for the normalized helminth model (3.5). Let $x_1 = s$, $x_2 = e$, $x_3 = i$, $x_4 = r$ and $x_5 = m$. Using the vector notation $\mathbf{X} = (x_1, x_2, x_3, x_4, x_5)^T$, then (3.5) can be written in the form $\dfrac{d\mathbf{X}}{dt} = \mathbf{F}(x)$ with $\mathbf{F} = (f_1, f_2, f_3, f_4, f_5)^T$. If we choose $\beta = \beta^*$ as the bifurcation parameter and solving for $\mathcal{R}_0 = 1$ we have:

$$\begin{cases} f_1 &= b + \gamma x_4 - (b + \dfrac{\beta^* x_5}{1 + x_5} - (d + \epsilon)x_3)x_1, \\ f_2 &= \dfrac{\beta^* x_5}{1 + x_5} x_1 - (b + \rho - (d + \epsilon)x_3)x_2, \\ f_3 &= \rho x_2 - (b + d + q + \epsilon - (d + \epsilon)x_3)x_3, \\ f_4 &= (q + \tau)x_3 - (b + \gamma - (d + \epsilon)x_3)x_4, \\ f_5 &= \epsilon x_3 - \mu_M x_5. \end{cases} \tag{3.20}$$

where,

$$\beta^* = \frac{\mu_M(b + \rho)(d + b + q + \epsilon + \tau)}{\epsilon\rho}$$

Now, the matrix W at DFE $\mathcal{E}_0$ of the equations (3.20) is:

$$W = \begin{pmatrix} -b & 0 & -(d + \epsilon) & \gamma & -\beta \\ 0 & -(b + \rho) & 0 & 0 & \beta \\ 0 & \rho & -(b + d + q + \epsilon) & 0 & 0 \\ 0 & 0 & q & -(b + \gamma) & 0 \\ 0 & 0 & \epsilon & 0 & -\mu_M \end{pmatrix} \tag{3.21}$$

At the value $\mathcal{R}_0 = 1$, the Jacobian W has simple zero eigenvalue whose corresponding left and right eigenvectors are expressed as :

$$w_1 = \left(\frac{\mu_M \gamma q - (b + \gamma)(\mu_M(d + \epsilon) + \epsilon\beta)}{b(b + \gamma)} \right) w_3, w_2 = \frac{\beta^* \epsilon w_3}{\mu_M(b + \rho)}, w_3 = w_3 > 0 \text{ is free,}$$
$$w_4 = \frac{q w_3}{b + \gamma}, w_5 = \frac{\epsilon w_3}{\mu_M} \text{ and,}$$
$$v_1 = v_4 = 0, v_2 = \frac{\rho v_3}{b + \rho}, v_3 = v_3 > 0 \text{ is free}, v_5 = \frac{\rho\beta^* v_3}{\mu_M(b + \rho)}.$$

Using the result in Castillo-Chavez and Song (2004), we need to compute the co-efficients **a** and **b** where,

$$\begin{aligned} \mathbf{a} &= \sum_{k,i,j=1}^{5} v_k w_i w_j \frac{\partial^2 f_k}{\partial x_i \partial x_j} (\mathcal{E}_0, \beta^*), \\ \mathbf{b} &= \sum_{k,i=1}^{5} v_k w_i \frac{\partial^2 f_k}{\partial x_i \partial \beta^*} (\mathcal{E}_0, \beta^*). \end{aligned} \tag{3.22}$$

Now, evaluating the partial derivatives of the system (3.20) at $(\mathcal{E}_0, \beta^*)$ we obtain

$$\frac{\partial^2 f_1}{\partial x_1 \partial x_5} = -\beta^*, \frac{\partial^2 f_1}{\partial x_3 \partial x_1} = d + \epsilon, \frac{\partial^2 f_2}{\partial x_1 \partial x_5} = \beta^*, \frac{\partial^2 f_2}{\partial x_3 \partial x_2} = d + \epsilon,$$
$$\frac{\partial^2 f_3}{\partial x_3^2} = 2(d + \epsilon), \frac{\partial^2 f_4}{\partial x_3 \partial x_4} = d + \epsilon.$$

Furthermore,

$$\frac{\partial^2 f_1}{\partial x_5 \partial \beta^*} = -1, \frac{\partial^2 f_2}{\partial x_5 \partial \beta^*} = 1.$$

Therefore,

$$\mathbf{a} = \frac{v_3 w_3^2 \rho}{b\mu_M (b+\rho)^2 (b+\gamma)} \epsilon \beta^* a_0 + 2(d+\epsilon) v_3 w_3^2. \tag{3.23}$$

where

$a_0 = (b+\rho)[\mu_M \gamma q - (b+\gamma)(\mu_M(d+\epsilon) + \epsilon\beta^*)] + b(b+\gamma)$.

and

$$\mathbf{b} = \frac{\rho \epsilon \beta^*}{\mu_M (b+\rho)^2} v_3 w_3. \tag{3.24}$$

The coefficient **b** is positive. By Castillo-Chavez and Song (2004), the coefficient **a** decides the local dynamics of $\mathcal{E}_0$. Therefore if $a_0 < 0$ then system (3.5) will exhibit forward bifurcation and if $a_0 > 0$ it undergoes backward bifurcation.

3.2.7 Sensitivity Analysis

Numerical sensitivity analysis was done by computing sensitivity indices of basic reproduction number $\mathcal{R}_0$ which measures the model robustness to parameter values (Chitnis *et al.*, 2006). A variable's forward sensitivity index to a parameter is a ratio of the variable's relative change to the parameter's relative change.

Definition 3.1

The normalized forward sensitivity index of a variable ω that depends differentiable on a parameter ς is defined as $r_\varsigma^\omega = \dfrac{\partial \omega}{\partial \varsigma} \times \dfrac{\varsigma}{\omega}$.

From equation (3.8), we compute the sensitivity indices of each parameter involved in $\mathcal{R}_0$ using the equation $r_\varsigma^{\mathcal{R}_0} = \dfrac{\partial \mathcal{R}_0}{\partial \varsigma} \times \dfrac{\varsigma}{\mathcal{R}_0}$. For example, the sensitivity index of parameter value with respect to β is given by $r_\beta^{\mathcal{R}_0} = \dfrac{\partial \mathcal{R}_0}{\partial \beta} \times \dfrac{\beta}{\mathcal{R}_0} = 1$, and other indices are $r_\rho^{\mathcal{R}_0}$, $r_\epsilon^{\mathcal{R}_0}$, $r_{\mu_M}^{\mathcal{R}_0}$, $r_b^{\mathcal{R}_0}$, $r_d^{\mathcal{R}_0}$, $r_q^{\mathcal{R}_0}$ were obtained and evaluated using parameter values in Table 6 as illustrated in Fig. 3.

To evaluate the most sensitive parameters for the model's dynamics, a sensitivity analysis was conducted to assess the model's robustness to parameter values. Clearly β, ρ and ϵ have positive indices with most sensitive parameter being β and the least positively sensitive parameter ρ. This implies that the endemicity of the disease increases when the parameters β, ρ and ϵ are increased while keeping other parameters constant. On the other hand the parameters μ_M, b, d and q have negative indices and

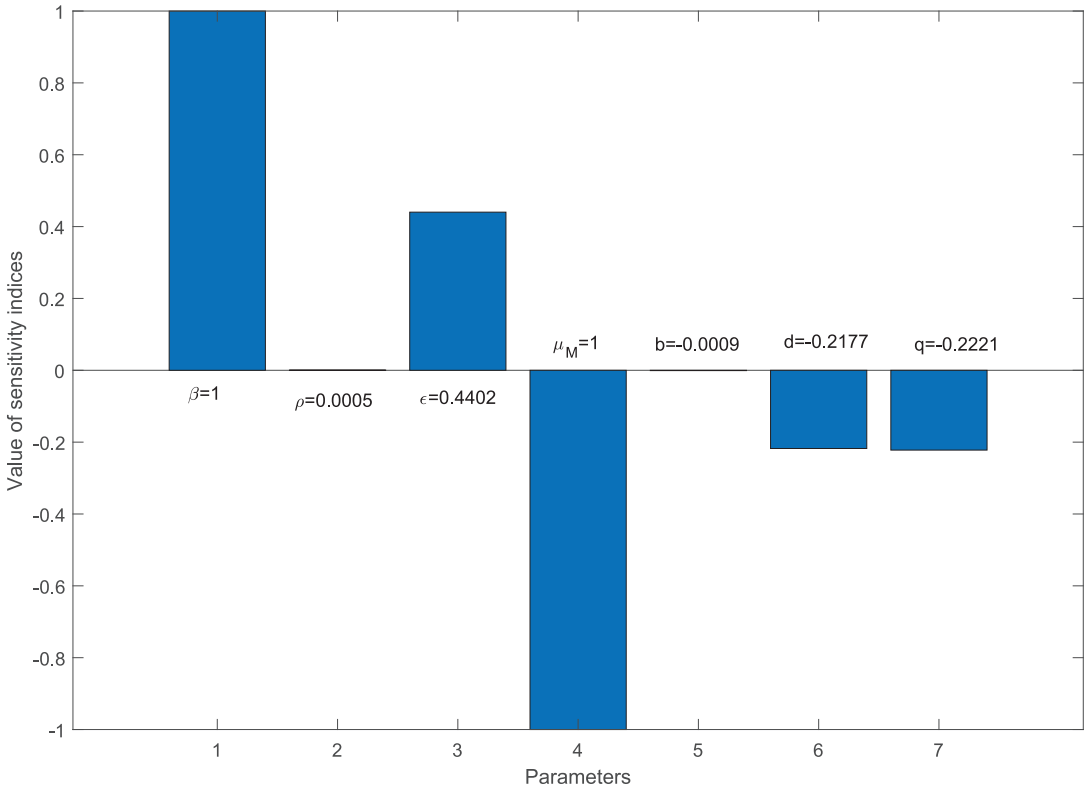

Figure 3: Sensitivity analysis of $\mathcal{R}_0$ with respect to each model parameter

when each of these are decreased while keeping the other parameters constant decreases the value of $\mathcal{R}_0$ implying that they decrease the endemicity of the disease. Thus based on these results we suggest the following interventions to be made for the control of the helminth infection from the endemic communities. The first intervention is the mass cleanliness to reduce the concentration of the parasites from contaminated environment. The other one is the use of anthelmintic drugs including MDA for both healthy and infected individuals which will in turn reduce the shedding rate of the parasite to the environment.

3.2.8 Extension of the Model to Optimal Control

In this section we extend the helminths model (3.2) by incorporating three time dependent control measures. The best intervention strategies will be identified from combination of these control measures so as to minimize the infection from the community. The optimal control model for helminth infection is formulated by considering the following controls:

(i) Health education control, $u_1(t)$ that aims to sensitize the susceptible population. This is done through provision of education materials for example through TV messages, radio, posters, and leaflets, educational messages which can be delivered by health practitioners or teachers in schools, education that improve hygiene awareness and behavior of people who defecate

outside the latrines and purchase of shoes to both pre-school aged and school aged children (Mascarini-Serra, 2011). Thus the force of infection is modified as $\lambda = \frac{(1-\kappa_1 u_1)\beta M}{K+M}$ where κ_1 is the effectiveness measure of health education control, where $\kappa_1 \in (0,1)$ such that if $\kappa_1 = 0$ then health education is not effective and $\kappa_1 = 1$ corresponds to completely effective health education, $0 < \kappa_1 < 1$ implies that health education is effective to some degree.

(ii) The use of mass drug administration (deworming) $\kappa_2 u_2(t)$, which is administered regularly without individual diagnosis is applied to the entire population (Brooker *et al.*, 2006). Application of this control moves the individuals in exposed class to the susceptible class and those in the infected class to the recovered class.

(iii) Sanitation control $(u_3(t))$ which measures the efforts to prevent susceptible from contracting the disease. This include drinking clean water, personal hygiene, avoiding eating row vegetables, cleaning of fruits and intensive cleanliness of the environment which helps to break the helminth transmission cycle (Brooker *et al.*, 2006). Thus the clearance of the parasite from the environment will be accelerated by $\mu_M + \kappa_3 u_1$, where κ_3 is the effectiveness of the control to protect susceptible population from contracting helminth infection.

After incorporating the controls and using the same parameters and variables as in (3.2), we obtain the modified model with controls for helminth infection given by:

$$\begin{aligned}
\frac{dS}{dt} &= bN + \gamma R - \mu S - (1-\kappa_1 u_1)\lambda S + \kappa_2 u_2 E,\\
\frac{dE}{dt} &= (1-\kappa_1 u_1)\lambda S - (\mu+\rho)E - \kappa_2 u_2 E,\\
\frac{dI}{dt} &= \rho E - (d+\mu+\epsilon)I - (q+\kappa_2 u_2)I,\\
\frac{dR}{dt} &= (q+\kappa_2 u_2)I - (\mu+\gamma)R,\\
\frac{dM}{dt} &= \epsilon I - (\mu_M + \kappa_3 u_3)M.
\end{aligned} \tag{3.25}$$

with $S(0) = S_0$, $E(0) = E_0$, $I(0) = I_0$, $R(0) = R_0$, $M(0) = M_0$. In this study, we assume that the control functions $u_1(t)$, $u_2(t)$, $u_3(t)$ are Lebesque integrable functions with $0 \leq u_i \leq 1$ for $i = 1, 2, 3$ to mean that when the control is zero there is no any control implemented and when the control is one there is maximum implementation of the control. The objective is to obtain the optimal levels of the control and state variables that optimize the objective functional given by:

$$J(u_1, u_2, u_3) = \int_0^{t_f} \left(A_1 I + A_2 u_2 N + \frac{1}{2}\sum_{i=1}^{3} w_i u_i^2 \right) dt. \tag{3.26}$$

Here we want to minimize the number of infected individual from the population while keeping the cost of controls low. In equation (3.26), A_1 is the relative weight of the infected individuals that accounts for the social cost while A_2u_2 is the individual cost for MDA of the entire population (pre-school and school aged children) because it is the most vulnerable population for helminth infection. Furthermore, w_i is the relative costs weight associated with background costs for each control measure u_i such as advisement costs, production of posters, ordering and transportation of drugs, water treatment and t_f is the final fixed time. In this work the cost is not linear as may result to bang bang which means that the optimal control take values at only upper and lower control set thus we choose to have quadratic cost on the control of the form $\frac{1}{2}w_iu_i^2$ [see (Joshi *et al.*, 2006)]. The problem becomes of determining the optimal triplet (u_1^*, u_2^*, u_3^*) such that:

$$J(u_1^*, u_2^*, u_3^*) = \min_{u_1,u_2,u_3 \in U} J(u_1, u_2, u_3). \tag{3.27}$$

where $U = \{(u_1, u_2, u_3)|$ each u_i is measurable with $0 \leq u_i \leq 1$ for $0 \leq t \leq t_f\}$ is the admissible set.

3.2.9 Existence of an Optimal Control

The solution of the helminth model (3.5) is proved to be bounded so we use this result to prove the existence of the optimal control. However, existence of optimal control is shown using the approach of Fleming and Richel; Mafuta *et al.* (2013) and later applied by other scholars (Mpeshe *et al.*, 2014; Mwanga *et al.*, 2015; Chuma *et al.*, 2019). For detailed proof see (Mafuta *et al.*, 2013) Theorem 4.1, p 68-69.

3.2.10 The Hamiltonian and Optimality System

To obtain the Hamiltonian H, we apply the principles of Pontryagin's Maximum Principle (Pontryagin, 2018) to derive necessary conditions for the optimal pair. Therefore, the Hamiltonian is expressed as:

$$\begin{aligned} H(S, E, I, R, M, t) = A_1I + A_2u_2N + \frac{1}{2}\sum_{i=1}^{3} w_iu_i^2 + \lambda_1\frac{dS}{dt} + \lambda_2\frac{dE}{dt} + \lambda_3\frac{dI}{dt} + \\ \lambda_4\frac{dR}{dt} + \lambda_5\frac{dM}{dt}. \end{aligned} \tag{3.28}$$

with $\lambda_i, i = 1, 2, 3, 4, 5$ denote the adjoint variables to be determined by taking the negative derivative the Hamiltnian function.

Theorem 3.4

Given the optimal set u_1, u_2, u_3 that minimizes J over U, there exist an adjoint variables

$\lambda_1, \lambda_2, \lambda_3, \lambda_4, \lambda_5$ such that:

$$\begin{aligned}
\frac{d\lambda_1}{dt} &= -A_2u_2 + \frac{(1-\kappa_1u_1)\beta M}{K+M}(\lambda_1-\lambda_2) + (\mu-b)\lambda_1,\\
\frac{d\lambda_2}{dt} &= -A_2u_2 + (\mu+\rho)\lambda_2 + \kappa_2u_2(\lambda_2-\lambda_1) - b\lambda_1 - \rho\lambda_3,\\
\frac{d\lambda_3}{dt} &= -A_1 - A_2u_2 - b\lambda_1 + (d+\mu+\epsilon)\lambda_3 + (q+\kappa_2u_2)(\lambda_3-\lambda_4) - \epsilon\lambda_5,\\
\frac{d\lambda_4}{dt} &= -A_2u_2 - (b+\gamma)\lambda_1 + (\mu+\gamma)\lambda_4,\\
\frac{d\lambda_5}{dt} &= \left(\frac{(1-\kappa_1u_1)S\beta}{K+M} - \frac{(1-\kappa_1u_1)SM\beta}{(K+M)^2}\right)(\lambda_1-\lambda_2) + (\mu_M+\kappa_3u_3)\lambda_5,
\end{aligned} \tag{3.29}$$

with transversality conditions, $\lambda_i(t_f) = 0, i = 1, 2, 3, 4, 5$. The characterization of the control set (u_1^*, u_2^*, u_3^*) using the technique of control bounds gives:

$$\begin{aligned}
u_1^*(t) &= \max\{0, \min(1, \Phi_1)\},\\
u_2^*(t) &= \max\{0, \min(1, \Phi_2)\},\\
u_3^*(t) &= \max\{0, \min(1, \Phi_3)\}.
\end{aligned}$$

where,

$$\begin{aligned}
\Phi_1 &= \frac{\kappa_1\beta MS}{w_1(K+M)}(\lambda_2-\lambda_1),\\
\Phi_2 &= \frac{\kappa_2E(\lambda_2-\lambda_1) + \kappa_2I(\lambda_3-\lambda_4)}{w_2} - \frac{A_2(S+E+I+R)}{w_2},\\
\Phi_3 &= \frac{\kappa_3M\lambda_5}{w_3}.
\end{aligned}$$

Proof. By using the Pontragian's Maximum Principle (Pontryagin, 2018) the adjoint system is the Euler-Lagrange equations obtained taking the negative of the partial derivative of the Hamiltonian in 3.28 with respect to the state variables. Thus the adjoint system can be written as:

$$\begin{aligned}
\frac{d\lambda_1}{dt} &= -\frac{\partial H}{dS} = -A_2u_2 + \frac{(1-\kappa_1u_1)\beta M}{K+M}(\lambda_1-\lambda_2) + (\mu-b)\lambda_1,\\
\frac{d\lambda_2}{dt} &= -\frac{\partial H}{dE} = -A_2u_2 + (\mu+\rho)\lambda_2 + \kappa_2u_2(\lambda_2-\lambda_1) - b\lambda_1 - \rho\lambda_3,\\
\frac{d\lambda_3}{dt} &= -\frac{\partial H}{dI} = -A_1 - A_2u_2 - b\lambda_1 + (d+\mu+\epsilon)\lambda_3 + (q+\kappa_2u_2)(\lambda_3-\lambda_4) - \epsilon\lambda_5,\\
\frac{d\lambda_4}{dt} &= -\frac{\partial H}{dR} = -A_2u_2 - (b+\gamma)\lambda_1 + (\mu+\gamma)\lambda_4,,\\
\frac{d\lambda_5}{dt} &= -\frac{\partial H}{dM} = \left(\frac{(1-\kappa_1u_1)S\beta}{K+M} - \frac{(1-\kappa_1u_1)SM\beta}{(K+M)^2}\right)(\lambda_1-\lambda_2) + (\mu_M+\kappa_3u_3)\lambda_5.
\end{aligned}$$

Using the same principle we get the controls by solving the equation obtained by taking the partial

derivative of the Hamiltonian with respect to each control.i.e:

$$\begin{aligned}
\frac{\partial H}{\partial u_1} &= w_1 u_1 + \frac{\kappa_1 \beta MS}{K+M}\lambda_1 - \frac{\kappa_1 \beta MS}{K+M}\lambda_2, \\
\frac{\partial H}{\partial u_2} &= w_2 u_2 + \kappa_2 E(\lambda_1 - \lambda_2) + \kappa_2 I(\lambda_3 - \lambda_4), \\
\frac{\partial H}{\partial u_3} &= w_3 u_3 - \kappa_3 M \lambda_5.
\end{aligned}$$

Now, setting $\dfrac{\partial H}{\partial u_i} = 0$ at u_1^* for $i = 1, 2, 3$ we obtain the controls set:

$$\begin{aligned}
u_1^*(t) &= \frac{\kappa_1 \beta MS}{w_1(K+M)}(\lambda_2 - \lambda_1), \\
u_2^*(t) &= \frac{\kappa_2 E(\lambda_2 - \lambda_1) + \kappa_2 I(\lambda_3 - \lambda_4)}{w_2} - \frac{A_2(S+E+I+R)}{w_2}, \\
u_3^*(t) &= \frac{\kappa_3 M \lambda_5}{w_3}.
\end{aligned}$$

The controls can then be written using standard control arguments with bounds on the controls as:

$$u_1^* = \begin{cases} \Phi_1 & \text{if } 0 < \Phi_1 < 1, \\ 0 & \text{if } \Phi_1 \leq 0, \\ 1 & \text{if } \Phi_1 \geq 1. \end{cases}$$

$$u_2^* = \begin{cases} \Phi_2 & \text{if } 0 < \Phi_2 < 1, \\ 0 & \text{if } \Phi_2 \leq 0, \\ 1 & \text{if } \Phi_2 \geq 1. \end{cases}$$

$$u_3^* = \begin{cases} \Phi_3 & \text{if } 0 < \Phi_3 < 1, \\ 0 & \text{if } \Phi_3 \leq 0, \\ 1 & \text{if } \Phi_3 \geq 1. \end{cases}$$

In compact notation we write,

$$\begin{aligned}
u_1^*(t) &= \max\{0, \min(1, \Phi_1)\}, \\
u_2^*(t) &= \max\{0, \min(1, \Phi_2)\}, \\
u_3^*(t) &= \max\{0, \min(1, \Phi_3)\}.
\end{aligned}$$

where,

$$\Phi_1 = \frac{\kappa_1 \beta M S}{w_1(K+M)}(\lambda_2 - \lambda_1),$$
$$\Phi_2 = \frac{\kappa_2 E(\lambda_2 - \lambda_1) + \kappa_2 I(\lambda_3 - \lambda_4)}{w_2} - \frac{A_2(S+E+I+R)}{w_2},$$
$$\Phi_3 = \frac{\kappa_3 M \lambda_5}{w_3}.$$

The optimality system consists of the state system (3.25) coupled with adjoint system (3.29) together with the characterization of the optimal control with the initial and transversality conditions. □

The state equations in 3.25 and the co-state(adjoint) equation in system (3.29) are bounded and satisfy Lipchitz condition, thus uniqueness of the optimality systems follows using the approaches by Joshi *et al.* (2006).

3.2.11 Cost-Effectiveness Analysis

Using the Incremental Cost Effective Ratio (ICER), cost effectiveness analyses were conducted to measure the cost effectiveness of various combinations of control strategies. When comparing two competing intervention methods, one is compared to the next less successful solution in this process (Okosun *et al.*, 2013; Seidu & Makinde, 2014; Mwanga *et al.*, 2015). The ICER formula is given by

$$ICER = \frac{\text{Difference in costs between strategies}}{\text{Difference in the total number of infection averted}}. \tag{3.30}$$

We sum the difference between the total number of exposed and untreated individuals without and with control to get the total number of infections averted. Also to obtain the total cost for each strategy we used the cost function as shown in Table 2.

ICER(Strategy (i)) $= \frac{7.8901\times10^5}{8.0089\times10^4} = 9.85$, ICER(Strategy (iv)) $= \frac{9.9591\times10^3 - 7.8901\times10^5}{8.0092\times10^4 - 8.0089\times10^4} = -259683.6$,

ICER(Strategy (ii)) $= \frac{1.1149\times10^4 - 9.9591\times10^3}{8.0098\times10^4 - 8.0092\times10^4} = 225.15$, ICER(Strategy (iii)) $=$

Table 2: Ranking of control strategies in ascending order of the number of infections averted

Strategy	Total infection averted	Total costs $
No strategy	0	0
Strategy (i)	8.0089×10^4	7.8901×10^5
Strategy (iv)	8.0092×10^4	9.9591×10^3
Strategy (ii)	8.0098×10^4	1.1149×10^4
Strategy (iii)	8.0176×10^4	3.3270×10^3

$\frac{3.3270\times10^3-1.1149\times10^4}{8.0176\times10^4-8.0098\times10^4} = -100.28.$

Comparing strategy (i) and (iv), strategy (i) is more costly and less effective than strategy iv. Hence, we omit strategy (i) and recompute ICER values as indicated in Table 3. From Table 3 we observe

Table 3: Computation of ICER after omitting strategy (i)

Strategy	Total infection averted	Total costs $	ICER
Strategy 4	8.0092×10^4	9.9591×10^3	-259,683.6
Strategy 2	8.0098×10^4	1.1149×10^4	225.15
Strategy 3	8.0176×10^4	3.3270×10^3	-100.28

that strategy (ii) has higher cost compared to strategy (iv), Hence we omit strategy (ii) and recompute ICER as indicated in Table 4

From table 4 we conclude that strategy (iii) (control with health education and sanitation) is more

Table 4: Computation of ICER after omitting strategy (ii)

Strategy	Total infection averted	Total costs $	ICER
Strategy 4	8.0092×10^4	9.9591×10^3	0.12
Strategy 3	8.0176×10^4	3.3270×10^3	-100.28

cost effective than strategy (iv) (control with health education, MDA and sanitation) implying that it is the cheapest of all the control strategies.

3.3 Inter-host Mathematical Model for Helminth and Mycobacterium Tuberculosis Co-infection with the application Optimal of Control Strategies

3.3.1 Model Formulation

The Helminth-Mtb infection model was formulated under the following assumptions:

(i) The susceptible individuals cannot simultaneously get infected by both diseases but rather get infected with one disease and later by the other disease.

(ii) The population is homogeneously mixed.

(iii) The incidence rate for helminth infection follows the logistic model while Mtb is assumed to be frequency dependent.

(iv) An individual get helminth infection after a sufficient contact with polluted environment.

(v) Due to the fact that Mtb infection is more severe than helminth infection, we assume that co-infected individuals seek for TB treatment rather than helminth infection.

(vi) The Bacille Calmette-Guérin (BCG) vaccine does not confer a total immunity.

The model was formulated by considering two populations namely the human population and the parasite population (M) that are present in contaminated environment. The human population is subdivided into nine classes namely: susceptible (S), the vaccinated against Mtb (V_T), those infected with Mtb but does not show clinical symptoms of TB (E_T), those with active TB (I_T), TB recovered individuals (R_T), those infected by helminths (I_H), those who have recovered from helminths (R_H) and those who are dually infected by helminths and Mtb (I_{HT}). Thus the total human population is given by $N = S+V_T+E_T+I_T+I_H+I_{HT}+R_T+R_H+R_{HT}$. The susceptible population increases by recruitment through birth at the rate $(1-\eta)bN$ and by those who lose their temporary immunity against the helminths and Mtb at rates γ_1 and γ_2 respectively. The susceptible individuals get infected with Mtb upon sufficient contact with an infectious individual with the force of infection $\lambda_T = \frac{\beta_T(I_T+\sigma I_{TH})}{N}$ where β_T is the transmission rate and $\sigma > 1$ is the modification parameter for co-infected individuals that models infectivity for susceptible individuals. The susceptible individuals also get infected by helminths after ingestion of eggs/larvae or skin penetration by infective larvae with the force of infection $\lambda_H = \frac{\beta_H M}{K+M}$ where β_H is the ingestion rate of parasitic worms and K is the density of parasites in the soil. The helminth infected individuals increase due to susceptible individuals being infected with helminths, Mtb vaccinated individuals infected with helminths and co-infected individuals who recover from Mtb at rate τ_2. Furthermore, due to the fact that BCG vaccine does not grant total protection (Nkamba *et al.*, 2019), then individuals exposed to Mtb increase due to Mtb vaccinated individuals losing their protection against Mtb and get infected at the rate $\varrho\lambda_T$, with $\varrho \in (0,1)$ such that $1-\varrho$ is the efficacy of the vaccine.

The chronic infection by helminths alter the chance of getting infection and the progression of co-infecting parasites (virus or bacteria) (Fenton, 2013) as a result, individuals infested with helminths are at higher risk of developing tuberculosis (DiNardo *et al.*, 2016). Therefore, individuals co-infected with helminth and Mtb is increased by helminth infected individuals being infected with Mtb at the force of infection $g\lambda_T$, where $g > 1$ is the modification parameter that models increased susceptibility to Mtb and Mtb exposed individuals getting infected by helminths at a force of infection λ_H. In addition, the number of individuals with active TB increases as individuals progress from the exposed class at rate k and the co-infected individuals who recover from helminth infection at the rate τ_1 and are decreased due to natural recovery at the rate τ_2. The parasite population in the

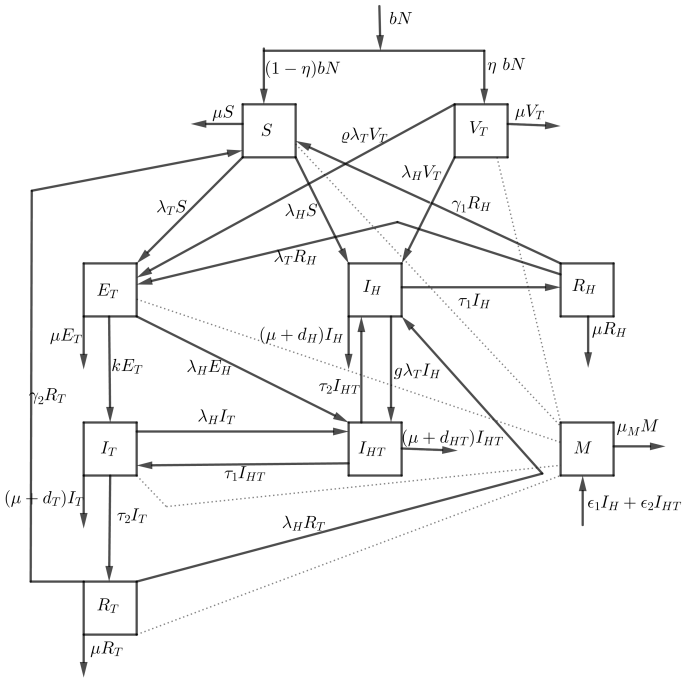

Figure 4: Compartmental diagram for the helminth and mycobactrium tuberculosis co-infection. The doted lines indicates the interaction of individuals with the polluted environment.

environment increase as they are released by the helminth infected individuals at the rate ϵ_1 and co-infected individuals at the rate ϵ_2 and are cleared from the environment at a rate μ_M. The description above is illustrated in Fig. 4 and the governing system of non-linear differential equations is as in model (3.31). The model parameters are described in Table 5.

$$
\begin{cases}
\dfrac{dS}{dt} &= (1-\eta)bN + \gamma_1 R_H + \gamma_2 R_T - (\mu + \lambda_T + \lambda_H)S, \\
\dfrac{dV_T}{dt} &= \eta bN - (\mu + \varrho\lambda_T + \lambda_H)V_T, \\
\dfrac{dE_T}{dt} &= \lambda_T S + \varrho\lambda_T V_T + \lambda_T R_H - (\mu + k + \lambda_H)E_T, \\
\dfrac{dI_T}{dt} &= kE_T + \tau_1 I_{HT} - (\mu + d_T + \tau_2 + \lambda_H)I_T, \\
\dfrac{dI_H}{dt} &= \lambda_H S + \lambda_H V_T + \lambda_H R_T + \tau_2 I_{TH} - (g\lambda_T + \mu + d_H + \tau_1 + \epsilon_1)I_H \\
\dfrac{dI_{HT}}{dt} &= g\lambda_T I_H + \lambda_H(E_T + I_T) - (\mu + d_{HT} + \tau_1 + \tau_2 + \epsilon_2)I_{HT}, \\
\dfrac{dR_T}{dt} &= \tau_2 I_T - (\lambda_H + \mu + \gamma_2)R_T, \\
\dfrac{R_H}{dt} &= \tau_1 I_H - (\lambda_T + \mu + \gamma_1)R_H, \\
\dfrac{dM}{dt} &= \epsilon_1 I_H + \epsilon_2 I_{HT} - \mu_M M.
\end{cases}
\tag{3.31}
$$

where,

$$\lambda_T = \frac{\beta_T(I_T + \sigma I_{HT})}{N}$$

and

$$\lambda_H = \frac{\beta_H M}{M + K}.$$

We reduce the model parameters in-order to simplify qualitative analysis of the model (3.31) using dimensionless version such that dimensionless variables are obtained by setting $s = \frac{S}{N}$, $v_T = \frac{V_T}{N}$, $e_T = \frac{E_T}{N}$, $i_T = \frac{I_T}{N}$, $i_H = \frac{I_H}{N}$, $i_{HT} = \frac{I_{HT}}{N}$, $r_T = \frac{R_T}{N}$, $r_H = \frac{R_H}{N}$, $r_{HT} = \frac{R_{HT}}{N}$ and $m = \frac{M}{K}$ replace the original variables S, V_T, E_T, I_T, I_H, I_{HT}, R_T, R_H, R_{HT}, M respectively in which the rate of change of the population at time t is given by:

$$\frac{dN}{dt} = (b - \mu)N + d_T I_T - (d_H + \epsilon_1)I_H - (d_{HT} + \epsilon_2)I_{HT}. \tag{3.32}$$

Upon differentiating dimensionless variables with respect to time and using equation (3.2), the system (3.31) becomes:

Table 5: Description of the model parameters

Parameters	Definition	Estimated value	Reference
b	Natural birth rate	$\frac{1}{18250}\text{day}^{-1}$	Slater *et al.* (2013)
β_T	Transmission rate for Mtb	0.42day^{-1}	Das *et al.* (2019)
μ	Natural death rate	$\frac{1}{(60 \times 365)}\text{day}^{-1}$	Mwanga *et al.* (2015)
γ_1	Loss of temporary immunity for helminth recovered individuals	$\frac{1}{70}\text{day}^{-1}$	Assumed
β_H	Ingestion rate of parasitic worms	1 parasites day^{-1}	Assumed
ϱ	Vaccine wane rate	0.7 Dimensionaless	Colditz *et al.* (1994)
τ_1	Natural recovery rate for helminth infected individuals	$\frac{1}{28}\text{day}^{-1}$	Assumed
d_H	Helminths disease induced death rate	$\frac{35}{1000}\text{day}^{-1}$	Slater *et al.* (2013)
γ_2	Loss of temporary immunity for Mtb recovered individuals	0.3day^{-1}	Yeketi *et al.* (2019)
τ_2	Natural recover rate for Mtb infected individuals	$\frac{0.2}{365}\text{day}^{-1}$	Dye *et al.* (1999)
d_T	Mtb disease induced death rate	0.08day^{-1}	Colditz *et al.* (1994)
d_{HT}	Helminths -Mtb disease induced death rate	0.08day^{-1}	Assumed
k	Progression to active TB	$\frac{0.00013}{365}\text{day}^{-1}$	Bhunu *et al.* (2008b)
μ_M	Clearance rate of parasitic worms	$\frac{13}{37500}\text{day}^{-1}$	Slater *et al.* (2013)
ϵ_1	Shading rate for helminth infected individuals	0.09day^{-1}	Assumed
K	Number of parasites in the environment	10^5 parasites	Assumed
ϵ_2	Shading rate for co-infected individuals	0.1day^{-1}	Assumed
g	Modification parameter	1.12 Dimensionless	Assumed
σ	Modification Parameter	1.5 Dimensionless	Assumed

$$
\begin{aligned}
\frac{ds}{dt} &= (1-\eta)b + \gamma_1 r_H + \gamma_2 r_T - (b + \lambda_T^* + \lambda_H^* - d_T i_T - (d_H + \epsilon_1) i_H \\
&\quad - (d_{HT} + \epsilon_2) i_{HT}) s, \\
\frac{dv_T}{dt} &= \eta b - (b + \varrho\lambda_T^* + \lambda_H^* - d_T i_T - (d_H + \epsilon_1) i_H - (d_{HT} + \epsilon_2) i_{HT}) v_T, \\
\frac{de_T}{dt} &= \lambda_T^* (s + \varrho v_T + r_H) - (b + k + \lambda_H^* - d_T i_T - (d_H + \epsilon_1) i_H - (d_{HT} + \epsilon_2) i_{HT}) e_T, \\
\frac{di_T}{dt} &= k e_T + \tau_1 i_{HT} - (b + d_T + \lambda_H^* + \tau_2 - d_T i_T - (d_H + \epsilon_1) i_H - (d_{HT} + \epsilon_2) i_{HT}) i_T, \\
\frac{di_H}{dt} &= \lambda_H^* (s + v_T + r_T) + \tau_2 i_{HT} - (b + d_H + \tau_1 + \epsilon_1 + g\lambda_T^* - d_T i_T - (d_H + \epsilon_1) i_H - \\
&\quad (d_{HT} + \epsilon_2) i_{HT}) i_H, \\
\frac{di_{HT}}{dt} &= g\lambda_T^* i_H + \lambda_H^* (e_T + i_T) - (b + \tau_1 + \tau_2 + \epsilon_2 + d_{HT} - d_T i_T - (d_H + \epsilon_1) i_H - \\
&\quad (d_{HT} + \epsilon_2) i_{HT}) i_{HT}, \\
\frac{dr_T}{dt} &= \tau_2 i_T - (b + \gamma_2 + \lambda_H^* - d_T i_T - (d_H + \epsilon_1) i_H - (d_{HT} + \epsilon_2) i_{HT}) r_T, \\
\frac{dr_H}{dt} &= \tau_1 i_H - (b + \gamma_1 + \lambda_T^* - d_T i_T - (d_H + \epsilon_1) i_H - (d_{HT} + \epsilon_2) i_{HT}) r_H, \\
\frac{dm}{dt} &= \epsilon_1 i_H + \epsilon_2 i_{HT} - \mu_M m,
\end{aligned}
\tag{3.33}
$$

subject to condition

$$
s + v_T + e_T + i_T + i_H + i_{HT} + r_T + r_H = 1. \tag{3.34}
$$

3.3.2 Helminth only Model

Before analyzing the full model (3.33), we first gain insight of the the helminth only model and Mtb only model.The helminth only model was obtained from equation (3.33) by setting $v_T = e_T = i_T = i_{HT} = r_T = \eta = 0$. Then we obtain:

$$
\begin{cases}
\frac{ds}{dt} &= b + \gamma_1 r_H - (b + \lambda_H^{**} - (d_H + \epsilon_1) i_H) s, \\
\frac{di_H}{dt} &= \lambda_H^{**} s - (b + d_H + \tau_1 + \epsilon_1 - (d_H + \epsilon_1) i_H) i_H, \\
\frac{dr_H}{dt} &= \tau_1 i_H - (b + \gamma_1 - (d_H + \epsilon_1) i_H) r_H, \\
\frac{dm}{dt} &= \epsilon_1 i_H - \mu_M m,
\end{cases}
\tag{3.35}
$$

where, $\lambda_H^{**} = \dfrac{\beta_H m}{1+m}$.

3.3.3 Positivity and Boundness of the Solution

The Helminth only model (3.35) is mathematically and epidemiologicaly well-posed in the region given by:

$$\Omega_H = \left\{(s, i_H, r_H, m) \in \mathbb{R}^3_+ \cup \mathbb{R}_+ : s + i_H + r_H \leq 1, 0 \leq m \leq 1\right\}. \tag{3.36}$$

Theorem 3.5

Supposing that the initial conditions are in Ω_H, then the system of equations for the Helminth model (3.35) has unique solution in Ω_H for $t > 0$.

3.3.4 Disease-Free Equilibrium (DFE) and Basic Reproduction Number

The disease-free equilibrium point of the helminth model (3.35) is obtained by letting the RHS of equation (3.35) to zero and evaluating at $i_H = r_H = m = 0$. Then, have $\mathcal{E}^0_H = (1, 0, 0, 0)$.

To obtain the basic reproduction number, we apply the next generation approach. From the equations:

$$\begin{aligned}
\frac{di_H}{dt} &= \lambda^{**}_H s - (b + d_H + \tau_1 + \epsilon_1 - (d_H + \epsilon_1)i_H)i_H, \\
\frac{dr_H}{dt} &= \tau_1 i_H - (b + \gamma_1 - (d_H + \epsilon_1)i_H)r_H, \\
\frac{dm}{dt} &= \epsilon_1 i_H - \mu_M m.
\end{aligned}$$

We have $p = \begin{pmatrix} \lambda^{**}_H s \\ 0 \\ 0 \end{pmatrix}$ and $q = \begin{pmatrix} (b + d_H + \tau_1 + \epsilon_1 - (d_H + \epsilon_1)i_H)i_H \\ (b + \gamma_1 - (d_H + \epsilon_1)i_H)r_H - \tau_1 i_H \\ \mu_M m - \epsilon_1 i_H \end{pmatrix}$, Then,

$$P = \begin{pmatrix} 0 & 0 & \beta_H \\ 0 & 0 & 0 \\ 0 & 0 & 0 \end{pmatrix}, Q^{-1} = \begin{pmatrix} \dfrac{\mu_M(b+\gamma_1)}{\mu_M(b+\gamma_1)(b+d_H+\epsilon_1+\tau_1)} & 0 & 0 \\ \dfrac{\tau_1}{\mu_M(b+\gamma_1)(b+d_H+\epsilon_1+\tau_1)} & \dfrac{1}{b+\gamma_1} & 0 \\ \dfrac{(b+\gamma_1)}{\mu_M(b+\gamma_1)(b+d_H+\epsilon_1+\tau_1)} & 0 & \dfrac{1}{\mu_M} \end{pmatrix},$$

$$PQ^{-1} = \begin{pmatrix} \dfrac{\beta_H \epsilon_1}{\mu_M(b+d_H+\epsilon_1+\tau_1)} & 0 & \frac{\beta_H}{\mu_M} \\ 0 & 0 & 0 \\ 0 & 0 & 0 \end{pmatrix}. \tag{3.37}$$

Therefore, we can easily note that the matrix in equation (3.37) has $\dfrac{\beta_H \epsilon_1}{\mu_M(b + d_H + \epsilon_1 + \tau_1)}$ as its spectral radius. Thus the basic reproduction number is

$$\mathcal{R}_H = \frac{\beta_H \epsilon_1}{\mu_M(b + d_H + \epsilon_1 + \tau_1)}. \tag{3.38}$$

3.3.5 Local Stability of the Disease-Free Equilibrium

Theorem 3.6

The disease free equilibrium point is locally asymptotically stable if $\mathcal{R}_H < 1$ *and unstable if* $\mathcal{R}_H > 1$.

Proof. We fist obtained the jacobean matrix at $\mathcal{E}_H^0$

$$J_H^0 = \begin{pmatrix} -b & d_H & \gamma_1 & -\beta_H \\ 0 & -(b+d_H+\tau_1+\epsilon_1) & 0 & \beta_H \\ 0 & \tau_1 & -(b+\gamma_1) & 0 \\ 0 & \epsilon_1 & 0 & -\mu_M \end{pmatrix}.$$

The characteristic polynomial of J_H^0 is given by:

$$P(x) = (b+x)(b-\gamma_1-x)(x^2+(b+d_H+\epsilon_1+\tau_1+\mu_M)x-\beta_H\epsilon_1+\mu_M(b+d_H+\epsilon_1+\tau_1)) \quad (3.39)$$

From equation (3.39), the eigenvalues of J_H^0 are $x_1 = -b < 0$, $x_2 = -(b+\gamma_1) < 0$, and

$$(x^2+(b+d_H+\epsilon_1+\tau_1+\mu_M)x + \frac{1}{\mu_M(b+d_H+\epsilon_1+\tau_1)}(1-\mathcal{R}_H) = 0. \quad (3.40)$$

Applying Routh-Hurwiz criteria on equation (3.40), it has strictly negative roots if $\mathcal{R}_H < 1$. Therefore the disease free equilibrium for the helminth only model is locally asymptotically stable if $\mathcal{R}_H < 1$ and unstable otherwise. □

3.3.6 Existance of Endemic Equilibrium

The helminth only model has endemic equilibrium which exist whenever $\mathcal{R}_H > 1$. Let $k^* = b - (d_H+\epsilon_1)i_H^*$ then solving equation (3.35) for the state variables, the endemic equilibrium in-terms of the force of infection is given by:

$$\begin{aligned}
s^* &= \frac{(\gamma_1+k^*)(d_H+k^*+\tau_1+\epsilon_1)b}{(\lambda_H)^*\left(\gamma_1(d_H+\epsilon_1)+k^*(\gamma_1+d_H+\tau_1+\epsilon_1)+(k^*)^2\right)+k^*(\gamma_1+k^*)k_1}, \\
i_H^* &= \frac{(\lambda_H)^*(\gamma_1+k^*)b}{(\lambda_H)^*\left(\gamma_1(d_H+\epsilon_1)+k^*(\gamma_1+d_H+\tau_1+\epsilon_1)+(k^*)^2\right)+k^*(\gamma_1+k^*)k_1}, \\
r_H^* &= \frac{\tau_1(\lambda_H)^*b}{\gamma_1\tau_1(\lambda_H)^*+(\gamma_1+k^*)((\lambda_H)^*+k^*)k_1}, \\
m^* &= \frac{\epsilon_1(\lambda_H)^*(\gamma_1+k^*)b}{\mu_M\left((\lambda_H)^*\left(\gamma_1(d_H+\epsilon_1)+k^*(\gamma_1+d_H+\tau_1+\epsilon_1)+(k^*)^2\right)+k^*(\gamma_1+k^*)k_1\right)}.
\end{aligned} \quad (3.41)$$

By using the force of infection $\lambda_H^{**} = \dfrac{\beta_H m^*}{1+m^*}$ and the equation (3.41),we have :

$$P(\lambda_H^{**}) = \lambda_H^{**}(A_1\lambda_H^{**}+B_1) = 0. \quad (3.42)$$

where,

$$
\begin{aligned}
k_1 &= (d_H + k^* + \tau_1 + \epsilon_1)\,, \\
A_1 &= \gamma_1(\epsilon_1(b+\mu_M) + \mu_M(d_H + k^*)) + k^*(\epsilon_1(b+\mu_M) + \mu_M(d_H + \tau_1 + k^*)) \\
B_1 &= \mu_M k^*(\gamma_1 + k^*)(d_H + \epsilon_1 + \tau_1 + k^*)(1 - \mathcal{R}_H).
\end{aligned} \tag{3.43}
$$

From equation (3.42), $\lambda_H^{**} = 0$ corresponds to the disease free equilibrium and the polynomial $P(\lambda_H^{**}) = 0$ corresponds to the endemic equilibrium point. Here we clearly observe that $A_1 > 0$ and $B_1 \geq 0$ whenever $\mathcal{R}_H < 1$ so that $\lambda_H^{**} = \frac{-B_1}{A_1} \leq 0$. Thus the helminth only model has endemic equilibrium when $R_H < 1$ which suggests the impossibility of backward bifurcation whenever $\mathcal{R}_H < 1$.

3.3.7 Mycobacterium Tuberculosis Only Model

The Mtb only model was obtained from equation (3.33) by setting $i_H = i_{HT} = r_H = m = 0$. Then we obtain:

$$
\begin{cases}
\dfrac{ds}{dt} &= (1-\eta)b + \gamma_2 r_T - (b + \lambda_T^{**} - d_T i_T)s, \\
\dfrac{dv_T}{dt} &= \eta b - (b + \varrho\lambda_T^{**} - d_T i_T)v_T, \\
\dfrac{de_T}{dt} &= \lambda_T^{**}(s + \varrho v_T) - (b + k - d_T i_T)e_T, \\
\dfrac{di_T}{dt} &= k e_T - (b + d_T + \tau_2 - d_T i_T)i_T, \\
\dfrac{dr_T}{dt} &= \tau_2 i_T - (b + \gamma_2 - d_T i_T)r_T.
\end{cases} \tag{3.44}
$$

where, $\lambda_T^{**} = \beta_T i_T$.

3.3.8 Positiviy and Boundness of the Solution

The Mtb only model (3.44) is epidemiologicaly and mathematically well posed in the region given by:

$$
\Omega_T = \{(s, v_T, e_T, i_T, r_T) \in \mathbb{R}_+^5 : s + v_T + e_T + i_T + r_T \leq 1\}. \tag{3.45}
$$

Theorem 3.7

Assuming that the initial conditions of the Mtb only model are in Ω_T, then the system of equations for the model (3.44) has unique solution for all $t > 0$.

3.3.9 Disease-Free Equilibrium (DFE) and Effective Reproduction Number

The disease free equilibrium of the Mtb only model is given by $\mathcal{E}_T^0 = (1-\eta), \eta, 0, 0, 0$. We use the principles of next generation matrix to obtain the effective reproduction number.

By considering the equations:

$$\begin{aligned}
\frac{de_T}{dt} &= \lambda_T^{**}(s + \varrho v_T) - (b + k - d_T i_T)e_T, \\
\frac{di_T}{dt} &= ke_T - (b + d_T + \tau_2 - d_T i_T)i_T, \\
\frac{dr_T}{dt} &= \tau_2 i_T - (b + \gamma_2 - d_T i_T)r_T.
\end{aligned} \tag{3.46}$$

We have:

$p_T = \begin{pmatrix} \lambda_T^{**}(s + \varrho v_{T_0}) \\ 0 \\ 0 \end{pmatrix}$ and $q_T = \begin{pmatrix} (b + k - d_T i_T)e_T \\ (b + d_T + \tau_2 - d_T i_T)i_T - ke_T \\ (b + \gamma_2 - d_T i_T)r_T - \tau_2 i_T \end{pmatrix}$, Then,

$P_T = \begin{pmatrix} 0 & \beta_T(s_0 + \varrho v_T) & 0 \\ 0 & 0 & 0 \\ 0 & 0 & 0 \end{pmatrix}$, and

$$Q_T^{-1} = \begin{pmatrix} \frac{1}{b+k} & 0 & 0 \\ \frac{k}{(b+k)(b+d_T+\tau_2)} & \frac{1}{b+d_T+\tau_2} & 0 \\ \frac{k\tau_2}{(b+k)(b+\gamma_2)(b+d_T+\tau_2)} & \frac{\tau_2}{(b+\gamma_2)(b+d_T+\tau_2)} & \frac{1}{b+\gamma_2} \end{pmatrix}$$

Therefore

$$P_T Q_T^{-1} = \begin{pmatrix} \frac{\beta_T k(s_0 + \varrho v_{T_0})}{(b+k)(b+d_T+\tau_2)} & \frac{\beta_T(s_0 + \varrho v_{T_0})}{(b+d_T+\tau_2} & 0 \\ 0 & 0 & 0 \\ 0 & 0 & 0 \end{pmatrix}. \tag{3.47}$$

Hence, the spectral radius of the next generation matrix (3.47) is $\frac{\beta_T k(s_0 + \varrho v_{T_0})}{(b+k)(b+d_T+\tau_2)}$. Thus, the effective reproduction of the Mtb only is given by

$$\mathcal{R}_T = \frac{\beta_T k(1 + (\varrho - 1)\eta)}{(b+k)(b+d_T+\tau_2)}. \tag{3.48}$$

3.3.10 Local Stability of the Disease-free Equilibrium

Theorem 3.8

The disease-free equilibrium point is locally asymptotically stable if $\mathcal{R}_T < 1$ and unstable if $\mathcal{R}_T > 1$.

Proof. We obtain the jacobean matrix at $\mathcal{E}_T^0$

$$J_T^0 = \begin{pmatrix} -b & 0 & 0 & (d_T - \beta_T)s_0 & \gamma_2 \\ 0 & -b & 0 & (d_T - \varrho\beta_T) & 0 \\ 0 & 0 & -(b+k) & \beta_T(s_0 + \varrho v_{T_0}) & 0 \\ 0 & 0 & k & -(b + d_T + \tau_2) & 0 \\ 0 & 0 & 0 & \tau_2 & -(b+\gamma_2) \end{pmatrix}. \tag{3.49}$$

It can be clearly observed that the first three eigenvalues of the jacobean matrix J_T^0 are $\lambda_{1,2} = -b < 0$ and $\lambda_3 = -(b + \gamma_2)$. The remaining two eigenvalues can be obtained from the characteristic polynomial of the block matrix $\widehat{J_T} = \begin{bmatrix} -(b+k) & \beta_T(s_0 + \varrho v_{T_0}) \\ k & -(b + d_T + \tau_2) \end{bmatrix}$. We can quickly make conclusion on the stability by obtaining the trace of matrix $\widehat{J_T}$.

Trace(tr) of $\widehat{J_T} = -(2b + k + d_T + \tau_2) < 0$. Here we only need the condition that $Det(\widehat{J_T}) > 0$ for the system (3.44) to be stable.

$Det(\widehat{J_T}) = (b+k)(b + d_T + \tau_2)[1 - \mathcal{R}_T]$ which is strictly positive whenever $\mathcal{R}_T < 1$.

Therefore the disease free equilibrium point of the Mtb only model is locally asymptotically stable if $\mathcal{R}_T < 1$ and unstable if $\mathcal{R}_T > 1$. □

3.3.11 Existence and Uniqueness of the Endemic Equilibrium

The endemic equilibrium point of the system (3.44) is given by $(s^*, v_T^*, e_T^*, i_T^*, r_T^*)$ and exists if the sub-populations is positive for future time. Let $h^* = b - d_T i_T^*$, then state variable can be obtained by equating the RHS of Eq. (3.44) equal to zero and solving to have:

$$\begin{aligned}
s^* &= \frac{b\left((1-\eta)d_T\left(\gamma_2 + h^*\right)\left(h^* + k\right)\left(h^* + \varrho\lambda_T^{**}\right) + (1-\eta)h^*\left(\gamma_2 + h^*\right)\left(h^* + k\right)\left(h^* + \tau_2\right) + h_1\right)}{\left(h^* + \varrho\lambda_T^{**}\right)\left(d_T\left(\gamma_2 + h^*\right)\left(h^* + k\right)\left(h^* + \lambda_T^{**}\right) + h^* h_2\right)}, \\
v_T^* &= \frac{b\eta}{h^* + \varrho\lambda_T^{**}}, \\
e_T^* &= \frac{b\left(\gamma_2 + h^*\right)\lambda_T^{**}\left(d_T + h^* + \tau_2\right)\left(\eta h^*(\varrho - 1) + h^* + \varrho\lambda_T^{**}\right)}{\left(h^* + \varrho\lambda_T^{**}\right)\left(d_T\left(\gamma_2 + h^*\right)\left(h^* + k\right)\left(h^* + \lambda_T^{**}\right) + h^* h_2\right)}, \\
i_T^* &= \frac{bk\left(\gamma_2 + h^*\right)\lambda_T^{**}\left(\eta h^*(\varrho - 1) + h^* + \varrho\lambda_T^{**}\right)}{\left(h^* + \varrho\lambda_T^{**}\right)\left(d_T\left(\gamma_2 + h^*\right)\left(h^* + k\right)\left(h^* + \lambda_T^{**}\right) + h^* h_2\right)}, \\
r_T^* &= \frac{bk\tau_2\lambda_T^{**}\left(\eta h^*(\varrho - 1) + h^* + \varrho\lambda_T^{**}\right)}{\left(h^* + \varrho\lambda_T^{**}\right)\left(d_T\left(\gamma_2 + h^*\right)\left(h^* + k\right)\left(h^* + \lambda_T^{**}\right) + h^* h_2\right)}.
\end{aligned} \tag{3.50}$$

Solving equation (3.50) into the equilibrium value for the force of infection λ_T^{**} we get:

$$\lambda_T^{**} g(\lambda_T^{**}) = \lambda_T^{**}(A_1 {\lambda_T}^{**2} + B_1 \lambda_T^{*} + C_1) = 0. \tag{3.51}$$

such that $\lambda_T^{**} = 0$ corresponds to the DFE and $g(\lambda_T^{**}) = 0$ corresponds to the existence of endemic equilibrium.

Where,

$h_1 = \varrho\lambda_T^{**}\left(\gamma_2\left(\tau_2\left((1-\eta)h^* + k\right) + (1-\eta)h^*\left(h^* + k\right)\right) + (1-\eta)h^*\left(h^* + k\right)\left(h^* + \tau_2\right)\right),$

$h_2 = \left(\left(\gamma_2 + h^*\right)\left(h^* + k\right)\left(h^* + \tau_2\right) + \lambda_T^{**}\left(\gamma_2\left(h^* + k + \tau_2\right) + \left(h^* + k\right)\left(h^* + \tau_2\right)\right)\right),$

$$\begin{aligned}
C_1 &= {h^*}^2(\gamma_2 + h^*)(k + h^*)(d_T + \tau_2 + h^*)(1 - \mathcal{R}_T),\\
B_1 &= h^*((1+\varrho)(k + h^*)(d_T(\gamma_2 + h^*) + h^*(\tau_2 + h^*)) + \gamma_2((1+\varrho)(k + h^*)h^*,\\
&\quad + \tau_2(k\varrho + (1+\varrho)h^*))) - bk\varrho\beta_T(\gamma_2 + h^*),\\
A_1 &= \varrho(d_T(k + h^*)(\gamma_2 + h^*) + h^*((k + h^*)(\tau_2 + h^*) + \gamma_2(k + \tau_2 + h^*))).
\end{aligned} \tag{3.52}$$

From the quadratic equation (3.51), we see that there is a unique endemic equilibrium if $A_1 > 0, B_2 < 0, C_2 = 0$ or $A_2 > 0, B_2 < 0$, $B_2^2 - 4A_2C_2 = 0$. Two equilibria occurs if $A_2 > 0$, $B_2 > 0$, $C_2 > 0$ and $B_1^2 - 4A_1C_1 > 0$.

Now from equation (3.51), the coefficient A_2 is always positive and C_2 is positive or negative if R_T is less than or greater than one. We therefore state the following result.

Lemma 3.1. *The system (3.44) has*

- *Precisely one unique endemic equilibrium if $A_2 > 0, B_2 < 0, C_2 = 0$ or $A_2 > 0, B_2 < 0$, $B_2^2 - 4A_2C_2 = 0$.*
- *Precisely two endemic equlibria if $A_2 > 0$, $B_2 > 0$, $C_2 > 0$ and $B_2^2 - 4A_2C_2 > 0$.*
- *None otherwise.*

To find the critical point where bifurcation occurs, we let the discriminant $B_2^2 - 4A_2C_2 = 0$ and express R_T in terms of other parameters to obtain:

$$R_T^c = 1 - \frac{B_2^2}{4A_1{h^*}^2(k + h^*)(\gamma_2 + h^*)(d_T + \tau_2 + h^*)}. \tag{3.53}$$

Therefore from (3.53) it is observed that backward bifurcation occurs in the range $R_T^c < R_T < 1$ [see Fig. 5].

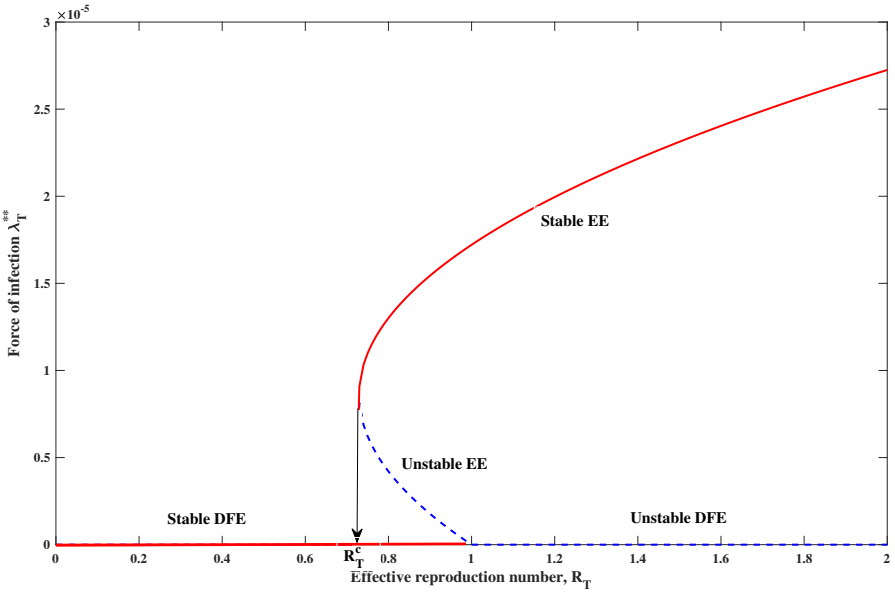

Figure 5: Backward bifurcation of the Mtb model

3.3.12 Existence of Backward Bifurcation

The backward bifurcation phenomenon can be proved by applying the center Manifold theory on the system (3.44). By adopting the center Manifold theorem of Castillo-Chavez and Song (2004), we perform bifurcation analysis by considering the transmission coefficient β_T as the bifurcation parameter if and only if $\mathcal{R}_T = 1$.

Let $\beta_T = \beta_T^* = \dfrac{(b+k)(b+d_T+\tau_2)}{k(1+(\varrho-1)\eta)}$. We make the following change of variable $s = x_1$, $v_T = x_2$, $e_T = x_3$, $i_T = x_4$, $r_T = x_5$. In addition, using the vector notation $\mathbf{x} = (x_1, x_2, x_3, x_4, x_5)^T$ then the Mtb-only model can be written in the form $\dfrac{dx}{dt} = F(\mathbf{x})$ as shown in the system (3.54).

$$\begin{aligned}
\frac{dx_1}{dt} &= f_1 = (1-\eta)b + \gamma_2 x_5 - (b + \beta_T^* x_4 - d_T x_4)x_1,\\
\frac{dx_2}{dt} &= f_2 = \eta b - (b + \varrho\beta_T^* x_4 - d_T x_4)x_2,\\
\frac{dx_3}{dt} &= f_3 = \beta_T^* x_4(x_1 + \varrho x_2) - (b + k - d_T x_4)x_3,\\
\frac{dx_4}{dt} &= f_4 = kx_3 - (b + d_T + \tau_2 - d_T x_4)x_4,\\
\frac{dx_5}{dt} &= f_5 = \tau_2 x_4 - (b + \gamma_2 - d_T x_4)x_5.
\end{aligned} \tag{3.54}$$

We then obtain the Jacobean of the system (3.54) at $\mathcal{E}_T^0$ given by:

$$J(\mathcal{E}_T^0) = \begin{pmatrix} -b & 0 & 0 & (d_T - \beta_T)s_0 & \gamma_2 \\ 0 & -b & 0 & (d_T - \varrho\beta_T) & 0 \\ 0 & 0 & -(b+k) & \beta_T(s_0 + \varrho v_{T_0}) & 0 \\ 0 & 0 & k & -(b + d_T + \tau_2) & 0 \\ 0 & 0 & 0 & \tau_2 & -(b+\gamma_2) \end{pmatrix}. \tag{3.55}$$

To apply the Center Manifold theorem, we need to calculate a and b. We begin by calculating the right and left eigenvalues of the system (3.55) denoted by $\mathbf{w}(w_1, w_2, w_3, w_4, w_5)^T$, and $\mathbf{v} = (v_1, v_2, v_3, v_4, v_5)^T$. We get

$$\begin{aligned} w_1 &= \frac{((b+\gamma_2)(d_T - \beta_T)s_0 + \gamma_2\tau_2)w_4}{b(b+\gamma_2)}, \\ w_2 &= \frac{(d_T - \varrho\beta_T^*)v_{T0}w_4}{b}, \\ w_3 &= \frac{\beta_T^*(s_0 + \varrho v_{T0})w_4}{b+k}, \\ w_4 &= w_4 > 0 \text{ is free}, \\ w_5 &= \frac{\tau_2 w_4}{b+\gamma_2}. \end{aligned} \tag{3.56}$$

and

$v_1 = v_2 = v_5 = 0$, $v_3 = \dfrac{kv_4}{b+k}$, $v_4 = v_4 > 0$ is free.

Using the aforementioned theorem the coefficients a and b are given by the expressions in equation (3.57).

$$\begin{aligned} a &= \sum_{k,i,j=1}^{5} v_k w_i w_j \frac{\partial^2 f_k}{\partial x_i \partial x_j}\left(\mathcal{E}_T^0, \beta_T^*\right), \\ b &= \sum_{k,i=1}^{5} v_k w_i \frac{\partial^2 f_k}{\partial x_i \partial \beta^*}\left(\mathcal{E}_T^0, \beta_T^*\right). \end{aligned} \tag{3.57}$$

From the system (3.55), we obtain the non-vanishing partial derivatives at $\mathcal{E}_T^0, \beta_T^*$ given by:

$$
\begin{aligned}
\frac{\partial^2 f_1}{\partial x_4 \partial x_1} &= -(\beta_T - d_T), \\
\frac{\partial^2 f_2}{\partial x_4 \partial x_2} &= -(\varrho\beta_T - d_T), \\
\frac{\partial^2 f_3}{\partial x_4 \partial x_3} &= d_T, \\
\frac{\partial^2 f_3}{\partial x_1 \partial x_4} &= \beta_T, \\
\frac{\partial^2 f_3}{\partial x_2 \partial x_4} &= \varrho\beta_T, \\
\frac{\partial^2 f_4}{\partial x_4^2} &= d_T, \\
\frac{\partial^2 f_5}{\partial x_4 \partial x_5} &= d_T.
\end{aligned} \tag{3.58}
$$

Furthermore,

$$
\begin{aligned}
\frac{\partial^2 f_1}{\partial \beta_T^* \partial x_4} &= -s_0, \\
\frac{\partial^2 f_2}{\partial \beta_T^* \partial x_4} &= -\varrho v_{T0}, \\
\frac{\partial^2 f_3}{\partial \beta_T^* \partial x_4} &= s_0 + \varrho v_{T0}.
\end{aligned} \tag{3.59}
$$

After tedious computations, it can be verified that:

$$
\begin{aligned}
a = \frac{\beta_T \left(d_T \left(\varrho(2b+k)v_T + s_0\left(2b+\gamma_2\right)\right) - \varrho(b+k)v_T\varrho\beta_T - s_0\left(b+\gamma_2\right)\beta_T + \gamma_2\tau_2\right) k v_4 w_4^2}{b(b+k)^2} \\
+ d_T v_4 w_4^2.
\end{aligned} \tag{3.60}
$$

and

$$
b = \frac{(s_0 + \varrho v_{T0})k w_4 v_4}{b+k}. \tag{3.61}
$$

The coefficient b is always positive. Hence by Castillo-Chavez and Song (2004), the coefficient a dictactes the local dynamics of $\mathcal{E}_T^0$. Thus the system (3.44) will undergo backward bifurcation if $a > 0$.

3.3.13 Analysis of the Full Model

We consider the complete Mtb-helminth co-infection model (3.33) after analyzing the dynamics of the two sub-models.

3.3.14 Disease-Free Equilibrium (DFE)

The DFE point of the system (3.33) is obtained by setting the right hand sides of the equations equal to zero with $e_T = 0$, $i_T = 0$, $i_H = 0$, $i_{HT} = 0$, $r_T = 0$, $r_H = 0$, $r_{HT} = 0$, and $m = 0$ to obtain the DFE $\mathcal{E}_0 = (1-\eta, \eta, 0, 0, 0, 0, 0, 0, 0)$.

3.3.15 Effective Reproduction Number

The principles of next-generation matrix by Van den Driessche and Watmough (2002) is used to obtain the effective reproduction number. It follows that the effective reproduction number of the Mtb-Helminth co-infection model (3.33), denoted by $\mathcal{R}_{HT}$ is given by $\mathcal{R}_{HT} = \max\{\mathcal{R}_H, \mathcal{R}_T\}$, where,

$$\mathcal{R}_H = \frac{\beta_H \epsilon_1}{\mu_M(b + d_H + \epsilon_1 + \tau_1)} \tag{3.62}$$

and

$$\mathcal{R}_T = \frac{\beta_T k(1 + \eta(\varrho - 1))}{(b + k)(b + d_T + \tau_2)} \tag{3.63}$$

corresponding to the reproduction numbers for helminth infection and Mtb transmission models obtained from sub-sections 3.3.4 and 3.3.9 respectively.

3.3.16 Local Stability of the Disease-Free Equilibrium

Theorem 3.9

The disease free equilibrium point is locally asymptotically stable if $\mathcal{R}_{HT} < 1$ *and unstable if* $\mathcal{R}_{HT} > 1$.

Proof. We first obtain the Jacobian matrix at the disease free equilibrium $\mathcal{E}_0$ in order to prove this theorem. The Jacobian Matrix is given by:

$$J_{\mathcal{E}_0} = \begin{pmatrix} -b & 0 & 0 & l_0 & -l_1 & -l_2 & \gamma_2 & \gamma_1 & -\beta_H s_0 \\ 0 & -b & 0 & (\varrho\beta_T - d_T)v_{T0} & -l_3 & -l_4 & 0 & 0 & -\beta_H v_{T0} \\ 0 & 0 & -(b+k) & \beta_T(s_0 + \varrho v_{T0}) & 0 & \beta_T\sigma(s_0 + \varrho v_{T0}) & 0 & 0 & 0 \\ 0 & 0 & k & -l_5 & 0 & \tau_1 & 0 & 0 & 0 \\ 0 & 0 & 0 & 0 & -l_6 & \tau_2 & 0 & 0 & \beta_H \\ 0 & 0 & 0 & 0 & 0 & -l_7 & 0 & 0 & 0 \\ 0 & 0 & 0 & \tau_2 & 0 & 0 & -l_8 & 0 & 0 \\ 0 & 0 & 0 & 0 & \tau_1 & 0 & 0 & -l_9 & 0 \\ 0 & 0 & 0 & 0 & \epsilon_1 & \epsilon_2 & 0 & 0 & -\mu_M \end{pmatrix}. \tag{3.64}$$

where,

$$\begin{aligned} l_0 &= (d_T - \beta_T)s_0, \\ l_1 &= (d_H + \epsilon_1)s_0, \\ l_2 &= (\sigma\beta_T - (d_{HT} + \epsilon_2))s_0, \\ l_3 &= (d_H + \epsilon_1)v_{T0}, \\ l_4 &= (\varrho\sigma\beta_T - (d_{HT} + \epsilon_2))v_{T0}, \\ l_5 &= (b + d_T + \tau_2), \\ l_6 &= (b + d_H + \tau_1), \\ l_7 &= (b + \tau_1 + \tau_2 + \epsilon_2 + d_{HT}), \\ l_8 &= (b + \gamma_2), \\ l_9 &= (b + \gamma_1). \end{aligned} \tag{3.65}$$

Now the characteristic polynomial of the Jacobian matrix $J_{\mathcal{E}_0}$ is given by:

$$\begin{aligned} p(\lambda) = (b+\lambda)^2 (b+\gamma_1+\lambda)(b+\gamma_2+\lambda)(b+d_{\text{HT}}+\tau_1+\tau_2+\lambda+\epsilon_2) \\ \left(\lambda^2 + (2b+k+d_T+\tau_2)\lambda + (b+k)(b+d_T+\tau_2)[1-\mathcal{R}_T]\right) \\ \left(\lambda^2 + (b+d_H+\epsilon_1+\mu_M+\tau_1)\lambda + \mu_M(b+d_H+\epsilon_1+\tau_1)[1-\mathcal{R}_H]\right). \end{aligned} \tag{3.66}$$

Clearly, from equation (3.66) the eigenvalues of $J_{\mathcal{E}_0}$ are as follows: $\lambda_{1,2} = -b < 0$, $\lambda_2 = -(b+\gamma_1) < 0$, $\lambda_3 = -(b+\gamma_2) < 0$, $\lambda_4 = -(b+d_{HT}+\tau_1+\tau_2+\epsilon_2) < 0$,

and

$$\begin{aligned} \left(\lambda^2 + (2b+k+d_T+\tau_2)\lambda + (b+k)(b+d_T+\tau_2)[1-\mathcal{R}_T]\right) \\ \left(\lambda^2 + (b+d_H+\epsilon_1+\mu_M+\tau_1)\lambda + \mu_M(b+d_H+\epsilon_1+\tau_1)[1-\mathcal{R}_H]\right) = 0. \end{aligned} \tag{3.67}$$

Applying Routh- Hurwitz conditions May (2019) on equation (3.5), it has strictly negative real roots if $\mathcal{R}_T < 1$ and $\mathcal{R}_H < 1$. Thus the DFE point $\mathcal{E}_0$ is locally asymptotically stable whenever $\mathcal{R}_{HT} < 1$ and unstable if either $\mathcal{R}_T > 1$ or $\mathcal{R}_H > 1$. □

3.3.17 Global Stability of Disease-Free Equilibrium

We investigate the global asymptotic stability of the disease free equilibrium of model (3.33) by using the theory applied by Castillo-Chavez *et al.* (2002). The system (3.33) is written as:

$$\begin{aligned} \frac{d\mathbf{X}}{dt} &= F(\mathbf{X}, \mathbf{Y}), \\ \frac{d\mathbf{Y}}{dt} &= G(\mathbf{X}, \mathbf{Y}), G(\mathbf{X}, 0) = 0, \end{aligned} \tag{3.68}$$

where, $\mathbf{X} = (s, v_T, r_T, r_H) \in \mathbb{R}^4_+$ represents the number of uninfected individuals and $\mathbf{Y} = (e_T, i_T, i_H, i_{HT}, m) \in \mathbb{R}^5_+$ represents the number of infected individuals including the latent and infectious individuals.

The DFE is given by $\mathcal{E}_0 = (X_0^*, 0)$, where $X_0^* = (1 - \eta, \eta)$. The conditions in equation (3.69) must be satisfied to guarantee local asymptotic:

$$\begin{aligned} \frac{d\mathbf{X}}{dt} &= F(X^*, 0), X^* \text{ is globally asmptotically stable(g.a.s) and} \\ G(\mathbf{X}, \mathbf{Y}) &= B\mathbf{Y} - \hat{G}(\mathbf{X}, \mathbf{Y}), \text{ where } \hat{G}(\mathbf{X}, \mathbf{Y}) \geq 0 \text{ for } (\mathbf{X}, \mathbf{Y}) \in \Sigma, \end{aligned} \tag{3.69}$$

and, $B = D_{\mathbf{Y}}\hat{G}(X^*, 0)$ is $M-$ matrix (That is, the off diagonal elements of matrix B are non negative), and Σ is the region where the model makes biological sense. If the equations in 3.33 satisfy the conditions in 3.69 then the following theorem holds:

Theorem 3.10

The fixed point $\mathcal{E}_0$ is globally asymptotically stable equilibrium of the system (3.33) given that $\mathcal{R}_{HT} < 1$ and that the conditions in 3.69 are fulfilled.

Proof. The system (3.33) as written in equation (3.69) can be re-written in a reduced form:

$$\frac{d\mathbf{X}}{dt}\Big|_{\mathbf{Y=0}} = \begin{pmatrix} (1-\eta)b - bs \\ \eta b - bv_T \\ 0 \end{pmatrix}. \tag{3.70}$$

Solving equation one in (3.70) gives $s(t) = (1 - \eta) + (s_0 - (1 - \eta))e^{-bt}$ implying that $s(t) \to 1 - \eta$ as $t \to \infty$. Similarly solving equation two in (3.15) gives $v_T(t) = \eta + (v_{T0} - \eta)e^{-bt}$ implying that

$v_T(t) \to \eta$ as $t \to 0$. Therefore the fist condition in 3.69 is satisfied.

Let

$$\begin{pmatrix} \hat{G}_1(\mathbf{X},\mathbf{Y}) \\ \hat{G}_2(\mathbf{X},\mathbf{Y}) \\ \hat{G}_3(\mathbf{X},\mathbf{Y}) \\ \hat{G}_4(\mathbf{X},\mathbf{Y}) \\ \hat{G}_5(\mathbf{X},\mathbf{Y}) \end{pmatrix} = \begin{pmatrix} \chi_1\lambda_T^*\left(1-\dfrac{s+\varrho v_T}{\chi_1}\right) - \lambda_T^* r_H + \lambda_H^* e_T - d_T i_T e_T - \chi_2 i_H e_T - \chi_3 i_{HT} e_T \\ \lambda_H^* i_T - d_T i_T^2 - \chi_2 i_H i_T - \chi_3 i_{HT} i_T \\ \beta_H m\left(1-\dfrac{s+v_T+r_T}{1+m}\right) + g\lambda_T^* i_H - d_T i_T i_H - \chi_2 i_H^2 - \chi_3 i_{HT} i_H \\ -g\lambda_T^* i_H - \lambda_H^*(e_T+i_T) - d_T i_T i_{HT} - \chi_2 i_H i_{HT} - \chi_3 i_{HT}^2 \\ 0 \end{pmatrix}. \tag{3.71}$$

and

$$B = \begin{pmatrix} -(b+k) & \beta_T(s_0+\varrho v_{T0}) & 0 & \beta_T\sigma(s_0+\varrho v_{T0}) & 0 \\ k & -(b+d_T+\tau_2) & 0 & \tau_1 & 0 \\ 0 & 0 & -(b+d_H+\tau_1+\epsilon_1) & \tau_2 & \beta_H \\ 0 & 0 & 0 & -\Gamma & 0 \\ 0 & 0 & \epsilon_1 & \epsilon_2 & -\mu_M \end{pmatrix}.$$

where $\chi_1 = (1+\eta(\varrho-1))$, $\chi_2 = d_H+\epsilon_1$, $\chi_3 = d_{HT}$+ϵ_3 and $\Gamma = b+\tau_1+\tau_2+\epsilon_2+d_{HT}$. From equation (3.71) we observe that $\widehat{G}_4(X,Y) < 0$ implying that the second condition in 3.69 is not fulfilled, so $\mathcal{E}_0$ may not be globally asymptotic stable. This suggests existence of multiple equlibria. □

3.3.18 The Effect of Helminth Infection on Mtb and Vice-versa

We analyze the effective reproduction number for helminth-Mtb co-infection model to determine the impact of helminth infection on Mtb by using approach by other scholars (Okosun & Robert, 2017; Tilahun *et al.*, 2018; Mushayabasa & Bhunu, 2011). This is done to determine how the rate of increase of infection by one disease affect the spread of the other disease in the community. The net effect of the co-infection and the interactions can have either positive or negative effect on each other. To analyze the effect of helminth infection on Mtb infection and vice-versa, we first express $\mathcal{R}_H$ in terms of $\mathcal{R}_T$. Then solve for b from the expression of $\mathcal{R}_T$ in equation (3.62) to get:

$$b = \frac{-\theta_1\mathcal{R}_T + \sqrt{\theta_2\mathcal{R}_T^2 + \theta_3\mathcal{R}_T}}{2\mathcal{R}_T}, \tag{3.72}$$

where $\theta_1 = k+d_T+\tau_2$, $\theta_2 = (k+d_T+\tau_2)^2 - 4k(d_T+\tau_2)$, $\theta_3 = 4\beta_T k(1+\eta(\varrho-1))$.

Then substituting b into the expression for $\mathcal{R}_H$ we get

$$\mathcal{R}_H = \frac{\beta_H \epsilon_1}{\mu_M \left(\frac{-\theta_1 R_T + \sqrt{\theta_2 R_T^2 + \theta_3 R_T}}{2R_T} + d_H + \epsilon_1 + \tau_1 \right)}. \tag{3.73}$$

Differentiating equation (3.73) partially with respect to $\mathcal{R}_T$ gives

$$\frac{\partial \mathcal{R}_H}{\partial \mathcal{R}_T} = \frac{\theta_3 \beta_H \epsilon_1 \mathcal{R}_T}{\mu_M \sqrt{\mathcal{R}_T(\theta_2 R_T + \theta_3)} \left(2\mathcal{R}_T(d_H + \epsilon_1 + \tau_1) - \theta_1 \mathcal{R}_T + \sqrt{\mathcal{R}_T(\theta_2 \mathcal{R}_T + \theta_3)} \right)^2}. \tag{3.74}$$

Now, whenever the right hand side of Eq. (3.74) is strictly positive, an increase in Mtb incidence in the society results in an increase in the incidence of helminth infection in the society.

If RHS of equation (3.74) is equal to zero, means that Mtb incidences have no influence on the spread of helminth infection.

Also, expressing b in terms of $\mathcal{R}_H$ from the expression of $\mathcal{R}_H$ in equation (3.63) we get:

$$b = \frac{\beta_H \epsilon_1 - \theta_6 \mathcal{R}_H}{\mu_M \mathcal{R}_H}, \tag{3.75}$$

where $\theta_6 = \mu_M(d_H + \tau_1)$. Then expressing $\mathcal{R}_T$ in terms of $\mathcal{R}_H$ we have

$$\mathcal{R}_T = \frac{\beta_T k(1 + \eta(\varrho - 1))\mu_M^2 \mathcal{R}_H^2}{(\beta_H \epsilon_1 + (\mu_M k - \theta_6)\mathcal{R}_H)(\beta_H \epsilon_1 + (\mu_M(d_T + \tau_2) - \theta_6)\mathcal{R}_H)} \tag{3.76}$$

Differentiating $\mathcal{R}_T$ with respect to $\mathcal{R}_H$ we get

$$\frac{\partial \mathcal{R}_T}{\partial \mathcal{R}_H} = \frac{k\epsilon_1 \mathcal{R}_H \mu_M^2 \beta_H \beta_T (1 + \eta(\varrho - 1))[\mathcal{R}_H(\mu_M(d_T + k + \tau_2) - 2\theta_6) + 2\beta_H \epsilon_1]}{(\mathcal{R}_H(k\mu_M - \theta_6) + \beta_H \epsilon_1)^2 (\mathcal{R}_H(\mu_M(d_T + \tau_2) - \theta_6) + \beta_H \epsilon_1)^2} \tag{3.77}$$

Whenever $\mu_M(d_T + k + \tau_2) \geq 2\theta_6$, then $\frac{\partial \mathcal{R}_T}{\partial \mathcal{R}_H}$ is strictly positive. This indicates that helminth infection incidence results in an increase in Mtb infection incidence in the society. Thus helminth infection enhances Mtb infection in the society.

3.3.19 Existance of Backward Bifurcation

To evaluate the endemic equilibrium's local asymptotic stability, we use the Centre Manifold Theorem, which was developed by Castillo-Chavez and Song (2004). To use the theory we make the subsequent change of variables: Let $x_1 = s$, $x_2 = v_T$, $x_3 = e_T$, $x_4 = i_T$, $x_5 = i_H$, $x_6 = i_{HT}$, $x_7 = r_T$, $x_8 = r_H$, $x_9 = m$. Then the model system (3.3) are often written within the form:

$$\frac{d\mathbf{X}}{dt} = \mathbf{F}(\mathbf{x}) = (f_1(\mathbf{x}), f_2(\mathbf{x}), f_3(\mathbf{x}), f_4(\mathbf{x}), f_5(\mathbf{x}), f_6(\mathbf{x}), f_7(\mathbf{x}), f_8(\mathbf{x}), f_9(\mathbf{x})) \tag{3.78}$$

where,

$$\begin{aligned}
\frac{dx_1}{dt} &= f_1(\mathbf{x}) = (1-\eta)b + \gamma_1 x_8 + \gamma_2 x_7 - (b + \beta_T(x_4 + \sigma x_6) - d_T x_4 - (d_H + \epsilon_1)x_5 \\
&\quad - (d_{HT} + \epsilon_2)x_6)x_1, \\
\frac{dx_2}{dt} &= f_2(\mathbf{x}) = \eta b - (b + \varrho\beta_T(x_4 + \sigma x_6) + \frac{\beta_H x_9}{1+x_9} - d_T x_4 - (d_H + \epsilon_1)x_5 - (d_{HT} + \epsilon_2)x_6)x_2, \\
\frac{dx_3}{dt} &= f_3(\mathbf{x}) = \beta_T(x_4 + \sigma x_6)(x_1 + \varrho x_2 + x_8) - (b + k + \frac{\beta_H x_9}{1+x_9} - d_T x_4 - (d_H + \epsilon_1)x_5 - \\
&\quad (d_{HT} + \epsilon_2)x_6)x_3, \\
\frac{dx_4}{dt} &= f_4(\mathbf{x}) = k x_3 + \tau_1 x_6 - (b + d_T + \tau_2 + \frac{\beta_H x_9}{1+x_9} - d_T x_4 - (d_H + \epsilon_1)x_5 - (d_{HT} + \epsilon_2)x_6)x_4, \\
\frac{dx_5}{dt} &= f_5(\mathbf{x}) = \frac{\beta_H x_9}{1+x_9}(x_1 + x_2 + x_7) + \tau_2 x_6 - (b + d_H + \tau_1 + \epsilon_1 + g\beta_T(x_4 + \sigma x_6) - d_T x_4 - \\
&\quad (d_H + \epsilon_1)x_5 - (d_{HT} + \epsilon_2)x_6)x_5, \\
\frac{dx_6}{dt} &= f_6(\mathbf{x}) = g\beta_T(x_4 + \sigma x_6)x_5 + \frac{\beta_H x_9}{1+x_9}(x_3 + x_4) - (b + \tau_1 + \tau_2 + \epsilon_2 + d_{HT} - d_T x_4 - \\
&\quad (d_H + \epsilon_1)x_5 - (d_{HT} + \epsilon_2)x_6)x_6, \\
\frac{dx_7}{dt} &= f_7(\mathbf{x}) = \tau_2 x_4 - (b + \gamma_2 + \frac{\beta_H x_9}{1+x_9} - d_T x_4 - (d_H + \epsilon_1)x_5 - (d_{HT} + \epsilon_2)x_6)x_7, \\
\frac{dx_8}{dt} &= f_8(\mathbf{x}) = \tau_1 x_5 - (b + \gamma_1 + \beta_T(x_4 + \sigma x_6) - d_T x_4 - (d_H + \epsilon_1)x_5 - (d_{HT} + \epsilon_2)x_6)x_8, \\
\frac{dx_{10}}{dt} &= f_9(\mathbf{x}) = \epsilon_1 x_5 + \epsilon_2 x_6 - \mu_M x_{10}.
\end{aligned} \tag{3.79}$$

So the Jacobian matrix of the system (3.79) at the disease-free ($\mathcal{E}_0$) is given by:

$$J_{\mathcal{E}_0} = \begin{pmatrix}
-b & 0 & 0 & J_0 & -J_1 & -J_2 & \gamma_2 & \gamma_1 & -\beta_H s_0 \\
0 & -b & 0 & (\varrho\beta_T - d_T)v_{T0} & -J_3 & -J_4 & 0 & 0 & -\beta_H v_{T0} \\
0 & 0 & -(b+k) & \beta_T^*(s_0 + \varrho v_{T0}) & 0 & \beta_T^*\sigma(s_0 + \varrho v_{T0}) & 0 & 0 & 0 \\
0 & 0 & k & -J_5 & 0 & \tau_1 & 0 & 0 & 0 \\
0 & 0 & 0 & 0 & -J_6 & \tau_2 & 0 & 0 & \beta_H \\
0 & 0 & 0 & 0 & 0 & -J_7 & 0 & 0 & 0 \\
0 & 0 & 0 & \tau_2 & 0 & 0 & -J_8 & 0 & 0 \\
0 & 0 & 0 & 0 & \tau_1 & 0 & 0 & -J_9 & 0 \\
0 & 0 & 0 & 0 & \epsilon_1 & \epsilon_2 & 0 & 0 & -\mu_M
\end{pmatrix}. \tag{3.80}$$

where,

$$
\begin{aligned}
J_0 &= (d_T - \beta_T)s_0,\\
J_1 &= (d_H + \epsilon_1)s_0,\\
J_2 &= (\sigma\beta_T - (d_{HT} + \epsilon_2))s_0,\\
J_3 &= (d_H + \epsilon_1)v_{T0},\\
J_4 &= (\varrho\sigma\beta_T^* - (d_{HT} + \epsilon_2))v_{T0},\\
J_5 &= (b + d_T + \tau_2),\\
J_6 &= (b + d_H + \tau_1),\\
J_7 &= (b + \tau_1 + \tau_2 + \epsilon_2 + d_{HT}),\\
J_8 &= (b + \gamma_2),\\
J_9 &= (b + \gamma_1).
\end{aligned}
\tag{3.81}
$$

Recall that $\mathcal{R}_{HT} = \max\{\mathcal{R}_H, \mathcal{R}_T\}$. If we consider $\mathcal{R}_{HT} = 1$ (that is $\mathcal{R}_H < \mathcal{R}_T = 1$), and let $\beta_T = \beta_T^*$ be a bifurcation parameter. Then, with $\mathcal{R}_T = 1$ gives

$$
\beta_T = \beta_T^* = \frac{(b + k)(b + d_T + \tau_2)}{k(1 + \eta(\varrho - 1))}. \tag{3.82}
$$

The Jacobian $J_{\mathcal{E}_0}$ has simple zero eigenvalue whose related right eigenvectors are denoted by $\mathbf{w} = [w_1, w_2, w_3, w_4, w_5, w_6, w_7, w_8, w_9]^T$.

where,

$$
\begin{aligned}
w_1 &= \left(\frac{J_8(d_T - \beta_T^*)s_0 + \gamma_2\tau_2}{bJ_8}\right)w_4 + \left(\frac{\mu_M\gamma_1\tau_1 - J_1J_9 - \beta_T^*\epsilon_1 s_0 J_9}{b\mu_M J_9}\right)w_5,\\
w_2 &= \frac{(\varrho\beta_T^* - d_T)v_{T0}}{b}w_4 - \frac{(\mu_M(d_H + \epsilon_1) + \beta_H\epsilon_1)}{b\mu_M}w_5,\\
w_3 &= \frac{\beta_T^*(s_0 + \varrho v_{T0})w_4}{b + k},\\
w_4 &= w_4 > 0 \text{ is free },\\
w_5 &= w_5 > 0 \text{ is free },\\
w_6 &= 0,\\
w_7 &= \frac{\tau_2 w_4}{J_8},\\
w_8 &= \frac{\tau_1 w_5}{J_9},\\
w_9 &= \frac{\epsilon_1 w_5}{\mu_M}.
\end{aligned}
\tag{3.83}
$$

The left eigenvectors of $J_{\mathcal{E}_0}$ associated with the simple eigenvalues are denoted by $\mathbf{v} = [v_1, v_2, v_3, v_4, v_5, v_6, v_7, v_8, v_9]^T$, where,

$$\begin{aligned}
&v_1 = v_2 = v_7 = v_8 = 0,\\
&v_3 = \frac{kv_4}{b+k},\\
&v_4 = v_4 > 0 \text{ is free },\\
&v_5 = v_5 > 0 \text{ is free },\\
&v_6 = \left(\frac{k\beta_T^*\sigma(s_0 + \varrho v_{T0}) + \tau_1(b+k)}{J_7(b+k)}\right) v_4 + \left(\frac{\tau_2\mu_M + \epsilon_2\beta_H}{J_7\mu_M}\right) v_5,\\
&v_9 = \frac{\beta_H v_5}{\mu_M}.
\end{aligned} \tag{3.84}$$

The coefficients a and b that decides the local dynamics of endemic equilibrium point are defined in equation (3.85) and (3.86):

$$a = \sum_{k,j,i=1}^{n} v_k w_i w_j \frac{\partial^2 f_k}{\partial x_i \partial x_j}(\mathcal{E}_0, \beta_T^*). \tag{3.85}$$

$$b = \sum_{k,i=1}^{n} v_k w_i \frac{\partial^2 f_k}{\partial x_i \partial \beta_T^*}(\mathcal{E}_0, \beta_T^*). \tag{3.86}$$

From the system (3.79), the non-zero partial derivatives of **F** related to a at DFE are given by:

$$
\begin{aligned}
\frac{\partial^2 f_1}{\partial x_4 \partial x_1} &= d_T - \beta_T^*, \\
\frac{\partial^2 f_1}{\partial x_5 \partial x_1} &= d_H + \epsilon_1, \\
\frac{\partial^2 f_1}{\partial x_6 \partial x_1} &= d_H + \epsilon_2 - \sigma\beta_T^*, \\
\frac{\partial^2 f_2}{\partial x_4 \partial x_2} &= d_T - \varrho\beta_T^*, \\
\frac{\partial^2 f_2}{\partial x_5 \partial x_2} &= d_H + \epsilon_1, \\
\frac{\partial^2 f_2}{\partial x_6 \partial x_2} &= d_{HT} + \epsilon_2 - \sigma\varrho\beta_T^*, \\
\frac{\partial^2 f_2}{\partial x_9 \partial x_2} &= -\beta_H, \\
\frac{\partial^2 f_3}{\partial x_4 \partial x_3} &= d_T, \\
\frac{\partial^2 f_3}{\partial x_5 \partial x_3} &= d_H + \epsilon_1, \\
\frac{\partial^2 f_3}{\partial x_6 \partial x_3} &= d_{HT} + \epsilon_2, \\
\frac{\partial^2 f_3}{\partial x_9 \partial x_3} &= -\beta_H, \\
\frac{\partial^2 f_3}{\partial x_4 \partial x_1} &= \beta_T, \\
\frac{\partial^2 f_3}{\partial x_6 \partial x_1} &= \sigma\beta_T, \\
\frac{\partial^2 f_3}{\partial x_4 \partial x_2} &= \varrho\beta_T, \\
\frac{\partial^2 f_3}{\partial x_6 \partial x_2} &= \varrho\sigma\beta_T, \\
\frac{\partial^2 f_3}{\partial x_4 \partial x_8} &= \beta_T, \\
\frac{\partial^2 f_3}{\partial x_6 \partial x_8} &= \sigma\beta_T, \\
\frac{\partial^2 f_4}{\partial x_4^2} &= d_T, \\
\frac{\partial^2 f_4}{\partial x_5 \partial x_4} &= d_H + \epsilon_1, \\
\frac{\partial^2 f_4}{\partial x_6 \partial x_4} &= d_{HT} + \epsilon_2, \\
\frac{\partial^2 f_4}{\partial x_9 \partial x_4} &= -\beta_H,
\end{aligned}
\tag{3.87}
$$

$$
\begin{aligned}
\frac{\partial^2 f_5}{\partial x_4 \partial x_5} &= d_T - g\beta_T^*, \\
\frac{\partial^2 f_5}{\partial x_5^2} &= d_H + \epsilon_1, \\
\frac{\partial^2 f_5}{\partial x_6 \partial x_5} &= d_{HT} + \epsilon_2 - g\sigma\beta_T^*, \\
\frac{\partial^2 f_5}{\partial x_9 \partial x_1} &= \beta_H, \\
\frac{\partial^2 f_5}{\partial x_9 \partial x_2} &= \beta_H, \\
\frac{\partial^2 f_5}{\partial x_9 \partial x_7} &= \beta_H, \\
\frac{\partial^2 f_6}{\partial x_4 \partial x_6} &= d_T, \\
\frac{\partial^2 f_6}{\partial x_5 \partial x_6} &= d_H + \epsilon_1 + g\sigma\beta_T^*, \\
\frac{\partial^2 f_6}{\partial x_6^2} &= d_{HT} + \epsilon_2, \\
\frac{\partial^2 f_6}{\partial x_4 \partial x_5} &= g\beta_T^*, \\
\frac{\partial^2 f_6}{\partial x_9 \partial x_3} &= \beta_H, \\
\frac{\partial^2 f_6}{\partial x_9 \partial x_4} &= \beta_H, \\
\frac{\partial^2 f_7}{\partial x_9 \partial x_7} &= -\beta_H, \\
\frac{\partial^2 f_7}{\partial x_4 \partial x_7} &= d_T, \\
\frac{\partial^2 f_7}{\partial x_5 \partial x_7} &= d_H + \epsilon_1, \\
\frac{\partial^2 f_7}{\partial x_6 \partial x_7} &= d_{HT} + \epsilon_2, \\
\frac{\partial^2 f_8}{\partial x_4 \partial x_8} &= d_T - \beta_T^*, \\
\frac{\partial^2 f_8}{\partial x_5 \partial x_8} &= d_H + \epsilon_1, \\
\frac{\partial^2 f_8}{\partial x_6 \partial x_8} &= d_{HT} + \epsilon_2 - \sigma\beta_T^*.
\end{aligned}
$$

Therefore equation (3.85) becomes:

$$
\begin{aligned}
a = &\left(\frac{a_0 w_4^2}{b(b+k)J_8} + \frac{a_1 w_4 w_5}{bJ\mu_M J_8 J_9 (b+k)}\right) v_3 + \left(d_T w_4^2 + \frac{(\mu_M(d_H+\epsilon_1) - \beta_H\epsilon_1)}{\mu_M} w_4 w_5\right) v_4 + \\
&\left(\frac{a_2 w_4 w_5}{bJ_8\mu_M^2} + \frac{a_3 w_5^2}{bJ_9\mu_M^2}\right) v_5 + \frac{a_4 w_4 w_5}{\mu_M(b+k)} v_6.
\end{aligned} \tag{3.88}
$$

where,

$$
\begin{aligned}
a_0 &= bd_T\beta_T^* J_8(s_0+\varrho v_{T0}) + J_8\varrho\beta_T^* v_{T0}(b+k)(\varrho\beta_T^* - d_T) + (J_8(d_T-\beta_T^*)s_0 + \gamma_2\tau_2)\sigma\beta_T^* \\
a_1 &= \beta_T^*(s_0+\varrho v_{T0})bJ_8J_9(\mu_M(d_H+\epsilon_1) - \beta_H\epsilon_1) + \beta_T^*\mu_M(b+k)(\sigma J_9(\mu_M\gamma_1\tau_1 - J_1J_8 - \\
&\quad \beta_T^*\epsilon_1 s_0 J_9) - b\tau_1 J_8) - \varrho\beta_T^* J_8 J_9 b(b+k)(\mu_M(d_H+\epsilon_1) + \beta_H\epsilon_1) \\
a_2 &= (d_T - g\beta_T^*)bJ_8\mu_M^2 + (J_8(d_T-\beta_T^*)s_0 + \gamma_2\tau_2)\epsilon_1\beta_H\mu_M + b\mu_M\epsilon_1\beta_H\tau_2 \\
a_3 &= bJ_9\mu_M^2(d_H+\epsilon_1) + \beta_H\epsilon_1(\mu_M\gamma_1\tau_1 - J_1J_9 - \beta_T^*\epsilon_1 s_0 J_9) \\
a_4 &= (\mu_M\beta_T^*(b+k) + \beta_T^*(s_0+\varrho v_{T0})\epsilon_1\beta_H + \beta_H\epsilon_1(b+k)).
\end{aligned}
\tag{3.89}
$$

To determine the sign of b, we find the subsequent non-vanishing partial derivatives of $\mathbf{F}$.

$$
\begin{aligned}
\frac{\partial^2 f_1}{\partial x_4 \partial \beta_T^*} &= -s_0, \\
\frac{\partial^2 f_1}{\partial x_6 \partial \beta_T^*} &= -\sigma s_0, \\
\frac{\partial^2 f_3}{\partial x_4 \partial \beta_T^*} &= s_0 + \varrho v_{T0}, \\
\frac{\partial^2 f_3}{\partial x_6 \partial \beta_T^*} &= \sigma(s_0 + \varrho v_{T0}).
\end{aligned}
\tag{3.90}
$$

Therefore,

$$
b = \frac{\beta_T^* k(s_0+\varrho v_{T0})^2}{(b+k)^2} w_4 v_4. \tag{3.91}
$$

Now, according to Castillo-Chavez and Song (2004), the signs of a and b dictates the local dynamics thus we have the following lemma.

Lemma 3.2. *Suppose that $b > 0$. Then we have*

(i) The system (3.33) undergoes backward bifurcation if the coefficient a is positive.

(ii) The system (3.33) will exhibit transcritical bifurcation if the coefficient a is negative.

3.3.20 Sensitivity Analysis

To evaluate the impact of each parameter on the effective reproduction number, we conduct a sensitivity analysis of the effective reproduction number subject to each parameter. Therefore we compute the forward sensitivity index of the effective reproduction number $\mathcal{R}_{HT}$ with respect to the parameters using the approach by Chitnis *et al.* (2006). Since $\mathcal{R}_{HT} = \max\{\mathcal{R}_H, \mathcal{R}_T\}$, then the sensitivity indices for $\mathcal{R}_H$ and $\mathcal{R}_T$ are computed. The normalized forward sensitivity index of a variable P with respect to parameter r is defined as $\zeta_r^P = \dfrac{r}{P}\dfrac{\partial P}{\partial r}$. For instance, the sensitivity index of $\mathcal{R}_T$ with respect to β_T is given by $\zeta_{\beta_T}^{\mathcal{R}_T} = \dfrac{\beta_T}{\mathcal{R}_T}\dfrac{\partial \mathcal{R}_T}{\partial \beta_T} = 1$, and other indices are evaluated using parameter values in Table 5. The remaining indices are given in Table 6 and Table 7.

Table 6: Sensitivity indices for reproduction number of Mtb infection $\mathcal{R}_T$

Parameter	Description	Sensitivity indices
β_T	Transmission rate for Mtb	+1.0000
k	Progression to active TB	+0.9935
η	Rate of vaccination	-0.5385
ϱ	Vaccine wane rate	+0.5385
d_T	Mtb disease induced death rate	-0.9691
τ_2	Natural recover rate for Mtb infected individuals	-0.0303

Table 7: Sensitivity indices for reproduction number of Helminth infection, $\mathcal{R}_H$

Parameter	Description	Sensitivity indices
β_H	Ingestion rate of parasitic worms	+1
ϵ_1	Shading rate for helminth infected individuals	+0.4402
μ_M	Clearance rate of parasitic worms	-1.0000
d_H	Helminths disease induced death rate	-0.2177
τ_1	Natural recovery rate for helminth infected individuals	-0.2221

From Table 6 and Table 7, the most positive parameter indices are β_T, k and β_H while the most negative parameter indices are b, d_T, and μ_M. This imply that when parameters β_T, k and β_H is increased, while the remaining are kept constant, increases the endemicity of the disease, while when the parameter μ_M is increased, the endemicity of disease is decreased. Increasing the natural birth rate and Mtb mortality rate does not make biological sense that the disease would be contained. Thus we suggest the application of optimal control to sensitive parameters such as β_H, β_T, and μ_M to study how effectively we can contain the Helminth-Mtb infection.

3.3.21 The Optimal Control Problem

In this section, the extension of the model (3.31) is formed by including four time-dependent controls so as to decide the optimal strategy for controlling the two diseases. The controls are defined as follows:

(i) Education campaign $u_1(t)$ that sensitize the parents to vaccinate more infants. Therefore the recruitment for the Mtb vaccinated individuals changes to $\eta N(1 + u_1(t))$ meaning that when this control is 100% implemented then the number of vaccinated babies doubles.

(ii) Treatment $\alpha_1 u_2(t)$ of individuals with active TB where α_1 is the drug efficacy use for Mtb infection. Therefore the Mtb recover rate changes to $\tau_2 + \alpha_1 u_2(t)$.

(iii) Deworming at a rate $\alpha_2 u_3(t)$ for the helminth infected individuals and co-infected individuals where α_2 is the drug efficacy use for the helminth infection. Therefore the helminth recover rate changes to $\tau_1 + \alpha_2 u_3(t)$.

(iv) Sanitation and proper hygiene u_4 that reduces the ingestion rate of parasites. Therefore the force of infection for the helminth infection is changed to $\lambda_H = \dfrac{(1-u_4)\beta_H M}{K+M}$.

After incorporating the controls $u_1(t)$, $u_2(t)$, $u_3(t)$, and $u_4(t)$ in the Mtb-helminth infection model (3.31), then the optimal control model becomes:

$$\begin{cases} \dfrac{dS}{dt} &= (1-\eta)bN + \gamma_1 R_H + \gamma_2 R_T - (\mu + \lambda_T + (1-u_4)\lambda_H)S, \\ \dfrac{dV_T}{dt} &= \eta b(1+u_1)N - (\mu + \varrho\lambda_T + (1-u_4)\lambda_H)V_T, \\ \dfrac{dE_T}{dt} &= \lambda_T S + \varrho\lambda_T V_T + \lambda_T R_H - (\mu + k + (1-u_4)\lambda_H)E_T, \\ \dfrac{dI_T}{dt} &= kE_T + (\tau_1 + \alpha_2 u_3)I_{HT} - (\mu + d_T + \tau_2 + (1-u_4)\lambda_H)I_T - (\tau_2 + \alpha_1 u_2)I_T, \\ \dfrac{dI_H}{dt} &= (1-u_4)\lambda_H S + (1-u_4)\lambda_H V_T + (1-u_4)\lambda_H R_T + \tau_2 I_{TH} - (g\lambda_T + \mu + d_H + \epsilon_1)I_H \\ &\quad -(\tau_1 + \alpha_2 u_3)I_H, \\ \dfrac{dI_{HT}}{dt} &= g\lambda_T I_H + (1-u_4)\lambda_H(E_T + I_T) - (\mu + d_{HT} + \tau_2 + \epsilon_2)I_{HT} - (\tau_1 + \alpha_2 u_3)I_{HT}, \\ \dfrac{dR_T}{dt} &= (\tau_2 + \alpha_1 u_2)I_T - ((1-u_4)\lambda_H + \mu + \gamma_2)R_T, \\ \dfrac{R_H}{dt} &= (\tau_1 + \alpha_2 u_3)I_H - (\lambda_T + \mu + \gamma_1)R_H, \\ \dfrac{dM}{dt} &= \epsilon_1 I_H + \epsilon_2 I_{HT} - \mu_M M. \end{cases} \tag{3.92}$$

We employ Pontryagin's Maximum Principle to figure out the required conditions for the optimal control of Helminth-Mtb co-infection. The control set U is Lebesgue measurable and is defined as $U = \{u_1(t), u_2(t), u_3(t), u_4(t) : 0 \leq u_i(t) \leq 1, 0 < t \leq t_f\}$. Then objective is to minimize individuals with active TB, individuals infested with helminth parasites and co-infected individuals while keeping the cost low. For this problem, we consider the objective functional defined by:

$$J = \int_{t_0}^{t_f} \{C_1 I_T + C_2 I_H + C_3 I_{HT} + \frac{1}{2}\sum_{i=1}^{4} w_i u_i^2\} dt. \tag{3.93}$$

where, C_1I_T, C_2I_H, C_3I_{HT} are the costs related to active tuberculosis individuals, infected with helminths individuals, and co-infected individuals respectively. The expression $\frac{1}{2}w_iu_i^2$ is related to the background costs with relative cost weights w_i for every control measure. The quadratic cost is tailored as utilized in other models with controls (Makinde & Okosun, 2011; Mwanga *et al.*, 2015). The particular value of the weights require intensive data processing, hence we elect estimate values for theoretical purposes.

The aim is to minimize the objective functional J as defined in 3.93 subject to model equations (3.92). Therefore we seek to get the optimal controls u_1^*, u_2^*, u_3^*, u_4^* such that:

$$J(u_1^*, u_2^*, u_3^*, u_4^*) = \min_{u_1,u_2,u_3,u_4 \in U} J(u_1, u_2, u_3, u_4) \tag{3.94}$$

where $U = \{(u_1, u_2, u_3, u_4)$ and therefore the controls u_1, u_2, u_3, u_4 are measurable with $0 \leq u_1 \leq 1, 0 \leq u_2 \leq 1, 0 \leq u_3 \leq 1$ and $0 \leq u_4 \leq 1$ for $t \in [t_0 \ \ t_f]\}$.

Theorem 3.11

Consider the control problem with the system of equations in 3.92. There exist $\boldsymbol{u}^* = (u_1^*, u_2^*, u_3^*, u_4^*) \in U$ *such that*

$$\min_{u_1,u_2,u_3,u_4 \in U} J(u_1, u_2, u_3, u_4,) = J(u_1^*, u_2^*, u_3^*, u_4^*).$$

The necessary conditions that an optimal solutions must satisfy is derived from Pontryagin Maximum Principle (Pontryagin, 2018). The principle converts equations (3.92)-(3.93) into the problem of minimizing the pointwise a Hamiltonian H, with reference to u_1, u_2, u_3, u_4. The Hamiltonian is given by:

$$\begin{aligned} H = {} & C_1I_T + C_2I_H + C_3I_{HT} + \frac{1}{2}(w_1u_1^2 + w_2u_2^2 + w_3u_3^2 + w_4u_4^2) + \lambda_S\{(1-\eta)bN + \\ & \gamma_1R_H + \gamma_2R_T - (\mu + \lambda_T + (1-u_4)\lambda_H)S\} + \lambda_{V_T}\{\eta b(1+u_1)N - (\mu + \varrho\lambda_T + (1-u_4) \\ & \lambda_H)V_T\} + \lambda_{E_T}\{\lambda_T S + \varrho\lambda_T V_T + \lambda_T R_H - (\mu + k + (1-u_4)\lambda_H)E_T + \lambda_{I_T}\{kE_T + (\tau_1 + \\ & \alpha_2u_3)I_{HT} - (\mu + d_T + (1-u_4)\lambda_H)I_T - (\tau_2 + \alpha_1u_2)I_T\} + \lambda_{I_H}\{(1-u_4)\lambda_H(S + V_T + R_T) \\ & + \tau_2I_{TH} - (\mu + d_H + \epsilon_1 + g\lambda_T)I_H - (\tau_1 + \alpha_2u_3)I_H\} + \lambda_{I_{HT}}\{g\lambda_T I_H + (1-u_4)\lambda_H(E_T + I_T) \\ & - (\mu + d_{HT} + \tau_2 + \epsilon_2)I_{HT} - (\tau_1 + \alpha_2u_3)I_{HT}\} + \lambda_{R_T}\{(\tau_2 + \alpha_1u_2)I_T - (\lambda_H + \mu + \gamma_2)R_T\} + \\ & \lambda_{R_H}\{(\tau_1 + \alpha_2u_3)I_H - (\lambda_T + \mu + \gamma_1)R_H\} + \lambda_M\{\epsilon_1I_H + \epsilon_2I_{HT} - \mu_M M\}. \end{aligned} \tag{3.95}$$

where λ_S, λ_{V_T}, λ_{E_T}, λ_{I_T}, λ_{I_H}, $\lambda_{I_{HT}}$, λ_{R_T}, λ_{R_H} and λ_M are the co-state variables or the adjoint variables. Now applying Pontryagin's Principle Pontryagin (2018) the problem has solution following the results of optimal control problem by Fleming and Rishel (2012).

Theorem 3.12

Given the optimal control u_i, for $i = 1, 2, 3, 4$ and the solution S, V_T, E_T, I_T, I_H, I_{HT}, R_T, R_H and M, the state system (3.92)-(3.93) that minimize $J(u_1, u_2, u_3, u_4)$ over U, there exists adjoint variables λ_S, λ_{V_T}, λ_{E_T}, λ_{I_T}, λ_{I_H}, $\lambda_{I_{HT}}$, λ_{R_T}, λ_{R_H} and λ_M satisfying

$$-\frac{d\lambda_i}{dt} = \frac{\partial H}{\partial x_i} \tag{3.96}$$

where $x_i = S, V_T, I_T, I_H, I_{HT}, R_T, R_H, M$ with transvesality conditions $\lambda_S(t_f) = \lambda_{V_T}(t_f) = \lambda_{E_T}(t_f) = \lambda_{I_T}(t_f) = \lambda_{I_H}(t_f) = \lambda_{I_{HT}}(t_f) = \lambda_{R_T}(t_f) = \lambda_{R_H}(t_f) = \lambda_M(t_f) = 0$
and the subsequent characterization holds on the interior of the control set U

$$\begin{aligned}
u_1^* &= \max\Big\{0, \min\Big\{1, -\frac{\eta b N \lambda_{V_T}}{w_1}\Big\}\Big\},\\
u_2^* &= \max\Big\{0, \min\Big\{1, \frac{\alpha_1 I_T(\lambda_{I_T} - \lambda_{R_T})}{w_2}\Big\}\Big\},\\
u_3^* &= \max\Big\{0, \min\Big\{1, \frac{\alpha_2 I_H(\lambda_{I_H} - \lambda_{R_H}) + \alpha_2 I_{HT}(\lambda_{I_{HT}} - \lambda_{I_T})}{w_3}\Big\}\Big\},\\
u_4^* &= \max\Big\{0, \min\Big\{1, \frac{\lambda_H \lambda_{I_H}(S + V_T + R_T) + \lambda_H \lambda_{I_{HT}}(E_T + I_T)}{w_4} -\\
&\qquad \frac{\lambda_H(S\lambda_S + V_T\lambda_{V_T} + E_T\lambda_{E_T} + I_T\lambda_{I_T})}{w_4}\Big\}\Big\}.
\end{aligned} \tag{3.97}$$

Proof. Fleming and Rishel (2012) provides the existence of an optimal control model (3.92) and the costate variables (3.96) due to boundness of state equations and the Lipschiz structure of the ordinary differential equations. Therefore applying the necessary conditions from Pontryagin Maximum Principle, we obtain the following system for costate variables:

$$\begin{aligned}
\frac{d\lambda_S}{dt} &= -(1-\eta)b\lambda_S + \frac{\beta_T(I_T + \sigma I_{HT})S}{N^2}(\lambda_{E_T} - \lambda_S) + \frac{\beta_T(I_T + \sigma I_{HT})V_T}{N^2}(\varrho\lambda_{E_T} - \lambda_{V_T})\\
&\quad - \eta b(1+u_1)\lambda_{V_T} + \frac{\beta_T(I_T + \sigma I_{HT})R_H}{N^2}(\lambda_{E_T} - \lambda_{R_H}) + \frac{\beta_T(I_T + \sigma I_{HT})}{N}(\lambda_S - \lambda_{E_T})\\
&\quad + \frac{g\beta_T(I_T + \sigma I_{HT})I_H}{N^2}(\lambda_{I_{HT}} - \lambda_{I_H}) + \frac{(1-u_4)\beta_H M}{K+M}(\lambda_S - \lambda_{I_H}) + \mu\lambda_S,\\
\frac{d\lambda_{V_T}}{dt} &= -(1-\eta)b\lambda_S + \frac{\beta_T(I_T + \sigma I_{HT})V_T}{N^2}(\varrho\lambda_{E_T} - \lambda_{V_T}) + \frac{\beta_T(I_T + \sigma I_{HT})R_H}{N^2}(\lambda_{E_T} - \lambda_{R_T})\\
&\quad - \eta b(1+u_1)\lambda_{V_T} + \frac{\beta_T(I_T + \sigma I_{HT})S}{N^2}(\lambda_{E_T} - \lambda_S) + \frac{\beta_T(I_T + \sigma I_{HT})}{N}(\lambda_{V_T} - \varrho\lambda_{E_T})\\
&\quad + \frac{g\beta_T(I_T + \sigma I_{HT})I_H}{N^2}(\lambda_{I_{HT}} - \lambda_{I_H}) + \frac{(1-u_4)\beta_H M}{K+M}(\lambda_{V_T} - \lambda_{I_H}) + \mu\lambda_{V_T},\\
\frac{d\lambda_{E_T}}{dt} &= -(1-\eta)b\lambda_S + \frac{\beta_T(I_T + \sigma I_{HT})S}{N^2}(\lambda_{E_T} - \lambda_S) + \frac{\varrho\beta_T(I_T + \sigma I_{HT})V_T}{N^2}(\lambda_{E_T} - \lambda_{V_T})\\
&\quad - \eta b(1+u_1)\lambda_{V_T} + \frac{\beta_T(I_T + \sigma I_{HT})R_H}{N^2}(\lambda_{E_T} - \lambda_{R_H}) + \frac{g\beta_T(I_T + \sigma I_{HT})I_H}{N^2}
\end{aligned}$$

$$
\begin{aligned}
&(\lambda_{I_{HT}} - \lambda_{I_H}) + \frac{(1-u_4)\beta_H M}{K+M}(\lambda_{E_T} - \lambda_{I_{HT}}) + k(\lambda_{E_T} - \lambda_{I_T}) + \mu\lambda_{E_T},\\
\frac{d\lambda_{I_T}}{dt} &= -C_1 - (1-\eta)b\lambda_S + \frac{\beta_T(I_T + \sigma I_{HT})S}{N^2}(\lambda_{E_T} - \lambda_S) + \frac{\varrho\beta_T(I_T + \sigma I_{HT})V_T}{N^2}(\lambda_{E_T} - \lambda_{V_T})\\
&- \eta b(1+u_1)\lambda_{V_T} + \frac{\beta_T(I_T + \sigma I_{HT})R_H}{N^2}(\lambda_{E_T} - \lambda_{R_H}) + \frac{\beta_T(S\lambda_S + V_T\lambda_{V_T} + I_T\lambda_{R_H})}{N}\\
&+ \frac{g\beta_T(I_T + \sigma I_{HT})I_H}{N^2}(\lambda_{I_{HT}} - \lambda_{I_H}) + \frac{(1-u_4)\beta_H M}{K+M}(\lambda_{I_T} - \lambda_{I_{HT}}) + (\mu + d_T)\lambda_{I_T}\\
&+ \frac{g\beta_T I_H}{N}(\lambda_{I_H} - \lambda_{I_{HT}}) + (\tau_2 + \alpha_1 u_2)(\lambda_{I_T} - \lambda_{R_H}), \qquad (3.98)\\
\frac{d\lambda_{I_H}}{dt} &= -C_2 - (1-\eta)b\lambda_S + \frac{\beta_T(I_T + \sigma I_{HT})S}{N^2}(\lambda_{E_T} - \lambda_S) + \frac{\varrho\beta_T(I_T + \sigma I_{HT})V_T}{N^2}(\lambda_{E_T} - \lambda_{V_T})\\
&- \eta b(1+u_1)\lambda_{V_T} + \frac{\beta_T(I_T + \sigma I_{HT})R_H}{N^2}(\lambda_{E_T} - \lambda_{R_H}) + \frac{g\beta_T(I_T + \sigma I_{HT})}{N}(\lambda_{I_H} - \lambda_{I_{HT}})\\
&+ \frac{g\beta_T(I_T + \sigma I_{HT})I_H}{N^2}(\lambda_{I_{HT}} - \lambda_{I_H}) + (\tau_1 + \alpha_2 u_3)(\lambda_{I_H} - \lambda_{R_H}) + (\mu + d_H + \epsilon_1)\lambda_{I_H}\\
&+ \epsilon_1\lambda_M,\\
\frac{d\lambda_{I_{HT}}}{dt} &= -C_3 - (1-\eta)b\lambda_S + \frac{\beta_T(I_T + \sigma I_{HT})S}{N^2}(\lambda_{E_T} - \lambda_S) + \frac{\varrho\beta_T(I_T + \sigma I_{HT})V_T}{N^2}(\lambda_{E_T} - \lambda_{V_T})\\
&- \eta b(1+u_1)\lambda_{V_T} + \frac{\beta_T(I_T + \sigma I_{HT})R_H}{N^2}(\lambda_{E_T} - \lambda_{R_H}) + \frac{\sigma g\beta_T(I_T + \sigma I_{HT})}{N}(\lambda_{I_H} - \lambda_{I_{HT}})\\
&+ \frac{g\beta_T(I_T + \sigma I_{HT})I_H}{N^2}(\lambda_{I_{HT}} - \lambda_{I_H}) + (\tau_1 + \alpha_2 u_3)(\lambda_{I_{HT}} - \lambda_{I_T}) + (\mu + d_{HT} + \tau_2 +\\
&\epsilon_2)\lambda_{I_{HT}} + \epsilon_2\lambda_M - \tau_2\lambda_{I_H} + \frac{\beta_T\sigma(S\lambda_S + \varrho V_T\lambda_{V_T} + R_H\lambda_{R_H})}{N} - \frac{\sigma\beta_T(S + \varrho V_T + R_H)}{N},\\
\frac{d\lambda_{R_T}}{dt} &= -(1-\eta)b\lambda_S + \frac{\beta_T(I_T + \sigma I_{HT})S}{N^2}(\lambda_{E_T} - \lambda_S) + \frac{\varrho\beta_T(I_T + \sigma I_{HT})V_T}{N^2}(\lambda_{E_T} - \lambda_{V_T})\\
&- \eta b(1+u_1)\lambda_{V_T} + \frac{\beta_T(I_T + \sigma I_{HT})R_H}{N^2}(\lambda_{E_T} - \lambda_{R_H}) + \gamma_2(\lambda_{R_T} - \lambda_S) + \mu\lambda_{R_T}\\
&+ \frac{g\beta_T(I_T + \sigma I_{HT})I_H}{N^2}(\lambda_{I_{HT}} - \lambda_{I_H}) + \frac{(1-u_4)\beta_H M}{K+M}(\lambda_{\lambda_{R_T}} - \lambda_{I_H}),\\
\frac{d\lambda_{R_H}}{dt} &= -(1-\eta)b\lambda_S + \frac{\beta_T(I_T + \sigma I_{HT})S}{N^2}(\lambda_{E_T} - \lambda_S) + \frac{\varrho\beta_T(I_T + \sigma I_{HT})V_T}{N^2}(\lambda_{E_T} - \lambda_{V_T})\\
&- \eta b(1+u_1)\lambda_{V_T} + \frac{\beta_T(I_T + \sigma I_{HT})R_H}{N^2}(\lambda_{E_T} - \lambda_{R_H}) + \gamma_1(\lambda_{R_H} - \lambda_S) + \mu\lambda_{R_H}\\
&+ \frac{g\beta_T(I_T + \sigma I_{HT})I_H}{N^2}(\lambda_{I_{HT}} - \lambda_{I_H}) + \frac{\beta_T(I_T + \sigma I_{HT})}{N}(\lambda_{\lambda_{R_H}} - \lambda_{E_T}),\\
\frac{d\lambda_M}{dt} &= \frac{(1-u_4)\beta_H MS}{(K+M)^2}(\lambda_{I_H} - \lambda_S) + \frac{(1-u_4)\beta_H MV_T}{(K+M)^2}(\lambda_{I_H} - \lambda_{V_T}) + \frac{(1-u_4)\beta_H MR_T}{(K+M)^2}\\
&(\lambda_{I_H} - \lambda_{R_T}) + \frac{(1-u_4)\beta_H ME_T}{(K+M)^2}(\lambda_{I_{HT}} - \lambda_{E_T}) + \frac{(1-u_4)\beta_H MI_T}{(K+M)^2}(\lambda_{I_{HT}} - \lambda_{I_T})\\
&+ \frac{(1-u_4)\beta_H(S\lambda_S + V_T\lambda_{V_T} + E_T\lambda_{E_T} + I_T\lambda_{I_T} + R_T\lambda_{R_T})}{K+M} + \mu_M\lambda_M -\\
&\frac{(1-u_4)\beta_H((S + V_T + R_T)\lambda_{I_H} + (E_T + I_T)\lambda_{I_{HT}})}{K+M}.
\end{aligned}
$$

To get the controls, we solve the equations $\frac{\partial H}{\partial u_i} = 0$ at u_i^* for $i = 1..., 4$ and obtained the following:

$$\begin{aligned}
u_1^* &= -\frac{\eta b N \lambda_{V_T}}{w_1}, \\
u_2^* &= \frac{\alpha_1 I_T(\lambda_{I_T} - \lambda_{R_T})}{w_2}, \\
u_3^* &= \frac{\alpha_2 I_H(\lambda_{I_H} - \lambda_{R_H}) + \alpha_2 I_{HT}(\lambda_{I_{HT}} - \lambda_{I_T})}{w_4}, \\
u_4^* &= \frac{\lambda_H \lambda_{I_H}(S + V_T + R_T) + \lambda_H \lambda_{I_{HT}}(E_T + I_T)}{w_4} - \lambda_H(S\lambda_S + V_T\lambda_{V_T} + E_T\lambda_{E_T} + I_T\lambda_{I_T}).
\end{aligned} \tag{3.99}$$

Then we write by standard control arguments involving the bounds on the controls as:

$$u_1^* = \begin{cases} \Theta_1 & \text{if } 0 < \Theta_1 < 1 \\ 0 & \text{if } \Theta_1 \leq 0 \\ 1 & \text{if } \Theta_1 \geq 1 \end{cases} \tag{3.100}$$

$$u_2^* = \begin{cases} \Theta_2 & \text{if } 0 < \Theta_2 < 1 \\ 0 & \text{if } \Theta_2 \leq 0 \\ 1 & \text{if } \Theta_2 \geq 1 \end{cases} \tag{3.101}$$

$$u_3^* = \begin{cases} \Theta_3 & \text{if } 0 < \Theta_3 < 1 \\ 0 & \text{if } \Theta_3 \leq 0 \\ 1 & \text{if } \Theta_3 \geq 1 \end{cases} \tag{3.102}$$

$$u_4^* = \begin{cases} \Theta_4 & \text{if } 0 < \Theta_4 < 1 \\ 0 & \text{if } \Theta_4 \leq 0 \\ 1 & \text{if } \Theta_4 \geq 1 \end{cases} \tag{3.103}$$

where,

$$\begin{aligned}
\Theta_1 &= -\frac{\eta b N \lambda_{V_T}}{w_1}, \\
\Theta_2 &= \frac{\alpha_1 I_T(\lambda_{I_T} - \lambda_{R_T})}{w_2}, \\
\Theta_3 &= \frac{\alpha_2 I_H(\lambda_{I_H} - \lambda_{R_H}) + \alpha_2 I_{HT}(\lambda_{I_{HT}} - \lambda_{I_T})}{w_4}, \\
\Theta_4 &= \frac{\lambda_H \lambda_{I_H}(S + V_T + R_T) + \lambda_H \lambda_{I_{HT}}(E_T + I_T)}{w_4} - \lambda_H(S\lambda_S + V_T\lambda_{V_T} + E_T\lambda_{E_T} + I_T\lambda_{I_T}).
\end{aligned} \tag{3.104}$$

□

3.4 Intra-host Mathematical Model for Mycobacterium Tuberculosis and Helminth Infection

3.4.1 Model formulation

The following assumptions guide the formulation of the model:

(i) The interaction that leads to the infection is between the Mtb bacteria and helminth parasites with macrophages.

(ii) The bacteria population replicates within the host macrophage.

(iii) The bacteria division follows a logistic growth.

(iv) The helminth parasites are too large to be phagocytosed by alveolar macrophages.

In this section we describe the interaction of the immune system of the host when challenged by the Mtb and parasitic worms. Due to complexity of the immune system, it is not possible to incorporate all of its components within a model for the co-infection of the Mtb and helminths at cellular level, hence we consider the interaction between Mtb, parasitic worms and the immune response as a feedback loop which comprises of three differential equations.

Infection by Mtb comprises intracelluar bacteria which are killed when the host macrophage is killed by apoptosis and extra-cellular bacteria that are killed by uninfected macrophages as a result of immune competence to clear invading pathogens. The bacteria population denoted by B grows logistically in the lung and is modeled by $\nu B(1-\frac{B}{\Pi})$ where ν is the constant growth rate and Π is the carrying capacity of the bacteria in the lung and they are eliminated as they interact with immune competence E at the rate δ_b. Therefore rate of change bacterial population within the host is described by the equation (3.105):

$$\frac{dB}{dt} = \nu B(1-\frac{B}{\Pi}) - \delta_b BE \tag{3.105}$$

On the other hand, helminth parasites are periodically ingested or penetrate the skin of human host when they come into contact with contaminated environment at the rate Λ_p and are eliminated within the body as they interact with the immune effectors at a rate propotional to the contact between worms and immune components. Therefore, the change of the helminth parasite population is given by the equation (3.106):

$$\frac{dP}{dt} = \Lambda_p P - \delta_p PE \tag{3.106}$$

Now, we consider three cases when there is infection by the two pathogens and in the absence of any infection as follows:

(i) The first case we consider the absence of Mtb or parasitic worms such that the dynamics of immune competence is given by the equation (3.107).

$$\frac{dE}{dt} = \Lambda_E - \delta_E E \tag{3.107}$$

where, Λ_E is the recruitment rate of the immune competence and δ_E is the loss of the immune competence because immune cells have limited life span.

(ii) The second case we consider is when helminth parasites enter the host prompting the immune response of the host to react. The helminths penetrate the skin or get ingested to infect the individual. The nonspecific precursor cell and not yet activated cells, cytotoxic T cells which lead to the immune competence against the parasites. The immune competence raised is assumed to be proportional to the density of parasites within the individual host at low density rates and at high densities it saturates, the stimulation of the immune system E as a result of this infection is modeled by the function $f(P)E$, where $f(P) = \dfrac{\theta_e P^n}{K_p + P^n}$ with positive parameters θ_e and K_p representing the strength of the immune competence on helminth parasites and half saturation constant respectively and n is a natural number.

The function $f(P)$ takes different shapes depending on the nature of immune competence either low-zone unresponsiveness or high unresponsiveness (decrease of immune response stimulation under high parasite load) (Mayer *et al.*, 1995). In our case, we consider the function to have two shapes when $n = 1$ and when $n > 1$ to mean small amounts of targets may be more or less ignored by host immune response [see Fig. 6]

(iii) The third case we consider when Mtb pathogen enter the body through inhalation of aerosol particles which trigger the immunity and consequently immune effector cells are supplied from the thymus. The bacteria results in the differentiation of naive T cells to T helper-1 and T helper-2 cells which activate the resting macrophages to clear the bacteria. If the immune system cannot kill the primary infection, then the granuloma is formed to prevent further differentiation of Mtb outside granuloma. The immune competence E as the ability of the immune system to eliminate Mtb bactria is modeled by the function $g(B)E$, where $g(B) = \dfrac{\theta_B B^n}{K_B + \varphi_B E + \alpha_B B^n}$, with positive parameters θ_B represents the strength of immune competence on Mtb bacteria and K_B is the half saturation constant. This process is inhibited by the presence of interleukin-4 cytokine with θ_B being the measure of inhibition. The graph of the function $g(B)$ looks like that in Fig. 6 for $n = 1$ and $n \geq 1$ respectively.

Now, combining expression in (b) and (c) equation (3.107) becomes;

$$\frac{dE}{dt} = \Lambda_E + f(P)E + g(B)E - \delta_E E. \tag{3.108}$$

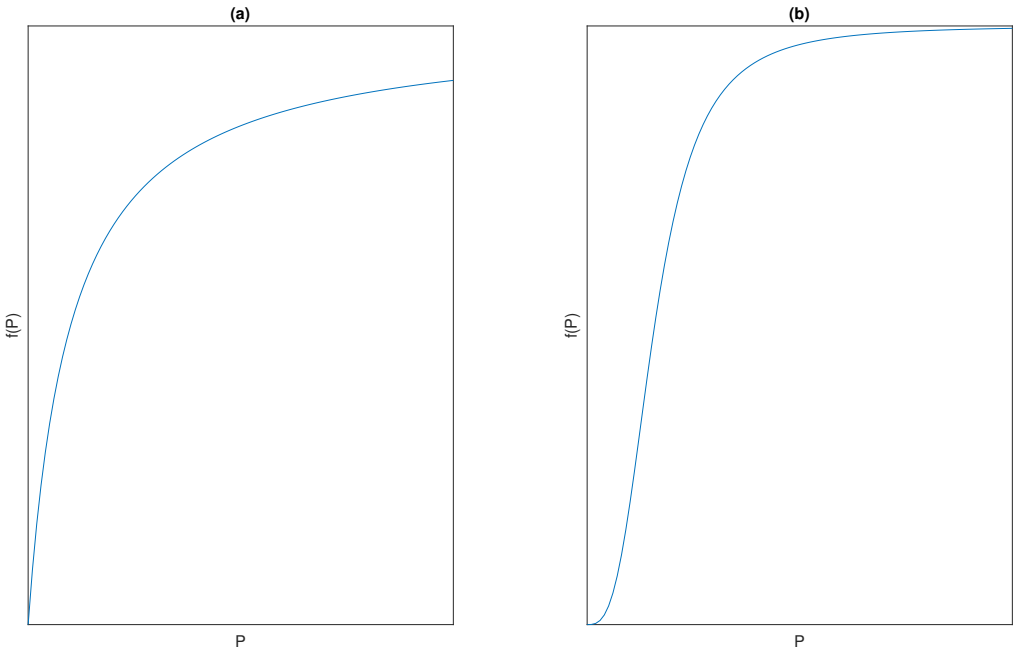

Figure 6: Graph of the immune competence for the function $f(P)$ (a) with $n = 1$; (b) with $n > 1$

We now consider the aforementioned mechanism which described the bacteria population, parasite population and the interaction of the two with immune system to form a mathematical model given by the system (3.109):

$$\begin{cases} \dfrac{dB}{dt} &= \nu B(1 - \frac{B}{\Pi}) - \delta_b BE, \\ \dfrac{dP}{dt} &= \Lambda_p P - \delta_p PE, \\ \dfrac{dE}{dt} &= \Lambda_E + f(P)E + g(B)E - \delta_E E, \end{cases} \tag{3.109}$$

with initial conditions $B(0) = B_0 \geq 0$, $P(0) = P_0 \geq 0$ and $E(0) = E_0 \geq 0$.

3.4.2 Qualitative Analysis of the Model

The dynamics of the model (3.109) is studied by simplifying the model to make analysis easy. We take $n = 1$ in the function $f(P)$ and $g(B)$. Hence the system (3.109) is reduced to:

$$\begin{cases} \dfrac{dB}{dt} &= \nu B(1-\frac{B}{\Pi}) - \delta_b BE, \\ \dfrac{dP}{dt} &= \Lambda_p P - \delta_p PE, \\ \dfrac{dE}{dt} &= \Lambda_E + \dfrac{\theta_e P}{K_p + P}E + \dfrac{\theta_B B}{K_B + \varphi_B E + \alpha_B B}E - \delta_E E. \end{cases} \tag{3.110}$$

3.4.3 Positivity of the Solution Trajectories of The Model (3.110)

We show that the solution of the system (3.110) are non-negative with the initial conditions $B(0) \geq 0$, $P(0) \geq 0$, $E(0) \geq 0$.

Theorem 3.13

The closed positive octant for the model (3.110) is positively invariant.

Proof. Clearly, $B = 0$ and $P = 0$ are the invariant planes for the model (3.110), we require to only show that $E(t) \geq 0$ for all future time.

Let us assume that there exits $t_0 > 0$ such that $E(t_0) = 0$ and $E(t) > 0$ for $0 < t < t_0$. Then

$$\frac{dE(t_0)}{dt} = \Lambda_E > 0. \tag{3.111}$$

It follows that $E(t) \geq 0$ for $t \geq t_0$. Thus $E(t) \geq 0$ for all future time. □

3.4.4 Boundness of the Solution

The model (3.110) describes the interaction of the helminth and Mtb pathogens with the immune system; hence it is important to show that the solution is bounded. In Fig. 6, the functions $f(B)$ and $f(P)$ are all continuous and bounded and hence the growth of the immune cells saturates.

Therefore, the pathogen population and the strength of the immune competence do not become negative or grow without bounds. Thus, the model in system (3.110) is mathematically and epidemeologically well posed and we can consider its dynamics in the proper subset (Hethcote, 2000).

3.4.5 Pathogen Free-Equilibrium Point and its Stability

We determine ability of the pathogens to invade an individual host and whether they are eliminated by the immune system or persist within an individual host. The pathogen free of the system (3.110)

denoted by H_0 is given by $(0, 0, \frac{e}{d})$. Linearizing the system 3.110 about H_0 gives

$$J_{H_0} = \begin{pmatrix} \nu - \frac{\delta_b \Lambda_E}{\delta_E} & 0 & 0 \\ 0 & \Lambda_p - \frac{\delta_p \Lambda_E}{\delta_E} & 0 \\ \frac{\theta_B \Lambda_E}{K_B \delta_E + \varphi_B \Lambda_E} & \frac{\theta_e \Lambda_E}{K_p \delta_E} & -\delta_E \end{pmatrix} \tag{3.112}$$

The condition that guarantee the local stability of the system at H_0 is that all eigenvalues of J_{H_0} must have negative real parts. Clearly, the matrix in equation (3.112) is a lower triangular matrix, hence its eigenvalues are the diagonal entries. It is evident that one of the eigenvalues is $-\delta_E < 0$ and for the remaining two to have negative real parts if $\nu - \frac{\delta_b \Lambda_E}{\delta_E} < 0$ and $\Lambda_p - \frac{\delta_p \Lambda_E}{\delta_E} < 0$. Therefore we have the following conditions.

$$\frac{\delta_E \nu}{\delta_b \Lambda_E} < 1 \text{ and } \frac{\delta_E \Lambda_p}{\delta_p \Lambda_E} < 1. \tag{3.113}$$

Hence, the basic reproduction number is given by $\mathcal{R}_{0BP} = \max\{\mathcal{R}_{0B}, \mathcal{R}_{0P}\}$, where $\mathcal{R}_{0B} = \frac{\delta_E \nu}{\delta_b \Lambda_E}$, and $\frac{\delta_E \Lambda_p}{\delta_p \Lambda_E}$. This result imply that the invasion of either Mtb or helminth parasites may not be able to result into an infection in an individual host. Hence individual host may recovery from primary infection by helminths or Mtb pathogen.

Using the condition in system (3.113), we have the following result.

Theorem 3.14

The pathogen free-equilibrium point H_0 of the system (3.110) is locally asymptotically stable if $\mathcal{R}_{0BP} < 1$ and unstable if either $\mathcal{R}_{0B} > 1$ or $\mathcal{R}_{0P} > 1$.

3.4.6 Endemic Equilibrium

In this section we discus the conditions for the existence and stability of endemic equilibrium points that is the Mtb equilibrium (i.e $B \neq 0, P = 0$), the helminth equilibrium (i.e $B = 0, P \neq 0$) and the co-infection when there is infection by Mtb and helminth parasites (i.e $B \neq 0, P \neq 0$). Using the results obtained in Theorem 3.14 and due to the complexities of the immune competence equation, the system (3.110) has endemic equilibria that corresponds to the following symmetric conditions:

(i) $\mathcal{R}_{0P} < 1$ (helminth infection dies out) and $\mathcal{R}_{0B} > 1$ (tuberculosis persist).

(ii) $\mathcal{R}_{0B} < 1$ (tuberculosis dies out) and $\mathcal{R}_{0P} > 1$ (helminth infection persist).

(iii) $\mathcal{R}_{0P} > 1$ (tuberculosis dies out) and $\mathcal{R}_{0B} > 1$ (helminth infection persist).

The results in Theorem 3.14 and the symmetric conditions in Fig. 7 imply that the endemic equilibrium is globally asymptotically stable for $\mathcal{R}_{0BP} > 1$.

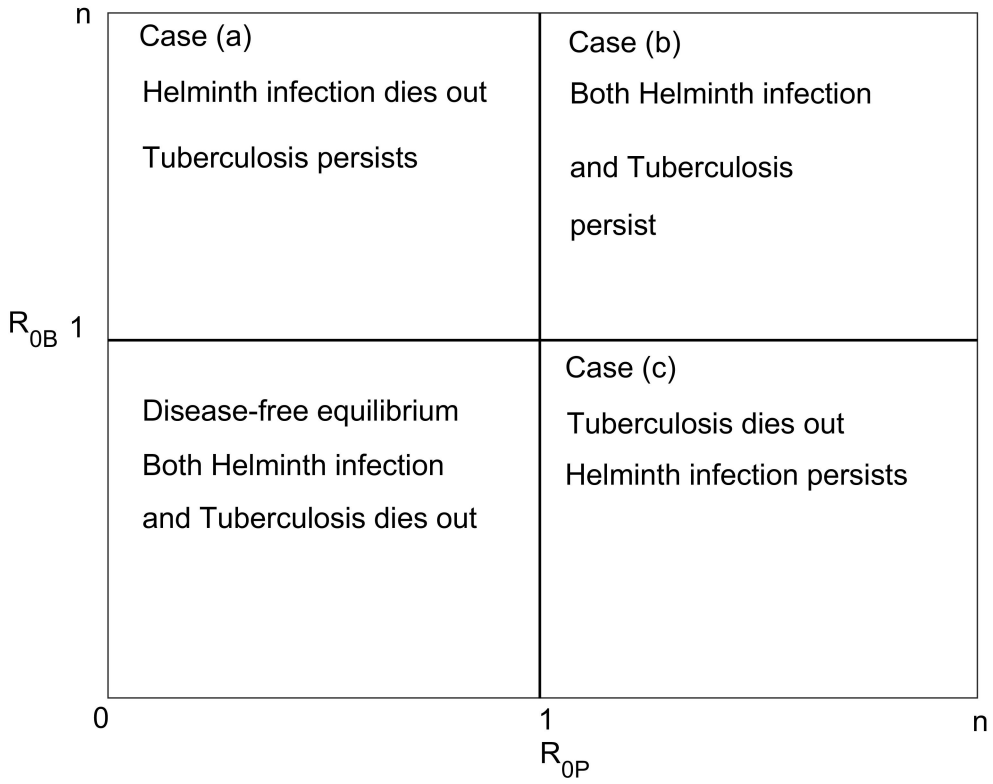

Figure 7: Equilibrium results showing the symmetric conditions for $\mathcal{R}_{0BP}$

3.4.7 The Impact of Helminth Parasites on Mtb Bacteria

To analyze the effects of helminth parasites on Mtb bactria and vice-versa, we write $\mathcal{R}_{0P}$ in-terms of $\mathcal{R}_{0B}$. From the expression of $\mathcal{R}_{0B}$, $\delta_E = \frac{\mathcal{R}_{0B}\delta_b\Lambda_E}{\nu}$. Substituting in the expression of $\mathcal{R}_{0P}$ we obtain:

$$\mathcal{R}_{0P}(\mathcal{R}_{0B}) = \frac{\Lambda_p\delta_b\mathcal{R}_{0B}}{\nu\delta_p} \tag{3.114}$$

Taking partial derivative of $\mathcal{R}_{0P}(\mathcal{R}_{0B})$ with respect to $\mathcal{R}_{0B}$, equation (3.114) becomes:

$$\frac{\partial\mathcal{R}_{0P}(\mathcal{R}_{0B})}{\partial\mathcal{R}_{0B}} = \frac{\Lambda_p\delta_b}{\nu\delta_p} \tag{3.115}$$

If the R.H.S of equation (3.115) is zero, this means that the helminth parasites has no effect on the dynamics of Mtb bacteria. Whereas if the R.H.S of (3.115) is greater than zero means that an increase in helminth parasites results in an increase in Mtb bacteria which indicates the occurrence of an endemic equilibrium for the helminth-Mtb co-infection.

3.4.8 The Impact of Mtb Bacteria on Helminth Parasites

Similarly, we express $\mathcal{R}_{0B}$ in-terms of $\mathcal{R}_{0P}$, so using the expression for $\mathcal{R}_{0P}$ we have $\delta_E = \frac{\delta_p \Lambda_E \mathcal{R}_{0P}}{\Lambda_p}$. Substituting into the expression for $\mathcal{R}_{0B}$ we obtain:

$$\mathcal{R}_{0B}(\mathcal{R}_{0P}) = \frac{\nu \delta_p \mathcal{R}_{0P}}{\delta_b \Lambda_p} \tag{3.116}$$

Taking partial derivative of $\mathcal{R}_{0B}(\mathcal{R}_{0P})$ with respect to $\mathcal{R}_{0P}$ we obtain:

$$\frac{\partial \mathcal{R}_{0B}(\mathcal{R}_{0P})}{\partial \mathcal{R}_{0P}} = \frac{\nu \delta_p}{\delta_b \Lambda_p} \tag{3.117}$$

If the R.H.S of equation (3.117) is equal to zero means that Mtb bacteria has no effect on the dynamics of helminth parasites. However, if the R.H.S of equation (3.117) is greater than zero implies that an increase in Mtb bacteria results in an increase in helminth parasites which suggest that whenever the two pathogens co-exist, they may stimulate one another and may give rise to chronic infection [see Fig. 8].

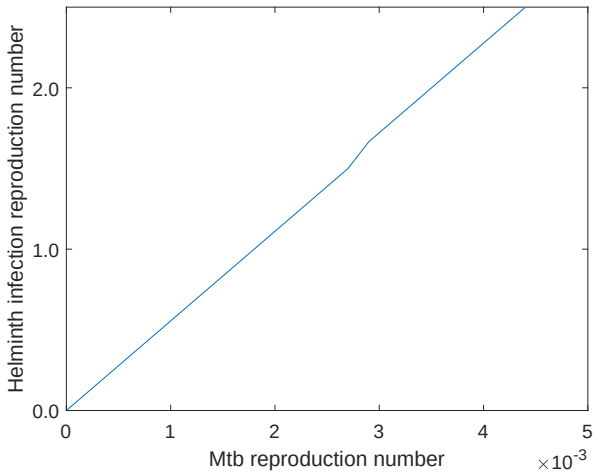

Figure 8: The relationship between helminth infection reproduction number and Mtb reproduction numbers

CHAPTER FOUR

RESULTS AND DISCUSSION

4.1 Numerical Simulation and Discussion of the Mathematical Model for the Optimal Control of Soil-transmitted Helminth Infection

The numerical simulation for the optimal control of the soil transmitted helminth model is performed using estimate parameter values indicated in Table 6 and others obtained from literature. Various optimal control strategies are applied to control the burden of helminth infection in the community. Starting with an initial guess for the optimal controls $u_1(t)$, $u_2(t)$ and $u_3(t)$, the state system (3.25) is solved numerically forward in time using the fourth order Runge-kutta method with initial conditions. Then the co-state (adjoint) system (3.29) is solved numerically backward in time using fourth order Runge-kutta method with the state variables and initial guess of the controls obtained earlier. All controls are updated using convex combination of the previous controls and its characterization then the process is repeated until convergence is achieved.

4.1.1 Discussion of Parameter and Initial Conditions Estimates

We were unable to get the ethical clearance on time so as to proceed with collection of secondary data. The inability to access the data on helminths and tuberculosis limits our ability to estimate model parameters, however using realistic set of parameters from clinical literature we analyze the future trends of helminth infection for various control strategies. For illustrative purpose we elected the parameters in realistic range as shown in Table 6. The actual value of the balancing weights requires intensive data mining and as such the following cost weights were used in the simulation : $A_1 = 800$, $A_2 = 0.15$, $w_1 = 15$, $w_2 = 30$ and $w_3 = 10$ with the efficacy rates $\kappa_1 = 0.7$, $\kappa_2 = 0.8$ and $\kappa_3 = 0.6$. The following initial conditions were used $S(0) = 1000$, $E(0) = 150$, $I(0) = 50$, $R(0) = 5$ and $M(0) = 200$.

4.1.2 Strategy (i): Control with Health Education and MDA

In this strategy we used combination of health education and MDA interventions to optimize the objective functional J while sanitation control was set to zero. Figure 8(a) shows that with this strategy there is significant effect in reducing the number of exposed individuals compared with the case when there were no control but does not bring the exposed individuals to zero at the final control period. The helminth infected individuals in Fig. 8(b) decreases to almost zero when the optimal

Table 6: Parameter values for soil transmitted helminth infection

Parameter	Symbol	Value	Source
Per capita birth rate	b	$\frac{1}{18250}day^{-1}$	Slater *et al.* (2013)
Per capita mortality rate	μ	$\frac{1}{(60\times365)}day^{-1}$	Mwanga *et al.* (2015)
Disease induced death rate	d	$\frac{35}{1000}day^{-1}$	Slater *et al.* (2013)
Ingestion rate of parasites	β	(1-7)7 parasites day^{-1}	Assumed
Carrying capacity of parasite in the environment	K	10^5 parasites	Assumed
Natural recovery rate	q	$\frac{1}{28}day^{-1}$	Assumed
Efficacy for MDA drug	κ_2	0.8	Vercruysse *et al.* (2011)
Immunity waning rate for recovered individuals	γ	$\frac{1}{7}day^{-1}$	Slater *et al.* (2013)
Clearance rate for parasitic worms	μ_M	$(\frac{5}{37500}-\frac{13}{37500})$ $\frac{13}{37500}day^{-1}$	Slater *et al.* (2013)
Shading rate of parasites to the environment	ϵ	0.09 day^{-1}	Assumed
Progression rate from exposed to infected class	ρ	$\frac{1}{10}day^{-1}$	Slater *et al.* (2013)

combination of health education and MDA are in place compared to when there were no control. In Fig. 8(c), we observed that the parasite population in the environment was reduced but does not reach zero at the final control period. This suggests that using combination of control measures, the infection can be lowered in the community but not completely removed in the specified control period. The control profile in Fig. 8(d) suggests that control combination with health education and MDA should be maximized and applied throughout the intervention period.

4.1.3 Strategy (ii): Control with MDA and Sanitation

Next, we consider the combination of MDA and sanitation interventions while the health education was set to zero. Figures 9(a) and 9(b) shows a similar trend as in Fig. 8(a) and Fig. 8(b) respectively but with this strategy more effective than the combination of health education and MDA. This was due to the fact that with MDA, anthelminthic drugs are regularly administered to the entire population (pre-school and school aged children) while using sanitation clears the density of parasites from the environment. The control profile in Fig. 9 suggests the control with MDA should be seized after

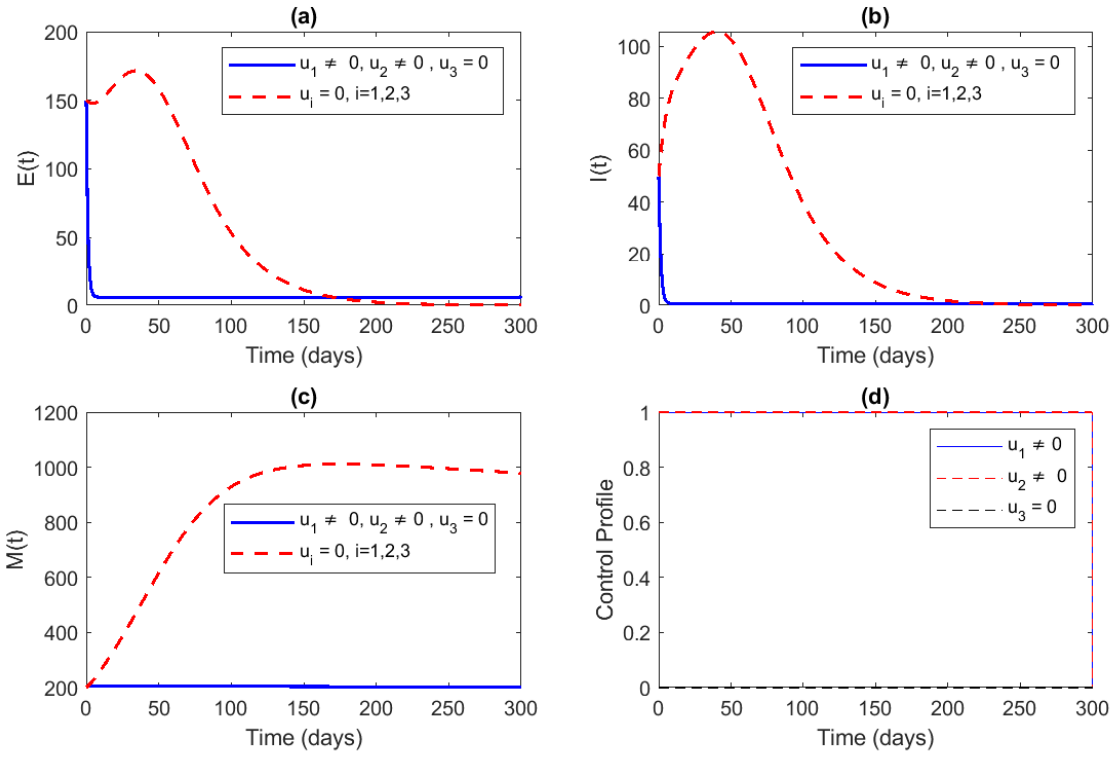

Figure 8: Simulations of the optimal control model with health education and MDA interventions

20 days while sanitation control should be kept at a maximum for approximately 20 days and then decreased to zero. Therefore, this results show that combination of these two controls measures can as well manage to control helminth infection in the community.

4.1.4 Strategy (iii): Control with Health Education and Sanitation

We next consider the control with combination of health education and sanitation in the absence of MDA. The health education and sanitation was used to optimize the objective functional J while MDA control were set to zero. In Fig. 10(a) shows that the number of exposed individuals were reduced and were totally controlled after 50 days. Figure 10(b) shows that the number of infected individuals were reduced and totally controlled at the final period. Figure 10(c) shows that the parasite population was reduced to minimum level. The control profile in Fig. 10(d) suggest that the control with health education should be maximized for 70 days while sanitation should be maximized for 65 days.

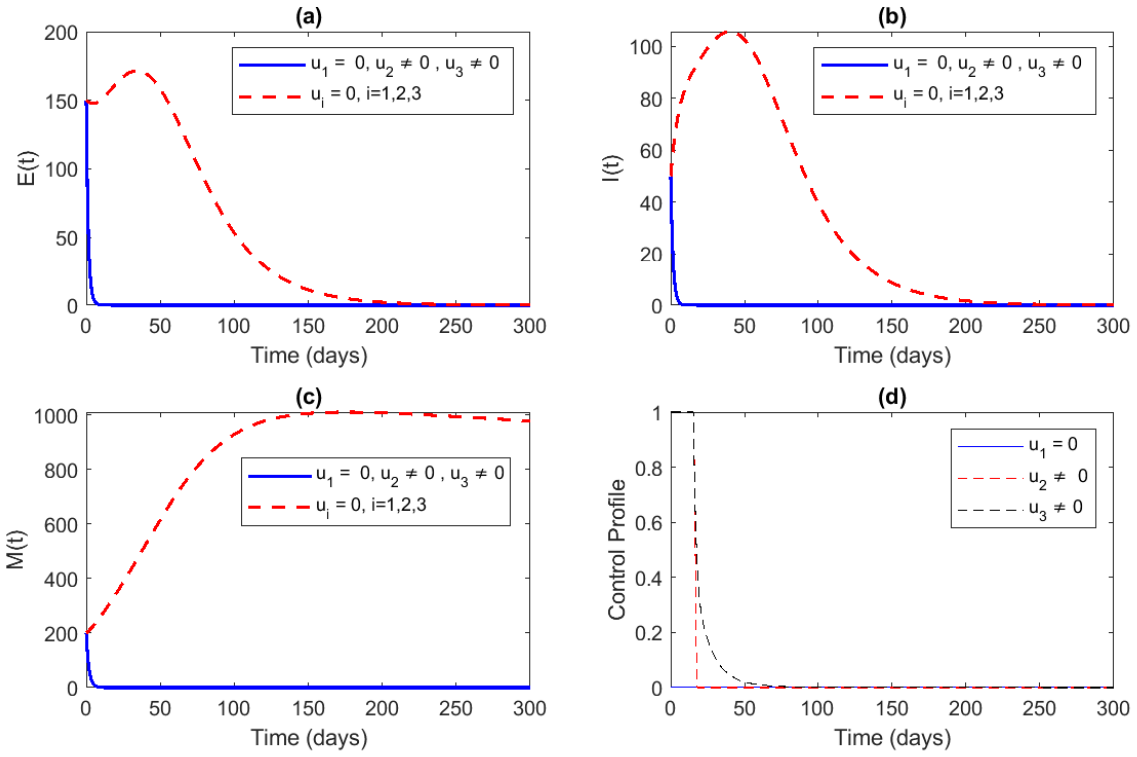

Figure 9: Simulations of the optimal control model with MDA and sanitation interventions

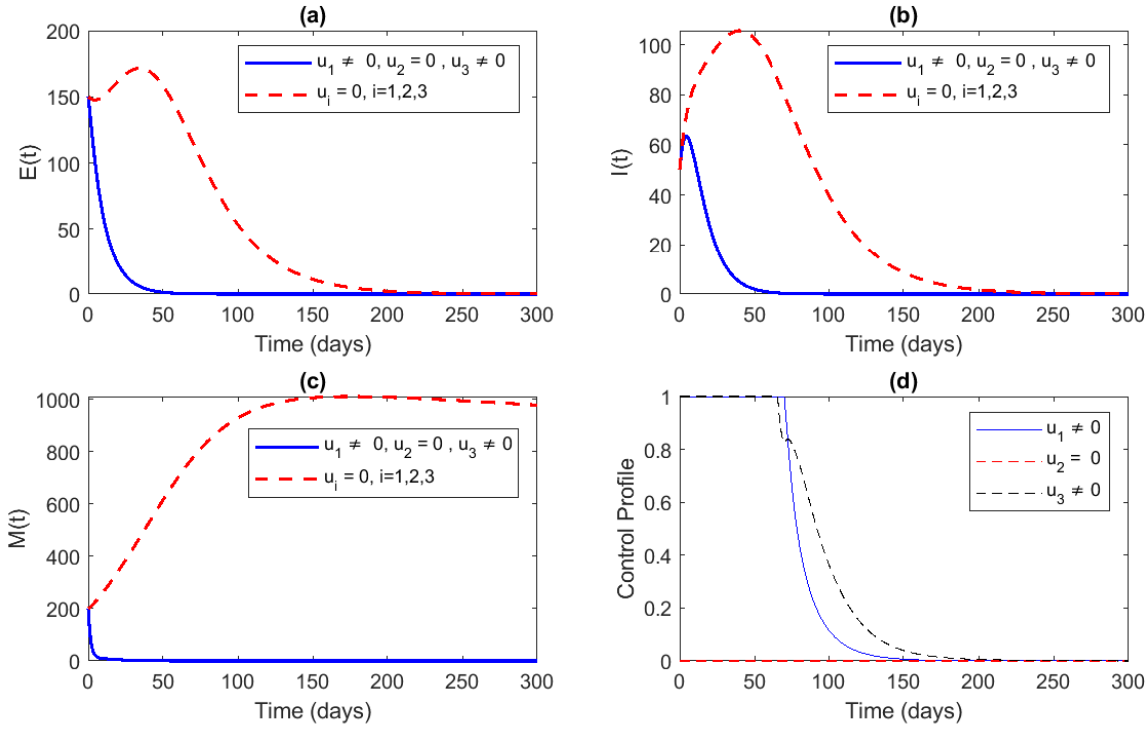

Figure 10: Simulations of the optimal control model with health education and sanitation interventions

4.1.5 Strategy (iv): Control with Health Education, MDA and Sanitation

Finally, we consider the case where all controls were in place. In this strategy the controls health education, MDA and sanitation were used to optimize the objective functional J. Figure 11(a) shows that the number of exposed individuals are totally controlled at the final control period. Figure 11(b) shows that the number of helminth infected individuals are also totally controlled at the final control period. Figure 11(c) shows that the parasite population is more reduced to zero at the final control time. Figure 11(d) suggest that the health education control should be maximized for 15 days, the MDA control be seized after 15 days while the sanitation should be maximized for 18 days and reduced to zero due to the fact that the infection has been cleared in the community.

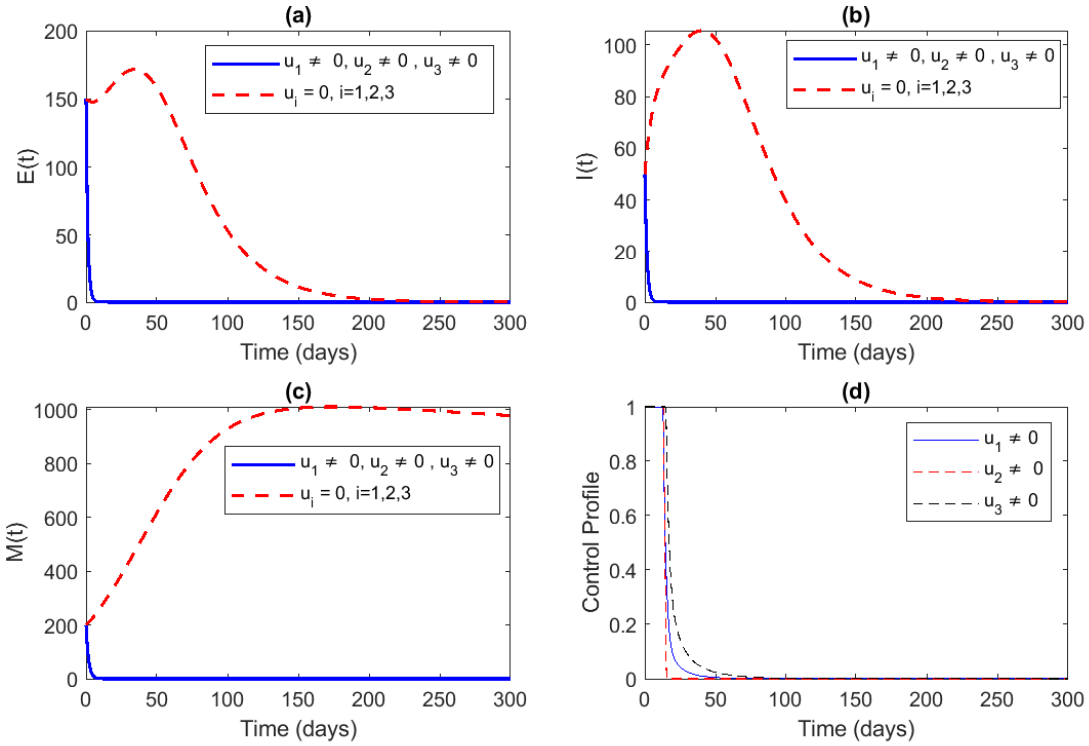

Figure 11: Simulations with health education, MDA and sanitation interventions

4.1.6 Model Validation

In the previous sections we developed and analyzed mathematical models for soil-transmitted helminths with the application of control strategies. We now compare the developed model with the data to perform model validation. Therefore, we fit into the model (3.25) the published data for reported cases of soil-transmitted helminths in Zanzibar following mass drug administration between 2000-2005 (Mohammed *et al.*, 2012). The best-fitted solution with Matlab and the data are plotted in Fig. 12. We compare the data with the simulation of our developed model. In Fig. 12, the dashed red

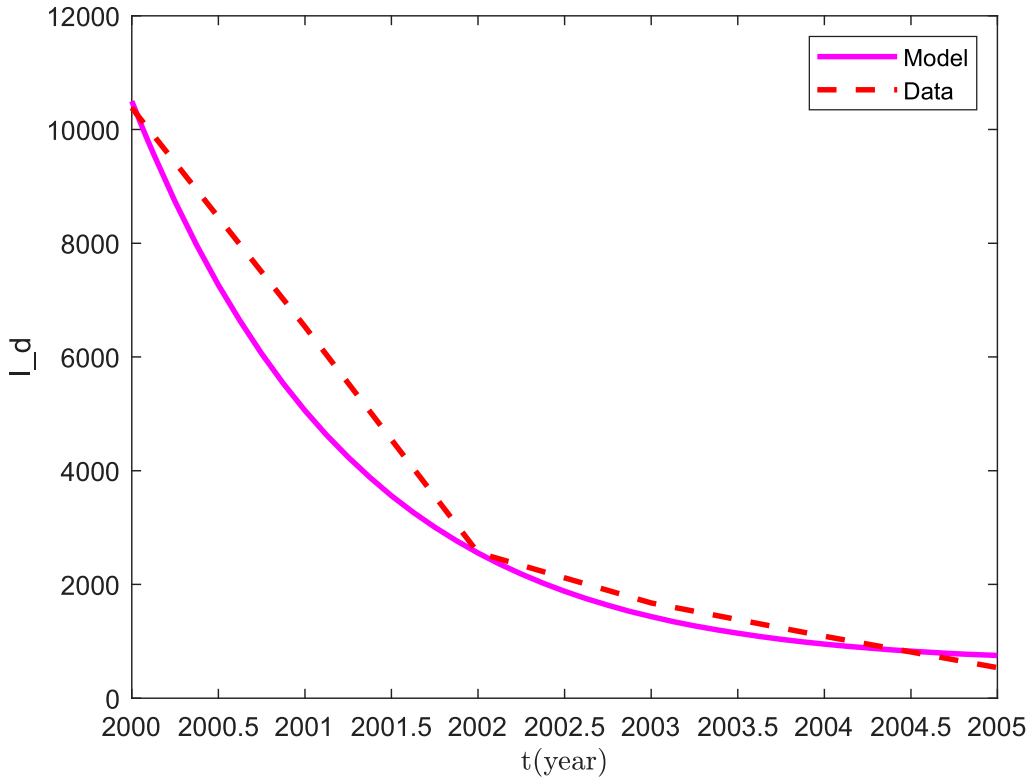

Figure 12: Model validation

lines indicate the data and the solid cyan line indicates the simulation of the model. We further examine the goodness of fit using Chi-Squire method. Matlab provides 95% confidence interval calculated from data and the expected observation from our simulation. Using the formula $\chi^2 = \sum_{i=1}^{n} \frac{(O_i - E_i)^2}{E_i}$, where E is the expected cases from the simulation of the model and O is the observed data, the calculated $\chi^2_{(calc)} = 81.88$ and from the table values $\chi^2_{(5\%,5)} = 1.145$ hence we conclude that their is no significance difference between the data and the model.

4.1.7 Concluding Remarks

In this chapter, we developed and analyzed a mathematical model for soil-transmitted helminths with the application of optimal control. Mathematical qualitative analyses were carried out and the model had a stable disease-free equilibrium point when the reproduction number is less than unity. Bifurcation analyses were also carried out using Center Manifold Theorem and the model exhibited backward bifurcation for some parameter values. Moreover, sensitivity analysis of $\mathcal{R}_0$ with respect to parameters β, ρ, ϵ, μ_M, b, d, q was done and results revealed that β was the most positive sensitive parameter while μ_M was the most negative sensitivity parameter. Furthermore, the model was extended to include control measures i.e health education, treatment by mass drug administration, and sanitation. The optimal control problem was solved by applying Pontryagin's

Maximum Principle by first obtaining the Hamiltonian, the adjoint variables, and the characterization of the controls. Applying a single control measure (health education or MDA or sanitation) alone is not sufficient to control the infection, thus a combination of control measures was used to optimize the objective functional J by considering the combination of health education with mass drug administration, a combination of mass drug administration with sanitation, a combination of health education with sanitation and all the three controls. Finally, we investigated the cost-effectiveness of the control strategies to ascertain the least and most expensive strategies. Based on our results, we conclude that a combination of health education and sanitation is the best strategy. Assessing the effectiveness of the model results (health education and sanitation strategy), we deduce that this strategy is highly likely to control the infection from the society if the health education control is maintained 100% for the first 70 days and sanitation control for the first 65 days. This is in agreement with the study by Campbell *et al.* (2014) which showed that WASH is a potential way of breaking the soil-transmitted helminth transmission cycle, though implementing WASH has enormous financial challenges. Whereas Anderson and May (1985) suggested that it is possible to quantify the level of antihelminthic treatment required in the community to suppress/eradicate the infection. In practice, our findings may be achieved, and that the health education and sanitation strategy will help to control the helminth infection otherwise the strategy may not be effective for containing the disease though practical difficulties may arise due to inadequate supply of resources.

4.2 Numerical Simulation and Discussion for the Inter-host Mathematical Model for Helminth and Mycobacterium Tuberculosis Co-infection with the Application of Control Strategies

Here, different optimal control strategies are used to investigate numerically their effect on the spread of helminth and Mtb co-infection. The state system (3.33), the adjoint system (3.98), and therefore the characterization in Equation (3.25) are solved numerically using an iterative scheme so as to attain the optimal control. Using the fourth-order Runge-Kutta scheme with the current state system solutions, we solve the state system forward in time and the adjoint system backward in time using the initial conditions for the state system and the transversality conditions for the adjoint system with the initial guess of the controls. The controls are then revised based on a convex combination of the controls and the characterization values (3.25). The solution of the state system and the adjoint system is repeated until when the present iteration are close to the previous iteration (Lenhart & Workman, 2007).

In numerical simulation, the weights are assumed to depend on the cost of investment and importance of the controls. For example, the cost associated with control u_2 require huge investment that include clinical examination of Mtb cases and procurement and transportation of the drugs. The cost associated with control u_2 require procurement and transportation of antihelminthic drugs and monitoring of the distribution of drugs. The true values of the weighs are unknown since they require broad field work and comprehensive data mining, so we choose the weights as: $C_1 = 5822$, $C_2 = 0.89$, $C_3 = 5822.89$, $w_1 = 20$, $w_2 = 40$, $w_3 = 30$, $w_4 = 10$, the initial state variables as: $S = 1500$, $V_T = 2000$, $E_T = 200$, $I_T = 150$, $I_H = 100$, $I_{HT} = 80$, $R_T = 5$, $R_H = 5$, $M = 200$. The efficacy parameters are $\alpha_1 = 0.75$, $\alpha_2 = 0.8$ and the remaining parameter values are given in Table 5.

4.2.1 Strategy (i): Control with Education Campaign (u_1) and Treatment of Individuals with Active TB (u_2)

The educational campaign control (u_1) and treatment of individuals with active TB (u_2) are used to optimize the objective functional J while the other controls (u_3) and (u_4) related to helminths were set to zero. We observed that in Fig. 13(b) the number of individuals with active TB was controlled but start to increase again until the end of the intervention period. This may be related to our previous analysis that helminth infection enhances Mtb infection. In this strategy, helminth infection is not controlled, Figs, 13(c) and 13(d) indicate that there is slight significance in the case with control and without control for helminth infected individuals and co-infected individuals respectively. Figure 13(e) indicates that the parasite population is not controlled with this strategy while Fig. 13(f) indicates that the educational campaign control should be seized after 158 days while treatment of individuals with active TB control should be kept maximum in the entire period of intervention.

4.2.2 Strategy (ii): Control with Mass Drug Administration (u_3) and Sanitation (u_4)

The mass drug administration (MDA) control (u_3) and sanitation control (u_4) were used to optimize the objective functional J. Again, we observe that Fig. 14(a) indicates the increase in vaccinated individuals. Also, Fig. 14(b) indicates that the people with active TB increases rapidly and eventually controlled after 55 days. An equivalent scenario is observed in Fig. 14(c) and Fig. 14(d) where the helminth infected individuals and co-infected individuals were effectively controlled. Figure 14(e) suggests that the parasite population is substantially controlled at the end of the intervention period. This strategy seems to be effective in controlling the two diseases from the community. Figure 14(f) indicate that MDA and sanitation controls should be kept maximum throughout the intervention period.

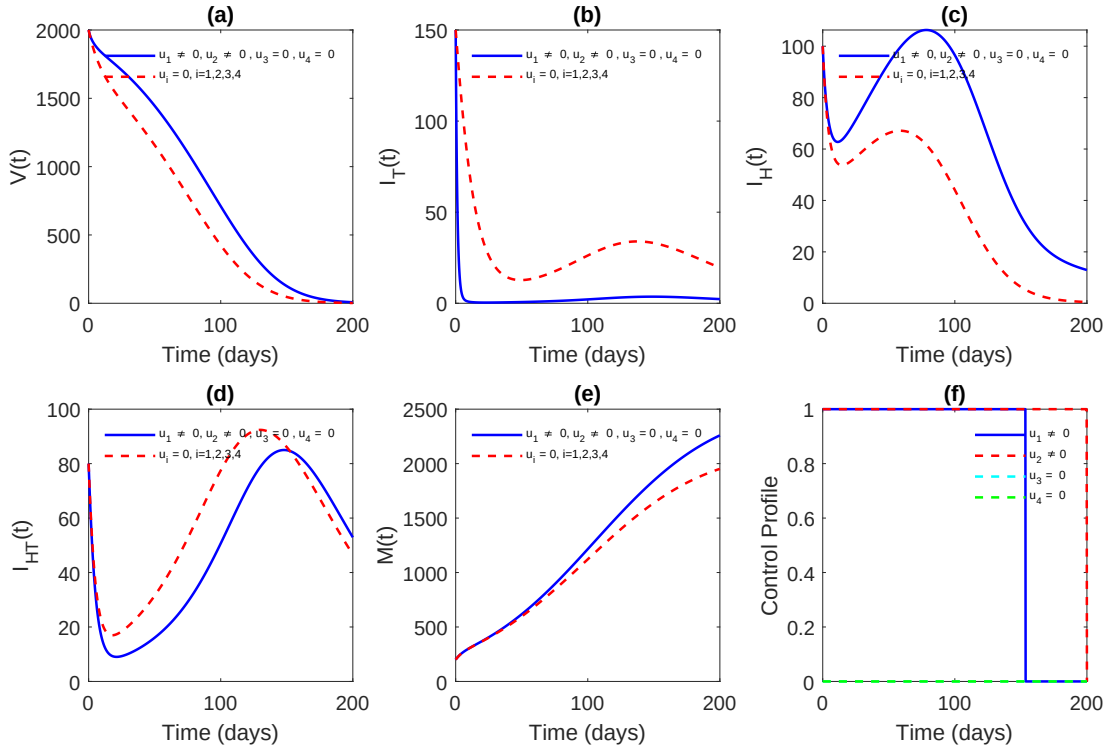

Figure 13: Simulations of helminth-Mtb co-infection model with the effect of education campaign and treatment of Mtb infected individuals

4.2.3 Strategy (iii): Control with Educational Campaign (u_1) and Sanitation (u_4)

The educational campaign control (u_1) and sanitation (u_4) are employed to optimize the objective functional J. This strategy has the same profiles as the strategy with mass drug administration and sanitation controls but takes a long time to control the two diseases. Figure 15(f) indicates that the educational campaign must be stopped after 30 days whereas sanitation control must be kept maximum in the entire period of intervention.

4.2.4 Strategy (iv): Control with Treatment of Individuals with Active TB (u_2) and MDA (u_3)

The treatment of individuals with active TB control (u_2) and MDA (u_3) are used to optimize the objective function J while the other controls (u_1) and (u_4) are set to zero. Figure 16(a) indicate a slight increase in the vaccinated individuals compared to strategy 4.2.1, 4.2.2, and 4.2.3 . Figure 16(b) and Fig. 16(d) indicate that the treatment of individuals with active TB and co-infected individuals are effectively controlled while Fig. 16(c) indicate a decrease in the helminth infected individuals but rise at the final intervention period. This is due to absence of preventive measures in this strategy. Figure 16(f) indicate that both controls should be kept maximum until the final intervention period.

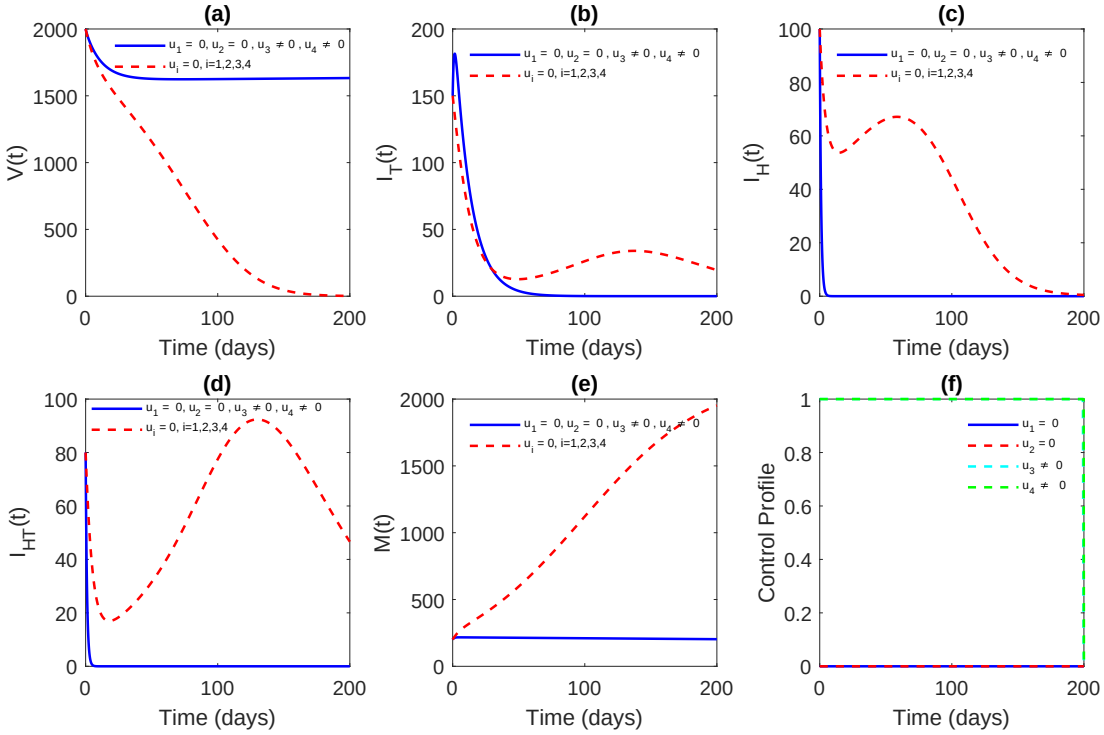

Figure 14: Simulations of helminth-Mtb co-infection model with the effect of MDA and sanitation

4.2.5 Strategy (v): Control with Educational Campaign (u_1), Treatment of Mtb Infected Individuals (u_2), MDA (u_3), and sanitation (u_4)

With this strategy, all four controls are employed to optimize the objective functional J. We observed that Fig. 17(a) indicates that the number of vaccinated individuals increases more at the end of the intervention period. Figure 17(b), Fig. 17(c), and Fig. 17(d) indicate that individuals with active TB, helminth infected and co-infected individuals are all effectively and efficiently controlled at the end of intervention period. Figure 17(e) depict that the parasite population is decreased to a number that cannot harm the human population. This strategy indicates that optimal educational campaigns, treatment of individuals with active TB, MDA, and sanitation would effectively control the helminth-Mtb infection at the end of the intervention period. Figure 17(f) suggests that the educational campaign should be stopped after 115 days whereas the remaining controls should be maintained maximum for the whole intervention period.

4.2.6 Concluding Remarks

With the application of optimal control strategies, we formulated and evaluated the inter-host mathematical model for the Helminth-Mtb co-infection model in this chapter. The analysis of the sub-

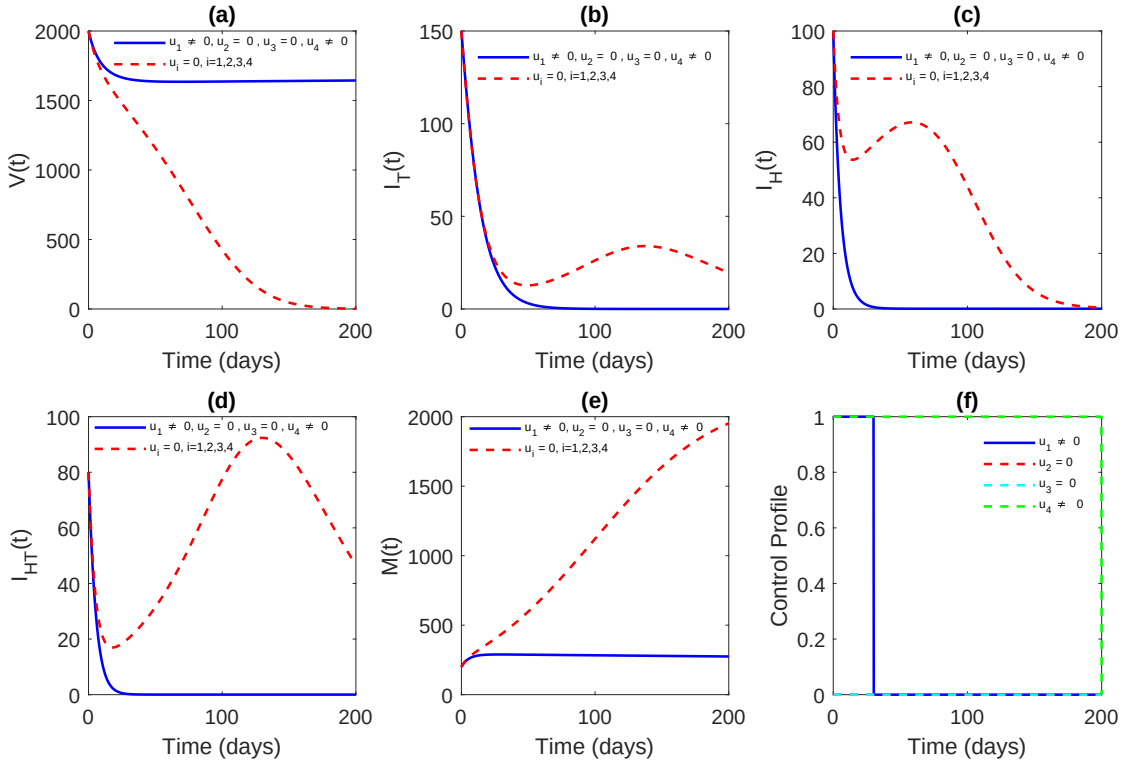

Figure 15: Simulations of helminth-Mtb co-infection model with the effect of educational campaign and sanitation

models (Helminth only sub-model and Mtb only sub-model) showed that the disease-free equilibrium point is globally asymptotically stable whenever their associated reproduction numbers is less than unity. The co-existence of the equilibria was observed for Mtb only model when the corresponding reproduction number is less than unity. Then the full co-infection model was considered and the effective reproduction number was obtained and used to gain insights into the dynamics of the two diseases. We again established the existence of backward or forward bifurcation using Center Manifold Theorem, then we investigated the impact the two diseases have on each other and found that helminth infection cases increase Mtb infection cases. Furthermore, the model was modified by incorporating four control measures, educational campaign to sensitize the parents to take babies to BCG vaccine clinic; treatment of individuals with active TB; mass drug administration for helminth and co-infected individuals; and sanitation to reduce the intake rate of parasites. The optimal control was analyzed using the Principle of Pontryagin's Maximum Pontryagin (2018), by first finding the Hamiltonian, co-state variables, the characterization of the controls, and the optimality system.

Then we solved numerically the optimality system by iterative scheme using Forward-Backward Sweep Method (FBSM) with the combination of the following control measures:

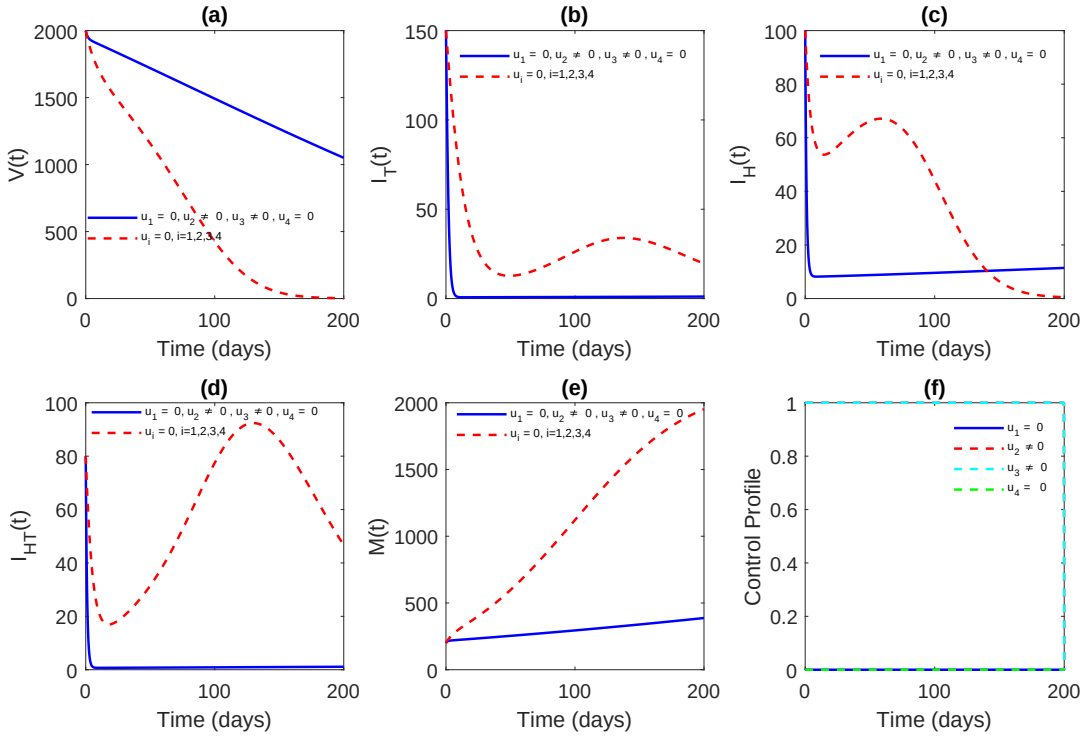

Figure 16: Simulations of the helminth-Mtb co-infection model with the effect of treatment of Mtb infected individuals and MDA

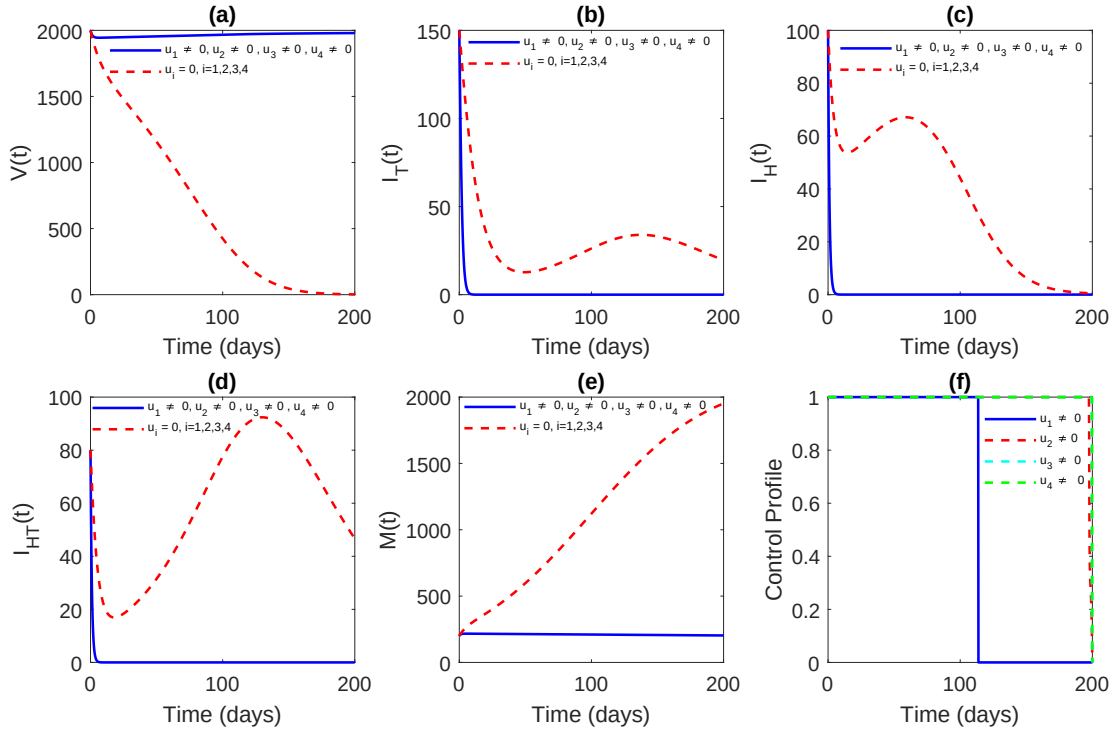

Figure 17: Simulations of the helminth-Mtb co-infection model with the effect of educational campaign, treatment of Mtb infected individuals, MDA, and sanitation

(i) By applying a combination of educational campaign and treatment of individuals with active TB.

(ii) By applying a combination of educational campaign and sanitation.

(iii) By applying a combination of treatment of individuals with active TB and mass drug administration.

(iv) By applying a combination of the education campaign, treatment of individuals with active TB, mass drug administration, and sanitation.

The control strategies which focus on TB only while helminths is not controlled would not lead to the efficient and effective control of TB or helminth infection. Moreover, control strategies that focus on helminths only while TB is not controlled would control both TB and helminth infection. This is linked to the increased susceptibility of Mtb for individuals infested with helminths. However, control strategies that include all control measures would effectively control the Helminth-Mtb co-infection at the end of the intervention period. Thus, we suggest to the public health stakeholders that in order to control the Helminth-Mtb co-infection, the intervention strategies that target controlling helminth infection and vaccination of babies with BCG after birth and treatment of individuals with active tuberculosis should be emphasized.

4.3 Numerical Simulation and Discussion of the Intra-host Mathematical Model for Mycobacterium Tuberculosis and Helminth Infection

In this section, we perform the numerical simulation of the model (3.110) by MATLAB using the inbuilt function ode45 solver. By using various initial conditions and the parameter values in Table 7, the behavior of the model (3.110) are illustrated hereunder:

Table 7: Description of the model parameters

Parameters	Definition	Estimated value	Reference
ν	Growth rate of bacteria	4×10^{-8}	Du *et al.* (2017)
δ_E	Loss of immune competence	0.02	Assumed
φ_B	Measure of inhibition	0.5	Assumed
K_p	Half saturation constant for parasites	10000	Assumed
K_B	Half saturation constant for Mtb	10000	Assumed
Π	Carrying capacity of the bacteria	10^8	Du *et al.* (2017)

δ_p	Clearance rate of helminth parasites	0.000685	Chiyaka *et al.* (2010)
Λ_E	Recruitment of immune cells	0.01	Assumed
Λ_p	Rate at which parasites are infecting individuals	0.8	Chiyaka *et al.* (2010)
δ_b	Clearance of Mtb bacteria	0.01	Du *et al.* (2017)
θ_e	Strength of immune cells on parasites	3	Assumed
θ_B	Strength of the immune cells on Mtb bacteria	2	Assumed

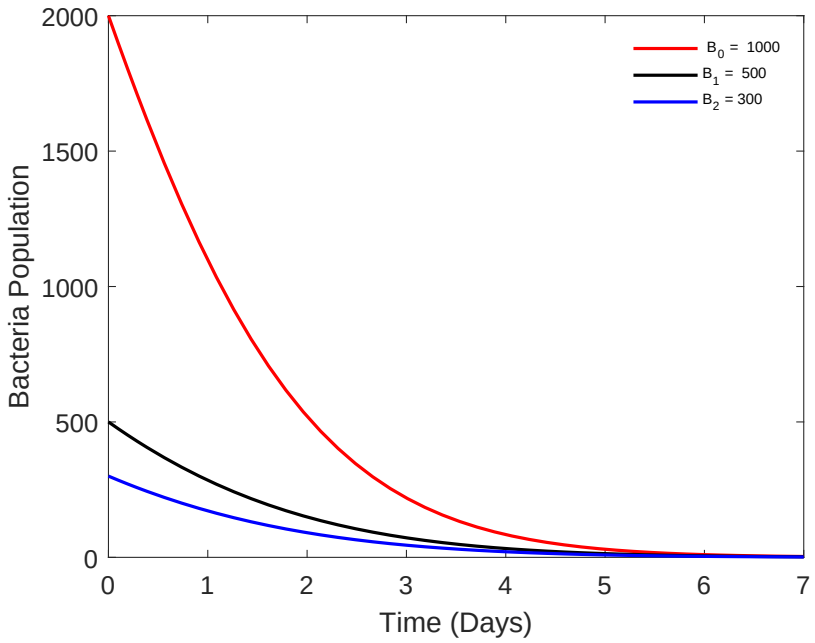

Figure 18: The solution of system (3.110) showing bacteria population convergence to the equilibrium point

Figures 18,19, and 20 indicate that the bacteria population, the parasite population and the immune competence all converge to the equilibrium H_0 when $R_{0BP} < 1$. This suggest that the infection by either helminth parasites or Mtb bacteria may be unsuccessful in an individual host and the host may recover from primary infection by Mtb or helminth parasites though helminths seams to persist within a host for quite longer time than Mtb bacteria. The later suggest infection by helminths parasites increase susceptibility to tuberculosis.

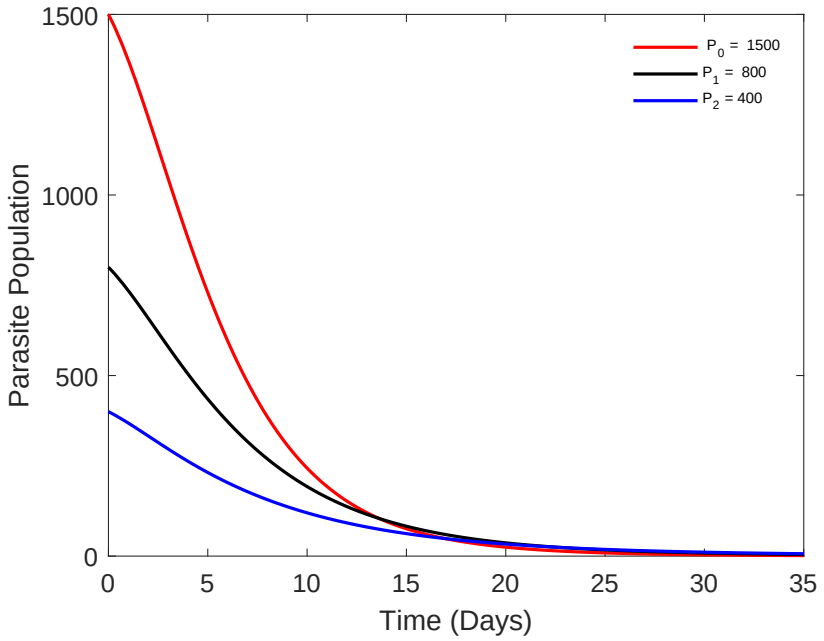

Figure 19: The solution of system (3.110) showing parasite population convergence to the equilibrium point

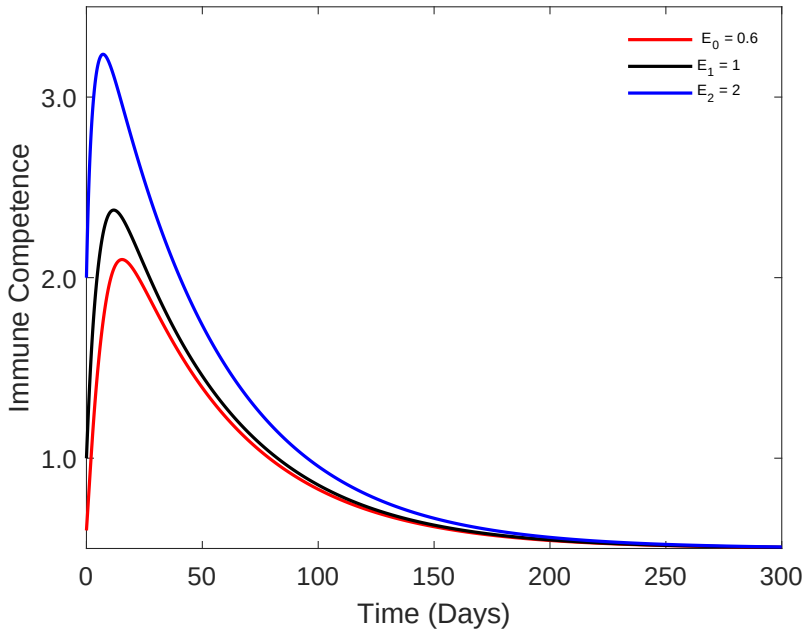

Figure 20: The solution of system (3.110) showing immune competence convergence to the equilibrium point

4.4 Concluding Remarks

In this chapter we formulated and analyzed a mathematical model for the interaction between helminth parasites, Mtb bacteria and the immune system. The model had four equilibrium points

i.e the pathogen free equilibrium point, the helminth equilibrium point (when the Mtb infection dies out), the Mtb equilibrium point (when helminth infection dies out), and the helminth-Mtb equilibrium point when both diseases persist in the community. The impact of helminth parasites on Mtb bacteria was investigated and the results indicated that infection by helminth enhances the chances of acquiring tuberculosis.

CHAPTER FIVE

CONCLUSION AND RECOMMENDATIONS

5.1 Conclusion

We used mathematical models to investigate the impact of helminth infection on Mtb transmission dynamics with the application of control strategies and the effect of immune responses caused by helminth parasites and Mtb bacteria infection in this research.

The model for soil-transmitted helminth with control strategies was developed to study the transmission dynamics and control of soil-transmitted helminth. The aim was to later couple the developed model with Mtb to form a co-infection model. A qualitative analysis of the model was made such that the basic reproduction number was determined and the disease-free equilibrium point was both locally and globally asymptotically stable whenever the basic reproduction number, $\mathcal{R}_0 < 1$ and unstable otherwise. The endemic equilibrium co-exists with the disease-free equilibrium point when $\mathcal{R}_0 < 1$. Moreover, sensitivity analysis of the reproduction number indicated that the ingestion rate of parasites was the most sensitive parameter for the transmission of the soil-transmitted helminth. The numerical simulation revealed that a combination of health education and sanitation is the best strategy to contain the disease.

The co-infection model was formulated by modifying the soil-transmitted model to form the co-infection model with control measures. The analysis of the sub-models was first considered and the full model was later analyzed. The disease-free equilibrium for the helminth only model was shown to be locally asymptotically stable when the reproduction number of the helminth model $\mathcal{R}_H < 1$ and unstable otherwise. However, the endemic equilibrium exists when $\mathcal{R}_H > 1$ with the impossibility of backward bifurcation. The Mtb only model has a stable disease-free equilibrium point when the effective reproduction number for Mtb model $\mathcal{R}_T < 1$ and the endemic equilibrium co-exist with the disease-free equilibrium point. The model exhibited backward bifurcation suggesting that making $\mathcal{R}_T < 1$ is not sufficient for eradicating tuberculosis from the community. The conditions for the existence of the disease-free equilibrium and endemic equilibrium for the full model were discussed. The possibility of the existence of backward bifurcation was established by using Centre Manifold Theorem and the results showed that the model undergoes backward bifurcation for some conditions. The optimal control model was then formed and analyzed to determine the optimal strategy for controlling the spread of the two diseases. Numerical simulation for optimal control problem

revealed that the target for controlling helminth infection and vaccinating babies with BCG and treatment of individuals with active tuberculosis should be emphasized to effectively control the disease. Furthermore, the analysis showed that infection by helminth results in increased susceptibility to tuberculosis.

The model for the interaction between the helminth infection and Mtb at the cellular level showed that primary infection with helminth parasites or Mtb bacteria was unsuccessful within an individual host when the basic reproduction number is less than a unit. Numerical simulation showed that the most virulent pathogen was the helminth parasites which could not be cleared completely by the immune cells. Even though the data used for simulations in understanding the transmission dynamics of the two diseases both at the cellular and population level, and the effect of control measures were adopted from literature, the models present a platform that can be used for future decision making and further modeling. In addition the models developed in this study are credible because they are developed based on the underling epidemiological and mathematical theories and the definition of the variables are justified. Sensitivity analysis (an important aspect of model validation) were conducted with multiple runs with small variability of parameter values that plausibly indicate the practicability of our model findings.

5.2 Recommendations

5.2.1 Recommendation from the Study

The following recommendation from our study are made:

(i) Mathematical model for soil-transmitted helminth with control strategies developed suggest that for effective control of helminth infection, the control with health education and sanitation should be emphasized. When the health education is maximized for the fist 70 days while the sanitation control is maximized for 65 days then individuals infected with helminth will be controlled after 50 days.

(ii) On the other hand the inter-host helminth and Mtb co-infection model developed suggest that infcetion by helminths enhances the chances of getting tuberculosis. Thus, whenever there is co-existence of helminth infection and tuberculosis, the model suggest inclusion of helminth infection control strategies with the tuberculosis control strategies for effective control of tuberculosis.

5.2.2 Recommendation for Future Study

The models developed in this dissertation can be expanded to include:

(i) Time delay to capture the outcome of the disease for the time span between when we acquire the infection and when clinical symptoms of the disease appear.

(ii) Linking the current model with the stochastic model, including seasonality, and linking the model with statistical models and demographic data.

(iii) The study sets the ground for assessment of the performance of various catalog of the control measures.

REFERENCES

Abate, E. (2013). The impact of helminth infection in patients with active tuberculosis. PhD thesis, Linköping University Electronic Press.

Anderson, R. M., & May, R. M. (1978). Regulation and stability of host-parasite population interactions: I. regulatory processes. *The journal of animal ecology*, 219–247.

Anderson, R. M., & May, R. M. (1982). Coevolution of hosts and parasites. *Parasitology*, 85(2), 411–426.

Anderson, R. M., & May, R. M. (1985). Helminth infections of humans: mathematical models, population dynamics, and control. *Advances in Parasitology*, 24, 1–101.

Anderson, R. M., & May, R. M. (1992). Infectious diseases of humans: Dynamics and control. Oxford University Press.

Babayan, S. A., Liu, W., Hamilton, G., Kilbride, E., Rynkiewicz, E. C., Clerc, M., & Pedersen, A. B. (2018). The immune and non-immune pathways that drive chronic gastrointestinal helminth burdens in the wild. *Frontiers in Immunology*, 9, 56.

Babu, S., & Nutman, T. B. (2016). Helminth-tuberculosis co-infection: an immunologic perspective. *Trends in Immunology*, 37(9), 597–607.

Bhunu, C., Garira, W., & Mukandavire, Z. (2009). Modeling HIV/AIDS and tuberculosis coinfection. *Bulletin of Mathematical Biology*, 71(7), 1745–1780.

Bhunu, C., Garira, W., Mukandavire, Z., & Zimba, M. (2008a). Tuberculosis transmission model with chemoprophylaxis and treatment. *Bulletin of Mathematical Biology*, 70(4), 1163–1191.

Bhunu, C., Garira, W., Mukandavire, Z., & Zimba, M. (2008b). Tuberculosis transmission model with chemoprophylaxis and treatment. *Bulletin of Mathematical Biology*, 70(4), 1163–1191.

Brooker, S., Clements, A. C., & Bundy, D. A. (2006). Global epidemiology, ecology and control of soil-transmitted helminth infections. *Advances in Parasitology*, 62, 221–261.

Campbell, S. J., Savage, G. B., Gray, D. J., Atkinson, J. M., Soares Magalhães, R. J., Nery, S. V., McCarthy, J. S., Velleman, Y., Wicken, J. H., & Traub, R. J. (2014). Water, sanitation, and hygiene (wash): a critical component for sustainable soil-transmitted helminth and schistosomiasis control. *PLoS Neglected Tropical Diseases*, 8(4), 2651.

Castillo-Chavez, C., Blower, S., Van den Driessche, P., Kirschner, D., & Yakubu, A. A. (2002). *Mathematical approaches for emerging and reemerging infectious diseases: models, methods, and theory*, volume 126. Springer Science & Business Media.

Castillo-Chavez, C., & Song, B. (2004). Dynamical models of tuberculosis and their applications. *Mathematical Biosciences and Engineering*, 1(2), 361–404.

CDC (2018). Helminths, Soil-Transmitted. accessed on: 29. 6 .2018.

Chatterjee, S., & Nutman, T. B. (2015). Helminth-induced immune regulation: Implications for immune responses to tuberculosis. *PLoS Pathogens*, 11(1), 1004582.

Chavez, C. C., Feng, Z., & Huang, W. (2002). On the computation of R0 and its role on global stability. *Mathematical Approaches for Emerging and Re-emerging Infection Diseases: An Introduction*, 125, 31–65.

Chitnis, N., Cushing, J. M., & Hyman, J. (2006). Bifurcation analysis of a mathematical model for malaria transmission. *SIAM Journal on Applied Mathematics*, 67(1), 24–45.

Chiyaka, E. T., Magombedze, G., & Mutimbu, L. (2010). Modelling within host parasite dynamics of schistosomiasis. *Computational and Mathematical Methods in Medicine*, 11(3), 255–280.

Chuma, F., Mwanga, G. G., & Masanja, V. G. (2019). Application of optimal control theory to newcastle disease dynamics in village chicken by considering wild birds as reservoir of disease virus. *Journal of Applied Mathematics*, 2019.

Coffeng, L. E., Bakker, R., Montresor, A., & de Vlas, S. J. (2015). Feasibility of controlling hookworm infection through preventive chemotherapy: A simulation study using the individual-based wormsim modelling framework. *Parasites & Vectors*, 8(1), 1–16.

Colditz, G. A., Brewer, T. F., Berkey, C. S., Wilson, M. E., Burdick, E., Fineberg, H. V., & Mosteller, F. (1994). Efficacy of BCG vaccine in the prevention of tuberculosis: Meta-analysis of the published literature. *Jama*, 271(9), 698–702.

Das, D. K., Khajanchi, S., & Kar, T. K. (2019). Influence of multiple re-infections in tuberculosis transmission dynamics: A mathematical approach. In *2019 8th International Conference on Modeling Simulation and Applied Optimization (ICMSAO)*, 1–5, IEEE.

Diekmann, O., & Heesterbeek, J. A. P. (2000). *Mathematical epidemiology of infectious diseases: model building, analysis and interpretation*, volume 5. John Wiley & Sons.

DiNardo, A. R., Mace, E. M., Lesteberg, K., Cirillo, J. D., Mandalakas, A. M., Graviss, E. A., Orange, J. S., & Makedonas, G. (2016). Schistosome soluble egg antigen decreases Mycobacterium tuberculosis–specific CD4+ T-cell effector function with concomitant arrest of macrophage phago-lysosome maturation. *The Journal of Infectious Diseases*, 214(3), 479–488.

Du, Y., Wu, J., & Heffernan, J. M. (2017). A simple in-host model for mycobacterium tuberculosis that captures all infection outcomes. *Mathematical Population Studies*, 24(1), 37–63.

Dye, C., Scheele, S., Pathania, V., & Raviglione, M. C. (1999). Global burden of tuberculosis: Estimated incidence, prevalence, and mortality by country. *Jama*, 282(7), 677–686.

Elliott, D. E., & Weinstock, J. V. (2012). Helminth–host immunological interactions: Prevention and control of immune-mediated diseases. *Annals of the New York Academy of Sciences*, 1247(1), 83–96.

Farrell, S. H., Coffeng, L. E., Truscott, J. E., Werkman, M., Toor, J., de Vlas, S. J., & Anderson, R. M. (2018). Investigating the effectiveness of current and modified world health organization guidelines for the control of soil-transmitted helminth infections. *Clinical Infectious Diseases*, 66(4), 253–259.

Fenton, A. (2013). Dances with worms: the ecological and evolutionary impacts of deworming on coinfecting pathogens. *Parasitology*, 140(9), 1119–1132.

Fleming, W. H., & Rishel, R. W. (2012). *Deterministic and stochastic optimal control*, volume 1. Springer Science & Business Media.

Harding, E. (2020). Who global progress report on tuberculosis elimination. *The Lancet Respiratory Medicine*, 8(1), 19.

Hethcote, H. W. (2000). The mathematics of infectious diseases. *SIAM review*, 42(4), 599–653.

Joshi, H. R., Lenhart, S., Li, M. Y., & Wang, L. (2006). Optimal control methods applied to disease models. *Contemporary Mathematics*, 410, 187–208.

Keeling, M. J., & Rohani, P. (2011). *Modeling infectious diseases in humans and animals*. Princeton university press.

Kirschner, D. (1999). Dynamics of co-infection with m. tuberculosisand HIV-1. *Theoretical Population Biology*, 55(1), 94–109.

Lenhart, S., & Workman, J. T. (2007). *Optimal control applied to biological models*. CRC press.

Mafuta, P., Mushanyu, J., Mushayabasa, S., & Bhunu, C. P. (2013). Transmission dynamics of trichomoniasis in bisexuals without the 'E'. *World Journal of Modelling and Simulation*, 9(4), 302–320.

Makinde, O. D., & Okosun, K. O. (2011). Impact of chemo-therapy on optimal control of malaria disease with infected immigrants. *BioSystems*, 104(1), 32–41.

Mascarini-Serra, L. (2011). Prevention of soil-transmitted helminth infection. *Journal of Global Infectious Diseases*, 3(2), 175.

May, R. M. (2019). *Stability and complexity in model ecosystems*, volume 1. Princeton university press.

Mayer, H., Zaenker, K., & An Der Heiden, U. (1995). A basic mathematical model of the immune response. *Chaos: An Interdisciplinary Journal of Nonlinear Science*, 5(1), 155–161.

Medley, G., Guyatt, H., & Bundy, D. (1993). A quantitative framework for evaluating the effect of community treatment on the morbidity due to ascariasis. *Parasitology*, 106(2), 211–221.

Mkhize-Kwitshana, Z. L., Tadokera, R., & Mabaso, M. H. (2017). Helminthiasis: A systematic review of the immune interactions present in individuals coinfected with hiv and/or tuberculosis. *Human Helminthiasis*.

Mohammed, K. A., Deb, R. M., Stanton, M. C., & Molyneux, D. H. (2012). Soil transmitted helminths and scabies in Zanzibar, Tanzania following mass drug administration for lymphatic filariasis-a rapid assessment methodology to assess impact. *Parasites & Vectors*, 5(1), 1–8.

Monin, L., Griffiths, K. L., Lam, W. Y., Gopal, R., Kang, D. D., Ahmed, M., Rajamanickam, A., Cruz-Lagunas, A., Zúñiga, J., & Babu, S. (2015). Helminth-induced arginase-1 exacerbates lung inflammation and disease severity in tuberculosis. *The Journal of Clinical Investigation*, 125(12), 4699–4713.

Mpeshe, S. C., Luboobi, L. S., & Nkansah-gyekye, Y. (2014). Optimal control strategies for the dynamics of rift valley fever. *Communications in Optimization Theory*, 3, 1–18.

Mushayabasa, S., & Bhunu, C. P. (2011). Modeling schistosomiasis and HIV/AIDS codynamics. *Computational and Mathematical Methods in Medicine*, 2011.

Mwanga, G. G., Haario, H., & Capasso, V. (2015). Optimal control problems of epidemic systems with parameter uncertainties: Application to a malaria two-age-classes transmission model with asymptomatic carriers. *Mathematical Biosciences*, 261, 1–12.

Nkamba, L. N., Manga, T. T., Agouanet, F., & Mann Manyombe, M. L. (2019). Mathematical model to assess vaccination and effective contact rate impact in the spread of tuberculosis. *Journal of Biological Dynamics*, 13(1), 26–42.

Okosun, K. O., Rachid, O., & Marcus, N. (2013). Optimal control strategies and cost-effectiveness analysis of a malaria model. *BioSystems*, 111(2), 83–101.

Okosun, K. O., & Robert, S. (2017). Optimal control analysis of malaria-schistosomiasis co-infection dynamics. *Mathematical Biosciences & Engineering*, 14(2), 377.

Ozcaglar, C., Shabbeer, A., Vandenberg, S. L., Yener, B., & Bennett, K. P. (2012). Epidemiological models of mycobacterium tuberculosis complex infections. *Mathematical Biosciences*, 236(2), 77–96.

Pontryagin, L. S. (2018). *Mathematical theory of optimal processes*. Routledge.

Pullan, R. L., Freeman, M. C., Gething, P. W., & Brooker, S. J. (2014). Geographical inequalities in use of improved drinking water supply and sanitation across sub-Saharan Africa: Mapping and spatial analysis of cross-sectional survey data. *PLoS Medicine*, 11(4), 1001626.

Salgame, P., Yap, G. S., & Gause, W. C. (2013). Effect of helminth-induced immunity on infections with microbial pathogens. *Nature Immunology*, 14(11), 1118.

Seidu, B., & Makinde, O. D. (2014). Optimal control of HIV/AIDS in the workplace in the presence of careless individuals. *Computational and Mathematical Methods in Medicine*, 2014.

Slater, H. C., Gambhir, M., Parham, P. E., & Michael, E. (2013). Modelling co-infection with malaria and lymphatic filariasis. *PLoS Comput Biol*, 9(6), 1003096.

Tasman, H. (2016). An optimal treatment control of TB-HIV coinfection. *International Journal of Mathematics and Mathematical Sciences*, 2016.

Tilahun, G. T., Makinde, O. D., & Malonza, D. (2018). Co-dynamics of pneumonia and typhoid fever diseases with cost effective optimal control analysis. *Applied Mathematics and Computation*, 316, 438–459.

Truscott, J., Turner, H., Farrell, S., & Anderson, R. (2016). Soil-transmitted helminths: Mathematical models of transmission, the impact of mass drug administration and transmission elimination criteria. *Advances in Parasitology*, 94, 133–198.

Uneke, C. (2010). Soil transmitted helminth infections and schistosomiasis in school age children in sub-Saharan Africa: Efficacy of chemotherapeutic intervention since world health assembly resolution 2001. *Tanzania Journal of Health Research*, 12(1), 86–99.

Van den Driessche, P., & Watmough, J. (2002). Reproduction numbers and sub-threshold endemic equilibria for compartmental models of disease transmission. *Mathematical Biosciences*, 180(1-2), 29–48.

Vercruysse, J., Behnke, J. M., Albonico, M., Ame, S. M., Angebault, C., Bethony, J. M., Engels, D., Guillard, B., Hoa, N. T. V., & Kang, G. (2011). Assessment of the anthelmintic efficacy of albendazole in school children in seven countries where soil-transmitted helminths are endemic. *PLoS Neglected Tropical Diseases*, 5(3), 948.

WHO (2018). Soil transimitted helminths infections. accessed on: 30. 6 .2018.

Xiao, D., & Bossert, W. H. (2010). An intra-host mathematical model on interaction between HIV and malaria. *Bulletin of Mathematical Biology*, 72(7), 1892–1911.

Yakob, L., Williams, G. M., Gray, D. J., Halton, K., Solon, J. A., & Clements, A. C. (2013). Slaving and release in co-infection control. *Parasites & Vectors*, 6(1), 1–9.

Yeketi, A. A., Othman, W. A. M., & Awang, M. O. (2019). The role of vaccination in curbing tuberculosis epidemic. *Modeling Earth Systems and Environment*, 5(4), 1689–1704.

APPENDICES

APPENDIX 1: MATLAB codes for Figure 3

```
syms beta rho epsilon mu1 b d q tau

v=[beta rho epsilon mu1 b d q];


R0=rho*epsilon*beta./(mu1*(b+rho)*(d+b+q+epsilon));
P=jacobian(R0,v)

v0=[7 1/10 0.09 13/37500 1/18250 35/1000 1/28];
v1=[1 2 3 4 5 6 7];

sensi= subs(P.*v/R0,v,v0)
double(sensi)
```

APPENDIX 2: MATLAB codes for Figures 4, 5, 6 and 7

```
clc
clear all
close all
t0 = 0; tf=300; N=1000; %case 3

time =linspace(t0,tf,N);

  y0  = [1000,150,50,5,200];% initial condition for STATE SYSTEM
%--- SOURCES OF CONSTANTS --
 Constant=[7 1/10 0.09 13/37500  1/18250 35/1000 1/28 1/7 0.000045
     0.7 0.8 0.6 800 0.15 15 30 10 100000 2000]
beta=Constant(1);
rho = Constant(2);
epsilon= Constant(3);
mu1 = Constant(4);
b = Constant(5);
d  = Constant(6);
q      = Constant(7);
gamma =  Constant(8);
mu     =Constant(9);
kappa1= Constant(10);
kappa2= Constant(11);
kappa3  = Constant(12);
A1     = Constant(13); % weight
A2    = Constant(14); % weight
B1    =Constant(15);
B2    =Constant(16);
B3    =Constant(17);
K     =Constant(18);
Nh     =Constant(19);

```

```
lf  = [0 0 0 0 0];
%% TEST SECTION
init =y0;
init2 =lf;
h = (tf-t0)/N;
u = linspace(0,0,N+1);
u1=u'; u2=u'; u3=u';
U = [u1 u2 u3];
%% IMPLIMENTATION OF THE ALGORITHM
%Test 1 stoping condition 1
delta = 0.001;
X=init;
i=0; %Initialize iteration counter
mm=size(X);
NumXX =10e10;
Xnew = rand(N+1,mm(2)).*(repmat(X,N+1,1));
DenXnew=norm(Xnew);
while  NumXX/DenXnew>delta
Xold =  Xnew;
oldu = U;
%FORWARD RUNGE KUTTA  FOR STATES
[Tx, X]=rk4foward(@kims,t0, tf,N, init,U,Constant);

% BACKWARD RUNGEKUTA FOR COSTATES
[Tp, P]=rk4back(@kims_costate,t0,tf,N,init2,U,X,Constant);

%UPDATE THE CONTROLS
x = X(1,:); y = X(2,:); v = X(3,:); z = X(4,:); l = X(5,:);
L1 = P(1,:); L2 = P(2,:); L3 = P(3,:); L4 = P(4,:); L5 = P(5,:);
g=x+y+v+z;

%Combination of health education and MDA
% Case1:u1\neq= 0, u2\neq= 0, u3= 0,
```

```
% u1 =max(0,min(1,((L2-L1).*beta.*l.*x*kappa1./(B1.*(K+l)))));
% u2 =max(0,min(1,(((L2-L1)*kappa2.*y+(L3-L4)*kappa2.*v)./B2-(A2*g
    )./B2)));
% u3 =zeros(1,N+1);

%Combination of MDA and sanitation
 % Case2::u1= 0, u2\neq= 0, u3\neq= 0,
% u1 =zeros(1,N+1);
% u2 =max(0,min(1,(((L2-L1)*kappa2.*y+(L3-L4)*kappa2.*v)./B2-(A2*g
    )./B2)));
% u3 =max(0,min(1,((kappa3.*l.*L5)./B3)));

%Combination of health education and sanitation
% Case3::u1=\ 0, u2= 0, u3\= 0,
% u1 =max(0,min(1,((L2-L1).*beta.*l.*x*kappa1./(B1.*(K+l)))));
% u2 =zeros(1,N+1);
% u3 =max(0,min(1,((kappa3.*l.*L5)./B3)));

%All controls
%Case4:u1=\ 0, u2\= 0, u3\= 0,
      u1 =max(0,min(1,((L2-L1).*beta.*l.*x*kappa1./(B1.*(K+l)))));
      u2 =max(0,min(1,(((L2-L1)*kappa2.*y+(L3-L4)*kappa2.*v)./B2-(
          A2*g)./B2)));
      u3 =max(0,min(1,((kappa3.*l.*L5)./B3)));

Uu=[u1' u2' u3'];
U = 0.5*Uu + 0.5*oldu; % Convex combination of the controls


Xnew =  X';
NumXX =abs(norm(Xnew-Xold));
DenXnew =norm(Xnew);
i=i+1 %Update iteration counter
```

```
94  end
95  %% PLOTING
96  X=X';
97  Tx =Tx';
98  XX=X(:,1); YY=X(:,2); VV=X(:,3); ZZ=X(:,4); LL=X(:,5);
99
100 Up = [0 0 0];
101 [T,Y] = ode45(@kims,time,y0,[],Up,Constant);
102
103 J =sum((A1.*VV(end)+A2.*Uu(:,2).*(XX(end)+YY(end)+VV(end)+ZZ(end))
        )+((B1/2)*Uu(:,1).*Uu(:,1)+(B2/2)*Uu(:,2).*Uu(:,2)+(B3/2)*Uu
        (:,3).*Uu(:,3))) %Change to the suitable objective function
104
105  S=[Tx,X];
106
107  save case5;
108  %save('case3State', 'S');
109  %save('case3Control', 'Uu');
110 %save('Cost', 'J');
111  figure(1)
112
113  subplot(2,2,1)
114  plot(Tx,X(:,2),'-b',T, Y(:,2),'--r','LineWidth',1.5);
115  %ylim([0 700])
116  ylabel('E(t)');
117  xlabel('Time (days)');
118  title('(a)')
119 legend('u_1 \neq 0, u_2 \neq 0 , u_3 = 0 ','u_i = 0, i=1,2,3 ')
120 %
121 subplot(2,2,2)
122  plot(Tx,X(:,3),'-b',T, Y(:,3),'--r','LineWidth',1.5);
123  %%ylim([0 700])
124  ylabel('I(t)');
```

```
125     xlabel('Time (days)');
126      title('(b)')
127  legend('u_1 \neq  0, u_2 \neq 0 , u_3 = 0 ','u_i = 0, i=1,2,3 ')
128
129  subplot(2,2,3)
130   plot(Tx,X(:,5),'-b',T, Y(:,5),'--r','LineWidth',1.5);
131  %ylim([250 800])
132   ylabel('M(t)');
133   xlabel('Time (days)');
134    title('(c)')
135  legend('u_1 \neq  0, u_2 \neq 0 , u_3 = 0 ','u_i = 0, i=1,2,3 ')
136
137  subplot(2,2,4)
138   plot(Tx,Uu(:,1),'-b',Tx,Uu(:,2),'--r',Tx,Uu(:,3),'--k',Tx,1.5);
139    ylim([0 1])
140   ylabel('Control Profile');
141   xlabel('Time (days)');
142    title('(d)')
143   legend('u_1 \neq 0','u_2 \neq  0 ','u_3 = 0 ')
144 % collect all the incidence terms in the ODE
145  X=XX'; % solution of the optimal control
146  U =[0 0 0]; % when no control
147 [Tx,Y] = ode45(@kims,time,y0,[],U,Constant);
148  Y=(Y);
149   Inew=sum(Y(:,2))-sum(X(:,2))+sum(Y(:,3))-sum(X(:,3)) % averted
```

Appendix 3: MATLAB codes for Figures 10, 11, 12, 13 and 14

```
clc
clear all
close all
w =2.5;

fs =12;

o = figure

t0 = 0; tf=200; N=1000; %case 3

time =linspace(t0,tf,N);

  y0  = [1500,2000,200,150,100,80,5,5,200];% initial condition for
      STATE SYSTEM

%--- SOURCES OF CONSTANTS --
Constant=[0.8 1/18250 0.09 0.1 1/70 0.3/365 1/(60*365) 0.42
    13/37500 1.7 0.7 1.12 100000 0.00013/365 0.75 0.8 0.08 35/1000 1
     0.08 1/28 0.2/365 5822 0.89 5822.89 20 40 30 10];

eta      = Constant(1);
b        = Constant(2);
epsilon1= Constant(3);
epsilon2= Constant(4);
gamma1   = Constant(5);
gamma2   = Constant(6);
mu       = Constant(7);
beta1    = Constant(8);
mu1      = Constant(9);
sigma    = Constant(10);
```

```
varrho   = Constant(11);
g        = Constant(12);
K        = Constant(13);
k        = Constant(14);
alpha1   = Constant(15);
alpha2   = Constant(16);
d1       = Constant(17);
d2       = Constant(18);
beta2    = Constant(19);
d3       = Constant(20);
tau1     = Constant(21);
tau2     = Constant(22);
C1       = Constant(23); % weight
C2       = Constant(24); % weight
C3       = Constant(25); % weight
B1       = Constant(26);
B2       = Constant(27);
B3       = Constant(28);
B4       = Constant(29);

lf   = [0 0 0 0 0 0 0 0 0 0];
%% TEST SECTION
init =y0;
init2 =lf;
h = (tf-t0)/N;
u = linspace(0,0,N+1);
u1=u'; u2=u'; u3=u'; u4=u';
U = [u1 u2 u3 u4];
%% IMPLIMENTATION OF THE ALGORITHM
%Test 1 stoping condition 1
delta = 0.001;
X=init;
i=0; %Initialize iteration counter
```

```
mm=size(X);
NumXX =10e10;
Xnew = rand(N+1,mm(2)).*(repmat(X,N+1,1));
DenXnew=norm(Xnew);
while  NumXX/DenXnew>delta
Xold =  Xnew;
oldu = U;
%FORWARD RUNGE KUTTA  FOR STATES
[Tx, X]=rk4foward(@stide,t0, tf,N, init,U,Constant);

% BACKWARD RUNGEKUTA FOR COSTATES
[Tp, P]=rk4back(@stide_costate,t0,tf,N,init2,U,X,Constant);

%UPDATE THE CONTROLS
x = X(1,:); y = X(2,:); v = X(3,:); z = X(4,:); l = X(5,:); q = X
    (6,:); r = X(7,:); s = X(8,:); m = X(9,:);
L1 = P(1,:); L2 = P(2,:); L3 = P(3,:); L4 = P(4,:); L5 = P(5,:);
   L6 = P(6,:); L7 = P(7,:); L8 = P(8,:); L9 = P(9,:);
g1=x+y+v+z+l+q+r+s+m;
lambda1=beta1.*(z+sigma.*q)./(g1);
lambda2=beta2*m./(K+m);
%% Case1_0:u1\neq= 0, u2\neq= 0,u3\neq= 0, u4= 0,
%  u1 =zeros(1,N+1);
%  u2 =zeros(1,N+1);
%  u3 =zeros(1,N+1);
%  u4 =zeros(1,N+1);
%Combination of educational campaign and  treatment of Mtb
    individuals
%% Case1_0:u1\neq= 0, u2\neq= 0,u3\neq= 0, u4= 0,
%  u1 =max(0,min(1,eta*b*g1.*L2./B1));
%  u2 =max(0,min(1,alpha1.*z.*(L4-L7)./B2));
%  u3 =zeros(1,N+1);
%  u4 =zeros(1,N+1);
```

```
%Combination of MDA and  sanitation
%% Case1_1:u1\neq 0, u2\neq 0,u3\neq 0, u4= 0,
%  u1 =zeros(1,N+1);
%  u2 =zeros(1,N+1);
%  u3 =max(0,min(1,(alpha2.*1.*(L5-L8)+alpha2.*q.*(L6-L4))./B3));
%  u4 =max(0,min(1,(lambda2.*L5.*(x+y+r)+lambda2.*L6.*(v+z)-
    lambda2.*x.*L1-lambda2.*y.*L2-lambda2.*v.*L3-lambda2.*z.*L4)./B4
    ));

%Combination of educational campaign and  sanitation
%% Case1_2:u1\neq 0, u2\neq 0,u3\neq 0, u4= 0,
%  u1 =max(0,min(1,eta*b*g1.*L2./B1));
%  u2 =zeros(1,N+1);
%  u3 =zeros(1,N+1);
%  u4 =max(0,min(1,(lambda2.*L5.*(x+y+r)+lambda2.*L6.*(v+z)-
    lambda2.*x.*L1-lambda2.*y.*L2-lambda2.*v.*L3-lambda2.*z.*L4)./B4
    ));
%Combination of treatment of Mtb and  MDA
%% Case1_3:u1\neq 0, u2\neq 0,u3\neq 0, u4= 0,
%  u1 =zeros(1,N+1);
%  u2 =max(0,min(1,alpha1.*z.*(L4-L7)./B2));
%  u3 =max(0,min(1,(alpha2.*1.*(L5-L8)+alpha2.*q.*(L6-L4))./B3));
%  u4 =zeros(1,N+1);

% Case1_4:u1\neq 0, u2\neq 0,u3\neq 0, u4= 0,
      u1 =max(0,min(1,eta*b*g1.*L2./B1));
      u2 =max(0,min(1,alpha1.*z.*(L4-L7)./B2));
      u3 =max(0,min(1,(alpha2.*1.*(L5-L8)+alpha2.*q.*(L6-L4))./B3))
          ;
      u4 =max(0,min(1,(lambda2.*L5.*(x+y+r)+lambda2.*L6.*(v+z)-
          lambda2.*x.*L1-lambda2.*y.*L2-lambda2.*v.*L3-lambda2.*z.*L4
          )./B4));
```

```
118 Uu=[u1' u2' u3' u4'];
119 U = 0.5*Uu + 0.5*oldu; % Convex combination of the controls
120 Xnew =  X';
121 NumXX =abs(norm(Xnew-Xold));
122 DenXnew =norm(Xnew);
123 i=i+1 %Update iteration counter
124 end
125 %% PLOTING
126 X=X';
127 Tx =Tx';
128 XX=X(:,1); YY=X(:,2); VV=X(:,3); ZZ=X(:,4); LL=X(:,5); QQ=X(:,6);
      RR=X(:,7); SS=X(:,8); MM=X(:,9);
129
130 Up = [0 0 0 0];
131 [T,Y] = ode45(@stide,time,y0,[],Up,Constant);
132
133 J =sum((C1.*ZZ(end)+C2.*LL(end)+C3.*QQ(end))+((B1/2)*Uu(:,1).*Uu
      (:,1)+(B2/2)*Uu(:,2).*Uu(:,2)+(B3/2)*Uu(:,3).*Uu(:,3)+(B4/2)*Uu
      (:,4).*Uu(:,4))) %Change to the suitable objective function
134
135  S=[Tx,X];
136
137  save case5;
138  save('case3State', 'S');
139  save('case3Control', 'Uu');
140 save('Cost', 'J');
141
142  figure(1)
143
144  subplot(2,3,1)
145  plot(Tx,X(:,2),'-b',T, Y(:,2),'--r','LineWidth',1.5);
146  %ylim([0 700])
147  ylabel('V(t)');
```

```
148  xlabel('Time (days)');
149  title('(a)')
150 legend({'u_1 \neq 0, u_2 \neq 0 , u_3 = 0 , u_4 = 0 ','u_i = 0,
       i=1,2,3,4 '},'FontSize',7)
151 legend boxoff
152 set(gca,'FontSize',fs)
153 %
154 subplot(2,3,2)
155  plot(Tx,X(:,4),'-b',T, Y(:,4),'--r','LineWidth',1.5);
156   %%ylim([0 700])
157  ylabel('I_T(t)');
158   xlabel('Time (days)');
159    title('(b)')
160 legend({'u_1 \neq 0, u_2 \neq 0 , u_3 = 0 , u_4 = 0 ','u_i = 0,
       i=1,2,3,4 '},'FontSize',7)
161 legend boxoff
162 set(gca,'FontSize',fs)
163
164 subplot(2,3,3)
165  plot(Tx,X(:,5),'-b',T, Y(:,5),'--r','LineWidth',1.5);
166  %ylim([0 600])
167  ylabel('I_H(t)');
168  xlabel('Time (days)');
169   title('(c)')
170
171 legend({'u_1 \neq 0, u_2 \neq 0 , u_3 = 0 , u_4 = 0 ','u_i = 0,
       i=1,2,3,4 '},'FontSize',7)
172 legend boxoff
173 set(gca,'FontSize',fs)
174
175 subplot(2,3,4)
176  plot(Tx,X(:,6),'-b',T, Y(:,6),'--r','LineWidth',1.5);
177  %ylim([250 800])
```

```
178  ylabel('I_{HT}(t)');
179  xlabel('Time (days)');
180   title('(d)')
181
182 legend({'u_1 \neq 0, u_2 \neq 0 , u_3 = 0 , u_4 = 0 ','u_i = 0,
       i=1,2,3,4 '},'FontSize',7)
183 legend boxoff
184 set(gca,'FontSize',fs)
185
186 subplot(2,3,5)
187  plot(Tx,X(:,9),'-b',T, Y(:,9),'--r','LineWidth',1.5);
188  %ylim([250 800])
189  ylabel('M(t)');
190  xlabel('Time (days)');
191   title('(e)')
192
193 legend({'u_1 \neq 0, u_2 \neq 0 , u_3 = 0 , u_4 = 0 ','u_i = 0,
       i=1,2,3,4 '},'FontSize',7)
194 legend boxoff
195 set(gca,'FontSize',fs)
196
197 subplot(2,3,6)
198  %plot(Tx,Uu(:,1),'-b',Tx,Uu(:,2),'--r',Tx,Uu(:,3),'--k',Tx,Uu
       (:,4),'-c', Tx);
199  plot(Tx,Uu(:,1),'-b',Tx,Uu(:,2),'--r',Tx,Uu(:,3),'--c',Tx,Uu(:,4)
       ,'--g','LineWidth',1.5);
200   ylim([0 1])
201  ylabel('Control Profile');
202  xlabel('Time (days)');
203   title('(f)')
204 legend({'u_1 \neq 0', 'u_2 \neq 0' , 'u_3 = 0' , 'u_4 = 0 '},'
      FontSize',7)
205 legend boxoff
```

```
206     set(gca,'FontSize',fs)
207
208 % collect all the incidence terms in the ODE
209  X=XX'; % solution of the optimal control
210  U =[0 0 0 0]; % when no control
211 [Tx,Y] = ode45(@stide,time,y0,[],U,Constant);
212  Y=(Y);
213  Inew=sum(Y(:,6))-sum(X(:,6)) % averted
214
215 % g=1:length(Y(:,6));
216 % figure(2)
217 %
218 % plot(g,Y(:,6),'b','LineWidth',1.5)
219
220 pause
221 set(gca, 'YTickLabel', num2cell(get(gca, 'YTick')))
222 set(o,'Units','Inches');
223
224 pos = get(o,'Position');
225
226 set(o,'PaperPositionMode','Auto','PaperUnits','Inches','PaperSize'
      ,[pos(3), pos(4)])
227  print(o,'C:\Users\DELL\Dropbox\Fluid\figures\figure1','-dpdf','-
       r1000')
```

APPENDIX 4: MATLAB codes for Figures 17, 18, and 19

```
clear all
close all
%w =2.5;

fs =12;



nu = 0.0004;
theta1=2;
theta2=3;
K1=10000;
K2=10000;
alpha1=0.01;
lambda1=0.05;
lambda2=0.01;
pi=10^8;
delta1=0.52;
delta2=0.12;
delta3=0.02;
varphi=0.9;


R1=delta3*nu./(delta1*lambda2)
R2=delta3*lambda1./(delta2*lambda2)

z = figure
fx1= @(t,x)[nu*x(1)*(1-x(1)./pi) - delta1*x(1)*x(3);
      lambda1*x(2)-delta2*x(2)*x(3);
      lambda2+(theta1*x(2)./(K1+x(2)))*x(3)+(theta2*x(1)./(K2+varphi
          *x(3)+alpha1*x(1)))*x(3)-delta3*x(3)];
```

```
[t,x1]=ode45(fx1,[0  14],[1000,1500,1]);
 figure (1)
plot(t,x1(:,1),'-r','lineWidth',1.5)
 grid off

xlabel('Time (Days)')
ylabel('Bacteria Population')
legend({' B_0 =  1000', 'B_1 =  500' , 'B_2 = 300'},'FontSize',7)
 legend boxoff
% ylim([0  1.5])
hold on
set(gca,'FontSize',fs)
fx1= @(t,x)[nu*x(1)*(1-x(1)./pi) - delta1*x(1)*x(3);
     lambda1*x(2)-delta2*x(2)*x(3);
     lambda2+(theta1*x(2)./(K1+x(2)))*x(3)+(theta2*x(1)./(K2+varphi
        *x(3)+alpha1*x(1)))*x(3)-delta3*x(3)];
[t,x1]=ode45(fx1,[0  14],[500,1500,1]);
figure (1)
plot(t,x1(:,1),'-k','lineWidth',1.5)
 grid off

xlabel('Time (Days)')
ylabel('Bacteria Population')
 %ylim([0  1.5])
 legend({' B_0 =  1000', 'B_1 =  500' , 'B_2 = 300'},'FontSize',7)
  legend boxoff
hold on
set(gca,'FontSize',fs)
fx1= @(t,x)[nu*x(1)*(1-x(1)./pi) - delta1*x(1)*x(3);
     lambda1*x(2)-delta2*x(2)*x(3);
      lambda2+(theta1*x(2)./(K1+x(2)))*x(3)+(theta2*x(1)./(K2+
         varphi*x(3)+alpha1*x(1)))*x(3)-delta3*x(3)];
[t,x1]=ode45(fx1,[0  14],[300,1500,1]);
```

```
62 plot(t,x1(:,1),'-b','lineWidth',1.5)%Graph of infected population
63  grid off
64
65 xlabel('Time (Days)')
66 ylabel('Bacteria Population')
67 %  ylim([0 1.5])
68 legend({' B_0 =  1000', 'B_1 =  500' , 'B_2 = 300'},'FontSize',7)
69  legend boxoff
70 set(gca,'FontSize',fs)
71 set(gca, 'YTickLabel', num2cell(get(gca, 'YTick')))
72 set(z,'Units','Inches');
73 pos = get(z,'Position');
74 set(z,'PaperPositionMode','Auto','PaperUnits','Inches','PaperSize'
     ,[pos(3), pos(4)])
75  print(z,'C:\Users\DELL\Dropbox\Fluid\figures\figure_01','-dpdf','
     -r1000')
76 hold off
77
78
79
80
81
82
83
84
85 %%%%SECOND FIGURE
86
87 z = figure
88 fx2= @(t,x)[nu*x(1)*(1-x(1)./pi) - delta1*x(1)*x(3);
89      lambda1*x(2)-delta2*x(2)*x(3);
90       lambda2+(theta1*x(2)./(K1+x(2)))*x(3)+(theta2*x(1)./(K2+
           varphi*x(3)+alpha1*x(1)))*x(3)-delta3*x(3)];
91
```

```
92  [t,x2]=ode45(fx2,[0  14],[1000,1500,1]);
93   figure (2)
94  plot(t,x2(:,2),'r','lineWidth',1.5)%Graph of infected population
95   grid off
96   %title ('Infectious Population before Intervension')
97  xlabel('Time (Days)')
98  ylabel('Parasite Population')
99  legend({' P_0 =  1500', 'P_1 =  800' , 'P_2 = 400'},'FontSize',7)
100  legend boxoff
101 hold on
102 set(gca,'FontSize',fs)
103
104 fx2= @(t,x)[nu*x(1)*(1-x(1)./pi) - delta1*x(1)*x(3);
105      lambda1*x(2)-delta2*x(2)*x(3);
106       lambda2+(theta1*x(2)./(K1+x(2)))*x(3)+(theta2*x(1)./(K2+
             varphi*x(3)+alpha1*x(1)))*x(3)-delta3*x(3)];
107
108 [t,x2]=ode45(fx2,[0  14],[1000,800,1]);
109  figure (2)
110 plot(t,x2(:,2),'k','lineWidth',1.5)%Graph of infected population
111  grid off
112  %title ('Infectious Population before Intervension')
113 xlabel('Time (Days)')
114 ylabel('Parasite Population')
115 legend({' P_0 =  1500', 'P_1 =  800' , 'P_2 = 400'},'FontSize',7)
116 hold on
117 set(gca,'FontSize',fs)
118
119 fx2= @(t,x)[nu*x(1)*(1-x(1)./pi) - delta1*x(1)*x(3);
120      lambda1*x(2)-delta2*x(2)*x(3);
121       lambda2+(theta1*x(2)./(K1+x(2)))*x(3)+(theta2*x(1)./(K2+
             varphi*x(3)+alpha1*x(1)))*x(3)-delta3*x(3)];
122
```

```
123 [t,x2]=ode45(fx2,[0  14],[1000,400,1]);
124   figure (2)
125 plot(t,x2(:,2),'b','lineWidth',1.5)%Graph of infected population
126  grid off
127  %title ('Infectious Population before Intervension')
128 xlabel('Time (Days)')
129 ylabel('Parasite Population')
130 legend({' P_0 =  1500', 'P_1 =  800' , 'P_2 = 400'},'FontSize',7)
131
132 set(gca,'FontSize',fs)
133
134 set(gca, 'YTickLabel', num2cell(get(gca, 'YTick')))
135 set(z,'Units','Inches');
136
137 pos = get(z,'Position');
138
139 set(z,'PaperPositionMode','Auto','PaperUnits','Inches','PaperSize'
      ,[pos(3), pos(4)])
140  print(z,'C:\Users\DELL\Dropbox\Fluid\figures\figure_02','-dpdf','
      -r1000')
141
142
143
144
145  %%%%THIRD FIGURE
146 z = figure
147 fx3= @(t,x)[nu*x(1)*(1-x(1)./pi) - delta1*x(1)*x(3);
148       lambda1*x(2)-delta2*x(2)*x(3);
149        lambda2+(theta1*x(2)./(K1+x(2)))*x(3)+(theta2*x(1)./(K2+
             varphi*x(3)+alpha1*x(1)))*x(3)-delta3*x(3)];
150
151 [t,x3]=ode45(fx3,[0  50],[1000,1500,0.6]);
152  figure (3)
```

```
153 plot(t,x3(:,3),'r','lineWidth',1.5)%Graph of infected population
154  grid off
155  %title ('Infectious Population before Intervension')
156 xlabel('Time (Days)')
157 ylabel('Immune Competence')
158 legend({' E_0 =  0.6', 'E_1 =  1' , 'E_2 = 2'},'FontSize',7)
159 hold on
160 set(gca,'FontSize',fs)
161
162 fx3= @(t,x)[nu*x(1)*(1-x(1)./pi) - delta1*x(1)*x(3);
163      lambda1*x(2)-delta2*x(2)*x(3);
164      lambda2+(theta1*x(2)./(K1+x(2)))*x(3)+(theta2*x(1)./(K2+varphi
           *x(3)+alpha1*x(1)))*x(3)-delta3*x(3)];
165
166 [t,x3]=ode45(fx3,[0  50],[1000,1500,1]);
167  figure (3)
168 plot(t,x3(:,3),'k','lineWidth',1.5)%Graph of infected population
169  grid off
170  %title ('Infectious Population before Intervension')
171 xlabel('Time (Days)')
172 ylabel('Immune Competence')
173 legend({' E_0 =  0.6', 'E_1 =  1' , 'E_2 = 2'},'FontSize',7)
174 hold on
175 set(gca,'FontSize',fs)
176
177
178 fx3= @(t,x)[nu*x(1)*(1-x(1)./pi) - delta1*x(1)*x(3);
179      lambda1*x(2)-delta2*x(2)*x(3);
180       lambda2+(theta1*x(2)./(K1+x(2)))*x(3)+(theta2*x(1)./(K2+
           varphi*x(3)+alpha1*x(1)))*x(3)-delta3*x(3)];
181
182 [t,x3]=ode45(fx3,[0  50],[1000,1500,2]);
183  figure (3)
```

```
184 plot(t,x3(:,3),'b','lineWidth',1.5)%Graph of infected population
185  grid off
186  %title ('Infectious Population before Intervension')
187 xlabel('Time (Days)')
188 ylabel('Immune Competence')
189 legend({' E_0 = 0.6', 'E_1 = 1' , 'E_2 = 2'},'FontSize',7)
190
191 set(gca,'FontSize',fs)
192
193
194 set(gca, 'YTickLabel', num2cell(get(gca, 'YTick')))
195 set(z,'Units','Inches');
196
197 pos = get(z,'Position');
198
199 set(z,'PaperPositionMode','Auto','PaperUnits','Inches','PaperSize'
    ,[pos(3), pos(4)])
200       ax=gca
201       ax.YTick = [0:1:5];
202      tix=get(gca,'ytick')';
203     set(gca,'yticklabel',num2str(tix,'%.1f'))
204     legend boxoff
205  print(z,'C:\Users\DELL\Dropbox\Fluid\figures\figure_03','-dpdf','
     -r1000')
```

RESEARCH OUTPUTS

1.0 Two puplications were made from this dissertation

1.1 Lambura, A. G., Mwanga G. G, Luboobi, L., & Kuznetsov, D. (2020). Mathematical model for optimal control of soil-Transmitted helminth infection. *Computational and Mathematical Methods in Medicine*, (2020), 1-15. https://doi.org/10.1155/2020/6721919

1.2 Lambura, A. G., Mwanga G. G., Luboobi, L., & Kuznetsov, D. (2020). Modeling the effects of helminth infection on the transmission dynamics of Mycobacterium tuberculosis under optimal control strategies. *Computational and Mathematical Methods in Medicine*, (2020), 1-21. https://doi.org/10.1155/2020/8869377

2.0 Poster on mathematical modeling for helminths and Mycobacterium tuberculosis co-infection

Hindawi
Computational and Mathematical Methods in Medicine
Volume 2020, Article ID 6721919, 15 pages
https://doi.org/10.1155/2020/6721919

Research Article

Mathematical Model for Optimal Control of Soil-Transmitted Helminth Infection

Aristide G. Lambura,[1,2] **Gasper G. Mwanga**,[3] **Livingstone Luboobi**,[1,4] **and Dmitry Kuznetsov**[1]

[1]*School of Computational and Communication Science and Engineering, The Nelson Mandela African, Institution of Science and Technology, P.O. Box 447, Arusha-, Tanzania*
[2]*Department of Computer Systems and Mathemmatics, Ardhi University, P.O. Box 35176, Dar es Salaam, Tanzania*
[3]*Department of Physcics, Mathematics and Informatics, University of Dar es Salaam, P.O. Box 2329, Dar es Salaam, Tanzania*
[4]*Institute of Mathematical Sciences, Strathmore University, P.O. Box 59857-00200, Nairobi, Kenya*

Correspondence should be addressed to Aristide G. Lambura; lamburaa@nm-aist.ac.tz

Received 14 March 2020; Revised 11 May 2020; Accepted 19 June 2020; Published 1 August 2020

Academic Editor: Konstantin Blyuss

In this paper, we study the dynamics of soil-transmitted helminth infection. We formulate and analyse a deterministic compartmental model using nonlinear differential equations. The basic reproduction number is obtained and both disease-free and endemic equilibrium points are shown to be asymptotically stable under given threshold conditions. The model may exhibit backward bifurcation for some parameter values, and the sensitivity indices of the basic reproduction number with respect to the parameters are determined. We extend the model to include control measures for eradication of the infection from the community. Pontryagian's maximum principle is used to formulate the optimal control problem using three control strategies, namely, health education through provision of educational materials, educational messages to improve the awareness of the susceptible population, and treatment by mass drug administration that target the entire population(preschool- and school-aged children) and sanitation through provision of clean water and personal hygiene. Numerical simulations were done using MATLAB and graphical results are displayed. The cost effectiveness of the control measures were done using incremental cost-effective ratio, and results reveal that the combination of health education and sanitation is the best strategy to combat the helminth infection. Therefore, in order to completely eradicate soil-transmitted helminths, we advise investment efforts on health education and sanitation controls.

1. Introduction

The worldwide burden of helminth (worm) infection cannot be underestimated. It is estimated that over 1.5 billion people worldwide are infected with helminths [1]. Soil-transmitted helminths are among the NTDs which mostly affect the poorest and the resource-constrained populations of the world. Soil-transmitted helminths are caused by interstinal parasitic nematode hookworm, Ascaries lumbriocoides and Trichuris trichiura species through ingesting eggs in unwashed undercooked vegetables and unpeeled fruits in contaminated water sources or ingestion of eggs by children who play in contaminated environment. More than 267 million preschool-aged children and more than 568 million school-aged children (SAC) live in endemic areas where these parasites are highly transmitted. This establishes chronic infections over time which hinders and impairs the developmental and cognitive growth of both preschool- and school-aged children which in turn affect their academic performance. It also has social and economic deficits [2]. The possibility of elimination of the helminth infection is by reducing the number of worms/parasites in a host, but this cannot be achieved without application of other means of reducing the density of

parasites from the contaminated environment. Hence proper treatment of the helminth infection and effective control strategy that target this group and infected adults is needed. Currently, there are control programmes to combat the disease which include regular treatment by mass drug administration (MDA), water sanitation, and health education. To reduce the morbidity of the soil-transmitted helminth, antihelminthic drugs like albendazole and benzimidazole have been used for decades but still there has not been an optimal application of the existing control measures with these treatment alternatives in endemic areas [3, 4].

Over years, mathematical models have helped to improve our understanding of population dynamics and provide tools for the assessment and evaluation of a number of control programmes in place. The mathematical model for the helminth infection can be traced back to the papers by [4–6]. Deterministic mathematical models inform policymakers to realize the effort required to increase control coverage for the achievement of less than one percent prevalence and intensity of soil-transmitted helminths by 2020 [7]. These models have been used intensively but none have applied optimal control for the soil-transmitted helminth infection.

However, optimization of the existing interventions tools for the helminth infection has been the priority research areas to examine their impact and sustainability [8]. The study on the implementation of these control measures and how to deliver them optimally is of great importance. Thus, in this study, we consider optimal control of the helminth mathematical model with the preventive measures (health education) to sensitize the susceptible population and treatment by mass drug administration and sanitation. The preventive measures include provision of education materials and educational messages and sanitation include proper provision of clean water, personal hygiene, and installation of public toilets while MDA is administered to the entire population (pre-SAC and SAC), but for the healthy individuals (susceptible and recovered), this treatment procedure becomes placebo.

2. Materials and Methods

2.1. Model Formulation. For modeling, the total human population is divided into four subpopulations $S(t)$, $E(t)$, $I(t)$, and $R(t)$. $S(t)$ represents the number of individuals who are not infected but can be infected by helminth parasites. $E(t)$ represents the number of individuals exposed to helminth infection but not infectious. $I(t)$ represents the number of individuals infested with parasitic worms. $R(t)$ represents the number of individuals recovered from the helminth infection. $M(t)$ represents the parasite population in the environment. Individuals in the susceptible class contract infection after a sufficient contact with the contaminated environment. All the newborns enter a susceptible class at the rate b and are moved to the exposed class at the rate λ. Individuals in the exposed class are being reinfected as they interact with contaminated environment but remain latent for a period of $1/\rho$, where ρ is the progression rate from the exposed to infective class. Again, we assume that an infected individual contaminate the environment at rate ε but do not acquire new infection; hence, individuals in the infected class are moved to the recovered class as the result of natural immunity at the rate q. Also, we assume that the recovered individuals are aware of infection so that individuals in this class may not interact with contaminated environment; furthermore, they have temporary immunity against the infection. Hence, individuals in the recovered class return to the susceptible class at a rate γ due to loss of immunity and awareness.

The infected individuals contaminate the environment at the rate ε as they defecate outside the latrines to increase the concentration of parasitic worms in the soil. The parasitic worms in the soil infect human population at the rate

$$\lambda = \frac{\beta M}{K + M}, \tag{1}$$

where β is the intake rate of eggs in contaminated food or larvae that has penetrated the skin to lead the transmission of infection and K is the number (density) of the helminths at which the infection rate is half the maximum rate. The natural mortality in each human class is denoted by μ, and the infectious individuals have added the helminth-induced death rate denoted by d. Further, we assume that the parasitic worms die naturaly at the rate μ_M. The aforementioned assumptions and explanation give the dynamics of the helminth model as illustrated in Figure 1. Model parameters are fully described in Table 1. The model has five nonlinear ordinary differential equations given by system (2).

$$\frac{dS}{dt} = bN + \gamma R - (\mu + \lambda)S, \tag{2}$$

$$\frac{dE}{dt} = \lambda S - (\mu + \rho)E, \tag{3}$$

$$\frac{dI}{dt} = \rho E - (d + \mu + q + \varepsilon)I, \tag{4}$$

$$\frac{dR}{dt} = qI - (\mu + \gamma)R, \tag{5}$$

$$\frac{dM}{dt} = \varepsilon I - \mu_M M, \tag{6}$$

with the condition $S + E + I + R = N$.

From equation (2), we have

$$\frac{dN}{dt} = (b - \mu)N - (d + \varepsilon)I. \tag{7}$$

Hence the dynamics of the helminth model can be investigated by normalizing model (2).

Let $s = S/N$, $e = E/N$, $i = I/N$, $r = R/N$, and $m = M/K$.

Then, equation (7) can be written in terms of fractional variables as

$$\frac{dN}{dt} = (b - \mu - (d + \varepsilon)i)N. \tag{8}$$

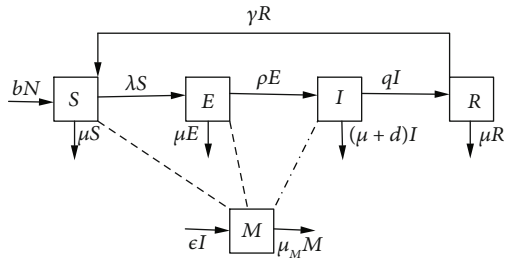

Figure 1: Compartmental diagram for the helminth model. The dashed lines indicate the interaction of human population with contaminated environment to ingest parasitic worms while the dashed line with dot indicate the rate at which individuals infested with helminths releases eggs to contaminate the environment.

Using equation (8) and differentiating the fractional variables with respect to t leads to the following normalized model:

$$\frac{ds}{dt} = b + \gamma r - \left(b + \frac{\beta m}{1+m} - (d+\varepsilon)i\right)s, \tag{9}$$

$$\frac{de}{dt} = \frac{\beta m}{1+m}s - (b + \rho - (d+\varepsilon)i)e, \tag{10}$$

$$\frac{di}{dt} = \rho e - (b + d + q + \varepsilon - (d+\varepsilon)i)i, \tag{11}$$

$$\frac{dr}{dt} = qi - (b + \gamma - (d+\varepsilon)i)r, \tag{12}$$

$$\frac{dm}{dt} = \varepsilon i - \mu_M m. \tag{13}$$

The solutions of system (9) enter the region that is positively invariant given by

$$\Omega = \left\{(s, e, i, r, m) \in \mathbb{R}_+^5 \mid s + e + i + r \le 1, 0 \le m \le 1\right\}. \tag{14}$$

The following theorem guarantees the well posedness of system (9) such that the solutions with nonnegative initial conditions will remain nonnegative for all future time.

Theorem 1. *The region $\Omega \in \mathfrak{R}_+^5$ is positively invariant with respect to system (9) and nonnegative solutions exist for all future time.*

Proof. Given the nonnegative initial conditions, it can be shown that the solutions to system (9), $s(t), e(t), i(t), r(t)$ and$m(t)$ are non-negative for $t > 0$ otherwise we assume a contradiction that there exists a first time t_0 such that $s(t_0) = 0$, $s'(t_0) \le 0$ and $s(t) > 0$, $e(t) > 0$, $i(t) > 0$, $r(t) > 0$, $m(t) > 0$ for $0 < t < t_0$; or there exists t_1 such that $e(t_1) = 0$, $e'(t_1) \le 0$ and $e(t) > 0$, $s(t) > 0$, $i(t) > 0$, $r(t) > 0$, $m(t) > 0$ for $0 < t < t_1$; or there exists t_2 such that $i(t_2) = 0$, $i'(t_2) \le 0$ and $i(t) > 0$, $s(t) > 0$, $e(t) > 0$, $r(t) > 0$, $m(t) > 0$ for $0 < t < t_2$; or there exists t_3 such that $r(t_3) = 0$, $r'(t_3) \le 0$ and $r(t) > 0$, $s(t) > 0$, $e(t) > 0$, $i(t) > 0$, $m(t) > 0$ for $0 < t < t_3$; or there exists t_4 such that $m(t_4) = 0$, $m'(t_4) \le 0$ and $m(t) > 0$, $s(t) > 0$, $e(t) > 0$, $i(t) > 0$, $r(t) > 0$ for $0 < t < t_4$ as in [9].

In the first case, consider the first equation of system (9)

$$\frac{ds(t_0)}{dt} = b + \gamma r(t_0) > 0, \tag{15}$$

which is a contradiction implying that $s(t) > 0$.

In the second case, we have

$$\frac{de(t_1)}{dt} = \frac{\beta m(t_1)s(t_1)}{1 + m(t_1)} \ge 0, \tag{16}$$

if this is true both $s(t_1) \ge 0$ and $m(t_1) \ge 0$. It follows that $e(t_1) \ge 0$ which is a contradiction implying that $e(t) > 0$.

In the third case, we have

$$\frac{di(t_2)}{dt} = \rho e(t_2) > 0, \tag{17}$$

which is a contradiction implying that $i(t) > 0$.

In the fourth case, we have

$$\frac{dr(t_3)}{dt} = (q + \tau)i(t_3) > 0, \tag{18}$$

which is a contradiction implying that $r(t) > 0$.

In the fifth case, we have

$$\frac{dm(t_4)}{dt} = \varepsilon i(t_4) > 0, \tag{19}$$

which is a contradiction implying that $m(t) > 0$.

Hence, in all cases, $s(t)$, $e(t)$, $i(t)$, $r(t)$, and m are all positive for all $t > 0$. Thus, the components of the solutions to system (9) remain positive for all $t > 0$.

Thus, the helminth model is well posed epidemiologically and mathematically. Thus, it is sufficient to consider the dynamics of (9) in Ω [10].

3. Model Analysis

The qualitative analysis of the normalized model (9) is considered in order to get an understanding of the dynamics of the helminth infection.

3.1. The Disease-Free Equilibrium and Basic Reproduction Number. The disease-free equilibrium of model (9) is obtained by equating all the derivatives to zero and then setting $e = 0$, $i = 0$, $r = 0$, and $m = 0$. Thus, we obtain the DFE as

$$\mathscr{E}_0 = (1, 0, 0, 0, 0). \tag{20}$$

The basic reproduction number denoted by $\mathscr{R}_0$ is the quantity that quantifies the ability of the disease to invade the community, and it is the quantity that governs the spread of the disease. Furthermore, it helps in deciding on control strategies to be adopted for disease eradication. Therefore,

Table 1: Parameter values for soil-transmitted helminth infection.

Parameter	Symbol	Value	Source
Per capita birth rate	b	$\frac{1}{18250}\,\text{day}^{-1}$	[27]
Per capita mortality rate	μ	$\frac{1}{(60\times 365)}\,\text{day}^{-1}$	[28]
Disease induced death rate	d	$\frac{35}{1000}\,\text{day}^{-1}$	[27]
Ingestion rate of parasites	β	7 parasites day^{-1}	Assumed
Carrying capacity of parasite in the environment	K	10^5 parasites	Assumed
Natural recovery rate	q	$\frac{1}{28}\,\text{day}^{-1}$	Assumed
Efficacy for MDA drug	κ_2,	0.8	[29]
Immunity waning rate for recovered individuals	γ	$\frac{1}{7}\,\text{day}^{-1}$	[27]
Clearance rate for parasitic worms	μ_M	$\frac{13}{37500}\,\text{day}^{-1}$	[27]
Shading rate of parasites to the environment	ε	0.09 day^{-1}	Assumed
Progression rate from exposed to infected class	ρ	$\frac{1}{10}\,\text{day}^{-1}$	[27]

in our case, $\mathscr{R}_0$ determines the role of parasitic worms/larvae present in the soil to produce secondary infections to the individual hosts.

The next-generation approach is used to obtain $\mathscr{R}_0$ following Diekmann et al. [11]. Using the principles of a next-generation matrix, let

$$\mathscr{F} = \left(\frac{\beta m}{1+m}s, 0, 0, 0\right)^T,$$

$$\mathscr{V} = ((b+\rho-(d+\varepsilon)i)e, (b+d+q+\tau+\varepsilon-(d+\varepsilon)i)i - \rho e, (b+\gamma-(d+\varepsilon)i)r-(\tau+q)i, (\mu_M-\theta)m-\varepsilon i)^T, \tag{21}$$

be the appearance of new infections and transfer on individuals between compartments, respectively. Applying the linearization technique, the Jacobian matrices of $\mathscr{F}$ and $\mathscr{V}$ at DFE $\mathscr{E}_0$ are

$$F = \begin{pmatrix} 0 & 0 & 0 & \beta \\ 0 & 0 & 0 & 0 \\ 0 & 0 & 0 & 0 \\ 0 & 0 & 0 & 0 \end{pmatrix}, \qquad V = \begin{pmatrix} b+\rho & 0 & 0 & 0 \\ -\rho & b+d+q+\varepsilon & 0 & 0 \\ 0 & -(\tau+q) & b+\gamma & 0 \\ 0 & -\varepsilon & 0 & \mu_M \end{pmatrix}. \tag{22}$$

The basic reproduction number $\mathscr{R}_0$ is the spectral radius of the next-generation matrix FV^{-1}. Thus,

$$\mathscr{R}_0 = \frac{\rho\varepsilon\beta}{\mu_M(b+\rho)(d+b+q+\varepsilon)}, \tag{23}$$

From (23), the fraction $\beta/(b+d+q+\varepsilon)$ represents the average number of susceptible individuals being infected during the infectious period, and the fraction $\rho/(b+\rho)$ represents the proportion of individuals that survives the latent period, while ε/μ_M represents the fraction of parasites diminished from the environment.

3.2. Stability of DFE. We state Theorem 2 for the stability of the DFE.

Theorem 2. *The disease-free equilibrium of model (9) is LAS if $\mathscr{R}_0 < 1$ and unstable if $\mathscr{R}_0 > 1$.*

Proof. To investigate the local stability of the DFE at $\mathscr{E}_0$, we obtain the Jacobian matrix of equation (9), i.e.,

$$J_{\mathscr{E}_0} = \begin{pmatrix} -b & 0 & -(d+\varepsilon) & \gamma & -\beta \\ 0 & -(b+\rho) & 0 & 0 & \beta \\ 0 & \rho & -(b+d+q+\varepsilon) & 0 & 0 \\ 0 & 0 & q & -(b+\gamma) & 0 \\ 0 & 0 & \varepsilon & 0 & -\mu_M \end{pmatrix}. \tag{24}$$

Clearly, $\lambda_1 = -b$ and $\lambda_2 = -(b+\gamma)$ are the first and second eigenvalues of the Jacobian matrix $J_{\mathscr{E}_0}$ which are strictly

negative. The remaining three can be obtained by considering the submatrix $J^1_{\mathscr{E}_0}$:

$$J^1_{\mathscr{E}_0} = \begin{pmatrix} -(b+\rho) & 0 & \beta \\ \rho & -(b+d+q+\varepsilon) & 0 \\ 0 & \varepsilon & -\mu_M \end{pmatrix}. \quad (25)$$

From equation (25), the characteristic equation is given by

$$f(\lambda) = \lambda^3 + d_2\lambda^2 + d_1\lambda + d_0 = 0, \quad (26)$$

where

$$d_2 = 2b + d + q + \rho + \varepsilon + \mu_M, \quad (27)$$

$$d_1 = (b+\rho)(b+d+q+\varepsilon) + \mu_M(2b+d+q+\rho+\varepsilon), \quad (28)$$

$$d_0 = \mu_M(b+\rho)(b+d+q+\varepsilon) - \varepsilon\rho\beta. \quad (29)$$

Applying the Routh-Hurwitz criteria [12], the conditions in (27) $d_0 > 0$,$d_1 > 0$, $d_2 > 0$, and $d_2d_1 > d_0$. Here, $d_1 > 0$, $d_2 > 0$, and $d_0 > 0$ when $\mathscr{R}_0 \le 1$, and then $d_2d_1 > d_0$. Hence, according to the Routh-Hurwitz criteria, the submatrix $J^1_{\mathscr{E}_0}$ has negative real parts whenever $\mathscr{R}_0 \le 1$.

Thus, the DFE, $\mathscr{E}_0$ is locally asymptotically stable if $\mathscr{R}_0 < 1$.

3.3. Global Stability of the Disease-Free Equilibrium. For the proof of global stability, we consider the theorem developed by Castillo-Chavez et al. [13] and later applied in [14, 15].

To apply the theorem, system (9) is written in the form

$$\frac{dX}{dt} = F(X, Z), \quad (30)$$

$$\frac{dZ}{dt} = G(X, Z), G(X, 0) = 0 \quad (31)$$

where $X = (s, r) \in \mathbb{R}^2_+$ denotes the number of uninfected components (individuals) and $Z = (e, i, m) \in \mathbb{R}^3_+$ denotes infected components (individuals) including the latent and infectious individuals.

The disease-free equilibrium is now denoted by $\mathscr{E}_0 = (X^*, 0) = (1, 0)$.

The conditions (H1) and (H2) in system (32) must be satisfied to guarantee local asymptotic stability:

$$H1 : \text{For } \frac{dX}{dt} = F(X^*, 0), X^* \text{ is globally asymptotically stable, and}$$

$$H2 : G(X, Z) = AZ - \widehat{G}(X, Z), \widehat{G}(X, Z) \ge 0 \text{ for } (X, Z) \in \Omega, \quad (32)$$

where $A = D_Z G(X^*, 0)$ is the Metzeler-matrix (the off-diagonal elements of A are nonnegative) and Ω is the region where the model makes biological sense.

If system (30) satisfies the two conditions in (32), then the following theorem holds.

Theorem 3. *The disease fixed point $\mathscr{E}_0 = (X^*, 0)$ is globally asymptotically stable of system (30) provided that $\mathscr{R}_0 < 1$ and that conditions H1 and H2 are satisfied.*

Proof. From system (9) we have,

$$F(X, Z) = \begin{pmatrix} b + \gamma r - \left(b + \dfrac{\beta m}{1+m} - (d+\varepsilon)i\right)s \\ qi - (b + \gamma - (d+\varepsilon)i)r \end{pmatrix}, \quad (33)$$

$$G(X, Z) = \begin{pmatrix} \dfrac{\beta m}{1+m}s - (b+\rho-(d+\varepsilon)i)e \\ \rho e - (b+d+q+\varepsilon-(d+\varepsilon)i)i \\ \varepsilon i - \mu_M m \end{pmatrix}, \quad (34)$$

Then, system (33) can be reduced to

$$\left.\frac{dX}{dt}\right|_{Z=0} = \begin{pmatrix} b - bs \\ 0 \end{pmatrix}. \quad (35)$$

Now, condition H1 is satisfied as it can be observed from the solution, namely, $s(t) = 1 + (s(0) - 1)e^{-bt}$. As $t \longrightarrow \infty$, the solution $s(t) \longrightarrow 1$ implying global convergence of solution of (35) in Ω. Thus, condition H1 is satisfied.

Let

$$A = \begin{pmatrix} -(b+\rho) & 0 & \beta \\ \rho & -(b+d+q+\varepsilon) & 0 \\ 0 & \varepsilon & -\mu_M \end{pmatrix}, \quad (36)$$

Then,

$$\widehat{G}(X, Z) = \begin{pmatrix} \widehat{G_1}(X, Z) \\ \widehat{G_2}(X, Z) \\ \widehat{G_3}(X, Z) \end{pmatrix} = \begin{pmatrix} \left(1 - \dfrac{s}{1+m}\right)\beta m - (d+\varepsilon)ie \\ -(d+\varepsilon)i^2 \\ 0 \end{pmatrix}. \quad (37)$$

From above, $\widehat{G}(X, Z) \ge 0$ if and only if $d = \varepsilon = 0$. Thus, $\mathscr{E}_0$ may not be globally asymptotically stable for some parameter values. This suggests the possibility of backward bifurcation of Section 3.5.

3.4. Existence of Endemic Equilibrium. The endemic equilibrium $\mathscr{E}^*$ of model (9) is defined as the steady state solution which occurs when disease persists in the community and is obtained by equating the derivatives of system (9) to zero. If we denote the force of infection as $\lambda^* = \beta m/1 + m$ at steady states and let $z^* = b - (d+\varepsilon)i^*$ for any choice of

i^* at the endemic equilibrium; then, the endemic equilibrium can be expressed in terms of the force of infection as

$$s^* = \frac{b(\gamma + z^*)(\rho + z^*)(d + q + z^* + \varepsilon)}{\Delta_3 + (z^*)^3(\lambda^* + \Delta_1) + (z^*)^2(\lambda^*\Delta_1 + \rho(\gamma + \Delta_2) + \gamma\Delta_2) + z^*\Delta_4 + (z^*)^4}, \tag{38}$$

$$e^* = \frac{b\lambda^*(\gamma + z^*)(\Delta_2 + z^*)}{(\gamma + z^*)(\lambda^* + z^*)(\rho + z^*)(\Delta_2 + z^*) - \gamma\lambda^* q\rho}, \tag{39}$$

$$i^* = \frac{b\lambda^*\rho(\gamma + z^*)}{\Delta_3 + (z^*)^3(\lambda^* + \Delta_1) + (z^*)^2(\lambda^*\Delta_1 + \rho(\gamma + \Delta_2) + \gamma\Delta_2) + z^*\Delta_4 + (z^*)^4}, \tag{40}$$

$$r^* = \frac{b\lambda^* q\rho}{\Delta_3 + (z^*)^3(\lambda^* + \Delta_1) + (z^*)^2(\lambda^*\Delta_1 + \rho(\gamma + \Delta_2) + \gamma\Delta_2) + z^*\Delta_4 + (z^*)^4}, \tag{41}$$

$$m^* = \frac{b\lambda^*\rho\varepsilon(\gamma + z^*)}{\mu_M\left(\Delta_3 + (z^*)^3(\lambda^* + \Delta_1) + (z^*)^2(\lambda^*\Delta_1 + \rho(\gamma + \Delta_2) + \gamma\Delta_2) + z^*\Delta_4 + (z^*)^4\right)}, \tag{42}$$

where

$$\begin{aligned}
\Delta_1 &= \gamma + d + q + \rho + \varepsilon,\\
\Delta_2 &= d + q + \varepsilon,\\
\Delta_3 &= \gamma\lambda^*\rho(d + \varepsilon),\\
\Delta_4 &= (\lambda^*(\rho(\gamma + \Delta_2) + \gamma\Delta_2) + \gamma\rho\Delta_2).
\end{aligned} \tag{43}$$

Using equation five of (38) and the force of infection $\lambda^* = \beta m^*/(1 + m^*)$ with the model parameters, then (38) satisfies the following polynomial:

$$\lambda^* P(\lambda^*) = \lambda^*(A\lambda^* + B) = 0, \tag{44}$$

where

$$\begin{aligned}
A &= \mu_M(\gamma\rho(d + \varepsilon) + z^*(\rho(\gamma + d + q + \varepsilon) + \gamma(d + q + \varepsilon)\\
&\quad + z^*(\gamma + d + q + \rho + z^* + \varepsilon))),\\
B &= \mu_M z^*(\gamma + z^*)(\rho + z^*)(d + q + \varepsilon + z^*)(1 - \mathscr{R}_0).
\end{aligned} \tag{45}$$

In equation (44), $\lambda^* = 0$ corresponds to the disease free equilibrium and the polynomial $P(\lambda^*) = 0$ corresponds to the existence of endemic equilibrium which co-exist with disease free equilibrium point when $\mathscr{R}_0 < 1$.

3.5. Bifurcation Analysis. To investigate the type of bifurcation model (9) exhibits, we use the center manifold theory of Castillo-Chavez and Song [16]. To apply the center manifold theory we make the change of variables for the normalized helminth model (9). Let $x_1 = s$, $x_2 = e$, $x_3 = i$, $x_4 = r$, and $x_5 = m$. Using the vector notation $X = (x_1, x_2, x_3, x_4, x_5)^T$, then (9) can be written in the form $dX/dt = F(x)$ with $F = (f_1, f_2, f_3, f_4, f_5)^T$. If we choose $\beta = \beta^*$ as the bifurcation parameter and solving for $\mathscr{R}_0 = 1$ we have:

$$\begin{cases}
f_1 &= b + \gamma x_4 - \left(b + \dfrac{\beta^* x_5}{1 + x_5} - (d + \varepsilon)x_3\right)x_1,\\
f_2 &= \dfrac{\beta^* x_5}{1 + x_5}x_1 - (b + \rho - (d + \varepsilon)x_3)x_2,\\
f_3 &= \rho x_2 - (b + d + q + \varepsilon - (d + \varepsilon)x_3)x_3,\\
f_4 &= (q + \tau)x_3 - (b + \gamma - (d + \varepsilon)x_3)x_4,\\
f_5 &= \varepsilon x_3 - \mu_M x_5,
\end{cases} \tag{46}$$

where

$$\beta^* = \frac{\mu_M(b + \rho)(d + b + q + \varepsilon + \tau)}{\varepsilon\rho}. \tag{47}$$

Now, the matrix W at DFE $\mathscr{E}_0$ of the equations (46) is

$$W = \begin{pmatrix}
-b & 0 & -(d + \varepsilon) & \gamma & -\beta\\
0 & -(b + \rho) & 0 & 0 & \beta\\
0 & \rho & -(b + d + q + \varepsilon) & 0 & 0\\
0 & 0 & q & -(b + \gamma) & 0\\
0 & 0 & \varepsilon & 0 & -\mu_M
\end{pmatrix}, \tag{48}$$

At the value $\mathscr{R}_0 = 1$, the Jacobian W has a simple zero eigenvalue whose corresponding left and right eigenvectors are expressed as

$$\begin{aligned} w_1 &= \left(\frac{\mu_M\gamma q - (b+\gamma)(\mu_M(d+\varepsilon)+\varepsilon\beta)}{b(b+\gamma)}\right)w_3,\\ w_2 &= \frac{\beta^*\varepsilon w_3}{\mu_M(b+\rho)},\\ w_3 &= w_3 > 0 \text{ is free},\\ w_4 &= \frac{qw_3}{b+\gamma},\\ w_5 &= \frac{\varepsilon w_3}{\mu_M},\\ v_1 &= v_4 = 0,\\ v_2 &= \frac{\rho v_3}{b+\rho},\\ v_3 &= v_3 > 0 \text{ is free},\\ v_5 &= \frac{\rho\beta^* v_3}{\mu_{M(b+\rho)}}. \end{aligned} \tag{49}$$

Using the result in [16], we need to compute the coefficients a and b where

$$\begin{aligned} a &= \sum_{k,i,j=1}^{5} v_k w_i w_j \frac{\partial^2 f_k}{\partial x_i \partial x_j}(\mathscr{E}_0, \beta^*),\\ b &= \sum_{k,i=1}^{5} v_k w_i \frac{\partial^2 f_k}{\partial x_i \partial \beta^*}(\mathscr{E}_0, \beta^*) \end{aligned} \tag{50}$$

Now, evaluating the partial derivatives of system (46) at $(\mathscr{E}_0, \beta^*)$, we obtain

$$\begin{aligned} \frac{\partial^2 f_1}{\partial x_1 \partial x_5} &= -\beta^*, \quad \frac{\partial^2 f_1}{\partial x_3 \partial x_1} = d+\varepsilon,\\ \frac{\partial^2 f_2}{\partial x_1 \partial x_5} &= \beta^*,\\ \frac{\partial^2 f_2}{\partial x_3 \partial x_2} &= d+\varepsilon,\\ \frac{\partial^2 f_3}{\partial x_3^2} &= 2(d+\varepsilon),\\ \frac{\partial^2 f_4}{\partial x_3 \partial x_4} &= d+\varepsilon. \end{aligned} \tag{51}$$

Furthermore,

$$\begin{aligned} \frac{\partial^2 f_1}{\partial x_5 \partial \beta^*} &= -1,\\ \frac{\partial^2 f_2}{\partial x_5 \partial \beta^*} &= 1. \end{aligned} \tag{52}$$

Therefore,

$$a = \frac{v_3 w_3^2 \rho}{b\mu_M(b+\rho)^2(b+\gamma)}\varepsilon\beta^* a_0 + 2(d+\varepsilon)v_3 w_3^2. \tag{53}$$

where

$$\begin{aligned} a_0 &= (b+\rho)[\mu_M\gamma q - (b+\gamma)(\mu_M(d+\varepsilon)+\varepsilon\beta^*)] + b(b+\gamma),\\ b &= \frac{\rho\varepsilon\beta^*}{\mu_M(b+\rho)^2}v_3 w_3. \end{aligned} \tag{54}$$

The coefficient b is positive. By Castillo-Chavez and Song [16], coefficient a decides the local dynamics of $\mathscr{E}_0$. Therefore, if $a_0 < 0$, then system (9) will exhibit forward bifurcation, and if $a_0 > 0$, it undergoes backward bifurcation.

3.6. Sensitivity Analysis of the Model Parameters. Numerical sensitivity analysis is done by computing sensitivity indices of basic reproduction number $\mathscr{R}_0$ which measures the model robustness to parameter values [17]. The forward sensitivity index of a variable to a parameter is a ratio of the relative change in the variable to the relative change in the parameter.

Definition 4. The normalized forward sensitivity index of a variable u that depends differentiable on a parameter ς is defined as $r_\varsigma^u = (\partial u/\partial\varsigma).\varsigma/u$.

From equation (23), we compute the sensitivity indices of each parameter involved in $\mathscr{R}_0$ using the equation $r_\varsigma^{\mathscr{R}_0} = (\partial\mathscr{R}_0/\partial\varsigma).(\varsigma/\mathscr{R}_0)$. For example, the sensitivity index of parameter value with respect to β is given by $r_\beta^{\mathscr{R}_0} = (\partial\mathscr{R}_0/\partial\beta).(\beta/\mathscr{R}_0) = 1$ and other indices are $r_\rho^{\mathscr{R}_0}$, $r_\varepsilon^{\mathscr{R}_0}$, $r_{\mu_M}^{\mathscr{R}_0}$, $r_b^{\mathscr{R}_0}$, $r_d^{\mathscr{R}_0}$, and $r_q^{\mathscr{R}_0}$ which were obtained and evaluated using parameter values in Table 1 as illustrated in Figure 2.

To determine the most sensitive parameters for the dynamics of the model, sensitivity analysis was carried out to determine the model robustness to parameter values. Clearly β, ρ, and ε have positive indices with most sensitive parameter be β and the least positively sensitive parameter ρ. This imply that the endemicity of the disease increases when the parameters β, ρ, and ε are increased while keeping other parameters constant. On the other hand, the parameters μ_M, b, d, and q have negative indices and when each of these are decreased, while keeping the other parameters constantly decreases the value of $\mathscr{R}_0$ implying that they decrease

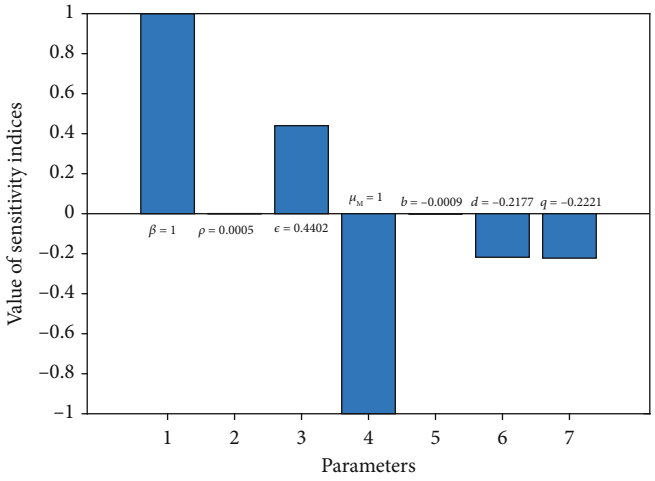

FIGURE 2: Sensitivity analysis of $\mathcal{R}_0$ with respect to each model parameter.

the endemicity of the disease. Thus, based on these results, we suggest the following interventions to be made for the eradication of the helminth infection from the endemic communities. The first intervention is the mass cleanliness to reduce the concentration of the parasites from the contaminated environment. The other one is the use of anthelmintic drugs including MDA for both healthy and infected individuals which will in turn reduce the shedding rate of the parasite to the environment.

3.7. Extension of the Model to Optimal Control. In this section, we extend the heminth model (2) by incorporating three time-dependent control measures. The best intervention strategies will be identified from combination of these control measures so as to minimize the infection from the community. The optimal control model for helminth infection is formulated by considering the following controls:

(1) Health education control $u_1(t)$ that is aimed at sensitizing the susceptible population. This is done through provision of education materials (TV messages, radio, posters, and leaflets), educational messages which can be delivered by health practitioners or teachers in schools, education that improve hygiene awareness and behavior of people who defecate outside the latrines, and purchase of shoes to both preschool-aged and school-aged children [18]. Thus. the force of infection is modified as $\lambda = ((1-\kappa_1 u_1)\beta M)/(K+M)$ where κ_1 is the effectiveness measure of health education control, where $\kappa_1 \in (0,1)$ such that if $\kappa_1 = 0$, then health education is not effective and $\kappa_1 = 1$ corresponds to completely effective health education, $0 < \kappa_1 < 1$ implies that health education is effective to some degree

(2) The use of mass drug administration (deworming) $\kappa_2 u_2(t)$, which is administered regularly without individual diagnosis is applied to the entire population [19]. Application of this control moves the individuals in exposed class to the susceptible class and those in the infected class to the recovered class

(3) Sanitation control $(u_3(t))$ which measures the efforts to prevent susceptible from contracting the disease. This include drinking clean water, personal hygiene, avoiding eating raw vegetables, cleaning of fruits, and intensive cleanliness of the environment which helps to break the helminth transmission cycle (see [19]). Thus, the clearance of the parasite from the environment will be accelerated by $\mu_M + \kappa_3 u_1$, where κ_3 is the effectiveness of the control to protect susceptible population from contracting helminth infection

After incorporating the controls and using the same parameters and variables as in (2), we obtain the modified model with controls for helminth infection given by

$$\frac{dS}{dt} = bN + \gamma R - \mu S - (1-\kappa_1 u_1)\lambda S + \kappa_2 u_2 E, \tag{55}$$

$$\frac{dE}{dt} = (1-\kappa_1 u_1)\lambda S - (\mu+\rho)E - \kappa_2 u_2 E, \tag{56}$$

$$\frac{dI}{dt} = \rho E - (d+\mu+\varepsilon)I - (q+\kappa_2 u_2)I, \tag{57}$$

$$\frac{dR}{dt} = (q+\kappa_2 u_2)I - (\mu+\gamma)R, \tag{58}$$

$$\frac{dM}{dt} = \varepsilon I - (\mu_M + \kappa_3 u_3)M. \tag{59}$$

with $S(0) = S_0$, $E(0) = E_0$, $I(0) = I_0$, $R(0) = R_0$, and $M(0) = M_0$. In this study, we assume that the control functions $u_1(t)$, $u_2(t)$, and $u_3(t)$ are Lebesque integrable functions with $0 \le u_i \le 1$ for $i = 1, 2, 3$ to mean that when the control is zero, there is no any control implemented and when the control is one there is maximum implementation of the control. The objective is to obtain the optimal levels of the control and state variables that optimize the objective functional given by

$$J(u_1, u_2, u_3) = \min_{u_1,u_2,u_3} \int_0^{t_f} \left(A_1 I + A_2 u_2 N + \frac{1}{2}\sum_{i=1}^{3} w_i u_i^2 \right) dt. \tag{60}$$

Here, we want to minimize the number of infected individual from the population while keeping the cost of controls low. In equation (60), A_1 is the relative weight of the infected individuals that accounts for the social cost while $A_2 u_2$ is the individual cost for MDA of the entire population(preschool- and school-aged children) because it the most vulnerable population for helminth infection. Furthermore, w_i is the relative costs weight associated with background costs for each control measure u_i such as advisement costs, production of posters, ordering and transportation of drugs and water treatment and t_f is the final fixed time. In this work, the cost is not linear as

may result to bang bang which means that the optimal control take values at only upper and lower control set; thus, we choose to have quadratic cost on the control of the form $(1/2)w_i u_i^2$ (see [20]). The problem becomes of determining the optimal triplet (u_1^*, u_2^*, u_3^*) such that

$$J(u_1^*, u_2^*, u_3^*) = \min_{u_1,u_2,u_3 \in U} J(u_1, u_2, u_3), \tag{61}$$

where $U = \{(u_1, u_2, u_3) \mid \text{each } u_i \text{ is measurable with } 0 \le u_i \le 1 \text{ for } 0 \le t \le t_f\}$ is the admissible set.

3.7.1. Existence of an Optimal Control. The solution of the helminth model (9) is proved to be bounded so we use this result to prove the existence of the optimal control. However, existence of optimal control is shown using the approach of Fleming and Richel [14] and later applied in [15, 21–23]. For detailed proof, (see [14], Theorem 4.1, p 68-69).

3.7.2. The Hamiltonian and Optimality Systems. To obtain the Hamiltonian H, we apply "Pontryagin's maximum principle" [24] to derive the necessary conditions for the optimal pair. Therefore, the Hamiltonian is expressed as

$$\begin{aligned} H(S, E, I, R, M, t) = {} & A_1 I + A_2 u_2 N + \frac{1}{2}\sum_{i=1}^{3} w_i u_i^2 + \lambda_1 \frac{dS}{dt} \\ & + \lambda_2 \frac{dE}{dt} + \lambda_3 \frac{dI}{dt} + \lambda_4 \frac{dR}{dt} + \lambda_5 \frac{dM}{dt}, \end{aligned} \tag{62}$$

with $\lambda_i, i = 1, 2, 3, 4, 5$ denotes the adjoint variables to be determined by taking the negative derivative of the Hamiltnian function.

Theorem 5. *Given the optimal set u_1, u_2, and u_3 that minimizes J over U, there exist an adjoint variables $\lambda_1, \lambda_2, \lambda_3, \lambda_4$, and λ_5 such that*

$$\frac{d\lambda_1}{dt} = -A_2 u_2 + \frac{(1-\kappa_1 u_1)\beta M}{K+M}(\lambda_1 - \lambda_2) + (\mu - b)\lambda_1, \tag{63}$$

$$\frac{d\lambda_2}{dt} = -A_2 u_2 + (\mu + \rho)\lambda_2 + \kappa_2 u_2(\lambda_2 - \lambda_1) - b\lambda_1 - \rho\lambda_3, \tag{64}$$

$$\begin{aligned} \frac{d\lambda_3}{dt} = {} & -A_1 - A_2 u_2 - b\lambda_1 + (d + \mu + \varepsilon)\lambda_3 + (q + \kappa_2 u_2) \\ & \cdot (\lambda_3 - \lambda_4) - \varepsilon\lambda_5, \end{aligned} \tag{65}$$

$$\frac{d\lambda_4}{dt} = -A_2 u_2 - (b + \gamma)\lambda_1 + (\mu + \gamma)\lambda_4, \tag{66}$$

$$\begin{aligned} \frac{d\lambda_5}{dt} = {} & \left(\frac{(1-\kappa_1 u_1)S\beta}{K+M} - \frac{(1-\kappa_1 u_1)SM\beta}{(K+M)^2}\right)(\lambda_1 - \lambda_2) \\ & + (\mu_M + \kappa_3 u_3)\lambda_5, \end{aligned} \tag{67}$$

with transversality conditions, $\lambda_i(t_f) = 0, i = 1, 2, 3, 4, 5$. The characterization of the control set $(u_1^*, u_2^*, \text{and } u_3^*)$ using the technique of control bounds gives

$$\begin{aligned} u_1^*(t) &= \max\{0, \min(1, \Phi_1)\}, \\ u_2^*(t) &= \max\{0, \min(1, \Phi_2)\}, \\ u_3^*(t) &= \max\{0, \min(1, \Phi_3)\}, \end{aligned} \tag{68}$$

where

$$\begin{aligned} \Phi_1 &= \frac{\kappa_1 \beta MS}{w_1(K+M)}(\lambda_2 - \lambda_1), \\ \Phi_2 &= \frac{\kappa_2 E(\lambda_2 - \lambda_1) + \kappa_2 I(\lambda_3 - \lambda_4)}{w_2} - \frac{A_2(S + E + I + R)}{w_2}, \\ \Phi_3 &= \frac{\kappa_3 M \lambda_5}{w_3}. \end{aligned} \tag{69}$$

Proof. By using ([24]), the adjoint system is the Euler-Lagrange equations obtained taking the negative of the partial derivative of the Hamiltonian in (62) with respect to the state variables. Thus, the adjoint system can be written as

$$\begin{aligned} \frac{d\lambda_1}{dt} &= -\frac{\partial H}{dS} = -A_2 u_2 + \frac{(1-\kappa_1 u_1)\beta M}{K+M}(\lambda_1 - \lambda_2) + (\mu - b)\lambda_1, \\ \frac{d\lambda_2}{dt} &= -\frac{\partial H}{dE} = -A_2 u_2 + (\mu + \rho)\lambda_2 + \kappa_2 u_2(\lambda_2 - \lambda_1) - b\lambda_1 - \rho\lambda_3, \\ \frac{d\lambda_3}{dt} &= -\frac{\partial H}{dI} = -A_1 - A_2 u_2 - b\lambda_1 + (d + \mu + \varepsilon)\lambda_3 \\ &\quad + (q + \kappa_2 u_2)(\lambda_3 - \lambda_4) - \varepsilon\lambda_5, \\ \frac{d\lambda_4}{dt} &= -\frac{\partial H}{dR} = -A_2 u_2 - (b + \gamma)\lambda_1 + (\mu + \gamma)\lambda_4, \\ \frac{d\lambda_5}{dt} &= -\frac{\partial H}{dM} = \left(\frac{(1-\kappa_1 u_1)S\beta}{K+M} - \frac{(1-\kappa_1 u_1)SM\beta}{K+M^2}\right)(\lambda_1 - \lambda_2) \\ &\quad + (\mu_M + \kappa_3 u_3)\lambda_5. \end{aligned} \tag{70}$$

Using the same principle, we get the controls by solving the equation obtained by taking the partial derivative of the Hamiltonian with respect to each control. For example,

$$\begin{aligned} \frac{\partial H}{\partial u_1} &= w_1 u_1 + \frac{\kappa_1 \beta MS}{K+M}\lambda_1 - \frac{\kappa_1 \beta MS}{K+M}\lambda_2, \\ \frac{\partial H}{\partial u_2} &= w_2 u_2 + \kappa_2 E(\lambda_1 - \lambda_2) + \kappa_2 I(\lambda_3 - \lambda_4), \\ \frac{\partial \mathrm{H}}{\partial u_3} &= w_3 u_3 - \kappa_3 M \lambda_5. \end{aligned} \tag{71}$$

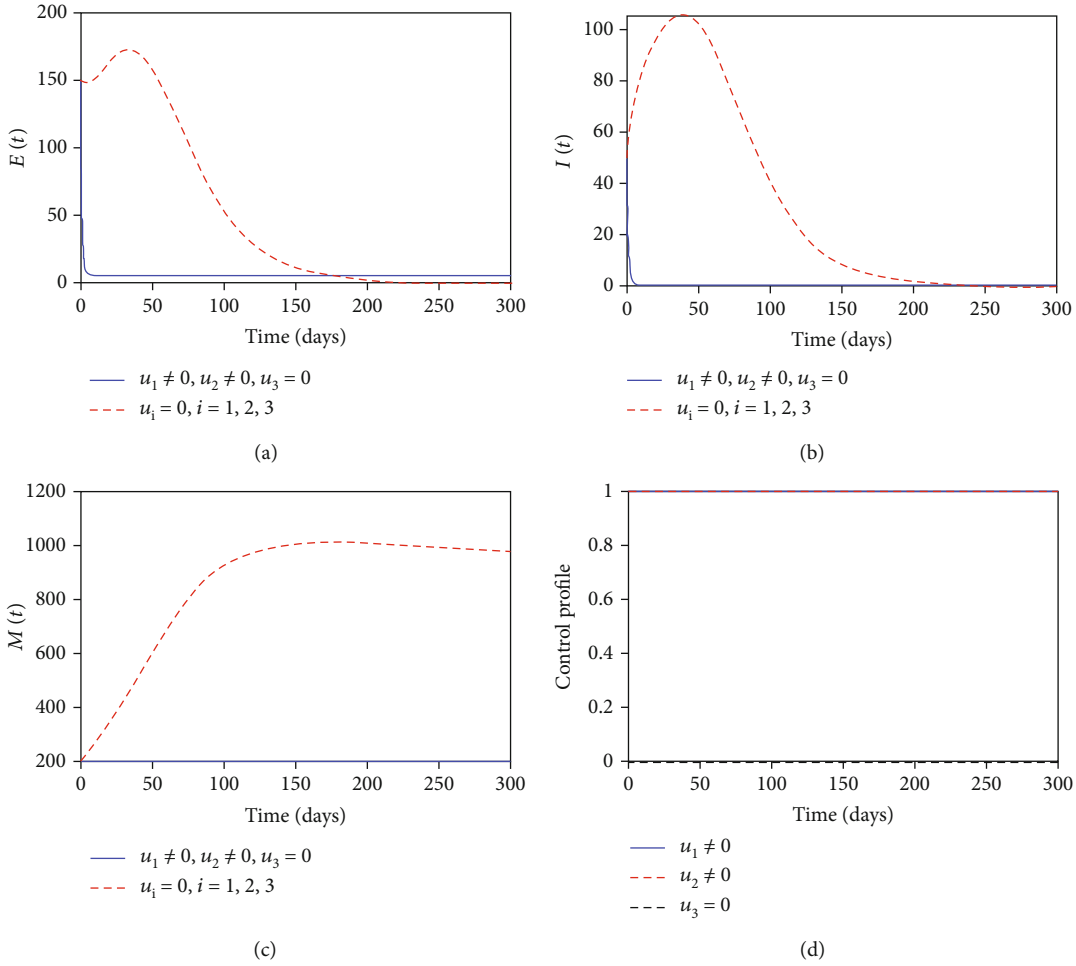

Figure 3: Simulations of the optimal control model with health education and MDA interventions.

Now, setting $\partial H/\partial u_i = 0$ at u_1^* for $i = 1, 2, 3$, we obtain the controls set:

$$u_1^*(t) = \frac{\kappa_1 \beta MS}{w_1(K+M)}(\lambda_2 - \lambda_1),$$
$$u_2^*(t) = \frac{\kappa_2 E(\lambda_2 - \lambda_1) + \kappa_2 I(\lambda_3 - \lambda_4)}{w_2} - \frac{A_2(S+E+I+R)}{w_2},$$
$$u_3^*(t) = \frac{\kappa_3 M \lambda_5}{w_3}. \tag{72}$$

The controls can then be written using standard control arguments with bounds on the controls as

$$u_1^* = \begin{cases} \Phi_1 \text{ if } 0 < \Phi_1 < 1, \\ 0 \text{ if } \Phi_1 \leq 0, \\ 1 \text{ if } \Phi_1 \geq 1. \end{cases}$$

$$u_2^* = \begin{cases} \Phi_2 \text{ if } 0 < \Phi_2 < 1, \\ 0 \text{ if } \Phi_2 \leq 0, \\ 1 \text{ if } \Phi_2 \geq 1. \end{cases}$$

$$u_3^* = \begin{cases} \Phi_3 \text{if } 0 < \Phi_3 < 1, \\ 0 \text{ if } \Phi_3 \leq 0, \\ 1 \text{ if } \Phi_3 \geq 1. \end{cases} \tag{73}$$

In compact notation, we writ,

$$u_1^*(t) = \max\{0, \min(1, \Phi_1)\},$$
$$u_2^*(t) = \max\{0, \min(1, \Phi_2)\}, \tag{74}$$
$$u_3^*(t) = \max\{0, \min(1, \Phi_3)\}.$$

where

$$\Phi_1 = \frac{\kappa_1 \beta MS}{w_1(K+M)}(\lambda_2 - \lambda_1),$$

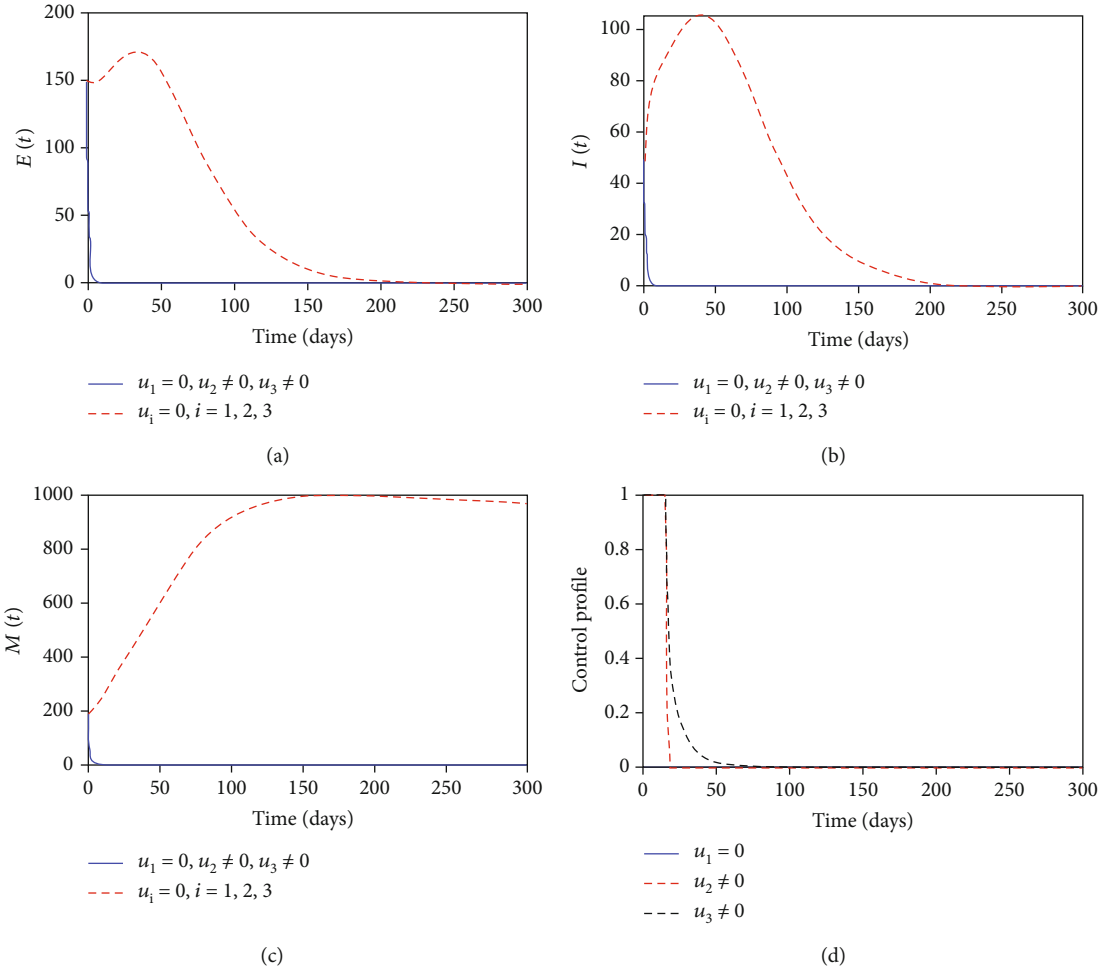

Figure 4: Simulations of the optimal control model with MDA and sanitation interventions.

$$\Phi_2 = \frac{\kappa_2 E(\lambda_2 - \lambda_1) + \kappa_2 I(\lambda_3 - \lambda_4)}{w_2} - \frac{A_2(S+E+I+R)}{w_2},$$

$$\Phi_3 = \frac{\kappa_3 M \lambda_5}{w_3}. \tag{75}$$

The optimality system consists of the state system (55) coupled with adjoint system (63) together with the characterization of the optimal control with the initial and transversality conditions.

The state equations in (55) and the costate (adjoint) equation in system (63) are bounded and satisfies the Lipchitz condition, thus uniqueness of the optimality systems follows using the approaches in [25, 26].

3.8. Numerical Simulation. We perform numerical simulation of the optimal control model using the parameter values given in Table 1. Various optimal control strategies are applied to control the burden of helminth infection in the community. Starting with an initial guess for the optimal controls $u_1(t)$, $u_2(t)$, and $u_3(t)$, state system (55) is solved numerically forward in time using the fourth-order Runge-Kutta method with initial conditions $S(0) = 1000$, $E(0) = 150$, $I(0) = 50$, $R(0) = 5$, and $M(0) = 200$. Then, co state (adjoint) system (63) is solved numerically backward in time using the fourth-order Runge-Kutta method with the state variables and initial guess of the controls obtained earlier. All controls are updated using convex combination of the previous controls and its characterization then the process is repeated until convergence is achieved. The following cost weights were used in the simulation: $A_1 = 800$, $A_2 = 0.15$, $w_1 = 15$, $w_2 = 30$, and $w_3 = 10$ with the efficacy rates $\kappa_1 = 0.7$, $\kappa_2 = 0.8$, and $\kappa_3 = 0.6$.

3.8.1. Control with Health Education and MDA. In this strategy, we used the combination of health education and MDA interventions to optimize the objective functional J while sanitation control is set to zero. Figure 3(a) shows that with this strategy there is a significant effect in reducing the number of exposed individuals compared with the case when there is no control but does not bring the exposed individuals to zero at the final control period. The helminth-infected individuals in Figure 3(b) decreases to almost zero when the optimal combination of health education and MDA are in place compared to when there is no control. In Figure 3(c), we observed that the parasite population in the

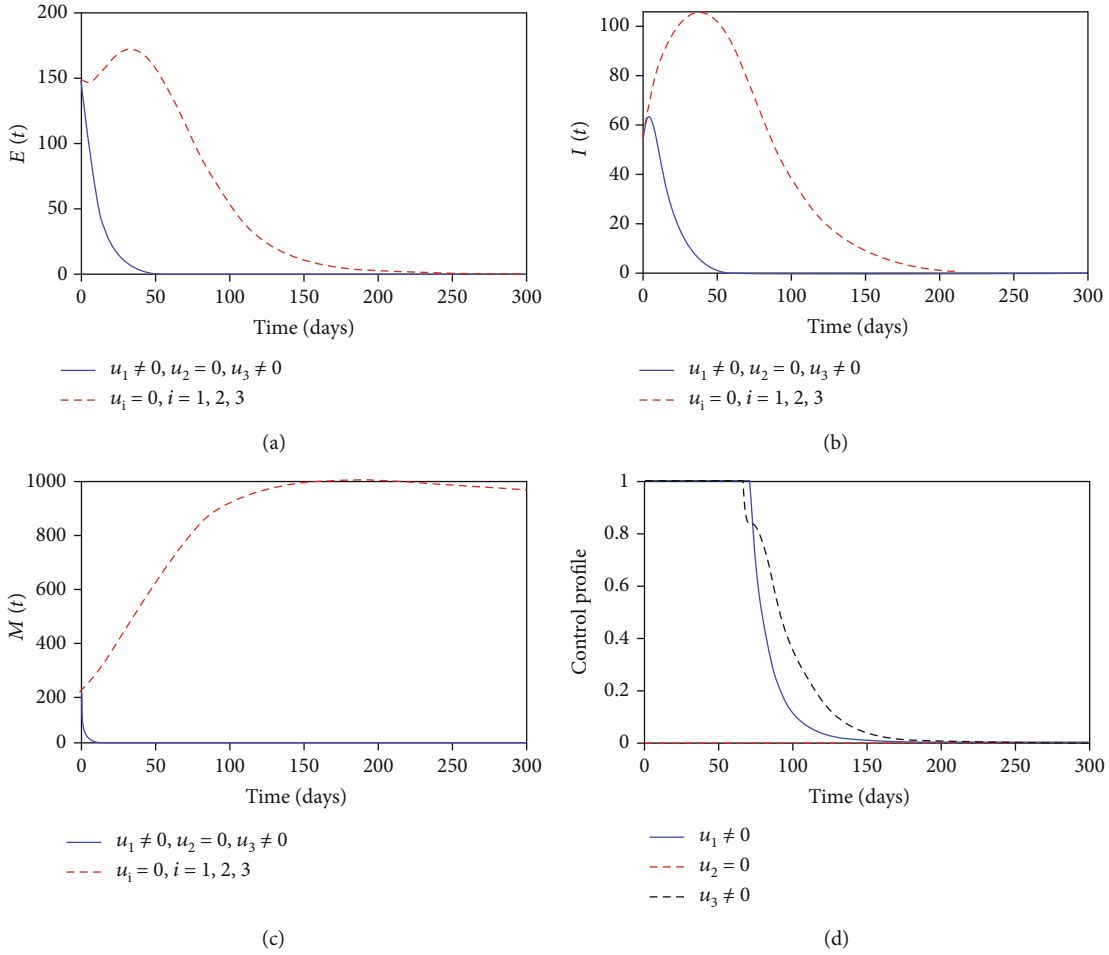

Figure 5: Simulations of the optimal control model with health education and sanitation interventions.

environment is reduced but does not reach zero at the final control period. This suggests that using combination of control measures, the infection can be lowered in the community but not completely removed in the specified control period. The control profile in Figure 3(d) suggests that control combination with health education and MDA should be maximized and applied throughout the intervention period.

3.8.2. Control with MDA and Sanitation. Next, we consider the combination of MDA and sanitation interventions while the health education is set to zero. Figures 4(a) and 4(b) show a similar trend as in Figures 3(a) and 3(b), respectively, but with this strategy more effective than the combination of health education and MDA. This is due to the fact that with MDA, anthelminthic drugs are regularly administered to the entire population (preschool- and school-aged children) while using sanitation clears the density of parasites from the environment. The control profile in Figure 4 suggests the control with MDA should be seized after 20 days while sanitation control should be kept at a maximum for approximately 20 days and then decreased to zero. Therefore, these results show that combination of these two controls measures can as well manage to control helminth infection in the community.

3.8.3. Control with Health Education and Sanitation. We next consider the control with combination of health education and sanitation in the absence of MDA. The health education and sanitation were used to optimize the objective functional J while MDA control was set to zero. Figure 5(a) shows that the number of exposed individuals were reduced and were totally controlled after 50 days. Figure 5(b) shows that the number of infected individuals were reduced and totally controlled at the final period. Figure 5(c) shows that the parasite population is reduced to the minimum level. The control profile in Figure 5(d) suggests that the control with health education should be maximized for 70 days while sanitation should be maximized for 65 days.

3.8.4. Control with Health Education, MDA, and Sanitation. Finally, we consider the case where all controls were in place. In this strategy the controls' health education, MDA, and sanitation were used to optimize the objective functional J. Figure 6(a) shows that the number of exposed individuals is totally controlled at the final control period. Figure 6(b) shows that the number of helminth-infected individuals is also totally controlled at the final control period. Figure 6(c) shows that the parasite population is more reduced to zero at the final control time. Figure 6(d)

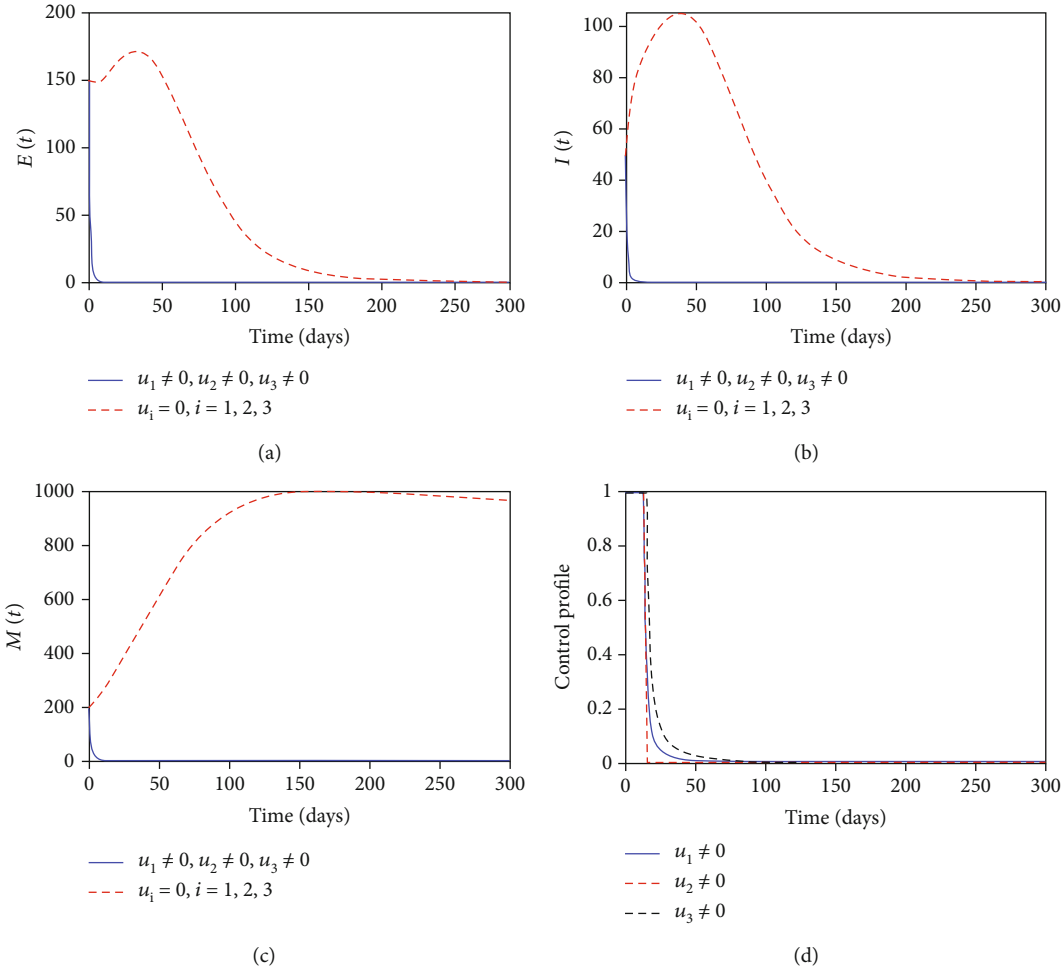

Figure 6: Simulations with health education, MDA, and sanitation interventions.

suggests that the health education control should be maximized for 15 days, the MDA control be seized after 15 days, while the sanitation should be maximized for 18 days and reduced to zero due to the fact that the infection has been cleared in the community.

3.9. Cost-Effectiveness Analysis. Cost effectiveness analysis is performed to quantify the cost effectiveness of different combinations of control strategies using Incremental Cost Effective Ratio (ICER). In this approach, when comparing two competing intervention strategies, one intervention is compared with the next less effective alternative [28, 30, 31]. The ICER formula is given by

$$\text{ICER} = \frac{\text{Difference in costs between strategies}}{\text{Difference in the totalnumber of infection averted}}. \tag{76}$$

To obtain the total number of infections averted, we take the sum of the difference between the total number of exposed and infected individuals without and with control. Also to obtain the total cost for each strategy, we used the cost function as shown in Table 2.

Table 2: Ranking of control strategies in ascending order of the number of infections averted.

Strategy	Total infection averted	Total costs ($)
No strategy	0	0
Strategy 3.8.1	8.0089×10^4	7.8901×10^5
Strategy 3.8.4	8.0092×10^4	9.9591×10^3
Strategy 3.8.2	8.0098×10^4	1.1149×10^4
Strategy 3.8.3	8.0176×10^4	3.3270×10^3

$\text{ICER}(3.8.1) = 7.8901 \times 10^5/8.0089 \times 10^4 = 9.85$, $\text{ICER}(3.8.4) = 9.9591 \times 10^3 - 7.8901 \times 10^5/8.0092 \times 10^4 - 8.0089 \times 10^4 = -259683.6$, $\text{ICER}(3.8.2) = 1.1149 \times 10^4 - 9.9591 \times 10^3/8.0098 \times 10^4 - 8.0092 \times 10^4 = 225.15$, $\text{ICER}(3.8.3) = 3.3270 \times 10^3 - 1.1149 \times 10^4/8.0176 \times 10^4 - 8.0098 \times 10^4 = -100.28$.

Comparing strategy 3.8.1 and 3.8.4, strategy 3.8.1 is more costly and less effective than strategy 3.8.4. Hence, we omit strategy 3.8.1 and recompute ICER values as indicated in Table 3.

From Table 3, we observe that strategy 3.8.2 has higher cost compared to strategy 3.8.4, Hence, we omit 3.8.2 and recompute ICER as indicated in Table 4.

Table 3: Computation of ICER after omitting strategy 3.8.1.

Strategy	Total infection averted	Total costs $	ICER
Strategy 3.8.4	8.0092×10^4	9.9591×10^3	-259,683.6
Strategy 3.8.2	8.0098×10^4	1.1149×10^4	225.15
Strategy 3.8.3	8.0176×10^4	3.3270×10^3	-100.28

Table 4: Computation of ICER after omitting strategy 3.8.2.

Strategy	Total infection averted	Total costs ($)	ICER
Strategy 3.8.4	8.0092×10^4	9.9591×10^3	0.12
Strategy 3.8.3	8.0176×10^4	3.3270×10^3	-100.28

From Table 4, we conclude that strategy 3.8.3 (control with health education and sanitation) is more cost effective than strategy 3.8.4 (control with health education, MDA and sanitation), implying that it is the cheapest of all the control strategies.

4. Discussions and Conclusions

In this paper, we formulated and analysed deterministic model for the helminth infection (soil-transmitted helminth).

In Section 3, we analysed the model by obtaining the feasible region and disease-free and endemic equilibrium points with their stability. Moreover, bifurcation analysis were carried out and the model exhibited backward bifurcation for some parameter values, and sensitivity analysis of $\mathscr{R}_0$ with respect to parameters β, ρ, ε, μ_M, b, d, q was done and results revealed that β was the most positive sensitive parameter while μ_M was the most negative sensitivity parameter. Furthermore, the helminth model developed in Section 2 was extended to include health education, treatment by mass drug administration and sanitation as control measures. We solved the optimal control problem using Pontryagin's maximum principle by first obtaining the Hamiltonian, the adjoint variables, and the characterization of the controls. Applying single-control measure (health education or MDA or sanitation) alone is not sufficient to control the infection; thus, combination of control measures were used to optimize the objective functional J by considering combination of health education with mass drug administration, combination of mass drug administration with sanitation, combination of health education with sanitation, and all the three controls. Finally, we investigated the cost effectiveness of the control strategies to ascertain the least and most expensive strategies. Based on our results, we conclude that the combination of health education and sanitation is the best strategy.

Data Availability

The data are available inside the manuscript and were obtained from related published articles. There is no restriction on the availability of the data.

Conflicts of Interest

The authors declare no conflict of interest.

Acknowledgments

We would like to express our appreciation to the African Development Bank for their financial support.

Supplementary Materials

The supplementary material contains the MatLab codes used for numerical simulations for sensitivity analysis and optimal control problem. *(Supplementary Materials)*

References

[1] E. Michael, M. N. Malecela-Lazaro, C. Kabali, L. C. Snow, and J. W. Kazura, "Mathematical models and lymphatic filariasis control: endpoints and optimal interventions," *Trends in Parasitology*, vol. 22, no. 5, pp. 226–233, 2006.

[2] WHO, *Soil transmitted helminths infections*, 2019, 2019, http://www.who.int/news-room/fact-sheets/detail/soil-transmitted-helminth-infections.

[3] M. Cappello, "Global health impact of soil-transmitted nematodes," *The Pediatric Infectious Disease Journal*, vol. 23, no. 7, pp. 663-664, 2004.

[4] R. M. Anderson and R. M. May, "Population dynamics of human helminth infections: control by chemotherapy," *Nature*, vol. 297, no. 5867, pp. 557–563, 1982.

[5] R. M. Anderson and R. M. May, "Regulation and stability of host-parasite population interactions: I. Regulatory processes," *The Journal of Animal Ecology*, vol. 47, no. 1, pp. 219–247, 1978.

[6] R. Anderson and R. May, "Directly transmitted infections diseases: control by vaccination," *Science*, vol. 215, no. 4536, pp. 1053–1060, 1982.

[7] J. E. Truscott, H. C. Turner, and R. M. Anderson, "What impact will the achievement of the current World Health Organisation targets for anthelmintic treatment coverage in children have on the intensity of soil transmitted helminth infections?," *Parasites & Vectors*, vol. 8, no. 1, 2015.

[8] World Health Organization and others, *Research priorities for helminth infections: technical report of the TDR disease reference group on helminth infections*, World Health Organization, 2012.

[9] Z. Qiu, J. Yu, and Y. Zou, "The asymptotic behavior of a chemostat model," *Discrete & Continuous Dynamical Systems-B*, vol. 4, no. 3, pp. 721–727, 2004.

[10] H. W. Hethcote, "The mathematics of infectious diseases," *SIAM Review*, vol. 42, no. 4, pp. 599–653, 2000.

[11] O. Diekmann and J. A. P. Heesterbeek, *Mathematical Epidemiology of Infectious Diseases: Model Building, Analysis and Interpretation, vol. 5*, John Wiley & Sons, West Sussex, 2000.

[12] R. M. May, *Stability and Complexity in Model Ecosystems*, no. 1, 2019Princeton university press, 2019.

[13] C. Castillo-Chavez, Z. Feng, and W. Huang, "On the computation of ro and its role on," in *Mathematical Approaches for Emerging and Reemerging Infectious Diseases: an Introduction*, vol. 1, p. 229, Springer Science & Business Media, 2002.

[14] W. H. Fleming and R. W. Rishel, *Deterministic and Stochastic Optimal Control*, no. 1, 2012Springer Science & Business Media, 2012.

[15] G. G. Mwanga, *Mathematical modeling and optimal control of malaria*, Lappeenranta University of Technology, 2014.

[16] C. Castillo-Chavez and B. Song, "Dynamical models of tuberculosis and their applications," *Mathematical Biosciences & Engineering*, vol. 1, no. 2, pp. 361–404, 2004.

[17] N. Chitnis, J. M. Cushing, and J. M. Hyman, "Bifurcation analysis of a mathematical model for malaria transmission," *SIAM Journal on Applied Mathematics*, vol. 67, no. 1, pp. 24–45, 2006.

[18] L. Mascarini-Serra, "Prevention of soil-transmitted helminth infection," *Journal of Global Infectious Diseases*, vol. 3, no. 2, pp. 175–182, 2011.

[19] S. Brooker, A. C. A. Clements, and D. A. P. Bundy, "Global epidemiology, ecology and control of soil-transmitted helminth infections," *Advances in Parasitology*, vol. 62, pp. 221–261, 2006.

[20] H. R. Joshi, S. Lenhart, M. Y. Li, and L. Wang, "Optimal control methods applied to disease models," *Contemporary Mathematics*, vol. 410, pp. 187–208, 2006.

[21] S. C. Mpeshe, L. S. Luboobi, and Y. A. W. Nkansah-gyekye, "Optimal control strategies for the dynamics of rift valley fever," *Communications in Optimization Theory*, vol. 3, pp. 1–18, 2014.

[22] G. M. Mlay, L. Luboobi, D. Kuznetsov, and F. Shahada, "Optimal treatment and vaccination control strategies for the dynamics of pulmonary tuberculosis," *International Journal of Advances in Applied Mathematics and Mechanics*, vol. 2, no. 3, pp. 196–207, 2015.

[23] F. Chuma, G. G. Mwanga, and V. G. Masanja, "Application of optimal control theory to Newcastle disease dynamics in village chicken by considering wild birds as reservoir of disease virus," *Journal of Applied Mathematics*, vol. 2019, Article ID 3024965, 14 pages, 2019.

[24] L. S. Pontryagin, *Mathematical Theory of Optimal Processes*, Routledge, 2018.

[25] K. R. Fister, S. Lenhart, and J. S. McNally, *Optimizing chemotherapy in an HIV model*, Texas State University, Department of Mathematics, 1998.

[26] H. R. Joshi, "Optimal control of an HIV immunology model," *Optimal Control Applications and Methods*, vol. 23, no. 4, pp. 199–213, 2002.

[27] H. C. Slater, M. Gambhir, P. E. Parham, and E. Michael, "Modelling co-infection with malaria and lymphatic filariasis," *PLoS Computational Biology*, vol. 9, no. 6, p. e1003096, 2013.

[28] G. G. Mwanga, H. Haario, and V. Capasso, "Optimal control problems of epidemic systems with parameter uncertainties: application to a malaria two-age-classes transmission model with asymptomatic carriers," *Mathematical Biosciences*, vol. 261, pp. 1–12, 2015.

[29] J. Vercruysse, J. M. Behnke, M. Albonico et al., "Assessment of the anthelmintic efficacy of albendazole in school children in seven countries where soil-transmitted helminths are endemic," *PLoS Neglected Tropical Diseases*, vol. 5, no. 3, p. e948, 2011.

[30] K. O. Okosun, O. Rachid, and N. Marcus, "Optimal control strategies and cost-effectiveness analysis of a malaria model," *BioSystems*, vol. 111, no. 2, pp. 83–101, 2013.

[31] B. Seidu and O. D. Makinde, "Optimal control of HIV/AIDS in the workplace in the presence of careless individuals," *Computational and Mathematical Methods in Medicine*, vol. 2014, Article ID 831506, 19 pages, 2014.

Hindawi
Computational and Mathematical Methods in Medicine
Volume 2020, Article ID 8869377, 21 pages
https://doi.org/10.1155/2020/8869377

Research Article

Modeling the Effects of Helminth Infection on the Transmission Dynamics of Mycobacterium tuberculosis under Optimal Control Strategies

Aristide G. Lambura,[1,2] **Gasper G. Mwanga**,[3] **Livingstone Luboobi**,[1,4] **and Dmitry Kuznetsov**[1]

[1]*School of Computational and Communication Science and Engineering, The Nelson Mandela African Institution of Science and Technology, P.O. Box 447, Arusha-, Tanzania*
[2]*Department of Computer Systems and Mathematics, Ardhi University, P.O. Box 35176, Dar es Salaam, Tanzania*
[3]*University of Dar es Salaam, P.O. Box 2329, Dar es Salaam, Tanzania*
[4]*Institute of Mathematical Sciences (IMS), Strathmore University, P.O. Box 59857-, 00200 Nairobi, Kenya*

Correspondence should be addressed to Aristide G. Lambura; lamburaa@nm-aist.ac.tz

Received 7 August 2020; Revised 19 October 2020; Accepted 28 October 2020; Published 18 November 2020

Academic Editor: Chung-Min Liao

A deterministic mathematical model for the transmission and control of cointeraction of helminths and tuberculosis is presented, to examine the impact of helminth on tuberculosis and the effect of control strategies. The equilibrium point is established, and the effective reproduction number is computed. The disease-free equilibrium point is confirmed to be asymptotically stable whenever the effective reproduction number is less than the unit. The analysis of the effective reproduction number indicates that an increase in the helminth cases increases the tuberculosis cases, suggesting that the control of helminth infection has a positive impact on controlling the dynamics of tuberculosis. The possibility of bifurcation is investigated using the Center Manifold Theorem. Sensitivity analysis is performed to determine the effect of every parameter on the spread of the two diseases. The model is extended to incorporate control measures, and Pontryagin's Maximum Principle is applied to derive the necessary conditions for optimal control. The optimal control problem is solved numerically by the iterative scheme by considering vaccination of infants for Mtb, treatment of individuals with active tuberculosis, mass drug administration with regular antihelminthic drugs, and sanitation control strategies. The results show that a combination of educational campaign, treatment of individuals with active tuberculosis, mass drug administration, and sanitation is the most effective strategy to control helminth-Mtb coinfection. Thus, to effectively control the helminth-Mtb coinfection, we suggest to public health stakeholders to apply intervention strategies that are aimed at controlling helminth infection and the combination of vaccination of infants and treatment of individuals with active tuberculosis.

1. Introduction

Soil-transmitted helminth infections are common infections that affect poor communities of the world. The species that infect people are the roundworm (*Ascaris lumbricoides*), the whipworm (*Trichuris trichiura*), and the hookworm (*Necator americanus*). These parasites reside in the intestine and release eggs to contaminate the soil [1]. Approximately 1.5 billion people are infected with soil-transmitted helminths worldwide which are widely distributed in tropical and subtropical areas, with the greatest numbers occurring in sub-Saharan Africa, America, China, and East Asia [1]. On the other hand, tuberculosis (TB) is an infectious disease that is caused by the bacillus Mycobacterium tuberculosis (Mtb). Approximately 5-10% of the estimated 1.7 billion people infected with Mtb develop active TB during their lifetime

[2]. The study by Watts et al. [3] suggests that infection by *trichuriasis* reduces the chance of latent tuberculosis (LTB) or blunts tuberculin skin tests (TST). Moreover, coinfection of helminth and Mtb has been a public health issue in developing countries [4]. The study by Dias et al. [5] suggests that intestinal helminth infection has a harmful effect to contain the Mtb infection and contributes to the development of active TB for coinfected individuals. Furthermore, coinfection with helminths increases the susceptibility to Mtb [6].

The usefulness of mathematical modeling for understanding and assessing the dynamics of infectious diseases cannot be underrated and has been used over the years to investigate the optimal mechanisms for intervention strategies in controlling the spread of infectious diseases. The transmission and dynamics of Mtb with other diseases have been studied by many researchers [7–9]. Bhunu et al. [7] developed an HIV/AIDS and TB coinfection model that considers the treatment of exposed and active TB individuals and therapy for AIDS. They found that the treatment of exposed and active forms of TB results in stuck commencement of the AIDS stage of HIV infection. Fatmawati and Tasman [8] proposed an optimal control model for the transmission of TB-HIV coinfection. They found that the best and effective strategy to lower the TB-HIV infection is to apply a combination of anti-TB and ARV treatment. Okosun [9] discussed the synergy between malaria and schistosomiasis in the presence of treatment. Their study revealed that an effective control of malaria could be achieved if efficient treatment and prevention of schistosomiasis are implemented. There is a need for modeling coinfection of infectious diseases in areas with neglected tropical diseases (NTD) which include helminth infections, Mtb, and malaria to list a few [10], due to their geographical overlap. To the best of our understanding, no study has been carried out to consider the helminth-Mtb coinfection with the use of optimal control theory.

In this paper, our emphasis is to propose a compartmental system for the codynamics of helminths and Mtb diseases and to explore the effect of helminths on Mtb and vice versa. The model is extended to incorporate four time-dependent controls, namely, educational campaign to sensitize the parents to take their babies to the Bacille Calmette-Guerin (BCG) vaccine clinic; treatment of individuals with active TB; treatment of individuals infected with helminth parasites through mass drug administration (MDA); and sanitation to lessen the ingestion rate of parasites from the polluted environment.

2. Materials and Methods

2.1. Model Formulation. The helminth-Mtb infection model is formulated under the following model assumptions:

(i) The susceptible individuals cannot simultaneously get infected by both diseases but rather get infected with one disease and later by the other disease

(ii) The population is homogeneously mixed

(iii) The incidence rate for helminth infection follows the logistic model while Mtb is assumed to be frequency-dependent

(iv) An individual gets helminth infection after sufficient contact with the polluted environment

(v) Due to the fact that Mtb infection is more severe than helminth infection, we assume that coinfected individuals seek TB treatment rather than helminth infection

(vi) The Bacille Calmette-Guerin (BCG) vaccine does not confer a total immunity

The model is formulated by considering two populations, namely, the human population and the parasite population (M) that are present in the contaminated environment. The human population is subdivided into nine classes, namely, susceptible (S), the vaccinated against Mtb (V_T), those infected with Mtb but do not show clinical symptoms of TB (E_T), those with active TB (I_T), TB-recovered individuals (R_T), those infected by helminths (I_H), those who have recovered from helminths (R_H), and those who are dually infected by helminths and Mtb (I_{HT}). Thus, the total human population is given by $N = S + V_T + E_T + I_T + I_H + I_{HT} + R_T + R_H + R_{HT}$. The susceptible population increases by recruitment through birth at the rate $(1-\eta)bN$ and by those who lose their temporary immunity against the helminths and Mtb at rates γ_1 and γ_2, respectively. The susceptible individuals get infected with Mtb upon sufficient contact with an infectious individual with the force of infection $\lambda_T = (\beta_T(I_T + \sigma I_{HT}))/N$, where β_T is the transmission rate and $\sigma > 1$ is the modification parameter for coinfected individuals that models infectivity for susceptible individuals. The susceptible individuals also get infected by helminths after ingestion of eggs/larvae or skin penetration by infective larvae with the force of infection $\lambda_H = \beta_H M/(K + M)$, where β_H is the ingestion rate of parasitic worms and K is the density of parasites in the soil. The helminth-infected individuals increase due to susceptible individuals being infected with helminths, Mtb-vaccinated individuals infected with helminths, and coinfected individuals who recover from Mtb at the rate τ_2. Furthermore, due to the fact that the BCG vaccine does not grant total protection [11], then individuals exposed to Mtb increase due to Mtb-vaccinated individuals losing their protection against Mtb and getting infected at the rate $\rho\lambda_T$, with $\rho \in (0, 1)$ such that $1 - \rho$ is the efficacy of the vaccine.

The chronic infection by helminths alters the chance of getting infected and the progression of coinfecting parasites (virus or bacteria) [12]; as a result, individuals infested with helminths are at higher risk of developing tuberculosis [13]. Therefore, individuals coinfected with helminth and Mtb are increased by helminth-infected individuals being infected with Mtb at the force of infection $g\lambda_T$, where $g > 1$ is the modification parameter that models increased susceptibility to Mtb, and Mtb-exposed

individuals getting infected by helminths at a force of infection λ_H. In addition, the number of individuals with active TB increases as individuals progressed from the exposed class at the rate$k$and coinfected individuals recovered from helminth infection at the rate$\tau_1$and decreases due to natural recovery at the rateτ_2. The parasite populations in the environment increase as they are released by the helminth-infected individuals at the rate ε_1 and coinfected individuals at the rate ε_2 and are cleared from the environment at a rate μ_M.The description above is illustrated in Figure 1, and the governing system of nonlinear differential equations is shown in model (1). The model parameters are described in Table 1.

$$\begin{cases} \dfrac{dS}{dt} = (1-\eta)bN + \gamma_1 R_H + \gamma_2 R_T - (\mu + \lambda_T + \lambda_H)S, \\ \dfrac{dV_T}{dt} = \eta bN - (\mu + \rho\lambda_T + \lambda_H)V_T, \\ \dfrac{dE_T}{dt} = \lambda_T S + \rho\lambda_T V_T + \lambda_T R_H - (\mu + k + \lambda_H)E_T, \\ \dfrac{dI_T}{dt} = kE_T + \tau_1 I_{HT} - (\mu + d_T + \tau_2 + \lambda_H)I_T, \\ \dfrac{dI_H}{dt} = \lambda_H S + \lambda_H V_T + \lambda_H R_T + \tau_2 I_{HT} - (g\lambda_T + \mu + d_H + \tau_1 + \varepsilon_1)I_H, \\ \dfrac{dI_{HT}}{dt} = g\lambda_T I_H + \lambda_H(E_T + I_T) - (\mu + d_{HT} + \tau_1 + \tau_2 + \varepsilon_2)I_{HT}, \\ \dfrac{dR_T}{dt} = \tau_2 I_T - (\lambda_H + \mu + \gamma_2)R_T, \\ \dfrac{R_H}{dt} = \tau_1 I_H - (\lambda_T + \mu + \gamma_1)R_H, \\ \dfrac{dM}{dt} = \varepsilon_1 I_H + \varepsilon_2 I_{HT} - \mu_M M, \end{cases} \tag{1}$$

where

$$\lambda_T = \frac{\beta_T(I_T + \sigma I_{HT})}{N}, \qquad \lambda_H = \frac{\beta_H M}{M + K}. \tag{2}$$

We perform a qualitative analysis of model (1) using a dimensionless version such that dimensionless variables obtained by setting $s = S/N$, $v_T = V_T/N$, $e_T = E_T/N$, $i_T = I_T/N$, $i_H = I_H/N$, $i_{HT} = I_{HT}/N$, $r_T = R_T/N$, $r_H = R_H/N$, $r_{HT} = R_{HT}/N$, and $m = M/K$ replace the original variables S, V_T, E_T, I_T, I_T, I_{HT}, R_T, R_H, R_{HT}, and M, respectively, in which the rate of change of the population at time t is given by

$$\frac{dN}{dt} = (b-\mu)N + d_T I_T - (d_H + \varepsilon_1)I_H - (d_{HT} + \varepsilon_2)I_{HT}. \tag{3}$$

Upon differentiating dimensionless variables with respect to time and using equation (3), system (1) becomes

$$\begin{aligned} \frac{ds}{dt} &= (1-\eta)b + \gamma_1 r_H + \gamma_2 r_T - (b + \lambda_T^* + \lambda_H^* \\ &\quad - d_T i_T - (d_H + \varepsilon_1)i_H - (d_{HT} + \varepsilon_2)i_{HT})s, \\ \frac{dv_T}{dt} &= \eta b - (b + \rho\lambda_T^* + \lambda_H^* - d_T i_T - (d_H + \varepsilon_1)i_H \\ &\quad - (d_{HT} + \varepsilon_2)i_{HT})v_T, \\ \frac{de_T}{dt} &= \lambda_T^*(s + \rho v_T + r_H) - (b + k + \lambda_H^* - d_T i_T \\ &\quad - (d_H + \varepsilon_1)i_H - (d_{HT} + \varepsilon_2)i_{HT})e_T, \\ \frac{di_T}{dt} &= ke_T + \tau_1 i_{HT} - (b + d_T + \lambda_H^* + \tau_2 - d_T i_T \\ &\quad - (d_H + \varepsilon_1)i_H - (d_{HT} + \varepsilon_2)i_{HT})i_T, \\ \frac{di_H}{dt} &= \lambda_H^*(s + v_T + r_T) + \tau_2 i_{HT} - (b + d_H + \tau_1 + \varepsilon_1 + g\lambda_T^* \\ &\quad - d_T i_T - (d_H + \varepsilon_1)i_H - (d_{HT} + \varepsilon_2)i_{HT})i_H, \\ \frac{di_{HT}}{dt} &= g\lambda_T^* i_H + \lambda_H^*(e_T + i_T) - (b + \tau_1 + \tau_2 + \varepsilon_2 + d_{HT} \\ &\quad - d_T i_T - (d_H + \varepsilon_1)i_H - (d_{HT} + \varepsilon_2)i_{HT})i_{HT}, \\ \frac{dr_T}{dt} &= \tau_2 i_T - (b + \gamma_2 + \lambda_H^* - d_T i_T - (d_H + \varepsilon_1)i_H \\ &\quad - (d_{HT} + \varepsilon_2)i_{HT})r_T, \\ \frac{dr_H}{dt} &= \tau_1 i_H - (b + \gamma_1 + \lambda_T^* - d_T i_T - (d_H + \varepsilon_1)i_H \\ &\quad - (d_{HT} + \varepsilon_2)i_{HT})r_H, \\ \frac{dm}{dt} &= \varepsilon_1 i_H + \varepsilon_2 i_{HT} - \mu_M m, \end{aligned} \tag{4}$$

subject to condition $s + v_T + e_T + i_T + i_H + i_{HT} + r_T + r_H = 1$.

2.2. Disease-Free Equilibrium (DFE). The DFE point of system (4) is obtained by setting the right-hand sides of the equations to zero with $e_T = 0$, $i_T = 0$, $i_H = 0$, $i_{HT} = 0$, $r_T = 0$, $r_H = 0$, $r_{HT} = 0$, and $m = 0$ to obtain the DFE $\mathscr{E}_0 = (1-\eta, \eta, 0, 0, 0, 0, 0, 0, 0, 0)$.

2.3. Effective Reproduction Number. The principles of the next-generation matrix [22] are used to obtain the effective reproduction number.

$$\mathscr{R}_T = \frac{\beta_T k(1 + \eta(\rho - 1))}{(b + k)(b + d_T + \tau_2)}, \tag{5}$$

$$\mathscr{R}_H = \frac{\beta_H \varepsilon_1}{\mu_M(b + d_H + \varepsilon_1 + \tau_1)}, \tag{6}$$

corresponding to the reproduction numbers for the Mtb and helminth infection transmission models obtained from the positive eigenvalues of the next-generation matrix, respectively.

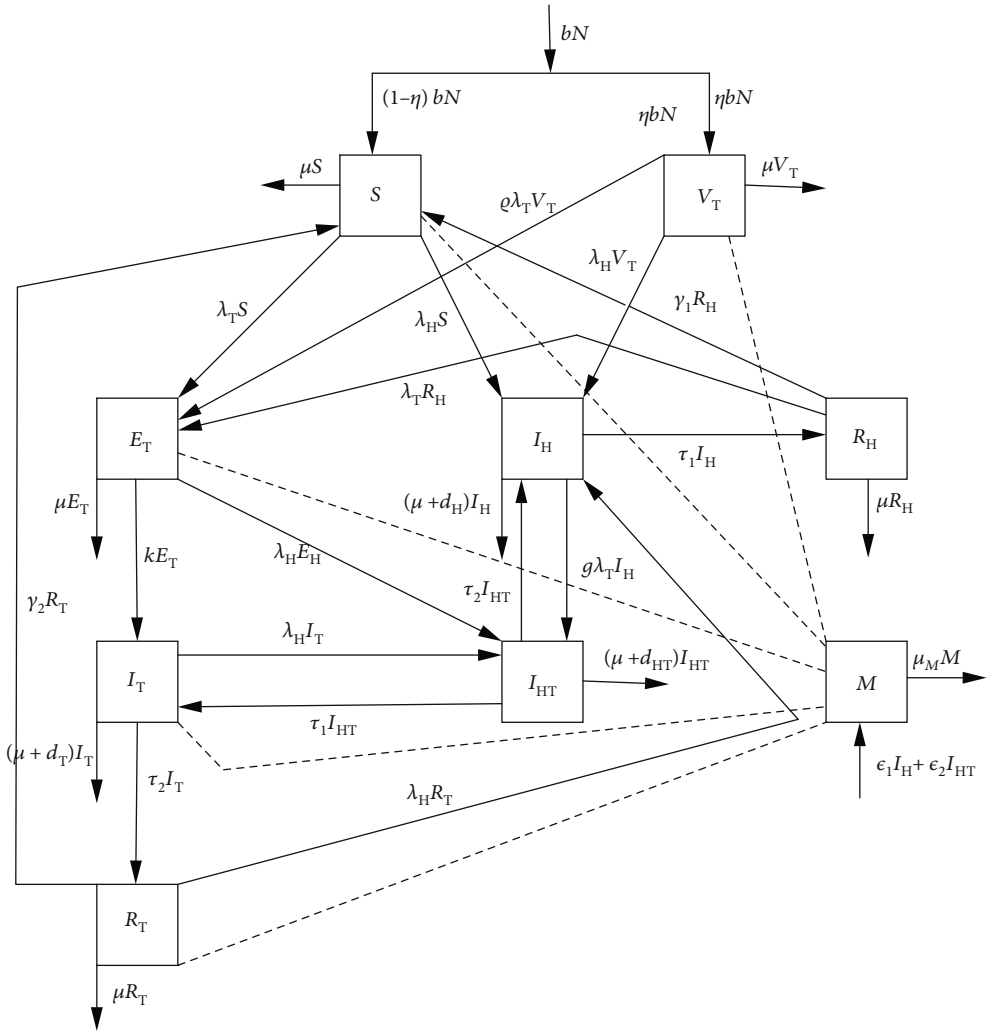

Figure 1: Compartmental diagram for the helminth and Mycobacterium tuberculosis coinfection. The dotted lines indicate the interaction of individuals with the polluted environment.

2.4. Local Stability of the Disease-Free Equilibrium

Theorem 1. *The disease-free equilibrium point is locally asymptotically stable if $\mathcal{R}_{HT} < 1$ and unstable if either $\mathcal{R}_T > 1$ or $\mathcal{R}_H > 1$.*

Proof. We first obtain the Jacobian matrix at the disease-free equilibrium $\mathcal{E}_0$ in order to prove this theorem. The Jacobian matrix is given by

$$J_{\mathcal{E}_0} = \begin{pmatrix} -b & 0 & 0 & l_0 & -l_1 & -l_2 & \gamma_2 & \gamma_1 & -\beta_H s_0 \\ 0 & -b & 0 & (\rho\beta_T - d_T)\nu_{T0} & -l_3 & -l_4 & 0 & 0 & -\beta_H \nu_{T0} \\ 0 & 0 & -(b+k) & \beta_T(s_0 + \rho\nu_{T0}) & 0 & \beta_T\sigma(s_0 + \rho\nu_{T0}) & 0 & 0 & 0 \\ 0 & 0 & k & -l_5 & 0 & \tau_1 & 0 & 0 & 0 \\ 0 & 0 & 0 & 0 & -l_6 & \tau_2 & 0 & 0 & \beta_H \\ 0 & 0 & 0 & 0 & 0 & -l_7 & 0 & 0 & 0 \\ 0 & 0 & 0 & \tau_2 & 0 & 0 & -l_8 & 0 & 0 \\ 0 & 0 & 0 & 0 & \tau_1 & 0 & 0 & -l_9 & 0 \\ 0 & 0 & 0 & 0 & \varepsilon_1 & \varepsilon_2 & 0 & 0 & -\mu_M \end{pmatrix}, \tag{7}$$

where

$$\begin{aligned} l_0 &= (d_T - \beta_T)s_0, \\ l_1 &= (d_H + \varepsilon_1)s_0, \\ l_2 &= (\sigma\beta_T - (d_{HT} + \varepsilon_2))s_0, \\ l_3 &= (d_H + \varepsilon_1)\nu_{T0}, \\ l_4 &= (\rho\sigma\beta_T - (d_{HT} + \varepsilon_2))\nu_{T0}, \\ l_5 &= (b + d_T + \tau_2), \\ l_6 &= (b + d_H + \tau_1), \\ l_7 &= (b + \tau_1 + \tau_2 + \varepsilon_2 + d_{HT}), \\ l_8 &= (b + \gamma_2), \\ l_9 &= (b + \gamma_1). \end{aligned} \tag{8}$$

Now, the characteristic polynomial of the Jacobian matrix $J_{\mathcal{E}_0}$ is given by

Table 1: Description of the model parameters.

Parameters	Definition	Estimated value	Reference
b	Natural birth rate	$1/18250\ \text{day}^{-1}$	[14]
β_T	Transmission rate for Mtb	$0.42\ \text{day}^{-1}$	[15]
μ	Natural death rate	$1/(60\times 365)\ \text{day}^{-1}$	[16]
γ_1	Loss of temporary immunity for helminth-recovered individuals	$1/70\ \text{day}^{-1}$	Assumed
β_H	Ingestion rate of parasitic worms	$1\ \text{parasite day}^{-1}$	Assumed
ρ	Vaccine wane rate	0.7 dimensionless	[17]
τ_1	Natural recovery rate for helminth-infected individuals	$1/28\ \text{day}^{-1}$	[18]
d_H	Helminth disease-induced death rate	$35/1000\ \text{day}^{-1}$	[14]
γ_2	Loss of temporary immunity for Mtb-recovered individuals	$0.3\ \text{day}^{-1}$	[19]
τ_2	Natural recovery rate for Mtb-infected individuals	$0.2/365\ \text{day}^{-1}$	[20]
d_T	Mtb disease-induced death rate	$0.08\ \text{day}^{-1}$	[17]
d_{HT}	Helminth-Mtb disease-induced death rate	$0.08\ \text{day}^{-1}$	Assumed
k	Progression to active TB	$0.00013/365\text{day}^{-1}$	[21]
μ_M	Clearance rate of parasitic worms	$13/37500\ \text{day}^{-1}$	[14]
ε_1	Shading rate for helminth-infected individuals	$0.09\ \text{day}^{-1}$	[18]
K	Number of parasites in the environment	10^5 parasites	[18]
ε_2	Shading rate for coinfected individuals	$0.1\ \text{day}^{-1}$	Assumed
g	Modification parameter	1.12 dimensionless	Assumed
σ	Modification parameter	1.5 dimensionless	Assumed

$$\begin{aligned} p(\lambda) = {} & (b+\lambda)^2(b+\gamma_1+\lambda)(b+\gamma_2+\lambda) \\ & \cdot (b+d_{HT}+\tau_1+\tau_2+\lambda+\varepsilon_2) \\ & \cdot \left(\lambda^2+(2b+k+d_T+\tau_2)\lambda+(b+k)\right) \\ & \cdot (b+d_T+\tau_2)[1-\mathscr{R}_T]\big)\big(\lambda^2+(b+d_H+\varepsilon_1 \\ & +\mu_M+\tau_1)\lambda+\mu_M(b+d_H+\varepsilon_1+\tau_1)[1-\mathscr{R}_H]\big). \end{aligned} \tag{9}$$

Clearly, from equation (9), the eigenvalues of $J_{\mathscr{E}_0}$ are as follows: $\lambda_{1,2}=-b<0$, $\lambda_2=-(b+\gamma_1)<0$, $\lambda_3=-(b+\gamma_2)<0$, $\lambda_4=-(b+d_{HT}+\tau_1+\tau_2+\varepsilon_2)<0$, and

$$\begin{aligned} & \left(\lambda^2+(2b+k+d_T+\tau_2)\lambda+(b+k)(b+d_T+\tau_2)[1-\mathscr{R}_T]\right) \\ & \cdot \left(\lambda^2+(b+d_H+\varepsilon_1+\mu_M+\tau_1)\lambda+\mu_M\right. \\ & \left.\cdot (b+d_H+\varepsilon_1+\tau_1)[1-\mathscr{R}_H]\right)=0. \end{aligned} \tag{10}$$

Applying Routh-Hurwitz conditions [23] on equation (10), it has strictly negative real roots if $\mathscr{R}_T<1$ and $\mathscr{R}_H<1$. Thus, the DFE point $\mathscr{E}_0$ is locally asymptotically stable whenever $\mathscr{R}_{HT}<1$ and unstable if either $\mathscr{R}_T>1$ or $\mathscr{R}_H>1$.

2.5. Global Stability of the Disease-Free Equilibrium. We investigate the global asymptotic stability of the disease-free equilibrium of model (9) by using the theory applied by Chavez et al. [24]. System (9) is written as

$$\begin{aligned} \frac{dX}{dt} &= F(X,Y), \\ \frac{dY}{dt} &= G(X,Y),\ G(X,0)=0, \end{aligned} \tag{11}$$

where $X=(s,v_T,r_T,r_H)\in\mathbb{R}_+^4$ represents the number of uninfected individuals and $Y=(e_T,i_T,i_H,i_{HT},m)\in\mathbb{R}_+^5$ represents the number of infected individuals including the latent and infectious individuals.

The DFE is given by $\mathscr{E}_0=(X_0^*,0)$, where $X_0^*=(1-\eta,\eta)$. The conditions in equation (12) must be satisfied to guarantee local asymptotic stability:

$$\frac{dX}{dt} = F(X^*, 0), \quad X^* \text{ is globally asmptotically stable (g.a.s)},$$
$$G(X, Y) = BY - \widehat{G}(X, Y), \quad \text{where } \widehat{G}(X, Y) \geq 0 \text{ for } (X, Y) \in \Sigma, \tag{12}$$

and $B = D_Y\widehat{G}(X^*, 0)$ is M-matrix (that is, the off-diagonal elements of matrix B are nonnegative); and Σ is the region where the model makes biological sense. If the equations in (4) satisfy the conditions in (12), then the following theorem holds.

Theorem 2. *The fixed point $\mathscr{E}_0$ is a globally asymptotically stable equilibrium of system (4) given that $\mathscr{R}_{HT} < 1$ and that the conditions in (12) are fulfilled.*

Proof. System (4) as written in equation (12) can be rewritten in a reduced form:

$$\left.\frac{dX}{dt}\right|_{Y=0} = \begin{pmatrix} (1-\eta)b - bs \\ \eta b - bv_{\mathrm{T}} \\ 0 \end{pmatrix}. \tag{13}$$

Solving equation one in (13) gives $s(t) = (1-\eta) + (s_0 - (1-\eta))e^{-bt}$ implying that $s(t) \longrightarrow 1-\eta$ as $t \longrightarrow \infty$. Similarly, solving equation two in (13) gives $v_{\mathrm{T}}(t) = \eta + (v_{\mathrm{T}0} - \eta)e^{-bt}$ implying that $v_{\mathrm{T}}(t) \longrightarrow \eta$ as $t \longrightarrow 0$. Therefore, the first condition in (12) is satisfied.

Let

$$\begin{pmatrix} \widehat{G}_1(X, Y) \\ \widehat{G}_2(X, Y) \\ \widehat{G}_3(X, Y) \\ \widehat{G}_4(X, Y) \\ \widehat{G}_5(X, Y) \end{pmatrix} = \begin{pmatrix} \chi_1\lambda_{\mathrm{T}}^*\left(1 - \dfrac{s + \rho v_{\mathrm{T}}}{\chi_1}\right) - \lambda_{\mathrm{T}}^* r_{\mathrm{H}} + \lambda_{\mathrm{H}}^* e_{\mathrm{T}} - d_{\mathrm{T}} i_{\mathrm{T}} e_{\mathrm{T}} - \chi_2 i_{\mathrm{H}} e_{\mathrm{T}} - \chi_3 i_{\mathrm{HT}} e_{\mathrm{T}} \\ \lambda_{\mathrm{H}}^* i_{\mathrm{T}} - d_{\mathrm{T}} i_{\mathrm{T}}^2 - \chi_2 i_{\mathrm{H}} i_{\mathrm{T}} - \chi_3 i_{\mathrm{HT}} i_{\mathrm{T}} \\ \beta_{\mathrm{H}} m\left(1 - \dfrac{s + v_{\mathrm{T}} + r_{\mathrm{T}}}{1+m}\right) + g\lambda_{\mathrm{T}}^* i_{\mathrm{H}} - d_{\mathrm{T}} i_{\mathrm{T}} i_{\mathrm{H}} - \chi_2 i_{\mathrm{H}}^2 - \chi_3 i_{\mathrm{HT}} i_{\mathrm{H}} \\ -g\lambda_{\mathrm{T}}^* i_{\mathrm{H}} - \lambda_{\mathrm{H}}^*(e_{\mathrm{T}} + i_{\mathrm{T}}) - d_{\mathrm{T}} i_{\mathrm{T}} i_{\mathrm{HT}} - \chi_2 i_{\mathrm{H}} i_{\mathrm{HT}} - \chi_3 i_{\mathrm{HT}}^2 \\ 0 \end{pmatrix},$$
$$B = \begin{pmatrix} -(b+k) & \beta_{\mathrm{T}}(s_0 + \rho v_{\mathrm{T}0}) & 0 & \beta_{\mathrm{T}}\sigma(s_0 + \rho v_{\mathrm{T}0}) & 0 \\ k & -(b + d_{\mathrm{T}} + \tau_2) & 0 & \tau_1 & 0 \\ 0 & 0 & -(b + d_{\mathrm{H}} + \tau_1 + \varepsilon_1) & \tau_2 & \beta_{\mathrm{H}} \\ 0 & 0 & 0 & -\Gamma & 0 \\ 0 & 0 & \varepsilon_1 & \varepsilon_2 & -\mu_M \end{pmatrix}, \tag{14}$$

where $\chi_1 = (1 + \eta(\rho - 1))$, $\chi_2 = d_{\mathrm{H}} + \varepsilon_1$, $\chi_3 = d_{\mathrm{HT}} + \varepsilon_3$, and $\Gamma = b + \tau_1 + \tau_2 + \varepsilon_2 + d_{\mathrm{HT}}$. From equation (14), we observe that $\widehat{G}_4(X, Y) < 0$ implying that the second condition in (12) is not fulfilled, so $\mathscr{E}_0$ may not be globally asymptotically stable. This suggests the existence of multiple equilibria.

2.6. The Effect of Helminth Infection on Mtb and Vice Versa. We analyze the effect of helminth infection on Mtb infection and vice versa, by first expressing $\mathscr{R}_{\mathrm{H}}$ in terms of $\mathscr{R}_{\mathrm{T}}$. We solve for b from the expression of $\mathscr{R}_{\mathrm{T}}$ in equation (5) to get

$$b = \frac{-\theta_1\mathscr{R}_{\mathrm{T}} + \sqrt{\theta_2\mathscr{R}_{\mathrm{T}}^2 + \theta_3\mathscr{R}_{\mathrm{T}}}}{2\mathscr{R}_{\mathrm{T}}}, \tag{15}$$

where $\theta_1 = k + d_{\mathrm{T}} + \tau_2$, $\theta_2 = (k + d_{\mathrm{T}} + \tau_2)^2 - 4k(d_{\mathrm{T}} + \tau_2)$, $\theta_3 = 4\beta_{\mathrm{T}}k(1 + \eta(\rho - 1))$.

Then, substituting b into the expression for $\mathscr{R}_{\mathrm{H}}$, we get

$$\mathscr{R}_{\mathrm{H}} = \frac{\beta_{\mathrm{H}}\varepsilon_1}{\mu_M\left(\left(\left(-\theta_1 R_{\mathrm{T}} + \sqrt{\theta_2 R_{\mathrm{T}}^2 + \theta_3 R_{\mathrm{T}}}\right)/2R_{\mathrm{T}}\right) + d_{\mathrm{H}} + \varepsilon_1 + \tau_1\right)}. \tag{16}$$

Differentiating equation (16) partially with respect to $\mathscr{R}_{\mathrm{T}}$ gives

$$\frac{\partial\mathscr{R}_{\mathrm{H}}}{\partial\mathscr{R}_{\mathrm{T}}} = \frac{\theta_3\beta_{\mathrm{H}}\varepsilon_1\mathscr{R}_{\mathrm{T}}}{\mu_M\sqrt{\mathscr{R}_{\mathrm{T}}(\theta_2 R_{\mathrm{T}} + \theta_3)}\left(2\mathscr{R}_{\mathrm{T}}(d_{\mathrm{H}} + \varepsilon_1 + \tau_1) - \theta_1\mathscr{R}_{\mathrm{T}} + \sqrt{\mathscr{R}_{\mathrm{T}}(\theta_2\mathscr{R}_{\mathrm{T}} + \theta_3)}\right)^2}. \tag{17}$$

Now, whenever the right-hand side of equation (17) is strictly positive, an increase in the Mtb incidence in the society results in an increase in the incidence of helminth infection in the society.

If RHS of equation (17) is equal to zero, it means that Mtb incidences have no influence on the spread of helminth infection.

Also, expressing b in terms of $\mathscr{R}_{\mathrm{H}}$ from the expression of $\mathscr{R}_{\mathrm{H}}$ in equation (6), we get

$$b = \frac{\beta_{\mathrm{H}}\varepsilon_1 - \theta_6\mathscr{R}_{\mathrm{H}}}{\mu_M\mathscr{R}_{\mathrm{H}}}, \tag{18}$$

where $\theta_6 = \mu_M(d_{\mathrm{H}} + \tau_1)$. Then, expressing $\mathscr{R}_{\mathrm{T}}$ in terms of $\mathscr{R}_{\mathrm{H}}$, we have

$$\mathscr{R}_{\mathrm{T}} = \frac{\beta_{\mathrm{T}}k(1+\eta(\rho-1))\mu_M^2\mathscr{R}_{\mathrm{H}}^2}{(\beta_{\mathrm{H}}\varepsilon_1 + (\mu_M k - \theta_6)\mathscr{R}_{\mathrm{H}})(\beta_{\mathrm{H}}\varepsilon_1 + (\mu_M(d_{\mathrm{T}}+\tau_2) - \theta_6)\mathscr{R}_{\mathrm{H}})}, \tag{19}$$

Differentiating $\mathscr{R}_{\mathrm{T}}$ with respect to $\mathscr{R}_{\mathrm{H}}$, we get

$$\frac{\partial\mathscr{R}_{\mathrm{T}}}{\partial\mathscr{R}_{\mathrm{H}}} = \frac{k\varepsilon_1\mathscr{R}_{\mathrm{H}}\mu_M^2\beta_{\mathrm{H}}\beta_{\mathrm{T}}(1+\eta(\rho-1))[\mathscr{R}_{\mathrm{H}}(\mu_M(d_{\mathrm{T}}+k+\tau_2) - 2\theta_6) + 2\beta_{\mathrm{H}}\varepsilon_1]}{(\mathscr{R}_{\mathrm{H}}(k\mu_M - \theta_6) + \beta_{\mathrm{H}}\varepsilon_1)^2(\mathscr{R}_{\mathrm{H}}(\mu_M(d_{\mathrm{T}}+\tau_2) - \theta_6) + \beta_{\mathrm{H}}\varepsilon_1)^2}. \tag{20}$$

Whenever $\mu_M(d_{\mathrm{T}} + k + \tau_2) \geq 2\theta_6$, then $\partial\mathscr{R}_{\mathrm{T}}/\partial\mathscr{R}_{\mathrm{H}}$ is strictly positive. This indicates that helminth infection incidence results in an increase in Mtb infection incidence in the society. Thus, helminth infection enhances Mtb infection in the society.

2.7. Existence of Backward Bifurcation. To determine the local asymptotic stability of the endemic equilibrium, we apply the Center Manifold Theorem developed by [25]. To use the theory, we make the subsequent change of variables: let $x_1 = s$, $x_2 = v_{\mathrm{T}}$, $x_3 = e_{\mathrm{T}}$, $x_4 = i_{\mathrm{T}}$, $x_5 = i_{\mathrm{H}}$, $x_6 = i_{\mathrm{HT}}$, $x_7 = r_{\mathrm{T}}$, $x_8 = r_{\mathrm{H}}$, and $x_9 = m$. Then, model system (4) is often written within the following form:

$$\frac{dX}{dt} = F(x) = (f_1(x), f_2(x), f_3(x), f_4(x), f_5(x), f_6(x), f_7(x), f_8(x), f_9(x)) \tag{21}$$

where

$$\begin{aligned}
\frac{dx_1}{dt} &= f_1(x) = (1-\eta)b + \gamma_1 x_8 + \gamma_2 x_7 - (b + \beta_{\mathrm{T}}(x_4 + \sigma x_6) \\
&\quad - d_{\mathrm{T}}x_4 - (d_{\mathrm{H}} + \varepsilon_1)x_5 - (d_{\mathrm{HT}} + \varepsilon_2)x_6)x_1, \\
\frac{dx_2}{dt} &= f_2(x) = \eta b - \left(b + \rho\beta_{\mathrm{T}}(x_4 + \sigma x_6) + \frac{\beta_{\mathrm{H}}x_9}{1+x_9}\right. \\
&\quad \left. - d_{\mathrm{T}}x_4 - (d_{\mathrm{H}} + \varepsilon_1)x_5 - (d_{\mathrm{HT}} + \varepsilon_2)x_6\right)x_2, \\
\frac{dx_3}{dt} &= f_3(x) = \beta_{\mathrm{T}}(x_4 + \sigma x_6)(x_1 + \rho x_2 + x_8) - \left(b + k + \frac{\beta_{\mathrm{H}}x_9}{1+x_9}\right. \\
&\quad \left. - d_{\mathrm{T}}x_4 - (d_{\mathrm{H}} + \varepsilon_1)x_5 - (d_{\mathrm{HT}} + \varepsilon_2)x_6\right)x_3,
\end{aligned}$$

where $J_0 = (d_{\mathrm{T}} - \beta_{\mathrm{T}})s_0$, $J_1 = (d_{\mathrm{H}} + \varepsilon_1)s_0$, $J_2 = (\sigma\beta_{\mathrm{T}} - (d_{\mathrm{HT}} + \varepsilon_2))s_0$, $J_3 = (d_{\mathrm{H}} + \varepsilon_1)\nu_{\mathrm{T0}}$, $J_4 = (\rho\sigma\beta_{\mathrm{T}}^* - (d_{\mathrm{HT}} + \varepsilon_2))\nu_{\mathrm{T0}}$, J_5 $= (b + d_{\mathrm{T}} + \tau_2)$, $J_6 = (b + d_{\mathrm{H}} + \tau_1)$, $J_7 = (b + \tau_1 + \tau_2 + \varepsilon_2 + d_{\mathrm{HT}})$, $J_8 = (b + \gamma_2)$, and $J_9 = (b + \gamma_1)$.

$$\begin{aligned}
\frac{dx_4}{dt} &= f_4(x) = kx_3 + \tau_1 x_6 - \left(b + d_{\mathrm{T}} + \tau_2 + \frac{\beta_{\mathrm{H}}x_9}{1+x_9} - d_{\mathrm{T}}x_4\right. \\
&\quad \left. - (d_{\mathrm{H}} + \varepsilon_1)x_5 - (d_{\mathrm{HT}} + \varepsilon_2)x_6\right)x_4, \\
\frac{dx_5}{dt} &= f_5(x) = \frac{\beta_{\mathrm{H}}x_9}{1+x_9}(x_1 + x_2 + x_7) + \tau_2 x_6 \\
&\quad - (b + d_{\mathrm{H}} + \tau_1 + \varepsilon_1 + g\beta_{\mathrm{T}}(x_4 + \sigma x_6) \\
&\quad - d_{\mathrm{T}}x_4 - (d_{\mathrm{H}} + \varepsilon_1)x_5 - (d_{\mathrm{HT}} + \varepsilon_2)x_6)x_5, \\
\frac{dx_6}{dt} &= f_6(x) = g\beta_{\mathrm{T}}(x_4 + \sigma x_6)x_5 + \frac{\beta_{\mathrm{H}}x_9}{1+x_9}(x_3 + x_4) \\
&\quad - (b + \tau_1 + \tau_2 + \varepsilon_2 + d_{\mathrm{HT}} - d_{\mathrm{T}}x_4 \\
&\quad - (d_{\mathrm{H}} + \varepsilon_1)x_5 - (d_{\mathrm{HT}} + \varepsilon_2)x_6)x_6, \\
\frac{dx_7}{dt} &= f_7(x) = \tau_2 x_4 - \left(b + \gamma_2 + \frac{\beta_{\mathrm{H}}x_9}{1+x_9} - d_{\mathrm{T}}x_4\right. \\
&\quad \left. - (d_{\mathrm{H}} + \varepsilon_1)x_5 - (d_{\mathrm{HT}} + \varepsilon_2)x_6\right)x_7, \\
\frac{dx_8}{dt} &= f_8(x) = \tau_1 x_5 - (b + \gamma_1 + \beta_{\mathrm{T}}(x_4 + \sigma x_6) \\
&\quad - d_{\mathrm{T}}x_4 - (d_{\mathrm{H}} + \varepsilon_1)x_5 - (d_{\mathrm{HT}} + \varepsilon_2)x_6)x_8, \\
\frac{dx_{10}}{dt} &= f_9(x) = \varepsilon_1 x_5 + \varepsilon_2 x_6 - \mu_M x_{10}.
\end{aligned} \tag{22}$$

So the Jacobian matrix of system (22) at the disease-free equilibrium ($\mathscr{E}_0$) is given by

$$J_{\mathscr{E}_0} = \begin{pmatrix} -b & 0 & 0 & J_0 & -J_1 & -J_2 & \gamma_2 & \gamma_1 & -\beta_H s_0 \\ 0 & -b & 0 & (\rho\beta_T - d_T)\nu_{T0} & -J_3 & -J_4 & 0 & 0 & -\beta_H \nu_{T0} \\ 0 & 0 & -(b+k) & \beta_T^*(s_0 + \rho\nu_{T0}) & 0 & \beta_T^*\sigma(s_0 + \rho\nu_{T0}) & 0 & 0 & 0 \\ 0 & 0 & k & -J_5 & 0 & \tau_1 & 0 & 0 & 0 \\ 0 & 0 & 0 & 0 & -J_6 & \tau_2 & 0 & 0 & \beta_H \\ 0 & 0 & 0 & 0 & 0 & -J_7 & 0 & 0 & 0 \\ 0 & 0 & 0 & \tau_2 & 0 & 0 & -J_8 & 0 & 0 \\ 0 & 0 & 0 & 0 & \tau_1 & 0 & 0 & -J_9 & 0 \\ 0 & 0 & 0 & 0 & \varepsilon_1 & \varepsilon_2 & 0 & 0 & -\mu_M \end{pmatrix}, \tag{23}$$

Recall that $\mathscr{R}_{HT} = \max\{\mathscr{R}_H, \mathscr{R}_T\}$. If we consider $\mathscr{R}_{HT} = 1$ (that is, $\mathscr{R}_H < \mathscr{R}_T = 1$), let $\beta_T = \beta_T^*$ be a bifurcation parameter. Then, $\mathscr{R}_T = 1$ gives

$$\beta_T = \beta_T^* = \frac{(b+k)(b+d_T+\tau_2)}{k(1+\eta(\rho-1))}. \tag{24}$$

The Jacobian $J_{\mathscr{E}_0}$ has a simple zero eigenvalue whose related right eigenvectors are denoted by $w = [w_1, w_2, w_3, w_4, w_5, w_6, w_7, w_8, w_9]^T$.where $w_1 = ((J_8(d_T - \beta_T^*)s_0 + \gamma_2\tau_2)/bJ_8)w_4 + ((\mu_M\gamma_1\tau_1 - J_1J_9 - \beta_T^*\varepsilon_1 s_0 J_9)/b\mu_M J_9)w_5$, $w_2 = (((\rho\beta_T^* - d_T)\nu_{T0})/b)w_4 - ((\mu_M(d_H + \varepsilon_1) + \beta_H\varepsilon_1)/b\mu_M)w_5$, $w_3 = \beta_T^*(s_0 + \rho\nu_{T0})w_4/(b+k)$, $w_4 = w_4 > 0$, $w_5 = w_5 > 0$, $w_6 = 0$, $w_7 = (\tau_2 w_4)/J_8$, $w_8 = (\tau_1 w_5)/J_9$, and $w_9 = (\varepsilon_1 w_5)/\mu_M$.

The left eigenvectors of $J_{\mathscr{E}_0}$ associated with the simple eigenvalues are denoted by $\nu = [\nu_1, \nu_2, \nu_3, \nu_4, \nu_5, \nu_6, \nu_7, \nu_8, \nu_9]^T$, where $\nu_1 = \nu_2 = \nu_7 = \nu_8 = 0$, $\nu_3 = k\nu_4/(b+k)$, $\nu_4 = \nu_4 > 0$, $\nu_5 = \nu_5 > 0$, $\nu_6 = ((k\beta_T^*\sigma(s_0 + \rho\nu_{T0}) + \tau_1(b+k))/J_7(b+k))\nu_4 + ((\tau_2\mu_M + \varepsilon_2\beta_H)/J_7\mu_M)\nu_5$, and $\nu_9 = (\beta_H\nu_5)/\mu_M$.

The coefficients a and b that decide the local dynamics of the endemic equilibrium point are defined in equations (25) and (26):

$$a = \sum_{k,j,i=1}^{n} \nu_k w_i w_j \frac{\partial^2 f_k}{\partial x_i \partial x_j}(\mathscr{E}_0, \beta_T^*), \tag{25}$$

$$b = \sum_{k,i=1}^{n} \nu_k w_i \frac{\partial^2 f_k}{\partial x_i \partial \beta_T^*}(\mathscr{E}_0, \beta_T^*). \tag{26}$$

From system (22), the nonzero partial derivatives of F related to a at DFE are given by

$$\frac{\partial^2 f_1}{\partial x_4 \partial x_1} = d_T - \beta_T^*,$$

$$\frac{\partial^2 f_1}{\partial x_5 \partial x_1} = d_H + \varepsilon_1,$$

$$\frac{\partial^2 f_1}{\partial x_6 \partial x_1} = d_H + \varepsilon_2 - \sigma\beta_T^*,$$

$$\frac{\partial^2 f_2}{\partial x_4 \partial x_2} = d_T - \rho\beta_T^*,$$

$$\frac{\partial^2 f_2}{\partial x_5 \partial x_2} = d_H + \varepsilon_1,$$

$$\frac{\partial^2 f_2}{\partial x_6 \partial x_2} = d_{HT} + \varepsilon_2 - \sigma\rho\beta_T^*,$$

$$\frac{\partial^2 f_2}{\partial x_9 \partial x_2} = -\beta_H,$$

$$\frac{\partial^2 f_3}{\partial x_4 \partial x_3} = d_T,$$

$$\frac{\partial^2 f_3}{\partial x_5 \partial x_3} = d_H + \varepsilon_1,$$

$$\frac{\partial^2 f_3}{\partial x_6 \partial x_3} = d_{HT} + \varepsilon_2,$$

$$\frac{\partial^2 f_3}{\partial x_9 \partial x_3} = -\beta_H,$$

$$\frac{\partial^2 f_3}{\partial x_4 \partial x_1} = \beta_T,$$

$$\frac{\partial^2 f_3}{\partial x_6 \partial x_1} = \sigma\beta_T,$$

$$\frac{\partial^2 f_3}{\partial x_4 \partial x_2} = \rho\beta_T,$$

$$\frac{\partial^2 f_3}{\partial x_6 \partial x_2} = \rho\sigma\beta_{\mathrm{T}},$$

$$\frac{\partial^2 f_3}{\partial x_4 \partial x_8} = \beta_{\mathrm{T}},$$

$$\frac{\partial^2 f_3}{\partial x_6 \partial x_8} = \sigma\beta_{\mathrm{T}},$$

$$\frac{\partial^2 f_4}{\partial x_4^2} = d_{\mathrm{T}},$$

$$\frac{\partial^2 f_4}{\partial x_5 \partial x_4} = d_{\mathrm{H}} + \varepsilon_1,$$

$$\frac{\partial^2 f_4}{\partial x_6 \partial x_4} = d_{\mathrm{HT}} + \varepsilon_2,$$

$$\frac{\partial^2 f_4}{\partial x_9 \partial x_4} = -\beta_{\mathrm{H}},$$

$$\frac{\partial^2 f_5}{\partial x_4 \partial x_5} = d_{\mathrm{T}} - g\beta_{\mathrm{T}}^*,$$

$$\frac{\partial^2 f_5}{\partial x_5^2} = d_{\mathrm{H}} + \varepsilon_1,$$

$$\frac{\partial^2 f_5}{\partial x_6 \partial x_5} = d_{\mathrm{HT}} + \varepsilon_2 - g\sigma\beta_{\mathrm{T}}^*,$$

$$\frac{\partial^2 f_5}{\partial x_9 \partial x_1} = \beta_{\mathrm{H}},$$

$$\frac{\partial^2 f_5}{\partial x_9 \partial x_2} = \beta_{\mathrm{H}},$$

$$\frac{\partial^2 f_5}{\partial x_9 \partial x_7} = \beta_{\mathrm{H}},$$

$$\frac{\partial^2 f_6}{\partial x_4 \partial x_6} = d_{\mathrm{T}},$$

$$\frac{\partial^2 f_6}{\partial x_5 \partial x_6} = d_{\mathrm{H}} + \varepsilon_1 + g\sigma\beta_{\mathrm{T}}^*,$$

$$\frac{\partial^2 f_6}{\partial x_6^2} = d_{\mathrm{HT}} + \varepsilon_2,$$

$$\frac{\partial^2 f_6}{\partial x_4 \partial x_5} = g\beta_{\mathrm{T}}^*,$$

$$\frac{\partial^2 f_6}{\partial x_9 \partial x_3} = \beta_{\mathrm{H}},$$

$$\frac{\partial^2 f_6}{\partial x_9 \partial x_4} = \beta_{\mathrm{H}},$$

$$\frac{\partial^2 f_7}{\partial x_9 \partial x_7} = -\beta_{\mathrm{H}},$$

$$\frac{\partial^2 f_7}{\partial x_4 \partial x_7} = d_{\mathrm{T}},$$

$$\frac{\partial^2 f_7}{\partial x_5 \partial x_7} = d_{\mathrm{H}} + \varepsilon_1,$$

$$\frac{\partial^2 f_7}{\partial x_6 \partial x_7} = d_{\mathrm{HT}} + \varepsilon_2,$$

$$\frac{\partial^2 f_8}{\partial x_4 \partial x_8} = d_{\mathrm{T}} - \beta_{\mathrm{T}}^*,$$

$$\frac{\partial^2 f_8}{\partial x_5 \partial x_8} = d_{\mathrm{H}} + \varepsilon_1,$$

$$\frac{\partial^2 f_8}{\partial x_6 \partial x_8} = d_{\mathrm{HT}} + \varepsilon_2 - \sigma\beta_{\mathrm{T}}^*. \tag{27}$$

Therefore, equation (25) becomes

$$\begin{aligned} a = {} & \left(\frac{a_0 w_4^2}{b(b+k)J_8} + \frac{a_1 w_4 w_5}{bJ\mu_M J_8 J_9 (b+k)}\right)\nu_3 \\ & + \left(d_{\mathrm{T}} w_4^2 + \frac{(\mu_M(d_{\mathrm{H}} + \varepsilon_1) - \beta_{\mathrm{H}}\varepsilon_1)}{\mu_M} w_4 w_5\right)\nu_4 \\ & + \left(\frac{a_2 w_4 w_5}{bJ_8\mu_M^2} + \frac{a_3 w_5^2}{bJ_9\mu_M^2}\right)\nu_5 + \frac{a_4 w_4 w_5}{\mu_M(b+k)}\nu_6, \end{aligned} \tag{28}$$

where

$$\begin{aligned} a_0 = {} & bd_{\mathrm{T}}\beta_{\mathrm{T}}^* J_8(s_0 + \rho\nu_{\mathrm{T}0}) + J_8\rho\beta_{\mathrm{T}}^*\nu_{\mathrm{T}0}(b+k)(\rho\beta_{\mathrm{T}}^* - d_{\mathrm{T}}) \\ & + (J_8(d_{\mathrm{T}} - \beta_{\mathrm{T}}^*)s_0 + \gamma_2\tau_2)\sigma\beta_{\mathrm{T}}^*, \\ a_1 = {} & \beta_{\mathrm{T}}^*(s_0 + \rho\nu_{\mathrm{T}0})bJ_8J_9(\mu_M(d_{\mathrm{H}} + \varepsilon_1) - \beta_{\mathrm{H}}\varepsilon_1) \\ & + \beta_{\mathrm{T}}^*\mu_M(b+k)(\sigma J_9(\mu_M\gamma_1\tau_1 - J_1J_8 - \beta_{\mathrm{T}}^*\varepsilon_1 s_0 J_9) - b\tau_1 J_8) \\ & - \rho\beta_{\mathrm{T}}^* J_8 J_9 b(b+k)(\mu_M(d_{\mathrm{H}} + \varepsilon_1) + \beta_{\mathrm{H}}\varepsilon_1), \\ a_2 = {} & (d_{\mathrm{T}} - g\beta_{\mathrm{T}}^*)bJ_8\mu_M^2 + (J_8(d_{\mathrm{T}} - \beta_{\mathrm{T}}^*)s_0 + \gamma_2\tau_2)\varepsilon_1\beta_{\mathrm{H}}\mu_M \\ & + b\mu_M\varepsilon_1\beta_{\mathrm{H}}\tau_2, \\ a_3 = {} & bJ_9\mu_M^2(d_{\mathrm{H}} + \varepsilon_1) + \beta_{\mathrm{H}}\varepsilon_1(\mu_M\gamma_1\tau_1 - J_1J_9 - \beta_{\mathrm{T}}^*\varepsilon_1 s_0 J_9), \\ a_4 = {} & (\mu_M\beta_{\mathrm{T}}^*(b+k) + \beta_{\mathrm{T}}^*(s_0 + \rho\nu_{\mathrm{T}0})\varepsilon_1\beta_{\mathrm{H}} + \beta_{\mathrm{H}}\varepsilon_1(b+k)). \end{aligned} \tag{29}$$

To determine the sign of b, we find the subsequent nonvanishing partial derivatives of F.

Table 2: Sensitivity indices for the reproduction number of Mtb infection $\mathscr{R}_T$.

Parameter	Description	Sensitivity indices
β_T	Transmission rate for Mtb	+1.0000
k	Progression to active TB	+0.9935
η	Rate of vaccination	-0.5385
ρ	Vaccine wane rate	+0.5385
b	Natural birth rate	-0.9942
d_T	Mtb disease-induced death rate	-0.9691
τ_2	Natural recovery rate for Mtb-infected individuals	-0.0303

$$\begin{aligned}
\frac{\partial^2 f_1}{\partial x_4 \partial \beta_T^*} &= -s_0,\\
\frac{\partial^2 f_1}{\partial x_6 \partial \beta_T^*} &= -\sigma s_0,\\
\frac{\partial^2 f_3}{\partial x_4 \partial \beta_T^*} &= s_0 + \rho v_{T0},\\
\frac{\partial^2 f_3}{\partial x_6 \partial \beta_T^*} &= \sigma(s_0 + \rho v_{T0}).
\end{aligned} \tag{30}$$

Therefore, $b = (\beta_T^* k(s_0 + \rho v_{T0})^2/(b+k)^2) w_4 v_4$.

Now, according to [25], the signs of a and b dictate the local dynamics; thus, we have the following lemma.

Lemma 3. *Suppose that $b > 0$. Then, we have the following:*

(i) System (4) undergoes backward bifurcation if the coefficient a is positive

(ii) System (4) will exhibit transcritical bifurcation if the coefficient a is negative

3. Sensitivity Analysis

In this section, we perform a sensitivity analysis of the effective reproduction number subject to each parameter in order to determine the impact of every parameter on the effective reproduction number. Therefore, we compute the forward sensitivity index of the effective reproduction number $\mathscr{R}_{HT}$ with respect to the parameters using the approach by Chitnis et al. [26]. Since $\mathscr{R}_{HT} = \max\{\mathscr{R}_H, \mathscr{R}_T\}$, then the sensitivity indices for $\mathscr{R}_H$ and $\mathscr{R}_T$ are computed. The normalized forward sensitivity index of a variable P with respect to parameter r is defined as $\zeta_r^P = (r/P)(\partial P/\partial r)$. For instance, the sensitivity index of $\mathscr{R}_T$ with respect to β_T is given by $\zeta_{\beta_T}^{\mathscr{R}_T} = (\beta_T/\mathscr{R}_T)(\partial \mathscr{R}_T/\beta_T) = 1$, and other indices are evaluated using parameter values in Table 1. The remaining indices are given in Tables 2 and 3.

Table 3: Sensitivity indices for the reproduction number of helminth infection $\mathscr{R}_H$.

Parameter	Description	Sensitivity indices
β_H	Ingestion rate of parasitic worms	+1
ε_1	Shading rate for helminth-infected individuals	+0.4402
μ_M	Clearance rate of parasitic worms	-1.0000
b	Natural birth rate	-0.0003
d_H	Helminth disease-induced death rate	-0.2177
τ_1	Natural recovery rate for helminth-infected individuals	-0.2221

From Tables 2 and 3, the most positive parameter indices are β_T, k, and β_H while the most negative parameter indices are b, d_T, and μ_M. This implies that when parameters β_T, k, and β_H are increased, and while the remaining are kept constant, the endemicity of the disease is increased, while when the parameter μ_M is increased, the endemicity of disease is decreased. Increasing the natural birth rate and Mtb mortality rate does not make biological sense that the disease would be contained. Thus, we suggest the application of optimal control to sensitive parameters such as β_H, β_T, and μ_M to study how effectively we can contain the helminth-Mtb infection.

4. The Optimal Control Problem

In this section, the extension of model (1) is formed by including four time-dependent controls so as to decide the optimal strategy for controlling the two diseases. The controls are defined as follows:

(i) Educational campaign $u_1(t)$ that sensitizes the parents to vaccinate more infants. Therefore, the recruitment for the Mtb-vaccinated individuals changes to $\eta N(1 + u_1(t))$ meaning that when this control is 100% implemented, then the number of vaccinated babies doubles

(ii) Treatment $\alpha_1 u_2(t)$ of individuals with active TB, where α_1 is the drug efficacy use for Mtb infection. Therefore, the Mtb recovery rate changes to $\tau_2 + \alpha_1 u_2(t)$

(iii) Deworming at a rate $\alpha_2 u_3(t)$ for the helminth-infected individuals and coinfected individuals, where α_2 is the drug efficacy use for helminth infection. Therefore, the helminth recovery rate changes to $\tau_1 + \alpha_2 u_3(t)$

(iv) Sanitation and proper hygiene u_4 that reduces the ingestion rate of parasites. Therefore, the force of infection for the helminth infection is changed to $\lambda_H = (1 - u_4)\beta_H M/(K + M)$

After incorporating the controls $u_1(t)$, $u_2(t)$, $u_3(t)$, and $u_4(t)$ in the Mtb-helminth infection model (4), then the optimal control model becomes

$$\begin{cases} \dfrac{dS}{dt} = (1-\eta)bN + \gamma_1 R_{\mathrm{H}} + \gamma_2 R_{\mathrm{T}} - (\mu + \lambda_{\mathrm{T}} + (1-u_4)\lambda_{\mathrm{H}})S, \\ \dfrac{dV_{\mathrm{T}}}{dt} = \eta b(1+u_1)N - (\mu + \rho\lambda_{\mathrm{T}} + (1-u_4)\lambda_{\mathrm{H}})V_{\mathrm{T}}, \\ \dfrac{dE_{\mathrm{T}}}{dt} = \lambda_{\mathrm{T}} S + \rho\lambda_{\mathrm{T}} V_{\mathrm{T}} + \lambda_{\mathrm{T}} R_{\mathrm{H}} - (\mu + k + (1-u_4)\lambda_{\mathrm{H}})E_{\mathrm{T}}, \\ \dfrac{dI_{\mathrm{T}}}{dt} = kE_{\mathrm{T}} + (\tau_1 + \alpha_2 u_3)I_{\mathrm{HT}} - (\mu + d_{\mathrm{T}} + \tau_2 + (1-u_4)\lambda_{\mathrm{H}})I_{\mathrm{T}} - (\tau_2 + \alpha_1 u_2)I_{\mathrm{T}}, \\ \dfrac{dI_{\mathrm{H}}}{dt} = (1-u_4)\lambda_{\mathrm{H}} S + (1-u_4)\lambda_{\mathrm{H}} V_{\mathrm{T}} + (1-u_4)\lambda_{\mathrm{H}} R_{\mathrm{T}} + \tau_2 I_{\mathrm{HT}} - (g\lambda_{\mathrm{T}} + \mu + d_{\mathrm{H}} + \varepsilon_1)I_{\mathrm{H}} - (\tau_1 + \alpha_2 u_3)I_{\mathrm{H}}, \\ \dfrac{dI_{\mathrm{HT}}}{dt} = g\lambda_{\mathrm{T}} I_{\mathrm{H}} + (1-u_4)\lambda_{\mathrm{H}}(E_{\mathrm{T}} + I_{\mathrm{T}}) - (\mu + d_{\mathrm{HT}} + \tau_2 + \varepsilon_2)I_{\mathrm{HT}} - (\tau_1 + \alpha_2 u_3)I_{\mathrm{HT}}, \\ \dfrac{dR_{\mathrm{T}}}{dt} = (\tau_2 + \alpha_1 u_2)I_{\mathrm{T}} - ((1-u_4)\lambda_{\mathrm{H}} + \mu + \gamma_2)R_{\mathrm{T}}, \\ \dfrac{R_{\mathrm{H}}}{dt} = (\tau_1 + \alpha_2 u_3)I_{\mathrm{H}} - (\lambda_{\mathrm{T}} + \mu + \gamma_1)R_{\mathrm{H}}, \\ \dfrac{dM}{dt} = \varepsilon_1 I_{\mathrm{H}} + \varepsilon_2 I_{\mathrm{HT}} - \mu_M M. \end{cases} \tag{31}$$

We employ Pontryagin's Maximum Principle to figure out the required conditions for the optimal control of helminth-Mtb coinfection. The control set U is Lebesgue measurable and is defined as $U = \{u_1(t), u_2(t), u_3(t), u_4(t): 0 \le u_i(t) \le 1, 0 < t \le t_f\}$. Then, the objective is to minimize individuals with active TB, individuals infested with helminth parasites, and coinfected individuals while keeping the cost low. For this problem, we consider the objective functional defined by

$$J = \int_{t_0}^{t_f} \left\{ C_1 I_{\mathrm{T}} + C_2 I_{\mathrm{H}} + C_3 I_{\mathrm{HT}} + \frac{1}{2}\sum_{i=1}^{4} w_i u_i^2 \right\} dt, \tag{32}$$

where $C_1 I_{\mathrm{T}}$, $C_2 I_{\mathrm{H}}$, are $C_3 I_{\mathrm{HT}}$ are the costs related to active tuberculosis individuals, individuals infected with helminths, and coinfected individuals, respectively. The expression $(1/2)w_i u_i^2$ is related to the background costs with relative cost weights w_i for every control measure. The quadratic cost is tailored as utilized in other models with controls (see [16, 27]). The particular value of the weights requires intensive data processing; hence, we elect estimate values for theoretical purposes.

The aim is to minimize the objective functional J as defined in (32) subject to model (31). Therefore, we seek to get the optimal controls u_1^*, u_2^*, u_3^*, and u_4^* such that

$$J(u_1^*, u_2^*, u_3^*, u_4^*) = \min_{u_1,u_2,u_3,u_4 \in U} J(u_1, u_2, u_3, u_4), \tag{33}$$

where $U = \{(u_1, u_2, u_3, u_4)$ and therefore the controls su_1, u_2, u_3, are u_4 are measurable with $0 \le u_1 \le 1$, $0 \le u_2 \le 1$, $0 \le u_3 \le 1$, and $0 \le u_4 \le 1$ for $t \in [t_0 t_f]\}$.

Theorem 4. *Consider the control problem with the system of equations in (31). There exist* $u^* = (u_1^*, u_2^*, u_3^*, u_4^*) \in U$ *such that*

$$\min_{u_1,u_2,u_3,u_4 \in U} J(u_1, u_2, u_3, u_4,) = J(u_1^*, u_2^*, u_3^*, u_4^*). \tag{34}$$

The necessary conditions that an optimal solution must satisfy are derived from Pontryagin's Maximum Principle [28]. The principle converts equations (31) and (32) into the problem of minimizing the pointwise Hamiltonian H, with reference to u_1, u_2, u_3, *and* u_4. *The Hamiltonian is given by*

$$
\begin{aligned}
H = {} & C_1 I_T + C_2 I_H + C_3 I_{HT} + \frac{1}{2}\left(w_1 u_1^2 + w_2 u_2^2 + w_3 u_3^2 + w_4 u_4^2\right) \\
& + \lambda_S\{(1-\eta)bN + \gamma_1 R_H + \gamma_2 R_T - (\mu + \lambda_T + (1-u_4)\lambda_H)S\} \\
& + \lambda_{V_T}\{\eta b(1+u_1)N - (\mu + \rho\lambda_T + (1-u_4)\lambda_H)V_T\} \\
& + \lambda_{E_T}\{\lambda_T S + \rho\lambda_T V_T + \lambda_T R_H - (\mu + k + (1-u_4)\lambda_H)E_T \\
& + \lambda_{I_T}\{kE_T + (\tau_1 + \alpha_2 u_3)I_{HT} - (\mu + d_T + (1-u_4)\lambda_H)I_T \\
& - (\tau_2 + \alpha_1 u_2)I_T\} + \lambda_{I_H}\{(1-u_4)\lambda_H(S + V_T + R_T) \\
& + \tau_2 I_{HT} - (\mu + d_H + \varepsilon_1 + g\lambda_T)I_H - (\tau_1 + \alpha_2 u_3)I_H\} \\
& + \lambda_{I_{HT}}\{g\lambda_T I_H + (1-u_4)\lambda_H(E_T + I_T) \\
& - (\mu + d_{HT} + \tau_2 + \varepsilon_2)I_{HT} - (\tau_1 + \alpha_2 u_3)I_{HT}\} \\
& + \lambda_{R_T}\{(\tau_2 + \alpha_1 u_2)I_T - (\lambda_H + \mu + \gamma_2)R_T\} \\
& + \lambda_{R_H}\{(\tau_1 \quad + \alpha_2 u_3)I_H - (\lambda_T + \mu + \gamma_1)R_H\} \\
& + \lambda_M\{\varepsilon_1 I_H + \varepsilon_2 I_{HT} - \mu_M M\}.
\end{aligned} \tag{35}
$$

where λ_S, λ_{V_T}, λ_{E_T}, λ_{I_T}, λ_{I_H}, $\lambda_{I_{HT}}$, λ_{R_T}, λ_{R_H}, and λ_M are the costate variables or the adjoint variables. Now, applying Pontryagin's Maximum Principle [28], the problem has a solution following the results of the optimal control problem in [29].

Theorem 5. *Given the optimal controlu_i, for$i = 1, 2, 3, 4$, and the solutions$S, V_T, E_T, I_T, I_H, I_{HT}, R_T, R_H$, and$M$, and the state systems (31) and (32) that minimize$J(u_1, u_2, u_3, u_4)$over$U$, there exist adjoint variables$\lambda_S, \lambda_{V_T}, \lambda_{E_T}, \lambda_{I_T}, \lambda_{I_H}, \lambda_{I_{HT}}, \lambda_{R_T}, \lambda_{R_H}$, and$\lambda_M$ satisfying*

$$
-\frac{d\lambda_i}{dt} = \frac{\partial H}{\partial x_i} \tag{36}
$$

where $x_i = S, V_T, I_T, I_H, I_{HT}, R_T, R_H, M$ with transversality conditions $\lambda_S(t_f) = \lambda_{V_T}(t_f) = \lambda_{E_T}(t_f) = \lambda_{I_T}(t_f) = \lambda_{I_H}(t_f) = \lambda_{I_{HT}}(t_f) = \lambda_{R_T}(t_f) = \lambda_{R_H}(t_f) = \lambda_M(t_f) = 0$, and the subsequent characterization holds on the interior of the control set U:

$$
\begin{aligned}
u_1^* &= \max\left\{0, \min\left\{1, -\frac{\eta b N \lambda_{V_T}}{w_1}\right\}\right\}, \\
u_2^* &= \max\left\{0, \min\left\{1, \frac{\alpha_1 I_T(\lambda_{I_T} - \lambda_{R_T})}{w_2}\right\}\right\}, \\
u_3^* &= \max\left\{0, \min\left\{1, \frac{\alpha_2 I_H(\lambda_{I_H} - \lambda_{R_H}) + \alpha_2 I_{HT}(\lambda_{I_{HT}} - \lambda_{I_T})}{w_3}\right\}\right\}, \\
u_4^* &= \max\left\{0, \min\left\{1, \frac{\lambda_H \lambda_{I_H}(S + V_T + R_T) + \lambda_H \lambda_{I_{HT}}(E_T + I_T)}{w_4}\right.\right. \\
&\quad \left.\left. - \frac{\lambda_H(S\lambda_S + V_T\lambda_{V_T} + E_T\lambda_{E_T} + I_T\lambda_{I_T})}{w_4}\right\}\right\}.
\end{aligned} \tag{37}
$$

Proof. Flemming and Rishel [23] provide the existence of an optimal control model (31) and the costate variables (36) due to the boundness of state equations and the Lipschitz structure of the ordinary differential equations. Therefore, applying the necessary conditions from Pontryagin's Maximum Principle, we obtain the following system for costate variables:

$$
\begin{aligned}
\frac{d\lambda_S}{dt} = {} & -(1-\eta)b\lambda_S + \frac{\beta_T(I_T + \sigma I_{HT})S}{N^2}(\lambda_{E_T} - \lambda_S) \\
& + \frac{\beta_T(I_T + \sigma I_{HT})V_T}{N^2}(\rho\lambda_{E_T} - \lambda_{V_T}) - \eta b(1+u_1)\lambda_{V_T} \\
& + \frac{\beta_T(I_T + \sigma I_{HT})R_H}{N^2}(\lambda_{E_T} - \lambda_{R_H}) + \frac{\beta_T(I_T + \sigma I_{HT})}{N}(\lambda_S - \lambda_{E_T}) \\
& + \frac{g\beta_T(I_T + \sigma I_{HT})I_H}{N^2}(\lambda_{I_{HT}} - \lambda_{I_H}) \\
& + \frac{(1-u_4)\beta_H M}{K+M}(\lambda_S - \lambda_{I_H}) + \mu\lambda_S,
\end{aligned}
$$

$$
\begin{aligned}
\frac{d\lambda_{V_T}}{dt} = {} & -(1-\eta)b\lambda_S + \frac{\beta_T(I_T + \sigma I_{HT})V_T}{N^2}(\rho\lambda_{E_T} - \lambda_{V_T}) \\
& + \frac{\beta_T(I_T + \sigma I_{HT})R_H}{N^2}(\lambda_{E_T} - \lambda_{R_T}) - \eta b(1+u_1)\lambda_{V_T} \\
& + \frac{\beta_T(I_T + \sigma I_{HT})S}{N^2}(\lambda_{E_T} - \lambda_S) + \frac{\beta_T(I_T + \sigma I_{HT})}{N}(\lambda_{V_T} - \rho\lambda_{E_T}) \\
& + \frac{g\beta_T(I_T + \sigma I_{HT})I_H}{N^2}(\lambda_{I_{HT}} - \lambda_{I_H}) \\
& + \frac{(1-u_4)\beta_H M}{K+M}(\lambda_{V_T} - \lambda_{I_H}) + \mu\lambda_{V_T},
\end{aligned}
$$

$$
\begin{aligned}
\frac{d\lambda_{E_T}}{dt} = {} & -(1-\eta)b\lambda_S + \frac{\beta_T(I_T + \sigma I_{HT})S}{N^2}(\lambda_{E_T} - \lambda_S) \\
& + \frac{\rho\beta_T(I_T + \sigma I_{HT})V_T}{N^2}(\lambda_{E_T} - \lambda_{V_T}) - \eta b(1+u_1)\lambda_{V_T} \\
& + \frac{\beta_T(I_T + \sigma I_{HT})R_H}{N^2}(\lambda_{E_T} - \lambda_{R_H}) + \frac{g\beta_T(I_T + \sigma I_{HT})I_H}{N^2}(\lambda_{I_{HT}} - \lambda_{I_H}) \\
& + \frac{(1-u_4)\beta_H M}{K+M}(\lambda_{E_T} - \lambda_{I_{HT}}) + k(\lambda_{E_T} - \lambda_{I_T}) + \mu\lambda_{E_T},
\end{aligned}
$$

$$
\begin{aligned}
\frac{d\lambda_{I_T}}{dt} = {} & -C_1 - (1-\eta)b\lambda_S + \frac{\beta_T(I_T + \sigma I_{HT})S}{N^2}(\lambda_{E_T} - \lambda_S) \\
& + \frac{\rho\beta_T(I_T + \sigma I_{HT})V_T}{N^2}(\lambda_{E_T} - \lambda_{V_T}) - \eta b(1+u_1)\lambda_{V_T} \\
& + \frac{\beta_T(I_T + \sigma I_{HT})R_H}{N^2}(\lambda_{E_T} - \lambda_{R_H}) + \frac{\beta_T(S\lambda_S + V_T\lambda_{V_T} + I_T\lambda_{R_H})}{N} \\
& + \frac{g\beta_T(I_T + \sigma I_{HT})I_H}{N^2}(\lambda_{I_{HT}} - \lambda_{I_H}) + \frac{(1-u_4)\beta_H M}{K+M}(\lambda_{I_T} - \lambda_{I_{HT}}) \\
& + (\mu + d_T)\lambda_{I_T} + \frac{g\beta_T I_H}{N}(\lambda_{I_H} - \lambda_{I_{HT}}) + (\tau_2 + \alpha_1 u_2)(\lambda_{I_T} - \lambda_{R_H}),
\end{aligned}
$$

$$
\begin{aligned}
\frac{d\lambda_{I_H}}{dt} = {} & -C_2 - (1-\eta)b\lambda_S + \frac{\beta_T(I_T + \sigma I_{HT})S}{N^2}(\lambda_{E_T} - \lambda_S) \\
& + \frac{\rho\beta_T(I_T + \sigma I_{HT})V_T}{N^2}(\lambda_{E_T} - \lambda_{V_T}) - \eta b(1+u_1)\lambda_{V_T} \\
& + \frac{\beta_T(I_T + \sigma I_{HT})R_H}{N^2}(\lambda_{E_T} - \lambda_{R_H}) + \frac{g\beta_T(I_T + \sigma I_{HT})}{N}(\lambda_{I_H} - \lambda_{I_{HT}}) \\
& + \frac{g\beta_T(I_T + \sigma I_{HT})I_H}{N^2}(\lambda_{I_{HT}} - \lambda_{I_H}) + (\tau_1 + \alpha_2 u_3)(\lambda_{I_H} - \lambda_{R_H}) \\
& + (\mu + d_H + \varepsilon_1)\lambda_{I_H} + \varepsilon_1\lambda_M,
\end{aligned}
$$

$$\begin{aligned}
\frac{d\lambda_{I_{HT}}}{dt} &= -C_3 - (1-\eta)b\lambda_S + \frac{\beta_T(I_T+\sigma I_{HT})S}{N^2}\left(\lambda_{E_T}-\lambda_S\right)\\
&+ \frac{\rho\beta_T(I_T+\sigma I_{HT})V_T}{N^2}\left(\lambda_{E_T}-\lambda_{V_T}\right) - \eta b(1+u_1)\lambda_{V_T}\\
&+ \frac{\beta_T(I_T+\sigma I_{HT})R_H}{N^2}\left(\lambda_{E_T}-\lambda_{R_H}\right) + \frac{\sigma g\beta_T(I_T+\sigma I_{HT})}{N}\left(\lambda_{I_H}-\lambda_{I_{HT}}\right)\\
&+ \frac{g\beta_T(I_T+\sigma I_{HT})I_H}{N^2}\left(\lambda_{I_{HT}}-\lambda_{I_H}\right) + (\tau_1+\alpha_2u_3)\left(\lambda_{I_{HT}}-\lambda_{I_T}\right)\\
&+ (\mu+d_{HT}+\tau_2+\varepsilon_2)\lambda_{I_{HT}} + \varepsilon_2\lambda_M - \tau_2\lambda_{I_H}\\
&+ \frac{\beta_T\sigma\left(S\lambda_S+\rho V_T\lambda_{V_T}+R_H\lambda_{R_H}\right)}{N} - \frac{\sigma\beta_T(S+\rho V_T+R_H)}{N},\\
\frac{d\lambda_{R_T}}{dt} &= -(1-\eta)b\lambda_S + \frac{\beta_T(I_T+\sigma I_{HT})S}{N^2}\left(\lambda_{E_T}-\lambda_S\right)\\
&+ \frac{\rho\beta_T(I_T+\sigma I_{HT})V_T}{N^2}\left(\lambda_{E_T}-\lambda_{V_T}\right) - \eta b(1+u_1)\lambda_{V_T}\\
&+ \frac{\beta_T(I_T+\sigma I_{HT})R_H}{N^2}\left(\lambda_{E_T}-\lambda_{R_H}\right) + \gamma_2\left(\lambda_{R_T}-\lambda_S\right)\\
&+ \mu\lambda_{R_T} + \frac{g\beta_T(I_T+\sigma I_{HT})I_H}{N^2}\left(\lambda_{I_{HT}}-\lambda_{I_H}\right)\\
&+ \frac{(1-u_4)\beta_H M}{K+M}\left(\lambda_{\lambda_{R_T}}-\lambda_{I_H}\right),\\
\frac{d\lambda_{R_T}}{dt} &= -(1-\eta)b\lambda_S + \frac{\beta_T(I_T+\sigma I_{HT})S}{N^2}\left(\lambda_{E_T}-\lambda_S\right)\\
&+ \frac{\rho\beta_T(I_T+\sigma I_{HT})V_T}{N^2}\left(\lambda_{E_T}-\lambda_{V_T}\right)\\
&- \eta b(1+u_1)\lambda_{V_T} + \frac{\beta_T(I_T+\sigma I_{HT})R_H}{N^2}\left(\lambda_{E_T}-\lambda_{R_H}\right)\\
&+ \gamma_1\left(\lambda_{R_H}-\lambda_S\right) + \mu\lambda_{R_H} + \frac{g\beta_T(I_T+\sigma I_{HT})I_H}{N^2}\left(\lambda_{I_{HT}}-\lambda_{I_H}\right)\\
&+ \frac{\beta_T(I_T+\sigma I_{HT})}{N}\left(\lambda_{\lambda_{R_H}}-\lambda_{E_T}\right),\\
\frac{d\lambda_M}{dt} &= \frac{(1-u_4)\beta_H MS}{(K+M)^2}\left(\lambda_{I_H}-\lambda_S\right) + \frac{(1-u_4)\beta_H MV_T}{(K+M)^2}\left(\lambda_{I_H}-\lambda_{V_T}\right)\\
&+ \frac{(1-u_4)\beta_H MR_T}{(K+M)^2}\left(\lambda_{I_H}-\lambda_{R_T}\right)\\
&+ \frac{(1-u_4)\beta_H ME_T}{(K+M)^2}\left(\lambda_{I_{HT}}-\lambda_{E_T}\right) + \frac{(1-u_4)\beta_H MI_T}{(K+M)^2}\left(\lambda_{I_{HT}}-\lambda_{I_T}\right)\\
&+ \frac{(1-u_4)\beta_H\left(S\lambda_S+V_T\lambda_{V_T}+E_T\lambda_{E_T}+I_T\lambda_{I_T}+R_T\lambda_{R_T}\right)}{K+M}\\
&+ \mu_M\lambda_M - \frac{(1-u_4)\beta_H\left((S+V_T+R_T)\lambda_{I_H}+(E_T+I_T)\lambda_{I_{HT}}\right)}{K+M}.
\end{aligned} \tag{38}$$

To get the controls, we solve the equations $\partial H/\partial u_i = 0$ at u_i^* for $i = 1, \cdots, 4$ and obtained the following:

$$\begin{aligned}
u_1^* &= -\frac{\eta bN\lambda_{V_T}}{w_1},\\
u_2^* &= \frac{\alpha_1 I_T\left(\lambda_{I_T}-\lambda_{R_T}\right)}{w_2},\\
u_3^* &= \frac{\alpha_2 I_H\left(\lambda_{I_H}-\lambda_{R_H}\right)+\alpha_2 I_{HT}\left(\lambda_{I_{HT}}-\lambda_{I_T}\right)}{w_4},\\
u_4^* &= \frac{\lambda_H\lambda_{I_H}(S+V_T+R_T)+\lambda_H\lambda_{I_{HT}}(E_T+I_T)}{w_4}\\
&\quad - \lambda_H\left(S\lambda_S+V_T\lambda_{V_T}+E_T\lambda_{E_T}+I_T\lambda_{I_T}\right).
\end{aligned} \tag{39}$$

Then, we write by standard control arguments involving the bounds on the controls as

$$\begin{aligned}
u_1^* &= \begin{cases} \Theta_1, & \text{if } 0 < \Theta_1 < 1,\\ 0, & \text{if } \Theta_1 \le 0,\\ 1, & \text{if } \Theta_1 \ge 1,\end{cases}\\
u_2^* &= \begin{cases} \Theta_2, & \text{if } 0 < \Theta_2 < 1,\\ 0, & \text{if } \Theta_2 \le 0,\\ 1, & \text{if } \Theta_2 \ge 1,\end{cases}\\
u_3^* &= \begin{cases} \Theta_3, & \text{if } 0 < \Theta_3 < 1,\\ 0, & \text{if } \Theta_3 \le 0,\\ 1, & \text{if } \Theta_3 \ge 1,\end{cases}\\
u_4^* &= \begin{cases} \Theta_4, & \text{if } 0 < \Theta_4 < 1,\\ 0, & \text{if } \Theta_4 \le 0,\\ 1, & \text{if } \Theta_4 \ge 1,\end{cases}
\end{aligned} \tag{40}$$

where

$$\begin{aligned}
\Theta_1 &= -\frac{\eta bN\lambda_{V_T}}{w_1},\\
\Theta_2 &= \frac{\alpha_1 I_T\left(\lambda_{I_T}-\lambda_{R_T}\right)}{w_2},\\
\Theta_3 &= \frac{\alpha_2 I_H\left(\lambda_{I_H}-\lambda_{R_H}\right)+\alpha_2 I_{HT}\left(\lambda_{I_{HT}}-\lambda_{I_T}\right)}{w_4},\\
\Theta_4 &= \frac{\lambda_H\lambda_{I_H}(S+V_T+R_T)+\lambda_H\lambda_{I_{HT}}(E_T+I_T)}{w_4}\\
&\quad - \lambda_H\left(S\lambda_S+V_T\lambda_{V_T}+E_T\lambda_{E_T}+I_T\lambda_{I_T}\right).
\end{aligned} \tag{41}$$

5. Numerical Simulation

In this section, different optimal control strategies are used to investigate numerically their effect on the spread of helminth and Mtb coinfection. The state system (31), the adjoint system (38), and therefore the characterization in equation (37) are solved numerically using an iterative scheme so as to attain the optimal control. Using the initial conditions for the state system and the transversality conditions for the adjoint system with the initial guess of the controls, we solve the state system forward in time and the adjoint system backward in time using the fourth-order Runge-Kutta scheme with the current solutions of the state system. Then, the controls are updated using a convex combination of the controls and the values from characterization (37). The solution of the state system and the adjoint system is repeated until the present iteration is close to the previous iteration [30].

In numerical simulation, the weights are assumed to depend on the cost of investment and importance of the controls. For example, the cost associated with control u_2 requires huge investment that includes clinical examination

of Mtb cases and procurement and transportation of the drugs. The cost associated with control u_2 requires procurement and transportation of antihelminthic drugs and monitoring of the distribution of drugs. We choose the weights as $C_1 = 5822$, $C_2 = 0.89$, $C_3 = 5822.89$, $w_1 = 20$, $w_2 = 40$, $w_3 = 30$, and $w_4 = 10$ and the initial state variables as $S = 1500$, $V_T = 2000$, $E_T = 200$, $I_T = 150$, $I_H = 100$, $I_{HT} = 80$, $R_T = 5$, $R_H = 5$, and $M = 200$. The efficacy parameters are $\alpha_1 = 0.75$ and $\alpha_2 = 0.8$, and the remaining parameter values are given in Table 1.

5.1. Control with Educational Campaign (u_1) and Treatment of Individuals with Active TB (u_2). The educational campaign control (u_1) and treatment of individuals with active TB control (u_2) are used to optimize the objective functional J while the other controls (u_3) and (u_4) related to helminths were set to zero. We observed that in Figure 2(b) the number of individuals with active TB was controlled but starts to increase again until the end of the intervention period. This may be related to our previous analysis that helminth infection enhances Mtb infection. In this strategy, helminth infection is not controlled; Figures 2(c) and 2(d) indicate that there is slight significance in the case with controls and without controls for helminth-infected individuals and coinfected individuals, respectively. Figure 2(e) indicates that the parasite population is not controlled with this strategy while Figure 2(f) indicates that the educational campaign control should be seized after 158 days while treatment of individuals with active TB control should be kept maximum in the entire period of intervention.

5.2. Control with Mass Drug Administration (u_3) and Sanitation (u_4). The mass drug administration (MDA) control (u_3) and sanitation control (u_4) were used to optimize the objective functional J. Again, we observe that Figure 3(a) indicates the increase in vaccinated individuals. Also, Figure 3(b) indicates that the number of people with active TB increases rapidly and is eventually controlled after 55 days. An equivalent scenario is observed in Figures 3(c) and 3(d) where the helminth-infected individuals and coinfected individuals were effectively controlled. Figure 3(e) suggests that the parasite population is substantially controlled at the end of the intervention period. This strategy seems to be effective in controlling the two diseases from the community. Figure 3(f) indicates that MDA and sanitation controls should be kept maximum throughout the intervention period.

5.3. Control with Educational Campaign (u_1) and Sanitation (u_4). The educational campaign control (u_1) and sanitation control (u_4) are employed to optimize the objective functional J. This strategy has the same profiles as the strategy with mass drug administration and sanitation controls but takes a long time to control the two diseases. Figure 4(f) indicates that the educational campaign must be stopped after 30 days whereas sanitation control must be kept maximum in the entire period of intervention.

5.4. Control with Treatment of Individuals with Active TB (u_2) and MDA (u_3). The treatment of individuals with active TB control (u_2) and MDA control (u_3) are used to optimize the objective functional J while the other controls (u_1) and (u_4) are set to zero. Figure 5(a) indicates a slight increase in vaccinated individuals compared to the other strategies (Sections 5.1, 5.2, and 5.3). Figures 5(b) and 5(d) indicate that the treatment of individuals with active TB and coinfected individuals is effectively controlled while Figure 5(c) indicates a decrease in the helminth-infected individuals but a rise at the final intervention period. This is due to the absence of preventive measures in this strategy. Figure 5(f) indicates that both controls should be kept maximum until the final intervention period.

5.5. Control with Educational Campaign (u_1), Treatment of Mtb-Infected Individuals (u_2), MDA (u_3), and Sanitation (u_4). With this strategy, all four controls are employed to optimize the objective functional J. We observed that Figure 6(a) indicates that the number of vaccinated individuals increases more at the end of the intervention period. Figures 6(b)–6(d) indicate that individuals with active TB, helminth-infected individuals, and coinfected individuals are all effectively and efficiently controlled at the end of the intervention period. Figure 6(e) depicts that the parasite population is decreased to a number that cannot harm the human population. This strategy indicates that optimal educational campaign, treatment of individuals with active TB, MDA, and sanitation would effectively control the helminth-Mtb infection at the end of the intervention period. Figure 6(f) suggests that the educational campaign should be stopped after 115 days whereas the remaining controls should be maintained maximum for the whole intervention period.

6. Discussions and Conclusions

In this paper, we described and formulated a deterministic model for the transmission dynamics and control of helminth-Mtb coinfection. The effective reproduction number was computed, and we explored the steadiness of the disease-free equilibrium point. We again established the existence of backward or forward bifurcation using the Center Manifold Theorem. Then, we investigated the impact the two diseases have on each other and found that helminth infection cases increase Mtb infection cases. In Section 4, we modified the helminth-Mtb model by incorporating four control measures: educational campaign to sensitize the parents to take babies to the BCG vaccine clinic, treatment of individuals with active TB, mass drug administration for helminth and coinfected individuals, and sanitation to reduce the intake rate of parasites. The optimal control was analyzed using Pontryagin's Maximum Principle [28], by first finding the Hamiltonian, the costate variables, the characterization of the controls, and the optimality system.

Then, we solved numerically the optimality system by the iterative scheme using the Forward-Backward Sweep Method (FBSM) with the combination of the following control measures:

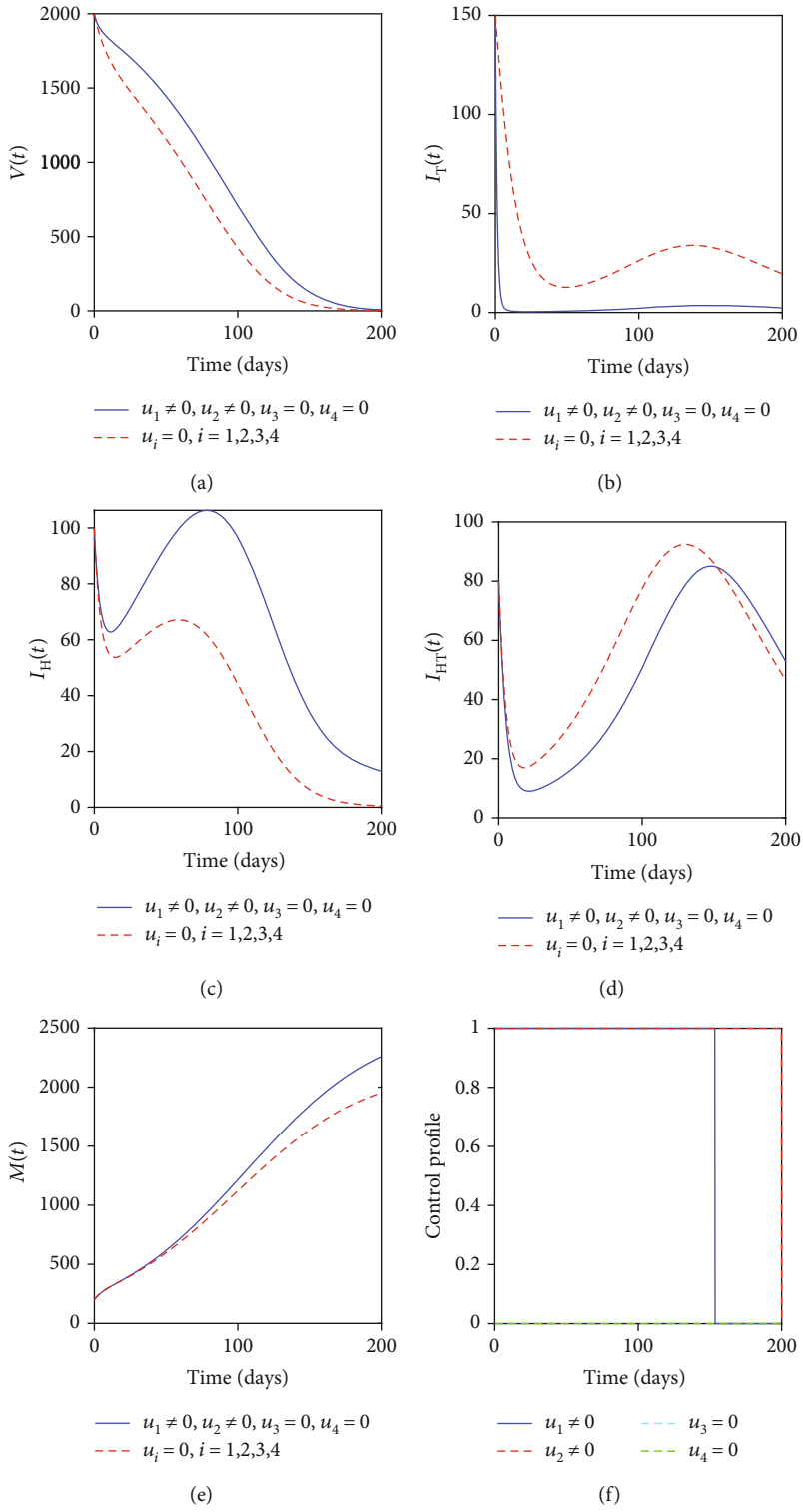

Figure 2: Simulations of the helminth-Mtb coinfection model with the effect of educational campaign and treatment of Mtb-infected individuals.

(i) By applying a combination of educational campaign and treatment of individuals with active TB

(ii) By applying a combination of mass drug administration (MDA) and sanitation

(iii) By applying a combination of educational campaign and sanitation

(iv) By applying a combination of treatment of individuals with active TB and mass drug administration

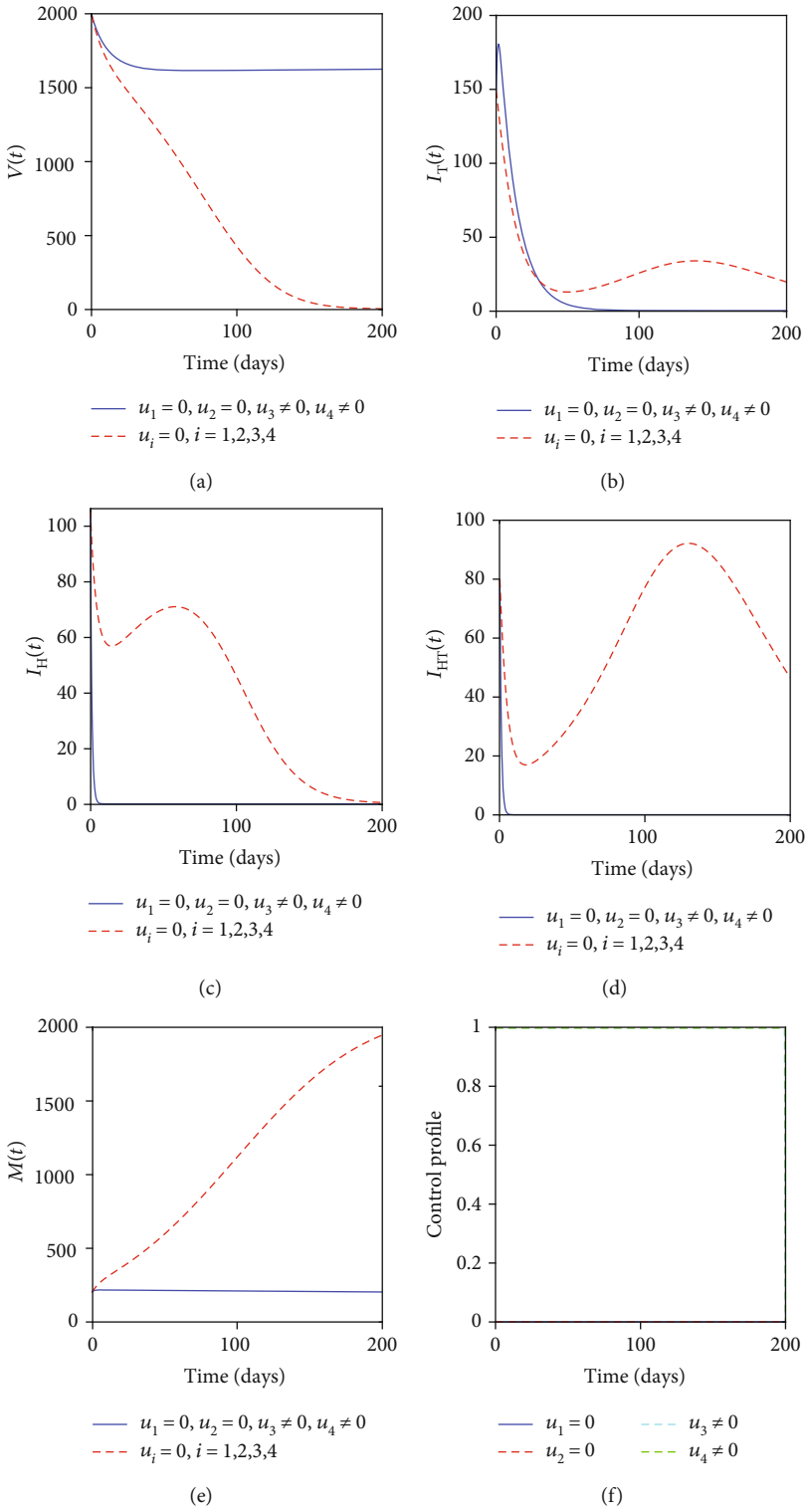

Figure 3: Simulations of the helminth-Mtb coinfection model with the effect of MDA and sanitation.

(v) By applying a combination of educational campaign, treatment of individuals with active TB, mass drug administration, and sanitation

The control strategies which focus on TB only while helminths are not controlled would not lead to the efficient and effective control of TB or helminth infection. Moreover,

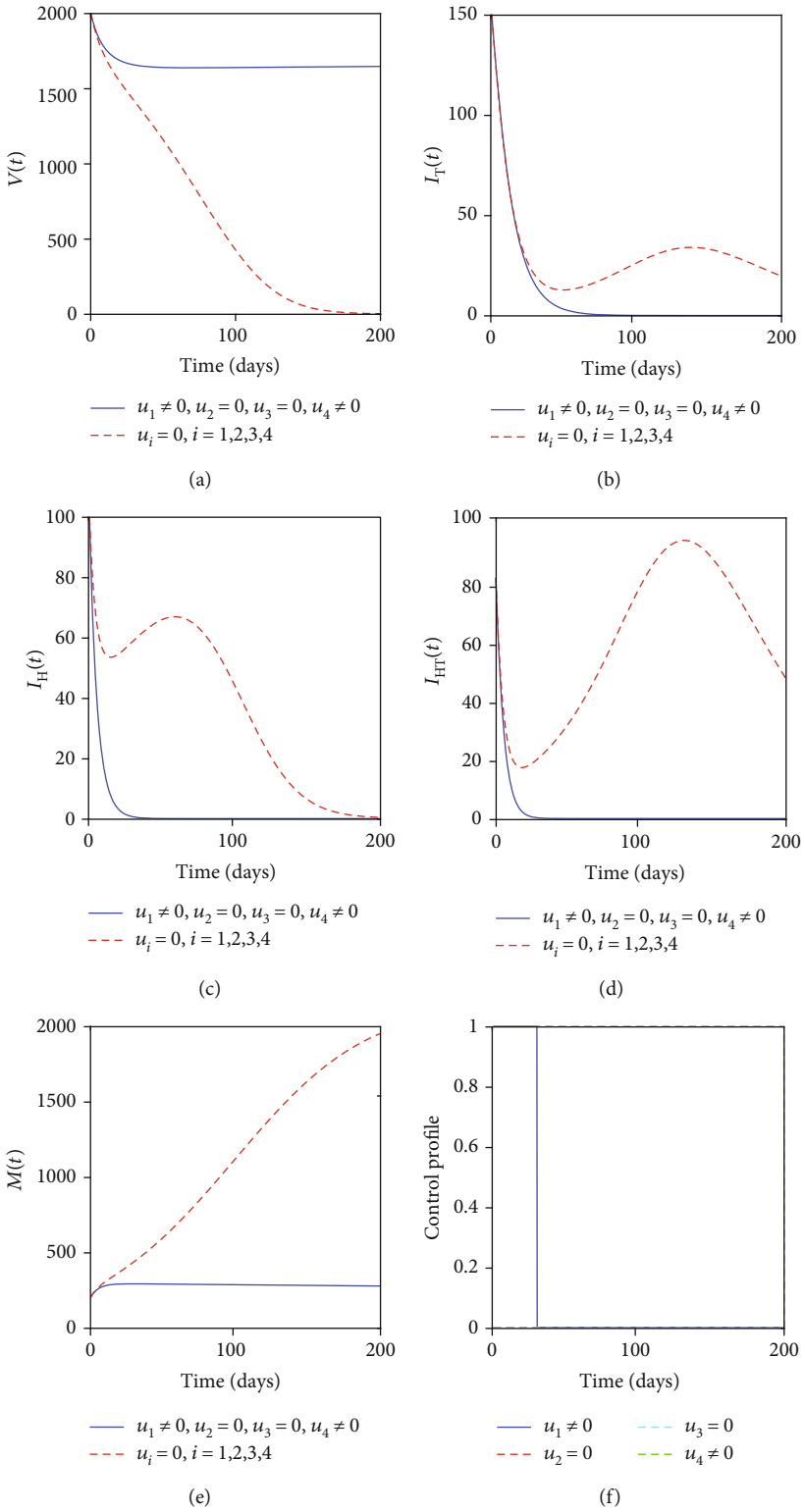

Figure 4: Simulations of the helminth-Mtb coinfection model with the effect of educational campaign and sanitation.

control strategies that focus on helminths only while TB is not controlled would control both TB and helminth infections. This is linked to the increased susceptibility of Mtb for individuals infested with helminths. However, control strategies that include all control measures would effectively control the helminth-Mtb

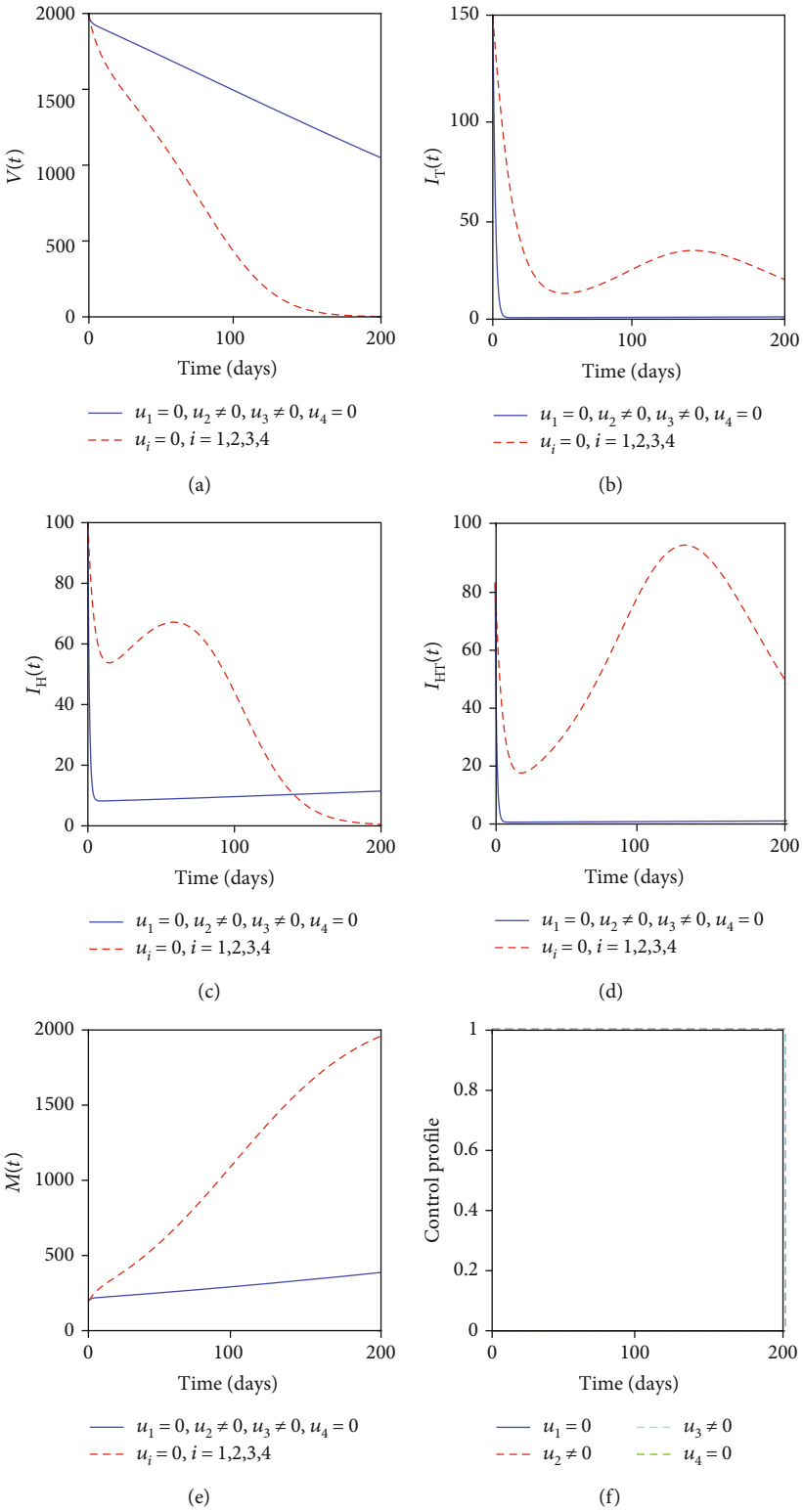

Figure 5: Simulations of the helminth-Mtb coinfection model with the effect of treatment of Mtb-infected individuals and MDA.

coinfection at the end of the intervention period. Thus, we suggest to the public health stakeholders that in order to control the helminth-Mtb coinfection, the intervention strategies that target controlling helminth infection and vaccination of babies with BCG after birth and treatment of individuals with active

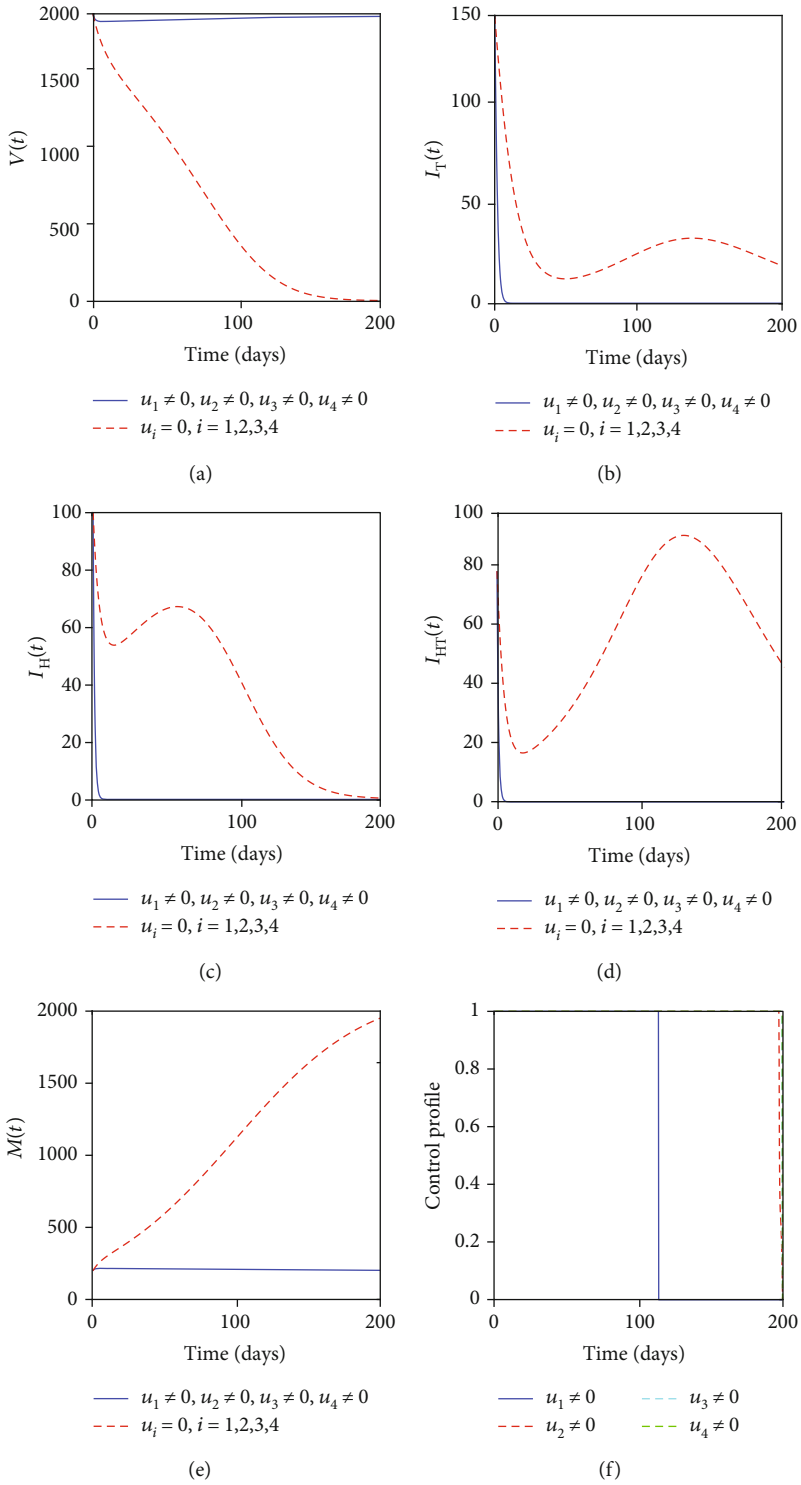

FIGURE 6: Simulations of the helminth-Mtb coinfection model with the effect of educational campaign, treatment of Mtb-infected individuals, MDA, and sanitation.

tuberculosis should be emphasized. One of the limitations of this study is the number of compartments involved that hinders some analytical analyses; however, numerical simulation shows the convergence.

Data Availability

The data are available inside the manuscript, and there is no restriction on the availability of the data.

Conflicts of Interest

The authors declare that they have no contesting interests regarding the publication of this article.

Acknowledgments

We acknowledge the financial support of the African Development Bank Group for this study.

Supplementary Materials

The supplementary material related to this article comprises the MATLAB codes used for numerical simulations. *(Supplementary Materials)*

References

[1] WHO, *Soil transimitted helminths infections*, 2020, June 2020, http://www.who.int/news-room/fact-sheets/detail/soil-transmitted-helminth-infections.

[2] B. Marais and A. Zumla, "Advancing global tuberculosis control after the UNGA-HLM," *Lancet*, vol. 392, no. 10153, pp. 1096-1097, 2018.

[3] N. S. Watts, M. M. Mizinduko, E. D. Barnett, L. F. White, and N. S. Hochberg, "Association between parasitic infections and tuberculin skin test results in refugees," *Travel Medicine and Infectious Disease*, vol. 16, pp. 35–40, 2017.

[4] A. Taghipour, M. Mosadegh, F. Kheirollahzadeh et al., "Are intestinal helminths playing a positive role in tuberculosis risk? A systematic review and meta-analysis," *PLoS One*, vol. 14, no. 10, article e0223722, 2019.

[5] A. T. Dias, S. B. R. de Castro, C. C. S. Alves et al., "Lower production of IL-17A and increased susceptibility to Mycobacterium bovis in mice coinfected with Strongyloides venezuelensis," *Memórias do Instituto Oswaldo Cruz*, vol. 106, no. 5, pp. 617–619, 2011.

[6] L. Monin, K. L. Griffiths, W. Y. Lam et al., "Helminth-induced arginase-1 exacerbates lung inflammation and disease severity in tuberculosis," *The Journal of Clinical Investigation*, vol. 125, no. 12, pp. 4699–4713, 2015.

[7] C. P. Bhunu, W. Garira, and Z. Mukandavire, "Modeling HIV/AIDS and tuberculosis coinfection," *Bulletin of Mathematical Biology*, vol. 71, no. 7, pp. 1745–1780, 2009.

[8] Fatmawati and H. Tasman, "An optimal treatment control of TB-HIV coinfection," *International Journal of Mathematics and Mathematical Sciences*, vol. 2016, Article ID 8261208, 11 pages, 2016.

[9] K. O. Okosun, "Optimal control analysis of malaria-schistosomiasis co-infection dynamics," *Mathematical Biosciences & Engineering*, vol. 14, p. 377, 2016.

[10] A. Kealey and R. Smith, "Neglected tropical diseases: infection, modeling, and control," *Journal of Health Care for the Poor and Underserved*, vol. 21, no. 1, pp. 53–69, 2010.

[11] L. N. Nkamba, T. T. Manga, F. Agouanet, and M. L. Mann Manyombe, "Mathematical model to assess vaccination and effective contact rate impact in the spread of tuberculosis," *Journal of Biological Dynamics*, vol. 13, no. 1, pp. 26–42, 2019.

[12] A. Fenton, "Dances with worms: the ecological and evolutionary impacts of deworming on coinfecting pathogens," *Parasitology*, vol. 140, no. 9, pp. 1119–1132, 2013.

[13] A. R. DiNardo, E. M. Mace, K. Lesteberg et al., "Schistosome soluble egg antigen decreases *Mycobacterium tuberculosis*–specific $CD4^+$ T-cell effector function with concomitant arrest of macrophage phago-lysosome maturation," *The Journal of Infectious Diseases*, vol. 214, no. 3, pp. 479–488, 2016.

[14] H. C. Slater, M. Gambhir, P. E. Parham, and E. Michael, "Modelling co-infection with malaria and lymphatic filariasis," *PLoS Computational Biology*, vol. 9, no. 6, article e1003096, 2013.

[15] D. K. Das, S. Khajanchi, and T. K. Kar, "Influence of multiple re-infections in tuberculosis transmission dynamics: a mathematical approach," in *2019 8th International Conference on Modeling Simulation and Applied Optimization (ICMSAO)*, pp. 1–5, Manama, Bahrai, April 2019.

[16] G. G. Mwanga, H. Haario, and V. Capasso, "Optimal control problems of epidemic systems with parameter uncertainties: application to a malaria two-age-classes transmission model with asymptomatic carriers," *Mathematical Biosciences*, vol. 261, pp. 1–12, 2015.

[17] G. A. Colditz, T. F. Brewer, C. S. Berkey et al., "Efficacy of BCG vaccine in the prevention of tuberculosis," *JAMA*, vol. 271, no. 9, pp. 698–702, 1994.

[18] A. G. Lambura, G. G. Mwanga, L. Luboobi, and D. Kuznetsov, "Mathematical model for optimal control of soil-transmitted helminth infection," *Computational and Mathematical Methods in Medicine*, vol. 2020, Article ID 6721919, 15 pages, 2020.

[19] A. A. Yeketi, W. A. M. Othman, and M. A. O. Awang, "The role of vaccination in curbing tuberculosis epidemic," *Modeling Earth Systems and Environment*, vol. 5, no. 4, pp. 1689–1704, 2019.

[20] C. Dye, S. Scheele, P. >Dolin, V. Pathania, M. C. Raviglione, and for the WHO Global Surveillance and Monitoring Project, "Global burden of tuberculosis," *JAMA*, vol. 282, no. 7, pp. 677–686, 1999.

[21] C. P. Bhunu, W. Garira, Z. Mukandavire, and M. Zimba, "Tuberculosis transmission model with chemoprophylaxis and treatment," *Bulletin of Mathematical Biology*, vol. 70, no. 4, pp. 1163–1191, 2008.

[22] P. Van den Driessche and J. Watmough, "Reproduction numbers and sub-threshold endemic equilibria for compartmental models of disease transmission," *Mathematical biosciences*, vol. 180, no. 1-2, pp. 29–48, 2002.

[23] W. Fleming and R. Rishel, *Deterministic and Sochastic Optimal Control*, Springer-Verlag, 1975.

[24] C. C. Chavez, Z. Feng, and W. Huang, "On the computation of r0 and its role on global stability," in *Mathematical Approaches for Emerging and Re-emerging Infection Diseases: An Introduction*, vol. 125, pp. 31–65, The IMA Volumes in Mathematics and Its Applications, 2002.

[25] C. Castillo-Chavez and B. Song, "Dynamical models of tuberculosis and their applications," *Mathematical Biosciences & Engineering*, vol. 1, no. 2, pp. 361–404, 2004.

[26] N. Chitnis, J. M. Cushing, and J. M. Hyman, "Bifurcation analysis of a mathematical model for malaria transmission," *SIAM Journal on Applied Mathematics*, vol. 67, no. 1, pp. 24–45, 2006.

[27] O. D. Makinde and K. O. Okosun, "Impact of chemo-therapy on optimal control of malaria disease with infected immigrants," *BioSystems*, vol. 104, no. 1, pp. 32–41, 2011.

[28] L. Pontryagin, V. Boltyanskij, R. Gamkrelidze, and E. Mishchenko, *The Mathematical Theory of Optimal Processes*, John Wiley & Sons, New York, NY, USA, 1962.

[29] W. H. Fleming and R. W. Rishel, *Deterministic and Stochastic Optimal Control*, vol. volume 1, Springer Science & Business Media, 2012.

[30] S. Lenhart and J. T. Workman, *Optimal Control Applied to Biological Models*, CRC Press, 2007.

MATHEMATICAL MODELING FOR HELMINTHS AND MYCOBACTERIUM TUBERCULOSIS CO-INFECTION

Introduction

- The study of both helminths and Mtb is important because of co-occurrence of these two diseases in same geographical location.
- Literature shows that in resource-poor areas, co-infection with helminth and Mtb pathogens frequently occurs [2].
- Furthermore, infection by helminth parasites increases the susceptibility to tuberculosis and the consequences associated with such dual infections are tremendously serious in the cognitive development of the pre-school and school aged children [1]

Sensitivity Analysis for helminth model

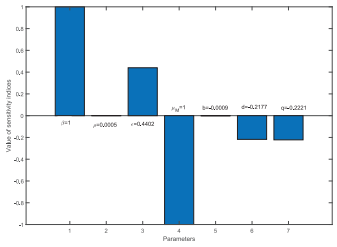

Numerical simulation for Helminth model

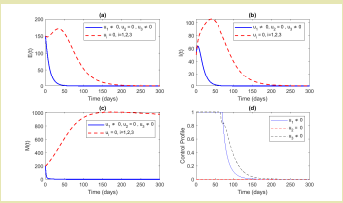

The co-infection model is formulated by extending the helminth model to incorporate the increased susceptibility to Mtb

The Helminth-Mtb co-infection model

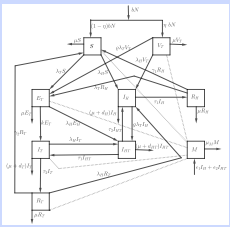

Numerical simulation for the co-infection model

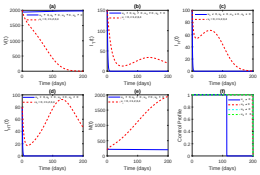

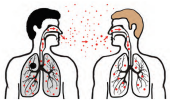

Impact of helminth parasites on Mtb and vice-versa

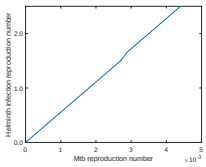

Numerical simulation for the intra-host model to show convergence to the equilibrium point

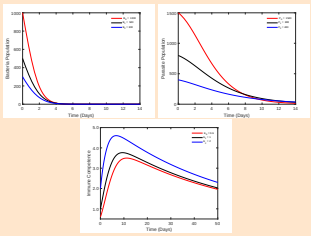

References

[1] Mkhize-Kwitshana, Zilungile L and Tadokera, Rebecca and Mabaso, Musawenkosi HL, *Helminthiasis: a systematic review of the immune interactions present in individuals coinfected with HIV and/or tuberculosis*, Human Helminthiasis.,IntechOpen, 2017.

[2] Uneke, CJ, *Soil transmitted helminth infections and schistosomiasis in school age children in sub-Saharan Africa: efficacy of chemotherapeutic intervention since World Health Assembly Resolution 2001*, Tanzania journal of health research, 12, 1,86–99,2010